
COSPAS-SARSAT 406 MHz FREQUENCY MANAGEMENT PLAN

C/S T.012
Issue 1 – Revision 18
October 2023

*This document has been
superseded by a later version*



COSPAS-SARSAT 406 MHz FREQUENCY MANAGEMENT PLAN**History**

<u>Issue</u>	<u>Revision</u>	<u>Date</u>	<u>Comments</u>
1	0	October 2002	Approved by CSC-29
1	1	October 2003	Approved by CSC-31
1	2	October 2004	Approved by CSC-33
1	3	November 2005	Approved by CSC-35
1	4	November 2007	Approved by CSC-39
1	5	October 2008	Approved by CSC-41
1	6	October 2009	Approved by CSC-43
1	7	October 2010	Approved by CSC-45
1	8	October 2012	Approved by CSC-49
1	9	October 2013	Approved by CSC-51
1	10	October 2014	Approved by CSC-53
1	11	October 2015	Approved by CSC-55
1	12	October 2016	Approved by CSC-57
1	13	February 2018	Approved by CSC-59
1	14	February 2019	Approved by CSC-61
1	15	March 2021	Approved by CSC-64
1	16	March 2022	Approved by CSC-66
1	17	November 2022	Approved by CSC-67
1	18	October 2023	Approved by CSC-69

TABLE OF CONTENTS

		Page
Document History		i
List of Pages.....		ii
Table of Contents.....		iii
1.	Introduction	1-1
1.1	Purpose.....	1-1
1.2	Scope.....	1-1
1.3	Background	1-2
1.4	Existing 406 MHz Channel Assignments Prior to the Adoption of the Frequency Management Plan.....	1-3
1.5	Reference Documents	1-3
2.	Cospas-Sarsat System Capacity	2-1
2.1	Definitions of LEOSAR and GEOSAR Capacity	2-1
2.2	LEOSAR System Capacity Model	2-2
2.3	GEOSAR System Capacity Model	2-3
2.4	Validation of Capacity Models	2-4
3.	Assessment of Capacity Requirements	3-1
3.1	Measure of Traffic Loads and System Capacity	3-1
3.2	406 MHz Beacon Population Assessment and Forecast	3-2
3.3	406 MHz Traffic Forecast.....	3-3
3.4	Interference and Faulty Beacons	3-4
4.	Cospas-Sarsat Channel Assignment Plan in the Band 406.0 - 406.1 MHz.....	4-1
4.1	Cospas-Sarsat 406 MHz Channel Assignment Plan	4-1
4.2	Cospas-Sarsat Policy on the Use of Assigned 406 MHz Channels.....	4-2
4.3	Bandwidth Requirements and Channel Assignment Strategies	4-3
4.4	Cospas-Sarsat System 406 MHz Frequency Protection Requirements	4-8
5.	Procedures for the Assignment of 406 MHz Channels.....	5-1
5.1	Description of LEOSAR and GEOSAR Satellite Constraints	5-1
5.2	Principles of 406 MHz Channel Assignment.....	5-2
5.3	Procedure for Deciding on New Channel Assignments.....	5-3

LIST OF ANNEXES**ANNEX A: List of Abbreviations and Acronyms****ANNEX B: Nominal Conditions Applicable for SARP, SARR and GEOSAR Capacity Definitions and Testing**

B.1	General	B-1
B.2	Nominal Conditions for LEOSAR SARP and SARR Systems	B-1
B.3	Nominal Conditions for GEOSAR Systems.....	B-3

ANNEX C: LEOSAR Capacity Model

C.1	Introduction	C-1
C.2	Basic LEOSAR System Characteristics	C-3
C.3	LEOSAR Capacity Analysis	C-8
C.4	Capacity of the SARP-1 LEOSAR System with Three Channels.....	C-22
C.5	Capacity of the SARP-2 LEOSAR System with 19 Channels	C-24

Appendix A to Annex C: Computation of the Probability of Collision in Frequency

C-A.1	Curves of Equal Doppler Shift	C-A-1
C-A.2	Probability of Collision in Frequency for a Beacon with a Doppler Ratio D (Single Channel)	C-A-2
C-A.3	Probability of Collision in Frequency for a Beacon with a Doppler Ratio D (Multiple Channels)	C-A-7
C-A.4	Results of the Computation of $P_c(D)$	C-A-9

Appendix B to Annex C: Analysis of a Multi-server Communication System with Poisson Arrivals

C-B.1	The Erlang-B Standard Model	C-B-1
C-B.2	Modified Erlang-B Model.....	C-B-3
C-B.3	Application to the LEOSAR SARP	C-B-4

Appendix C to Annex C: Probability of Successful Doppler Processing and LEOSAR System Capacity

C-C.1	Probability of Successful Doppler Processing	C-C-1
C-C.2	Comparison of the Probability of Doppler Processing for Various CTAs.....	C-C-2

Appendix D to Annex C: Results of a Simulation of the LEOSAR SARP Multiple Access

C-D.1	Objectives of the Simulation	C-D-1
C-D.2	Methodology	C-D-1
C-D.3	Results of the SARP-2 Multiple Access Simulation	C-D-4

ANNEX D: GEOSAR Capacity Model

D.1	Introduction	D-1
D.2	Basic GEOSAR System Characteristics.....	D-3
D.3	GEOSAR Capacity Analysis.....	D-8
D.4	GEOSAR System Capacity	D-24

Appendix A to Annex D: Analysis of Frequency Channel Separation

D-A.1	Scope and Objectives	D-A-1
D-A.2	Methodology	D-A-1

D-A.3	Operational Beacons' Frequency Distribution	D-A-2
D-A.4	Probability of Frequency Collisions within a Channel	D-A-3
D-A.5	Probability of Frequency Collisions for Beacons in Adjacent Channels	D-A-4
D-A.6	Probability of Frequency Collisions for the GEOSAR Channel Capacity Model	D-A-5
Appendix B to Annex D: Analysis of Collisions in Time over “M” Successive Bursts with Fixed Periods and Randomised Transmission Times		
D-B.1	Synchronised Transmissions with Random Spreading	D-B-1
D-B.2	Probability of Collisions as a Function of the Period Separation (Δ) of Synchronised Beacon Transmissions.....	D-B-2
D-B.3	Probability of Successful GEOSAR Processing for Beacon “A” Messages with a Period Separation $ \Delta < \tau$	D-B-13
D-B.4	Non-Conditional (Average) Probability of Successful GEOSAR Processing with Fixed Periods and Randomised Transmission Times	D-B-14
D-B.5	Summary of Conclusions of the Analysis of Collisions Over “M” Successive Bursts from Beacons with Fixed Repetition Periods and Randomised Transmission Times	D-B-16
Appendix C to Annex D: Analysis of Collisions in Time with Randomised Repetition Periods		
D-C.1	Transmission Times with Random Period Spreading	D-C-1
D-C.2	Transmission Times Spreading Over “n” Successive Bursts from Beacon “A” ...	D-C-2
D-C.3	Evolution of the Probability of Collision in Time Between Bursts from Beacons “A” and “B” Assuming an Initial Collision, or No Collision at T_1 ...	D-C-8
D-C.4	Probability of Collision in Time, Assuming N Active Beacons	D-C-11
D-C.5	Probability of Collision Assuming N Active Beacons AND At Least One Collision at T_1	D-C-17
D-C.6	Discussion of the Probabilities of Collision Under the Hypothesis of Random Repetition Periods	D-C-18
D-C.7	GEOSAR System Performance Under the Hypothesis of Randomised Repetition Periods	D-C-19
Appendix D to Annex D: GEOSAR Capacity Computer Simulation		
D-D.1	Scope and Objectives of Computer Simulations	D-D-1
D-D.2	Computer Simulation Methodology	D-D-1
D-D.3	Results of the Computer Simulations for Various Distributions of Transmission Times	D-D-4
D-D.4	Comparison of Computer Simulations Results with the Results of the Mathematical Analysis.....	D-D-7
ANNEX E: Test Procedures for Validating the GEOSAR Capacity Model		
E.1	Background	E-1
E.2	Test Procedure Using a Beacon Simulator	E-2
E.3	Data Reduction, Analysis and Results.....	E-3
Appendix A to Annex E: Sample Procedure for GEOSAR Capacity Testing using Transmissions with Time Overlaps		
Appendix B to Annex E: Sample Procedure for GEOSAR Capacity Testing using Non-Interfering Background Transmissions		
ANNEX F: Forecast of 406 MHz Beacon Population		
F.1	Potential Long Term 406 MHz Beacon Population	F-1
F.2	Beacon Population Forecast	F-2

ANNEX G: Cospas-Sarsat 406 MHz Message Traffic Model

G.1	Sources of 406 MHz Traffic.....	G-1
G.2	Beacon Population and 406 MHz Message Traffic.....	G-3
G.3	Model of 406 MHz Beacon Message Traffic.....	G-7
G.4	Estimation of the Message Traffic Model Parameters.....	G-11
G.5	Application of the Beacon Message Traffic Model to the LEOSAR and GEOSAR Systems.....	G-19

ANNEX H: Cospas-Sarsat 406 MHz Channel Assignment Plan**LIST OF FIGURES**

Figure 4.1:	LEOSAR Capacity and Bandwidth Requirements.....	4-4
Figure 4.2:	Comparison of Channel Assignment Strategies for combined LEO/GEO Operation.....	4-7
Figure C.1:	Beacon Burst Collisions in Time and Frequency.....	C-3
Figure C.2:	SARP Block Diagram.....	C-5
Figure C.3	LEOSAR Satellite Visibility Area.....	C-6
Figure C.4	Geometry of the Satellite to Beacon Line of Sight.....	C-11
Figure C.5	Geometry of the Satellite Visibility Area.....	C-11
Figure C.6	Probability of Frequency Collision as a Function of the Doppler Shift.....	C-12
Figure C.7(a)	Probability of Frequency Collisions for Five Adjacent Channels.....	C-14
Figure C.7(b)	Probability of Frequency Collisions for Ten and Twenty Adjacent Channels.....	C-15
Figure C.8	Diagram of SARP State's Transitions.....	C-16
Figure C.9	Probability of Successful Doppler Processing for CTA = 22°, Single Channel, Short and Long Beacon Message Formats, and Valid Long Messages.....	C-19
Figure C.10	Probability of Successful Doppler Processing for CTA = 22°, Short Beacon Message Format, with 5, 10 and 20 Frequency Channels.....	C-20
Figure C.11	Probability of Frequency Collision in Channel 406.025°MHz (3-Channel System).....	C-23
Figure C.12	Probability of Successful Doppler Processing for CTA = 22°.....	C-24
Figure C.13	LEOSAR Capacity Under Various Channel Assignment Schemes.....	C-25
Figure C-A.1	Integration Domain of C-A/E.10.....	C-A-4
Figure C-A.2	Combination of Probabilities of Frequency Collision for Three Adjacent Channels.....	C-A-8
Figure C-A.3	Probability of Frequency Collisions as a Function of the Doppler Shift.....	C-A-9
Figure C-B.1	Diagram of System State's Transitions.....	C-B-2
Figure C-B.2	Evolution of P_U as a Function of P_f	C-B-5

Figure C-B.3	$P_U(N)$ for: (a) $P_{f(\min)} = 0.0996$, and (b) $P_{f(\max)} = 0.2043$	C-B-5
Figure C-C.1	Probability of Successful Doppler Processing, Short Messages, Single Channel, Satellite Passes with $CTA \leq 22^\circ$ (Number of bursts received during pass ≥ 5)	C-C-3
Figure C-D.1	Simulation of Collisions in Time and Frequency with Variable Time Overlap....	C-D-2
Figure C-D.2	Determination of an “Average” Probability of Reception $P_R(N)$	C-D-3
Figure C-D.3	Ratio of Theoretical to Measured P_R as a Function of Beacon Density	C-D-5
Figure D.1	Short and Long Formats of 406 MHz Beacon Messages	D-4
Figure D.2	Probability of Collision in Time for the First Part of Long Messages	D-12
Figure D.3	Probability of Receiving at least “K” Messages with No Collisions Within 5 Minutes (Short Format Messages)	D-14
Figure D.4	Probability of Receiving at least “K” Messages with No Collisions Within 10 Minutes (Short Format Messages)	D-14
Figure D.5	Evolution of the Capacity Computed with Various Probabilities for Short Format Messages and for Processing Times = 5 Minutes and 10 Minutes	D-16
Figure D.6	Evolution of the Capacity Computed with Various Probabilities for Complete Long Format Messages and for Processing Times = 5 Minutes and 10 Minutes....	D-17
Figure D.7	Comparison of GEOSAR Capacity as Computed for:	D-19
	- Complete Long Messages (90% within 5 minutes and 99% within 10 minutes)	
	- Short Messages (95% within 5 minutes), and	
	- Valid Long Messages (First Protected Field, 95% within 5 minutes)	
Figure D.8	Message Transfer Times at Various EIRPs.....	D-22
Figure D.9	Comparison of Analysis and Simulation Results – Probability of Confirmed Complete Long Messages for Non-Conditional and “Worst-Case” Scenarios	D-28
Figure D.10	Evolution in Time of Non-Conditional and Conditional Probability of Confirmed Valid / Complete Long Messages With $K=3$ and 14 Active Beacons (Appendix B Weighted Average and Worst-Case Scenario).....	D-28
Figure D.11	Comparison of Analysis and Simulation Results - Probability of Confirmed Complete Long Messages for $K=4$ and $K=5$	D-29
Figure D.12	GEOSAR Channel Performance for $K \geq 3$ - Evolution of the Probability of Confirmed Messages with Time for Nominal ($K=3$) and Degraded Links ($K=4, 5$) - Non-Conditional and Conditional (Worst-Case) Probabilities	D-30
Figure D-A.1	FMCC Statistics on Operational Beacon Carrier Frequencies (1999)	D-A-1
Figure D-B.1	Fixed Repetition Period with Randomised Transmission Times	D-B-1
Figure D-B.2	Spreading of Second Bursts of A and B after One Period T	D-B-2
Figure D-B.3	Probability of First Burst Collision $P_1(\Delta)$	D-B-4
Figure D-B.4	Second and Subsequent Bursts Collisions.....	D-B-5
Figure D-B.5	Probability of Second and Subsequent Bursts Collisions $P_2(\Delta)$	D-B-8

Figure D-B.6	Comparison of the Probability of Collisions Under the Hypothesis of Uniform Distribution and for Fixed Periods with Randomised Transmission Times, Conditional ($\Delta \leq \tau$) and Non-Conditional Probabilities	D-B-12
Figure D-B.7	Evolution of the Probability of Successful Processing (Assuming $K = 3$) Under the Condition $ \Delta < \tau$, for 5 and 10 Minute Processing Time	D-B-13
Figure D-B.8	Comparison of Probability of Successful Processing (Valid Long Messages, 5 Minutes)	D-B-16
	a) Uniform Distribution of Burst Arrival Times	
	b) Non-Conditional - App.B Weighted Average, and	
	c) Conditional - App.B Worst-Case	
Figure D-C.1	Transmission Times with Randomised Repetition Period	D-C-1
Figure D-C.2	Transmission Times Spreading	D-C-2
Figure D-C.3	Density of Probability of Transmission Times of “A”	D-C-7
Figure D-C.4	Transmission Spreading After First Burst Collision	D-C-8
Figure D-C.5	Comparison of Probabilities of Collision for Individual Bursts Assuming a Uniform Distribution (Annex D), or Randomised Periods (Appendix C).....	D-C-18
Figure D-C.6	Comparison of Probabilities of Collision for Individual Bursts Assuming a Uniform Distribution (Annex D), or Randomised Periods (Appendix C), or Fixed Periods and Randomised Transmission Times (Appendix B)	D-C-20
Figure D-D.1	Uniform Distribution of Transmission Times	D-D-2
Figure D-D.2	Fixed Period and Randomised Transmission Times	D-D-2
Figure D-D.3	C/S T.001 Specification Transmission Times	D-D-3
Figure D-D.4	Simulation Results – Probability of Collision for N Active Beacons	D-D-4
Figure D-D.5	Analysis and Simulation Results – Probability of Collision for N Active Beacons and Valid Long Messages	D-D-6
Figure D-D.6	Analysis and Simulation Results – Probability of Success for N Active Beacons, for Valid Long Messages within 5 Minutes	D-D-6
Figure D-D.7	Comparison of Analysis and Simulation Results – Probability of Processing Success within 10 minutes for Single Complete Long Messages (Worst-Case Scenario) and Confirmed Complete Long Messages	D-D-9
Figure E.1	Graph Depicting Capacity of a 406 MHz Channel in a GEOSAR System	E-4
Figure F.1	Forecast of Beacon Population.....	F-2
Figure G.1	Global traffic Data To Be Collected by France and the USA for the Determination of the Rate of Activation (R_a), the Estimated Total Population (ETP), and the Average Transmission Duration (D)	G-12
Figure G.2	Distribution of GEO Traffic in Time	G-16
Figure G.3	Distribution of LEO Traffic in Time	G-17
Figure G.4	LEOSAR and GEOSAR Beacon Message Traffic Forecast	G-18

LIST OF TABLES

Table 4.1	Comparison of LEO/GEO Capacity for Various Channel Assignment Strategies	4-6
Table C.1	Capacity of the LEOSAR System with a Single Frequency Channel, and with “M” Adjacent-Channels	C-21
Table C.2	Capacity of the SARP-1 LEOSAR System with Three Channels (Probability of successful Doppler processing computed at edge of coverage assuming a uniform distribution of beacons among 3 channels)	C-23
Table C.3	Capacity of the SARP-2 LEOSAR System with 19 Channels (Probability of successful Doppler processing computed at edge of coverage assuming a uniform distribution of beacons among 19 channels)	C-25
Table C.4	LEOSAR Capacity for Various Channel Assignments	C-26
Table C-A.1	Probability of Collisions in the Frequency Domain	C-A-9
Table C-D.1	Simulation Results for One, Three or Five Channels	C-D-4
Table C-D.2	Simulation Results for Ten Channels	C-D-5
Table C-D.3	Maximum Number of Active Beacons Providing a 95% and 98% Probability of Successful Doppler Processing	C-D-6
Table D.1	GEOSAR Capacity as a Function of the Number of Non-Interfering Bursts Required (Short Format Messages)	D-15
Table D.2	GEOSAR Capacity as a Function of the Number of Non-Interfering Bursts Required (Complete Long Format Messages)	D-17
Table D.3	Comparison of Capacity for Various Probabilities of Retrieving Valid Short and Long Messages and Complete Long Messages	D-18
Table D.4	Message Transfer Times as a Function of Beacon EIRPs	D-21
Table D.5	Summary of GEOSAR Performance with 14 Active Beacons ($K = 3$) - Probability of Successful Processing of Single Valid or Complete Long Messages	D-26
Table D.6	Summary of GEOSAR Performance with a Traffic Load Equal to the Channel Capacity (14 Active Beacons, $K = 3$) - Probability of Confirmed Valid or Complete Long Messages	D-29
Table D-A.1	Analysis of Beacon Carrier Frequency Distribution	D-A-2
Table D-A.2	Probability of Frequency Collision as a function of the Channel Separation	D-A-5
Table D-B.1	Conditional Probability of Successful Processing for N Active Beacons, Assuming $K=3$ and At Least One Period Separation $ \Delta < \tau$	D-B-14
Table D-B.2	Non-Conditional Probability of successful Processing for N Active Beacons - Weighted Average for Valid and Complete Long Messages, Assuming $K=3$	D-B-15
Table D-D.1	Comparison of Mathematical Analysis and Computer Simulation Results Obtained for Valid Long Messages with Various Distributions of the Bursts Transmission Times	D-D-8

Table D-D.2	Comparison of Mathematical Analysis and Computer Simulation Results Obtained for Confirmed Complete Long Messages with Various Distributions of the Bursts Transmission Times.....	D-D-10
Table E.1	Data to be Collected for GEOSAR Capacity Test	E-3
Table E.2	Sample Table for Capacity Statistics.....	E-3
Table E-B.1	Bsim HEX ID	E-B-3
Table F.1:	Estimate of Potential 406 MHz Beacon Population	F-1
Table F.2:	406 MHz Beacon Population Model	F-3
Table G.1	Ten-Year Forecast of the Beacon Message Traffic	G-19
Table H.1:	Summary of 406 MHz Beacon Population Forecast, Capacity Requirements and Channel Requirements	H-1
Table H.2	Cospas-Sarsat 406 MHz Channel Assignment Table.....	H-2

This document has been
superseded by a later version

1. INTRODUCTION

The Cospas-Sarsat System provides distress alert and location data for search and rescue (SAR), using spacecraft and ground facilities to detect and locate the signals of distress radiobeacons operating on 406 MHz. To ensure that the System satisfies future capacity requirements and remains capable of servicing the growing 406 MHz beacon population, the use of the band 406.0 to 406.1 MHz by Cospas-Sarsat must be monitored and procedures for its efficient management must be defined.

1.1 Purpose

The purpose of this document is to describe the policies, procedures, and detailed technical analyses developed by Cospas-Sarsat for managing the use of the 406.0 - 406.1 MHz frequency band. Cospas-Sarsat Council decisions in respect of 406 MHz channel assignments are summarised at Annex H in the Cospas-Sarsat 406 MHz Channel Assignment Plan. Specifically this document provides:

- a. mathematical models for determining the capacity of the Cospas-Sarsat System;
- b. procedures for assessing the current and future 406 MHz distress beacon population;
- c. procedures for assessing the current and future 406 MHz beacon message traffic load on the System;
- d. a description of the channelisation of the 406 MHz band used by Cospas-Sarsat;
- e. procedures for meeting System capacity requirements by opening new channels in the 406 MHz band, as required to satisfy the growth of the 406 MHz traffic load; and
- f. the current status of the use of the 406.0 to 406.1 MHz frequency band by Cospas-Sarsat and a record of the Cospas-Sarsat Council decisions in respect of the future use of additional frequency channels, as required to accommodate the forecast 406 MHz beacon population.

1.2 Scope

This document presents the analysis of relevant issues concerning the assessment of capacity requirements, and a description of the policies and procedures adopted by Cospas-Sarsat for managing its use of the 406 MHz band.

Section 2 provides definitions of the capacity of the LEOSAR and GEOSAR systems, a general description of the 406 MHz LEOSAR and GEOSAR systems' capacity models and their validation.

Section 3 provides a description of how 406 MHz message traffic requirements are assessed and forecast by Cospas-Sarsat.

Section 4 describes the overall 406 MHz channel assignment plan and the Cospas-Sarsat policy on the use of assigned frequency channels.

Section 5 details the procedures used by Cospas-Sarsat to decide on the assignment of new frequency channels in the 406.0 to 406.1 MHz frequency band.

The detailed analysis of the LEOSAR and GEOSAR system capacity, the current and forecast 406 MHz beacon population and message traffic, and the approved 406 MHz Channel Assignment Plan are provided in the Annexes to this document.

1.3 Background

The International Telecommunication Union (ITU) has allocated the 406.0 - 406.1 MHz frequency band for the dedicated use of low power satellite position-indicating radiobeacons (see ITU Radio Regulations, Article S5, note S5.266). Since the overall capacity of the Cospas-Sarsat System is directly related to the distribution of beacon carrier frequencies within the band, there is a requirement to assess and manage the number of beacons operating in various portions of the allocated spectrum. Cospas-Sarsat has determined that the best way to ensure that the distress beacon message traffic does not exceed the System capacity in any portion of the available frequency band, is to divide the 406.0 - 406.1 MHz frequency band into channels, and to open the channels for beacon production as demand dictates.

The schedule for opening new channels for beacon production must account for:

- a. the capability of Cospas-Sarsat equipment; i.e. Cospas-Sarsat must ensure that space and ground segment equipment capable of processing beacon transmissions in a given channel will be available prior to opening that channel for use;
- b. the capacity of each frequency channel; i.e. the number of beacons operating simultaneously in a given channel that can be successfully processed by the Cospas-Sarsat System;
- c. the forecast 406 MHz traffic load resulting from the beacon population and other sources of 406 MHz signals (e.g. test and reference beacons);
- d. the advance notice required by administrations and organizations to adapt their regulations to authorise 406 MHz beacon operation in new frequency channels; and
- e. the advance notice required by beacon manufacturers to design and produce beacons which will operate in new 406 MHz channels.

In addition, there may be a need to develop procedures for terminating the production of beacons operating in channels that are approaching their capacity limit.

1.4 Existing 406 MHz Channel Assignments Prior to the Adoption of the Frequency Management Plan

The first Cospas-Sarsat channel opened for use by operational beacons was established with a centre frequency at 406.025 MHz. To accommodate the forecast growth of the population of beacons operating at 406.025 MHz, Cospas-Sarsat has required that all System beacons (orbitography and other reference beacons used for System calibration) be moved to the channel 406.022 MHz.

Following the closure of channel 406.025 MHz, new channels were available for Cospas-Sarsat type approval of beacon models at 406.028 MHz from 1 January 2000 until 1 January 2007, 406.037 MHz from 1 January 2004 until 1 January 2012 and 406.040 MHz from 1 January 2010 until 1 January 2017. New beacon models submitted for Cospas-Sarsat type approval after 1 January 2017 are required to operate at 406.031 MHz as provided in the Cospas-Sarsat 406 MHz Channel Assignment Table (see Annex H). Beacon models type approved for operation in channels that had been closed may continue to be produced at that frequency after their closure date. However, to ensure that the capacity in closed channels will not be exceeded in future, manufacturers of Cospas-Sarsat beacons type approved for operation in closed channels are encouraged to move the carrier frequency of these models to 406.031 MHz or other assigned channels as appropriate, subject to the demonstration by the manufacturer that the beacon model continues to meet the requirements of document C/S T.001 (406 MHz beacon specification).

1.5 Reference Documents

- a. C/S G.003: Introduction to the Cospas-Sarsat System;
- b. C/S S.011: Cospas-Sarsat Glossary;
- c. C/S T.001: Specification for Cospas-Sarsat 406 MHz Distress Beacons;
- d. C/S T.002: Cospas-Sarsat LEOLUT Performance Specification and Design Guidelines;
- e. C/S T.003: Description of the Payloads Used in the Cospas-Sarsat LEOSAR System;
- f. C/S T.005: Cospas-Sarsat LEOLUT Commissioning Standard;
- g. C/S T.007: Cospas-Sarsat 406 MHz Distress Beacon Type Approval Standard;
- h. C/S T.009: Cospas-Sarsat GEOLUT Performance Specification and Design Guidelines;
- i. C/S T.010: Cospas-Sarsat GEOLUT Commissioning Standard;
- j. C/S T.011: Description of 406 MHz Payloads Used in the Cospas-Sarsat GEOSAR System; and
- k. C/S A.003: Cospas-Sarsat System Monitoring and Reporting.

2. COSPAS-SARSAT SYSTEM CAPACITY

2.1 Definitions of LEOSAR and GEOSAR Capacity

The capacity of Cospas-Sarsat LEOSAR and GEOSAR systems is the number of 406 MHz distress beacons active in the field of view of a satellite that can be successfully processed, with a stated probability, under nominal conditions.

Each Cospas-Sarsat processing channel (i.e. the GEOSAR, LEOSAR SARR and LEOSAR SARP channels) must be analysed separately, since the method of processing 406 MHz beacon signals and the results produced are different for each system. For example, GEOLUTs in the GEOSAR system are designed to integrate bursts received from individual beacons until they are able to decode the 406 MHz beacon message, whereas the LEOSAR system search and rescue processor (SARP) and search and rescue repeater (SARR) processing channels are designed to decode individual beacon messages and produce Doppler locations.

Therefore, specific capacity definitions are given for the GEOSAR and for the LEOSAR processing channels.

The “nominal conditions” quoted in the definitions refer to applicable detailed technical parameters and ambient conditions. The nominal conditions applicable to each definition are provided at Annex B.

2.1.1 Definition of Cospas-Sarsat LEOSAR SARP and SARR System Capacity

The number of 406 MHz distress beacons operating simultaneously in the field of view of the LEOSAR satellite that can be successfully processed by the SARP or the SARR channel to provide beacon message and Doppler location information, under nominal conditions, 95% of the time.

2.1.2 Definition of Cospas-Sarsat GEOSAR System Capacity

The number of 406 MHz distress beacons operating simultaneously in the field of view of a GEOSAR satellite that can be successfully processed by the System to provide beacon message information, under nominal conditions, within 5 minutes of beacon activation 95% of the time.

The GEOSAR capacity analysis shows that, if the above probability of successful processing within 5 minutes is satisfied, then the probability of successful processing within 10 minutes is greater than 99% in the worst-case scenario, under nominal conditions, or 99.9% on average.

2.2 LEOSAR System Capacity Model

Annex C provides a detailed description of the LEOSAR capacity model and the results of the capacity computations for beacons with short and long message formats, under the following hypotheses that characterise the LEOSAR system operation:

- the beacons are evenly distributed in the LEOSAR satellite visibility area;
- the beacon burst arrival times at the satellite follow a Poisson distribution;
- beacon bursts that overlap in time and frequency cannot be successfully processed;
- the probability of collision between beacon bursts takes into account all beacons in the satellite visibility area defined with a 0° elevation angle;
- although a Doppler position can be computed with only 3 frequency measurements (and possibly with only two measurements complemented by an independent measurement of the beacon transmit frequency), under nominal conditions a successful Doppler processing requires the reception of at least four beacon messages; and
- the required probability of successful Doppler processing must be achieved for all beacons that have a maximum cross-track angle (CTA) of 22° , which provides for the possible reception of five bursts with an elevation angle of at least five degrees.

The analysis shows that the probability of beacon burst collision in the frequency domain is not uniform, but depends on the Doppler shift that affects the received burst (i.e. on the position of the beacon in the satellite visibility area). It also shows that, because of a Doppler spreading of ± 9 kHz, frequency channels separated by 3 kHz are not independent and the transmissions from beacons in one channel may interfere with transmissions from beacons in other channels. Therefore, because of inter-channel interference, the total capacity does not increase linearly with the number of available frequency channels.

For consistency with the GEOSAR capacity model the 95% probability criterion should be applied to the successful Doppler processing of valid long messages, with a population of beacons transmitting only long messages. The analysis detailed at Annex C, and simulations of the system performance, show that this would result in an overly conservative LEOSAR capacity figure, considering in particular that the 95% probability criterion is applied to beacons with a CTA of 22° , which is already a very conservative constraint. The LEOSAR capacity figures would significantly increase if the calculations were based on beacon events with a CTA less than 22° (i.e. satellite passes that provide for the possible reception of more than 5 bursts with a minimum elevation of 5°). Therefore, the nominal LEOSAR capacity will be based on the maximum number of active beacons in the satellite visibility circle that allows for a 95% probability of successful Doppler processing of a beacon with a CTA of 22° , assuming a population of beacons transmitting short messages.

On the basis on the above hypotheses, and in particular because of the choice of a scenario for achieving the required probability of successful Doppler processing that specifically addresses beacons at the edge of the satellite visibility area (i.e. with a CTA of 22°), the model used in the computation of the LEOSAR capacity is conservative. Nevertheless, the capacity figures provided by this model indicate that a worldwide beacon population greater than one million can be supported by a single frequency channel, and that a beacon population of about

3.15 million can be supported if the available frequency band is used in accordance with the optimum channel assignment scheme (see section 4).

In respect of the management of the 406.0 – 406.1 MHz frequency band, it is important to note that, for a capacity computation based on the specific case of beacon events characterised by a CTA of 22°, three adjacent channels provide less capacity than a single frequency channel, and five adjacent channels provide less capacity than three channels. To increase the LEOSAR system capacity, it is necessary to separate the new channels by at least 9 kHz to ensure a degree of independence between the channels. Total independence in term of frequency collisions between channels in the LEOSAR system would require a separation of 18 kHz.

The detailed analysis of the optimum frequency assignment scheme is provided in section 4.

2.3 GEOSAR System Capacity Model

Annex D provides a detailed analysis of the GEOSAR capacity model and the results of the capacity computations performed under the following hypotheses:

- GEOSAR channels separated by at least 3 kHz are independent (bursts from beacons in different channels do not collide in frequency);
- for the first burst transmitted by a beacon, all burst arrival times at the satellite antenna, from other beacons in the same channel, are assumed to be uniformly distributed over the duration of the repetition period;
- for subsequent transmissions of the same beacon, the probability of collision in time is affected by the random spreading of the repetition period as specified in document C/S T.001 (i.e. 50 seconds +/- 5 %);
- for a beacon satisfying the nominal conditions described at Annex B, a successful GEOLUT processing requires at least 3 beacon bursts received with no collisions; and
- the total system capacity increases linearly with the number of channels in use (the total load on the satellite repeater has no impact on the channel capacity).

The analysis of the GEOSAR capacity provided at Annex D demonstrates that the requirement for a 95% probability of successful processing within 5 minutes is always more restrictive than a requirement for 99% within 10 minutes. Therefore, the determination of the nominal GEOSAR capacity on the basis of a 95% probability of successful processing is consistent with the conservative approach adopted for the LEOSAR capacity model.

However, this criterion will be applied to the successful recovery of valid long messages (i.e. the recovery of the first protected field of a long message, assuming all beacons are transmitting long format messages), noting that a valid long message is sufficient to generate a GEOSAR alert, and that a complete long message (first and second protected fields) will be retrieved within 10 minutes with a probability of 99.9% (see Table D.5 of Annex D).

In addition, the analysis shows that, under the criterion 95% of valid messages successfully processed within 5 minutes, a complete long message will be confirmed (second successful processing of an identical message) within 10 minutes with a probability greater than 96%, or within 15 minutes with a probability greater than 99% in the worst-case scenario (see Table D.6 of Annex D)

With the above hypotheses the nominal GEOSAR channel capacity is 14 beacons in the visibility area of a GEOSAR satellite that are simultaneously active in the same channel.

The performance of the GEOSAR system is highly dependent upon the quality of the link, which itself depends on a number of factors (e.g. beacon EIRP). This link quality is reflected in the GEOSAR capacity model with the selection of the parameter K: minimum number of bursts required, with no frequency collisions, to ensure successful processing. The selection of $K = 3$ reflects a conservative approach to the determination of the nominal GEOSAR capacity and, under nominal conditions, some GEOSAR systems are expected to exhibit higher capacity performance than described above.

2.4 Validation of Capacity Models

The system capacity figures derived from the models described above must be verified on the basis of controlled tests, using real 406 MHz beacons and/or beacon simulators to generate known traffic loads in one or several 406 MHz channels. The output from Cospas-Sarsat LEOLUTs or GEOLUTs in presence of the simulated traffic load will be analysed to determine the performance of the system. The process is repeated for increasing (or decreasing) traffic loads, until the tested system exhibits a performance commensurate with the probability level of the capacity definition (i.e. 0.95).

The test procedures used to validate the GEOSAR and LEOSAR (SARP/SARR) capacity models are provided at Annex E.

3. ASSESSMENT OF CAPACITY REQUIREMENTS

The Cospas-Sarsat System capacity requirement is the load of 406 MHz transmissions from operational beacons or other sources that the System should be able to process or accommodate. The list below identifies the sources which contribute to this load:

- a. 406 MHz distress beacons which have been activated in their operational mode;
- b. 406 MHz distress beacons which have been activated in their self-test mode;
- c. transmissions from faulty 406 MHz beacons;
- d. Cospas-Sarsat System beacons (i.e. orbitography and reference beacons);
- e. 406 MHz test beacons; and
- f. interference.

3.1 Measure of Traffic Loads and System Capacity

The load on the System caused by a single active beacon transmitting a short format message, or a long format message, and operating in accordance with the requirements of document C/S T.001 (406 MHz beacon specification), is a well-defined and well understood amount of traffic which can be used as a unit of measure. Therefore, it is practical to convert all components of the 406 MHz traffic load into an equivalent number of active beacons as defined above.

For example, knowing the technical characteristics of 406 MHz beacon self-test mode signals, it is possible to represent the average load resulting from self-test mode transmissions which may occur in the system, as an equivalent number of simultaneously active beacons.

The end result is that the overall capacity requirement corresponding to the sum of all sources of 406 MHz transmissions can be expressed as an equivalent number of simultaneously active beacons. This approach provides a standard unit of measure that can also be used in the definition of System capacity, the capacity models, and Cospas-Sarsat test procedures for assessing capacity. Because this standard unit of 406 MHz traffic is used in all these applications, it allows a simple comparison of capacity requirements against the actual or forecast System capacity.

An estimate of 406 MHz transmission loads on the System requires:

- a. an assessment of the 406 MHz beacon population;
- b. a method for determining the traffic load on the System caused by the distress beacon population, actual or forecast, expressed as an equivalent number of active beacons; and

- c. appropriate methods for converting other components of the load into an equivalent number of active 406 MHz beacons.

Considering that the Cospas-Sarsat 406 MHz system includes satellites in low-altitude polar Earth orbit (LEOSAR system) and in geostationary orbit (GEOSAR system), and since each of these systems has unique operating characteristics, it is necessary to establish the capacity requirements for the LEOSAR and GEOSAR systems separately. Furthermore, since the use of the 406 MHz band is managed by controlling the number of beacons in each 406 MHz channel, there is a requirement to determine the traffic load generated in each 406 MHz channel.

3.2 406 MHz Beacon Population Assessment and Forecast

An accurate assessment of the 406 MHz beacon population and a forecast of its evolution are essential for determining current and future System capacity requirements (i.e. the beacon message traffic to be supported by the System).

The capacity of the System depends on the bandwidth available for beacon use. Therefore, to satisfy the capacity requirements resulting from the growth of the beacon population, the carrier frequency of 406 MHz beacons must be spread over an increasing number of frequency channels in the 406.0 to 406.1 MHz band. Each channel contributes a specific capacity figure which cannot be exceeded if the specified System performance is to be maintained in the channel. Therefore, the beacon population and the corresponding capacity requirements must be assessed and forecast for each Cospas-Sarsat 406 MHz frequency channel.

3.2.1 Total Beacon Population

The total 406 MHz beacon population is determined from the results of a survey of manufacturers of type approved beacons conducted annually by the Cospas-Sarsat Secretariat. This survey requests the manufacturer to provide:

- a. the number of distress beacons that were manufactured in the previous calendar year;
- b. the number of those beacons that were purchased as replacements for 406 MHz beacons which had been removed from service; and
- c. an estimate of the growth rate of the number of beacons that manufacturers will produce in future years.

This information is consolidated with information obtained from other sources (e.g. reports provided by national Administrations and international organizations) to produce a 10 year forecast of the overall 406 MHz beacon population. A model of the 406 MHz beacon population forecast is provided at Annex F.

As a check to ensure that the forecast beacon population remains consistent with the size of the potential user population, an analysis of available statistical data on aircraft and vessel fleets has been conducted. The potential beacon population is based on the size

of fleets for each category of aircraft and vessel, assuming an estimated maximum percentage of each category could be equipped, and a global estimate of the total personal locator beacon (PLB) market. A summary of this analysis is also provided at Annex F.

3.2.2 Beacon Population per Channel

The actual beacon population operating in each 406 MHz channel (P_{channel}) can be estimated by tracking the ratio of Cospas-Sarsat alerts received from each channel to the total number of alerts received, and applying this ratio to the total beacon population.

$$P_{\text{Channel}} = \frac{\text{Number of alerts received in channel}}{\text{Total number of alerts received}} \times \text{Total beacon population}$$

Having determined the actual beacon population in a channel, the forecast of the population in that channel can be developed on the basis of responses to the annual survey of beacon manufacturers by applying appropriate growth ratios. However, the forecast of the population in individual channels requires detailed information and complex analyses which may not be as reliable as global production figures or growth ratios. In particular, it may prove extremely difficult to predict on a long term basis reliable figures of beacon model production, or the termination of production of a beacon model and the replacement rate of existing beacons with new models.

Because of the difficulty of forecasting the beacon population in individual frequency channels, and the corresponding traffic demand, adequate margins will need to be introduced in the forecast of capacity requirements per channel when deciding on the use of additional frequency channels.

3.3 406 MHz Traffic Forecast

To determine capacity requirements, it is necessary to forecast the average and peak traffic loads in each 406 MHz channel. As described above, the load is comprised of 406 MHz transmissions from many sources, including operational beacons, System beacons, test beacons, and interference. The various sources of 406 MHz transmissions and the mathematical model used to forecast the 406 MHz beacon message traffic in the LEOSAR and GEOSAR systems are detailed at Annex G. An outline of the traffic model is provided below. The impact of faulty beacons and interference is further addressed in section 3.4.

The peak traffic load in the coverage area of a GEOSAR or LEOSAR satellite is obtained by:

- a. monitoring the 406 MHz band to assess the contribution of each source to the total load;
- b. conducting analyses to forecast long-term changes in the load contributed from each source (e.g. develop methods for assessing trends in the traffic load resulting from active beacons, self-test mode transmissions, test beacons, etc.);
- c. converting the load generated from each source into an equivalent number of operational beacons active world-wide;

- d. determining the corresponding load in the coverage area of the system considered (LEOSAR or GEOSAR) by applying the satellite coverage area to earth surface area ratio to each component of the load, as appropriate;
- e. monitoring the load from each source to determine fluctuations which are function of time or geographic regions, taking into account the systems' coverage area;
- f. applying the fluctuation factors described above (peak-time factor and geographic density ratio), to obtain worse case loads from each source; and
- g. summing the load from each source to establish the peak total traffic load.

The process described above provides capacity requirements for the LEOSAR and the GEOSAR systems, expressed as an equivalent number of active beacons, which are a function of the actual or forecast beacon population. Similar computations can also be performed for each 406 MHz channel, on the basis of the actual or forecast proportion of the total beacon population in each channel, to ensure that the capacity of each individual channel is not exceeded.

The detailed computation of the 406 MHz peak traffic load for each source of 406 MHz transmissions is described in detail in the "Cospas-Sarsat 406 MHz Message Traffic Model" provided at Annex G.

3.4 Interference and Faulty Beacons

Non-beacon transmitters which emit signals in the 406 MHz band and defective beacons can seriously impact on the System capacity.

Every effort is made by Cospas-Sarsat to identify and locate the sources of 406 MHz interference, using in particular the LEOSAR system and Doppler location techniques, so that these sources may be eliminated with the assistance of responsible Administrations. However, such elimination requires lengthy efforts and, during this period of time, interference can affect the System's capability to detect and locate 406 MHz distress alerts in some areas of the globe.

One particular beacon failure mode has been observed by Cospas-Sarsat. Some 406 MHz beacons transmit repetitively in the self-test mode (see document C/S T.001) a message with an inverted frame synchronisation pattern which is not processed by the System but does generate a 406 MHz traffic load. Additional tests have been introduced in the type approval process to eliminate this problem in future. However, in the interim, faulty beacons can have a significant impact on the total 406 MHz traffic at a particular time due to very short repetition periods of the self-test mode transmissions.

Having monitored the impact of such emissions for extended periods of time, Cospas-Sarsat concluded, that:

- a. although some channels in the 406.0 to 406.1 MHz frequency band seem to experience periodic interference patterns, it is not possible to reliably predict when interference

sources or faulty beacons will be active, the duration that they will be active, nor their impact while they are active;

- b. therefore, it is not possible to estimate a “typical load” that could be used to assess their impact on the 406 MHz traffic; and
- c. consequently, the Cospas-Sarsat 406 MHz traffic model should not include an additional traffic level to account for faulty beacons or interference.

However, it is also recognised that, during particular periods of time, in some geographic areas and within particular 406 MHz beacon channels, the System capacity could be affected by interference or faulty beacon transmissions and these aspects should be taken into account in the management of the use of the 406 MHz band.

- END OF SECTION 3 -

*This document has been
superseded by a later version*

4. COSPAS-SARSAT CHANNEL ASSIGNMENT PLAN IN THE BAND 406.0 - 406.1 MHz

The following sections discuss the rationale for the development of a Cospas-Sarsat 406 MHz channel assignment plan, the Cospas-Sarsat policy in respect of the use of assigned 406 MHz frequency channels, the 406 MHz bandwidth needed to satisfy capacity requirements for both the LEOSAR and GEOSAR systems, and the strategy for ensuring an optimum use of the available frequency spectrum.

The procedures developed by Cospas-Sarsat for the management of the 406 MHz beacon message traffic demand through the opening of additional frequency channels in the assignment table are discussed in section 5 of this document.

4.1 Cospas-Sarsat 406 MHz Channel Assignment Plan

Pursuant to Article 9 of the International Cospas-Sarsat Programme Agreement, the functions of the Cospas-Sarsat Council include, inter alia:

- the development of the necessary technical, administrative and operational plans;
- the preparation, consideration and adoption of technical specifications for the System space and ground facilities and radiobeacons, as well as the adoption of Cospas-Sarsat technical and operational documentation; and
- the assessment of the need for technical and operational enhancements of the System.

To ensure adequate system performance and the timely adjustment of the System capacity as demand requires, the Cospas-Sarsat Council must ensure that 406 MHz beacons are produced in accordance with a co-ordinated frequency assignment plan. The frequency assignment plan shall take into account:

- the constraints of the space segment (see section 5);
- the constraints of 406 MHz beacon development, production and testing, in particular the manufacturers' need for sufficient advance notice for implementing any changes to their beacon development and production programmes;
- the constraints of Administrations and international organisations responsible for regulatory matters; and
- the need to optimise the use of the available spectrum and reserve bandwidth for future system evolution, including the possible development of new types of 406 MHz distress beacons.

As decisions on matters of beacon specification, testing and type approval may impact on Administrations and users world-wide, the Cospas-Sarsat Council decisions in respect of the use of 406 MHz frequency channels for new beacon models must be co-ordinated with Administrations and the responsible international organisations, and publicised with sufficient advance notice.

In view of its responsibilities, the manufacturing and regulatory constraints described above and the need for advance planning and co-ordination, the Cospas-Sarsat Council has decided to adopt a long term Cospas-Sarsat 406 MHz Channel Assignment Plan, and to publicise the Cospas-Sarsat 406 MHz Channel Assignment Table, as provided at Annex H to this document. The Cospas-Sarsat 406 MHz Channel Assignment Table summarises the current assignments of 406 MHz channels for the production of type approved beacons and for type approval of new models of Cospas-Sarsat 406 MHz beacons. It also provides a summary of future channel assignments in the 406.0 to 406.1 MHz frequency band as planned by Cospas-Sarsat to ensure that future capacity requirements will be met.

4.2 Cospas-Sarsat Policy on the Use of Assigned 406 MHz Channels

The use of assigned frequency channels will be monitored on an annual basis. Cospas-Sarsat will update its forecast of capacity requirements and make changes to the 406 MHz Channel Assignment Plan as required. To allow for appropriate co-ordination with manufacturers, Administrations, and competent international organisations, Cospas-Sarsat will endeavour to decide on any changes to the 406 MHz Channel Assignment Plan with a minimum advance notice of three years before the date such changes would become applicable. The Cospas-Sarsat 406 MHz Channel Assignment Table provided at Annex H defines the current and planned status of channels in the 406.0-406.1 MHz band, as assigned by Cospas-Sarsat for type approval of 406 MHz beacon models.

The Cospas-Sarsat policy for the use of assigned 406 MHz channels is summarised as follows:

- a. Beacon models submitted for Cospas-Sarsat type approval testing shall comply with the applicable carrier frequency assignment as at the date the beacon is submitted to a Cospas-Sarsat accepted laboratory for type approval testing.
- b. If a beacon model is designed to operate in several 406 MHz frequency channels, Cospas-Sarsat will determine the frequency channel(s) in which production beacons of that model should operate, in accordance with the Channel Assignment Table (Annex H), and/or any applicable restrictions, depending on the particular design characteristics of the beacon model submitted for type approval and the type approval testing performed on that model.
- c. After successful completion of the Cospas-Sarsat type approval testing procedure, the Secretariat will issue a Cospas-Sarsat type approval certificate. The Cospas-Sarsat type approval certificate shall indicate the nominal carrier frequency, or frequencies, at which production beacons of that model should operate, as per the type approval testing performed on the model provided by the manufacturer.
- d. The nominal carrier frequency(ies) for a beacon model, as stated on the Cospas-Sarsat type approval certificate, will be published in the document Cospas-Sarsat System Data, updated by the Cospas-Sarsat Secretariat on an annual basis, and will be made available on the Cospas-Sarsat web-site.
- e. When issuing national type approval for a beacon model, or licences for the use of a beacon, Administrations should ensure that 406 MHz beacons of the model are operating in the appropriate frequency channel(s), as provided in the Cospas-Sarsat type approval

certificate and in accordance with the Cospas-Sarsat 406 MHz Channel Assignment Table.

- f. The Cospas-Sarsat 406 MHz Channel Assignment Table will be amended as required on an annual basis, and publicised in the revisions of this Cospas-Sarsat 406 MHz Frequency Management Plan (C/S T.012), issued by the Cospas-Sarsat Secretariat after approval of the Cospas-Sarsat Council.
- g. If the 406 MHz beacon message traffic in a particular frequency channel approaches its capacity limit, the Cospas-Sarsat Council may decide, as appropriate, to:
- close that channel for type approval of new beacon models and amend the 406 MHz Channel Assignment Table accordingly;
 - request manufacturers to switch their production to another frequency channel, subject to the beacon model continuing to satisfy Cospas-Sarsat performance requirements; and
 - recommend that Administrations consider amending their national regulations / legislation to encourage the transition to alternative frequency channels.

4.3 Bandwidth Requirements and Channel Assignment Strategies

Analysis conducted by Cospas-Sarsat has determined that the most effective way to manage the 406 MHz band was to divide the available spectrum into individual channels and open these channels for operational use as demand requires. The following sections discuss the bandwidth requirements for the GEOSAR and the LEOSAR systems, on the basis of 3 kHz frequency channels, and the optimum channel assignment strategy.

The Cospas-Sarsat frequency channels in the 406.0 - 406.1 MHz band are defined by the nominal carrier frequency of the beacons operating in the channel.

4.3.1 Bandwidth Requirements for the GEOSAR System

Based on the observed spectral characteristics of operational 406 MHz beacons, Cospas-Sarsat has determined that the nominal separation of beacon carrier frequencies should be at least 3 kHz in order to minimise inter-channel interference between adjacent channels in the GEOSAR system and ensure that adjacent channels can be considered as independent in terms of the GEOSAR system capacity. As the channels are independent, the total GEOSAR system capacity is the sum of the capacity of individual channels open for beacon operation.

4.3.2 Bandwidth Requirements for the LEOSAR System

The analysis of the LEOSAR system capacity shows that, due to a Doppler spreading of about +/- 9 kHz, frequency channels separated by 3 kHz are not independent in the LEOSAR system. Furthermore, the analysis provided at Annex C to this document, shows that a single channel has considerable capacity, but because of mutual interference between channels, three adjacent channels have less capacity than a single channel, and five adjacent channels have less capacity than three channels. This paradox is the result

of the increase in the probability of frequency collision for beacon bursts received with small Doppler shifts.

If required, a capacity increase can only be achieved by opening new channels separated from existing channels by at least 9 kHz. Total independence between existing and new channels would require a separation of 18 kHz.

Figure 4.1 illustrates the LEOSAR capacity (number of active beacons in the satellite visibility area) achieved when various channels or groups of channels are open for use, with channel A corresponding to 406.022 MHz (reserved for System beacons), and channel S corresponding to 406.079 MHz (channel 19). The capacity figure for a group of channels is plotted with reference to the highest channel in the group, e.g. the capacity corresponding to channels ABC+FG+JK is plotted as channel K (i.e. 11).

Figure 4.1: LEOSAR Capacity and Bandwidth Requirements

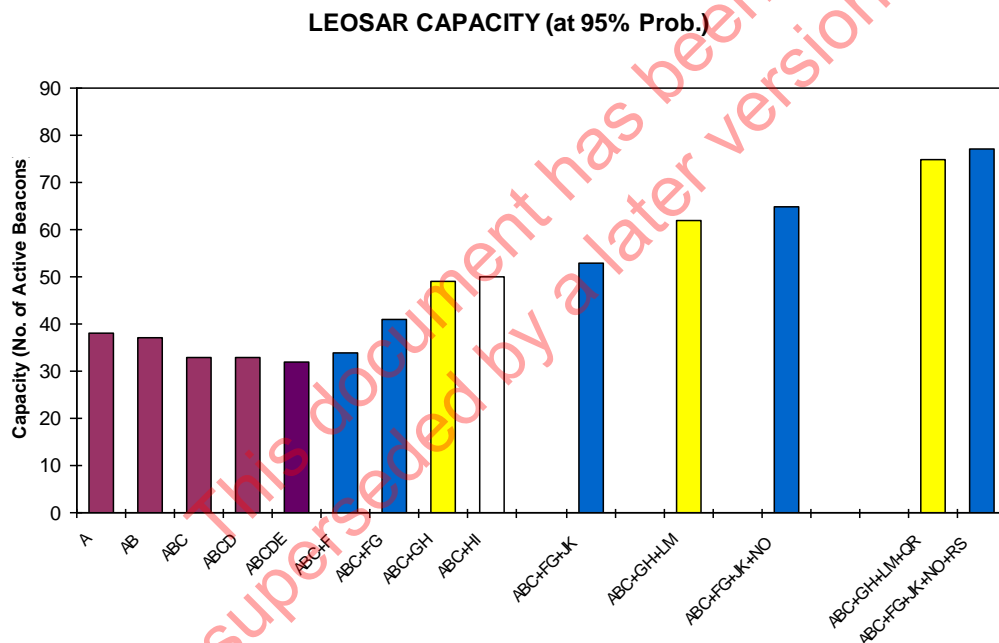


Figure 4.1 shows that:

- opening new channels adjacent to the three channels already in use (ABC) does not increase the LEOSAR capacity;
- the best result is achieved with pairs of adjacent channels separated by 12 kHz (i.e. ABC+G or ABC+GH); and
- a similar result is achieved with a separation of 9 kHz between pairs of channels (i.e. ABC+FG+JK+ etc.), but with less efficiency from a LEOSAR perspective as more channels need to be opened for the same end result.

The computed LEOSAR capacities illustrated in Figure 4.1, expressed as a number of active beacons in the satellite visibility circle, are provided in Table 4.1 below.

Note that the case of single additional channels (e.g., ABC+F, or ABC+G) has also been considered but would not provide for sufficient GEOSAR capacity (see section 4.3.3).

4.3.3 Optimum Channel Assignment Strategy

The capacity of a single independent channel in the LEOSAR system is considerably higher than the capacity of a single independent channel in the GEOSAR system. However, because of cross channel interference in the LEOSAR system, the LEOSAR system capacity does not increase linearly with the number of channels, while the capacity of the GEOSAR system does increase linearly with the number of channels opened for use. To achieve optimum use of the frequency spectrum, the strategy for assigning new channels, or groups of channels, with the appropriate frequency separation, should ensure that the LEOSAR and GEOSAR capacities remain balanced.

Taking into account the three channels already opened for use (i.e. 406.022 MHz, 406.025 MHz and 406.028 MHz), and the fact that the channel 406.022 MHz is currently reserved for System beacons (orbitography and reference beacons), Table 4.1 provides a comparison of the LEOSAR and GEOSAR capacities achieved under various channel assignment schemes. As the beacon message traffic models are different for the LEO and the GEO systems, the equivalent numbers of active beacons that correspond to the capacity of the LEOSAR and the GEOSAR systems cannot be compared directly. Therefore, for the purpose of this comparison, the capacity is expressed as the worldwide population of operational beacons that can be accommodated while maintaining adequate system performance.

From the above remark, it should be noted that the capacity, expressed as the worldwide beacon population that can be accommodated by the System, may vary with the model of beacon message traffic, while the capacity expressed as a number of active beacons in the satellite visibility area is only dependent upon the system performance and will remain constant, unless the system performance is enhanced/degraded.

Columns 1 to 3 of Table 4.1 identify the various channels and column 4 (Channels in Use) illustrates possible combinations of channels for a variety of assignment strategies.

Columns 5 (LEO Capa) and 7 (GEO Capa) provide the respective capacity of the LEOSAR and GEOSAR systems expressed as the number of active beacons in a satellite visibility area that can be processed with the required level of system performance, and computed using the capacity models provided at Annexes C and D. Note that the GEOSAR capacity is 0 for 406.022 MHz as this channel is reserved for System beacons. The LEOSAR capacity for 406.022 MHz is provided as illustration of a single independent LEOSAR channel capacity.

Columns 6 (LEO Channels) and 8 (GEO Channels) provide the LEO and GEO systems' capacity figures expressed in terms of the worldwide beacon population assessed in accordance with the 406 MHz beacon message traffic models detailed at Annex G.

Table 4.1: Comparison of LEO/GEO Capacity for Various Channel Assignment Strategies

	Channels	MHz	Channels in Use	LEO Capa	LEO-Channels	GEO Capa	GEO-Channels
1	1 - A	406.022	A	38	3,279,122	0	0
2	2 - B	406.025	AB	37	3,179,755	14	1,384,630
3	3 - C	406.028	ABC	33	2,782,285	28	3,146,886
4	4 - D	406.031	ABCD	33	2,782,285	42	4,909,142
5	5 - E	406.034	ABCDE	32	2,682,918	56	6,671,398
6	6 - F	406.037	ABC+F	34	2,881,653	42	4,909,142
7	7 - G	406.040	ABC+FG	41	3,577,224	56	6,671,398
8	8 - H	406.043	ABC+GH	49	4,372,163	56	6,671,398
9	9 - I	406.046	ABC+HI	50	4,471,530	56	6,671,398
10	10 - J	406.049					
11	11 - K	406.052	ABC+FG+JK	53	4,769,632	84	10,195,910
12	12 - L	406.055					
13	13 - M	406.058	ABC+GH+LM	62	5,663,938	84	10,195,910
14	14 - N	406.061					
15	15 - O	406.064	ABC+FG+JK+NO	65	5,962,040	112	13,720,422
16	16 - P	406.067					
17	17 - Q	406.070					
18	18 - R	406.073	ABC+GH+LM+QR	75	6,955,714	112	13,720,422
19	19 - S	406.076	ABC+FG+JK+NO+RS	77	7,154,448	140	17,244,934

Note: The worldwide beacon populations (LEO-Channels, GEO Channels) are computed on the basis of the 2023 LEO and GEO traffic models.

Table 4.1 shows that, with Channel A reserved for System beacons, the GEOSAR system would limit the capacity of the group of channels (ABC) to about 3.1 million. If channels D and E are used, the GEOSAR capacity would increase to about 6.7 million, but the LEOSAR capacity would not increase with these channel assignments.

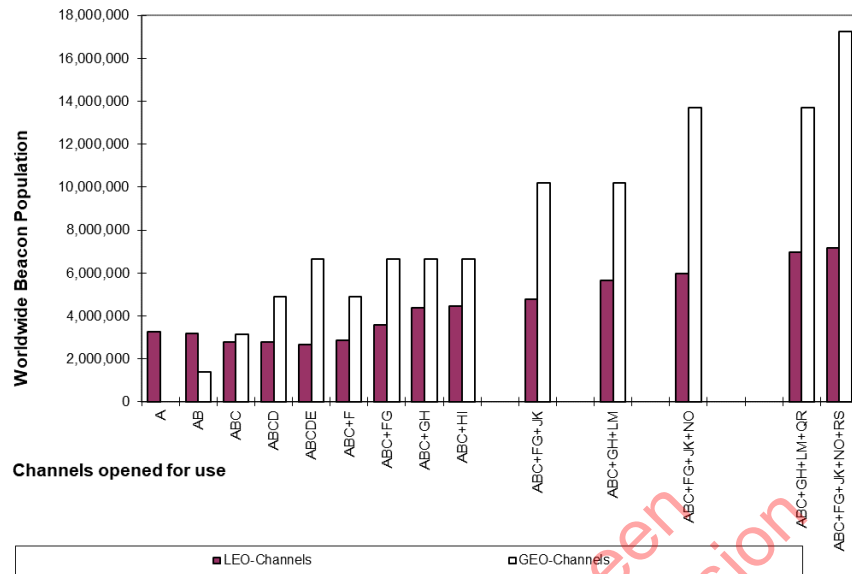
Therefore, a better strategy would be to open channels F and G (or G and H), which would significantly increase the LEOSAR capacity to 3.6 (or 4.3) million and allow for growth. Based on the 2023 LEO and GEO traffic models, the optimum assignment would be channels ABC+HI, which would provide a capacity of about 4.5 and 6.7 million for LEO and GEO systems.

Figure 4.2 illustrates the LEOSAR and GEOSAR capacities given in Table 4.1, and in particular two possible assignment schemes:

- a) the channels ABC plus additional groups of two adjacent channels separated by 9 kHz (e.g., ABC+FG+JK+NO+RS); and
- b) the channels ABC plus additional groups of two adjacent channels separated by 12 kHz (e.g., ABC+GH+LM+QR).

Note that the worldwide beacon population figures given in Figure 4.2 are derived from the capacity expressed as the equivalent number of beacons simultaneously active in the field of view of a satellite. These population figures are therefore dependent on the traffic model used and are significantly different from those obtained in 2002, when document C/S T.012 was first issued, which were more conservative. It should also be noted that these population figures assume that each available channel accommodates the maximum population allowed (i.e., matching the capacity).

Figure 4.2: Comparison of Channel Assignment Strategies for Combined LEO/GEO Operation



Note: Worldwide beacon population is based on 2023 LEO and GEO traffic models.

From Figure 4.2 and Table 4.1 it can be seen that:

- a separation of 12 kHz between channel pairs (ABC+GH+LM+QR) is more “efficient” from a LEOSAR perspective, as it provides the required capacity with the minimum spectrum occupancy; and
- a separation of 9 kHz between channel pairs (ABC+FG+JK+NO+RS) provides the maximum capacity within the 19 available channels (7.8 million) and maintains a reasonable match between the LEOSAR and the GEOSAR capacities.

On the basis of the traffic model available in 2002 which showed more balanced LEO and GEO capacities using the 9 kHz separation, Cospas-Sarsat has selected a channel assignment strategy which calls for the opening, when required by the expected growth of the beacon population, of pairs of adjacent channels separated by 9 kHz from the previous pair (i.e., alternating pairs of empty channels and pairs of channels open for use).

This channel assignment strategy is illustrated in the Channel Assignment Plan provided at Annex H to this document.

4.4 Cospas-Sarsat System 406 MHz Frequency Protection Requirements

Even though not all channels have been made available for use, the 406 MHz Cospas-Sarsat satellite payloads in orbit are relaying/processing transmissions in the complete 406.0 - 406.1 MHz frequency band. Therefore, any energy radiated in that band may have an impact on both the LEOSAR and GEOSAR system capacity. In particular, interference in the frequency band can severely affect the capability of the system to detect and process 406 MHz distress beacon transmissions.

For the reasons outlined above:

- any party planning to make use of non-assigned channels, or of channels assigned for use in future by Cospas-Sarsat 406 MHz beacons, should undertake appropriate co-ordination with Cospas-Sarsat, in accordance with the applicable ITU co-ordination procedures; and
- out-of-band transmissions should not generate a spectral power flux density in the 406.0 - 406.1 MHz band, as received by the Cospas-Sarsat satellites, in excess of the levels shown in ITU Recommendation ITU-R M.1478 (protection requirements for the Cospas-Sarsat SARP instruments).

- END OF SECTION 4 -

This document has been superseded by a later version

5. PROCEDURES FOR THE ASSIGNMENT OF 406 MHz CHANNELS

The 406.0 to 406.1 MHz available spectrum is divided into 3 kHz channels which are assigned for use as required, taking into account the following factors:

- a. the bandwidth of Cospas-Sarsat LEOSAR space segment instruments and the induced Doppler frequency shift on 406 MHz beacon transmissions;
- b. the bandwidth of Cospas-Sarsat GEOSAR space segment equipment;
- c. the total capacity requirements, current and forecast, as a function of the existing and forecast beacon population;
- d. the existing and forecast traffic loads in each active channel; and
- e. particular circumstances which may affect the capacity of specific channels.

The following sections describe the constraints imposed by LEOSAR and GEOSAR space segment instruments, the Cospas-Sarsat procedure applied for determining the need for new frequency channels, and the methods available to Cospas-Sarsat for managing capacity requirements.

5.1 Description of LEOSAR and GEOSAR Satellite Constraints

5.1.1 Bandwidth of LEOSAR Space Segment Instruments

As described in Cospas-Sarsat System document C/S T.003, entitled “Description of the Payloads Used in the Cospas-Sarsat LEOSAR System”, the future generations of SARP instruments will be able to receive signals in the band 406.01 - 406.09 MHz. Therefore, taking into account a maximum Doppler shift of about ± 9 kHz caused by the relative velocity between the satellite and the beacon, plus a 1 kHz margin at the edge to provide for some spreading of the beacon carrier frequency around the central frequency of a channel, the channel assignment plan should not include operational channels below 406.02 MHz (406.01 MHz + 10 kHz) or above 406.08 MHz (406.09 MHz - 10 kHz) to ensure compatibility with the second generation (SARP-2) instruments of the LEOSAR system.

5.1.2 Bandwidth of GEOSAR Space Segment Instruments

The bandwidth of GEOSAR satellite payloads is described in Cospas-Sarsat System document C/S T.011, entitled “Description of 406 MHz Payloads Used in the Cospas-Sarsat GEOSAR System”. Since, for management purposes, the bandwidth constraints imposed by GEOSAR space segment instruments need not include additional overhead to accommodate Doppler shift, the entire bandwidth covered by GEOSAR satellites (406.01 - 406.09 MHz) would be suitable for GEOSAR use.

5.2 Principles of 406 MHz Channel Assignment

The objective of the Cospas-Sarsat 406 MHz channel assignment process is to ensure that the number of 406 MHz beacons operating in a given channel does not generate a peak traffic load in excess of the channel capacity. To achieve this, the actual number of beacons produced for operation in each channel must be monitored, and its growth must be forecast to allow for decisions to be taken with sufficient advance notice.

However, Cospas-Sarsat does not have direct control of the production of 406 MHz beacons in each frequency channel, or of their sale. Cospas-Sarsat can only influence the production of beacons through the Cospas-Sarsat 406 MHz beacon type approval process, and by working closely with Administrations and international organizations which mandate or provide specification requirements for 406 MHz beacons.

5.2.1 Assignment of Frequency Channels for Type Approval of New Beacon Models

To ensure that 406 MHz beacons are compatible with Cospas-Sarsat satellite instruments and ground processing equipment, and do not adversely impact on the System performance, Cospas-Sarsat has established specific technical requirements and testing procedures for 406 MHz beacons. The technical requirements are described in the document “Specification for Cospas-Sarsat 406 MHz Distress Beacons” (C/S T.001) and the testing procedures are defined in the document “Cospas-Sarsat 406 MHz Distress Beacon Type Approval Standard” (C/S T.007). Upon successful completion of the testing of a beacon model in accordance with the requirements of C/S T.001 and C/S T.007, a Cospas-Sarsat type approval certificate is issued by the Cospas-Sarsat Secretariat to the manufacturer.

Cospas-Sarsat Participants, and the majority of Administrations from other countries, require that manufacturers obtain a Cospas-Sarsat type approval certificate before authorising the use and registration of 406 MHz beacon models in accordance with their national legislation and/or regulations.

Therefore, through the Cospas-Sarsat type approval procedure, Cospas-Sarsat can influence the production of new beacon models in a particular frequency channel by imposing that, from a given date, new models submitted for Cospas-Sarsat type approval operate in specific frequency channels. However, Cospas-Sarsat has no mandate to control the actual production of beacons and, once issued, the Cospas-Sarsat type approval certificate remains valid with no time-limit, unless the produced beacons of the type cease to meet the specified performance requirements. The production of type approved beacon models can continue for as long as the manufacturer decides, i.e., many years after the frequency channel has been closed for use by new beacon models.

As a consequence, Cospas-Sarsat must consider the need to open new frequency channels on the basis of production forecast, well before the active channels approach their capacity limit. This advance notice is also required by manufacturers who must plan in advance the design and production of new beacon models, as well as regulatory Administrations that may have to adapt the applicable regulation/licensing requirements.

In view of the above constraints, Cospas-Sarsat has agreed to:

- a. decide on opening new frequency channels for type approval of new beacon models with a minimum three year advance notice; and
- b. adopt type approval testing procedures which allow a particular beacon model to be tested and type approved for a range of frequency channels, provided that the manufacturer accepts the commitment to cease the production of the beacon model in frequency channels closed for type approval, and to transition its production to other channels open for type approval, as provided in the Cospas-Sarsat 406 MHz Channel Assignment Table (see Annex H).

5.2.2 Transition of Type Approved Beacon Models to New Frequency Channels

Because beacon models type approved for operation in a single channel can continue to be produced after the frequency channel has been closed for type approval of new models, the population of beacons in a particular channel could eventually grow beyond the capacity limit for that channel. Therefore, it may be necessary for Cospas-Sarsat to encourage the transition of production of these beacon models to other channels.

To facilitate such transition, Cospas-Sarsat has adopted streamlined retesting requirements for beacon models already type approved, to permit their operation in new frequency channels. However, Cospas-Sarsat relies on co-ordination with Administrations to enforce the transition on a national basis and may take measures, in coordination with beacon manufacturers and using C/S T.007 certification procedures, to transition beacon production, should the termination of production in a designated channel become an urgent requirement to ensure adequate System performance.

5.3 Procedure for Deciding on New Channel Assignments

As Cospas-Sarsat cannot directly control the actual number of beacons operating in a given 406 MHz channel, it is not possible to wait until a channel is at full capacity before requiring new beacon models to be type approved to operate in a different frequency channel. Instead, the schedule for closing channels for type approval of new beacon models must take into account the long-term production estimate of all type approved beacons designed to operate in the 406 MHz channel under consideration. Furthermore, since beacon model production rates are difficult to estimate, it is necessary to develop a schedule for opening and closing channels that provides for a reasonable channel capacity margin.

Taking into account the various factors which could affect beacon population growth, a channel should be closed for the type approval of new beacon models at the date when the forecast channel load would reach 75% of the nominal channel capacity.

To assist Council decisions and provide adequate advance notice to manufacturers and Administrations of the opening and closing of frequency channels for type approval of new beacon models, a ten-year frequency channel assignment plan has been developed on the basis of the forecast growth of the 406 MHz beacon population. The plan will be reviewed on an

annual basis to ensure consistency with the actual evolution of the beacon population. The annual review of the plan will also need to consider:

- a. the actual and forecast evolution of the beacon population and 406 MHz traffic in all channels open for the production of type approved beacons; and
- b. the actual and forecast growth of the beacon population and 406 MHz traffic in channels open for type approval of new beacon models.

As wide variations of the production of particular beacon models can significantly affect the forecast channel traffic, appropriate adjustments of the planned dates for opening new channels for type approval might be required. Co-ordination with Administrations and manufacturers will be undertaken if it becomes necessary to consider a transition of the production of type approved models into new channels.

- END OF SECTION 5 -

*This document has been
superseded by a later version*

**ANNEXES
TO THE COSPAS-SARSAT
406 MHz FREQUENCY
MANAGEMENT PLAN**

*This document has been
superseded by a later version*

This document has been
superseded by a later version

ANNEX A

LIST OF ABBREVIATIONS AND ACRONYMS

COSPAS	COsmicheskaya Sistema Poiska Avarinykh Sudov (Satellite System for the Search of Vessels in Distress)
CTA	Cross-track angle
C/S	Cospas-Sarsat
DRU	Data Recovery Unit of the SARP instrument
EIRP	Equivalent Isotropically Radiated Power
ELT	Emergency Locator Transmitter
EPIRB	Emergency Position Indicating Radio Beacon
GEO	Geostationary Earth Orbit
GEOLUT	Local User Terminal (LUT) in the GEOSAR System
GEOSAR	Geostationary Satellite System for Search and Rescue
ITU	International Telecommunication Union
ITU-R	ITU Radiocommunication Sector
kHz	Kilohertz
LUT	Local User Terminal
LEO	Low-altitude Earth Orbit
LEOLUT	LUT in the LEOSAR system
LEOSAR	Low-altitude Earth Orbit System for Search and Rescue
MHz	Megahertz
MCC	Mission Control Centre
N/A	not applicable
NOCR	Notification of country of beacon registration message
PLB	Personal Locator Beacon
PSK	Phase-shift keying (modulation)
SAR	Search And Rescue
SARP	Search And Rescue Processor
SARR	Search And Rescue Repeater
SARSAT	Search And Rescue Satellite Aided Tracking
SPOC	SAR point of contact

TCA	Time of closest approach
WRC	World Radiocommunication Conference (ITU)

- END OF ANNEX A -

*This document has been
superseded by a later version*

ANNEX B

NOMINAL CONDITIONS APPLICABLE FOR SARP, SARR AND GEOSAR CAPACITY DEFINITIONS AND TESTING

B.1 GENERAL

The capacity of Cospas-Sarsat 406 MHz channels are affected by many factors, such as the performance and technical characteristics of the beacon, satellite performance, the presence of interferers in the channel, and the performance of the ground processing equipment. Although these factors must be defined and quantified for the definition of Cospas-Sarsat capacity to be technically complete and for conducting capacity testing and analysis, the detailed values for these parameters are not required for a general understanding of capacity. In view of this, all such factors have been grouped together and are collectively referred to as “nominal conditions”. The nominal conditions applicable for each Cospas-Sarsat system (i.e., GEOSAR, LEOSAR SARP and LEOSAR SARR) are described below.

B.2 NOMINAL CONDITIONS FOR LEOSAR SARP AND SARR SYSTEMS

- a. Ambient Conditions. There are no significant sources of interference operating in the LEOSAR satellite uplink or downlink bands.
- b. 406 MHz Beacon Performance. The 406 MHz distress beacons satisfy the requirements of Cospas-Sarsat document C/S T.001 (beacon specification).
- c. Beacon Transmit Frequency. The beacon transmit frequencies in each channel follow a Gaussian distribution, with a mean value equal to the channel centre frequency and a standard deviation of 300 Hz.
- d. Beacon Message Processing. The beacon event is considered to have been successfully processed if the LEOLUT produces a valid* message. The nominal condition for achieving successful message processing is a beacon to satellite elevation angle of at least 5° .
- e. Doppler Processing. The Doppler processing is considered to have been successful if the Doppler solution is accurate to within 20 km. For the purpose of capacity computation and testing, the probability of successful Doppler processing should be achieved for all beacon events characterised by a cross-track angle less than, or equal to 22° (this allows for the possible reception of at least five beacon messages with an elevation angle $\geq 5^{\circ}$).

* The definition of a valid beacon message is provided in the Cospas-Sarsat LEOLUT Performance Specification and Design Guidelines (document C/S T.002).

- f. Coverage Area. In respect of beacon message processing and Doppler processing (see d. and e. above), a beacon is considered to be in the coverage area of the SARP / SARR channel if:
- (i) SARP. The beacon to satellite elevation angle at TCA is equal to or greater than 6.2° (this allows for the possible reception of at least 4 bursts with an elevation angle to the LEOSAR satellite of at least 5°).
 - (ii) SARR. The beacon to satellite elevation angle at TCA is equal to or greater than 6.2° and a LEOLUT was also in the field of view of the satellite during this period of time.

However, for the purpose of evaluating the beacon message traffic, and for the purpose of assessing the probability of burst collisions, a coverage area at 0° elevation angle will be considered.

- g. Satellite Performance. The Cospas-Sarsat LEOSAR satellite conforms to the description of document C/S T.003 (Description of the Payloads Used in the Cospas-Sarsat LEOSAR System).
- h. LEOLUT Performance. The LEOLUT satisfies the requirements detailed in the document, "Cospas-Sarsat LEOLUT Performance Specification and Design Guidelines" (C/S T.002).
- i. Relationship Between Beacon Population and 406 MHz Channels. When assessing the maximum LEOSAR system capacity, the beacons in the field of view of the satellite are assumed to be spread equally amongst the 406 MHz channels specified by Cospas-Sarsat. However, the assessment of the capacity of individual frequency channels (or group of channels) should also be performed for non-even distributions of the population among the available frequency channels.
- j. Distribution of Beacon Transmissions in Time. Beacon activations occur randomly in time, and the repetition period of beacon transmissions satisfies the C/S T.001 requirement, i.e., $50 \text{ seconds} \pm 5 \%$.
- k. Geographical Distribution of Beacons. The active beacons are evenly distributed throughout the field of view of the satellite.
- l. SARP Memory Limitation. There are no SARP memory limitations that affect the capacity.
- m. Distribution of Short and Long Format Messages. Unless otherwise specified, the capacity figures assume that all beacons transmit short format messages.

B.3 NOMINAL CONDITIONS FOR GEOSAR SYSTEMS

- a. Ambient Conditions. There are no significant sources of interference operating in the GEOSAR satellite uplink or downlink bands.
- b. 406 MHz Beacon Performance. The 406 MHz distress beacons satisfy the requirements of Cospas-Sarsat document C/S T.001 (beacon specification), and the beacons' EIRP in the direction of the satellite is greater than or equal to [32 dBm].
- c. Beacon Transmit Frequency. The beacon transmit frequencies in each channel follow a Gaussian distribution, with a mean value equal to the channel centre frequency and a standard deviation of 300 Hz.
- d. Beacon Message Processing. Beacons are considered to have been successfully processed if the GEOLUT produces a valid* message.
- e. Coverage Area. Beacons are considered to be in the coverage area of a GEOSAR satellite if the beacon to satellite elevation angle is equal to or greater than 4°, and there are no obstructions shielding the beacon from the satellite.
- f. Satellite Performance. The Cospas-Sarsat GEOSAR satellite conforms to the description of document C/S T.011 (Description of the 406 MHz Payloads Used in the Cospas-Sarsat GEOSAR System).
- g. GEOLUT Performance. The GEOLUT satisfies the requirements detailed in the document, "Cospas-Sarsat GEOLUT Performance Specification and Design Guidelines" (C/S T.009).
- h. Relationship Between Beacon Population and 406 MHz Channels. When assessing the GEOSAR system capacity, the beacons in the field of view of the satellite are assumed to be spread equally amongst the 406 MHz channels specified by Cospas-Sarsat.
- i. Distribution of Beacon Transmissions in Time. Beacon activations occur randomly in time, and the repetition period of beacon transmissions satisfies the C/S T.001 requirement, i.e., 50 seconds \pm 5 %.
- j. Geographical Distribution of Beacons. The active beacons are evenly distributed throughout the field of view of the satellite.
- k. Distribution of Short and Long Format Messages. Unless otherwise specified, the capacity figures assume that all beacons transmit long format messages.

- END OF ANNEX B -

* The definition of a valid beacon message is provided in the Cospas-Sarsat GEOLUT Performance Specification and Design Guidelines (document C/S T.009).

ANNEX C

LEOSAR CAPACITY MODEL

C.1 INTRODUCTION

The capacity of the Cospas-Sarsat 406 MHz LEOSAR system is defined as follows (see also C/S T.012, section 2):

“The number of 406 MHz distress beacons operating simultaneously in the field of view of the LEOSAR satellite that can be successfully processed by the SARP or the SARR channel to provide beacon message and Doppler location information, under nominal conditions, 95% of the time.”

Although the nominal capacity is defined for a single probability of success (i.e., 95%), the numerical results of the analysis are provided for two values of the probability of successful processing (i.e., 95% and 98%).

A conservative approach has been systematically taken for the development of the LEOSAR capacity model. In particular, the selected capacity figures correspond to the worst-case scenario, where the probability of successful Doppler processing is achieved for a beacon transmitting at the edge of the satellite visibility area (i.e., with a cross-track angle (CTA) of 22° , corresponding to a short duration pass of the satellite in visibility of the beacon, which allows for the recovery of only 5 beacon bursts). In all other circumstances, characterised by lower CTAs (i.e., longer duration passes), the probability of successful Doppler processing for a traffic load corresponding to the nominal capacity would be significantly higher than the 95% required by the definition. This is illustrated at Appendix C of this Annex, which provides the probability of successful Doppler processing for a given number of beacons in the satellite visibility area, and for various pass durations (i.e., with an increasing number of bursts that can be received during a satellite pass). This is also confirmed by simulations reported at Appendix D, which characterise an “average” probability of success, with no constraints on the CTA of the beacon.

Similarly, we have assumed that two beacon messages (or bursts) that collide in time and frequency are both lost as a result of such collision. This is not always the case and the burst of higher power is frequently correctly recovered, while the burst of lower power is lost (see also the simulations reported at Appendix D to Annex C).

The conservative approach compensates for some of the hypotheses made in developing the capacity model, such as the uniform distribution of beacons in the satellite visibility area and amongst the available frequency channels. These ideal conditions are rarely satisfied in real-world situations. However, to avoid an overly conservative assessment of the LEOSAR capacity, the nominal capacity figure is determined on the basis of a population of beacons that transmit the short message format, instead of a population of beacons transmitting the long message format. This matter is further discussed in section C.3.7.

The results of the capacity computations provided in Table C.1 indicate a single channel capacity of 21 beacons in the satellite visibility area at 98% probability and 38 beacons at 95% probability. These capacity computations correspond to the scenario of a satellite pass with a CTA of 22° .

Appendix C to this Annex shows that 100 beacons in the satellite visibility area can be successfully processed with 96% probability for all CTAs $\leq 20^{\circ}$, and with a 98% probability for all CTAs $\leq 19^{\circ}$.

Similarly, Appendix D to Annex C shows that a capacity computed on an “average” probability of success (i.e., with no constraint on the beacon CTA) would be considerably higher than the determination presented in this Annex.

Despite the conservative approach of the capacity model, the LEOSAR system still retains a large capacity in terms of the maximum beacon population that can be accommodated worldwide.

However, the capacity model also shows that decisions concerning the spreading of beacon carrier frequencies, primarily required for ensuring adequate capacity in the GEOSAR system, should take into account some specific characteristics of the LEOSAR system, in particular the fact that adjacent channels are not independent. This characteristic of the LEOSAR system has a direct bearing on the selection of the strategy to be used for spreading the beacon carrier frequencies within the 406.0 - 406.1 MHz frequency band, as shown in section 4.3 of document C/S T.012.

*This document has been
superseded by a later version*

C.2 BASIC LEOSAR SYSTEM CHARACTERISTICS

C.2.1 Random Access with Time and Frequency Diversity

Beacon transmission times are not synchronised and beacon message (also referred to as beacon burst in the capacity analysis) arrival times at the satellite receiver antenna are random. Therefore, bursts from different beacons may overlap in time.

The carrier frequency of a 406 MHz beacon is assigned to particular frequency channels in accordance with the frequency Management Plan (e.g., 406.025 MHz for the first generation beacons). Within a channel, the beacon carrier frequencies are distributed around the specified centre frequency of the channel, due to variations in oscillator frequencies, aging, temperature, etc. In addition, the frequency of the bursts received by the satellite is affected by a variable Doppler shift, which is a function of the satellite speed relative to the beacon. Therefore, at the satellite, 406 MHz bursts may overlap in both time and frequency and interfere with each other.

The probability of mutual interference between beacon bursts will increase with the number of active beacons in visibility of the satellite. This, in turn, determines the probability of successfully recovering a valid message and producing a Doppler location, as defined in the LEOLUT specification and design guidelines (C/S T.002).

Figure C.1: Beacon Burst Collisions in Time and Frequency

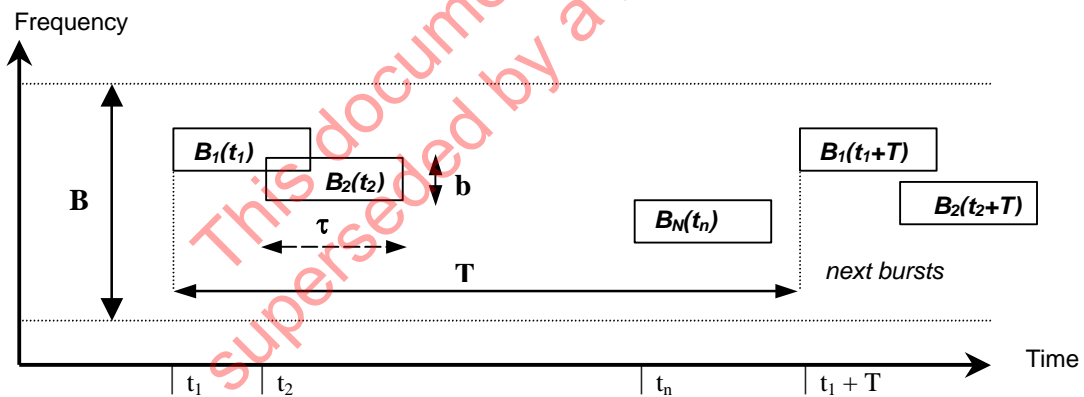


Figure C.1 illustrates a collision in the time and frequency domains of two beacon bursts $B_1(t_1)$ and $B_2(t_2)$, each of duration ' τ ' and occupying a frequency bandwidth ' b '. Assuming a different Doppler shift after the beacon repetition period T , the frequency overlap may disappear at $(t+T)$. As the message repetition period of beacons B_1 and B_2 may also be slightly different, a collision in time may not necessarily repeat itself in successive transmissions. However, for the purpose of the capacity analysis, only one repetition period should be considered, with random burst arrival times.

Data bits in the message transmitted by Cospas-Sarsat 406 MHz beacons are directly modulated on the carrier frequency using a narrow band PSK modulation. Any overlap in time and frequency between two beacon messages with an equivalent signal power typically results in the loss of both messages. If the overlapping messages are of distinctly different power, then some form of power capture may come into play and the stronger beacon message may be received correctly while the weaker message is lost (see Appendix D to Annex C).

In accordance with a prudent approach to the evaluation of the LEOSAR system capacity, the analysis performed in section C.3 assumes that, if two beacon bursts overlap in time and frequency, they are both destroyed by this collision. However, as discussed in section C.3, we will apply this constraint to short messages, instead of long format messages.

C.2.2 Single Frequency Channel Capacity and Total LEOSAR System Capacity

Cospas-Sarsat has determined that the optimum separation of frequency channels in the GEOSAR system was 3 kHz. Channels with this frequency separation can be considered as independent in the GEOSAR system capacity analysis, and the GEOSAR capacity increases as a linear function of the number of channels (see Annex D).

For the LEOSAR capacity analysis, Cospas-Sarsat has also determined that, due to the frequency diversity generated by the variable Doppler shifts of beacon carrier frequencies, and the relatively small visibility area of LEOSAR satellites (in comparison with the visibility area of GEOSAR satellites), the LEOSAR system has a much higher single channel capacity than the GEOSAR system. However, because of a maximum frequency shift of about 9 kHz, frequency channels separated by 3 kHz are not independent in the LEOSAR system (i.e., beacon bursts from a beacon in a given frequency channel can collide in time and frequency with bursts from beacons in other frequency channels).

Therefore, the LEOSAR capacity does not increase as a linear function of the number of 3 kHz channels.

An analysis is provided in section C.3 for a single frequency channel in the LEOSAR system, and for the total LEOSAR system capacity when all frequency channels are occupied and the total beacon population is evenly distributed amongst all available frequency channels. In this last configuration, all channels are assumed to be identical and the total system capacity can be assumed to be evenly distributed among all frequency channels. The individual channel capacity is then the total system capacity divided by the number of channels, but it should be noted that this individual channel capacity is less than the single frequency channel capacity previously considered.

C.2.3 SARP and SARR Processing Channels

Two different processing channels are indicated in the definition of the LEOSAR capacity: the Search and Rescue Processor (SARP) channel and the Search and Rescue Repeater (SARR) channel.

406 MHz beacon messages received through the Search and Rescue Processor (SARP) channel are processed on board the satellite to retrieve the message data and generate, for each beacon message, a time-tagged frequency measurement. This data is stored on board the spacecraft and continuously broadcast for transmission to a LEOLUT. The LEOLUT processes the data to compute a Doppler position and generates a distress message for distribution to SAR services. The SARP channel, which includes a satellite memory unit, provides the system global coverage as simultaneous satellite visibility of a LEOLUT and a beacon is not required to receive the beacon messages.

406 MHz beacon messages received through the Search and Rescue Repeater (SARR) channel are only repeated by the satellite SARR instrument, and all processing is performed in the

LEOLUT (i.e., data recovery, timing, frequency shift measurement and Doppler location computation).

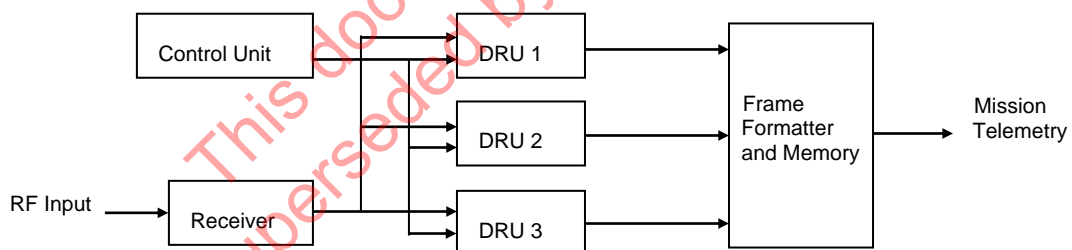
There are two physical limitations that impact on the SARP channel capacity, but not on the SARR channel capacity:

- a) the number of on board processing units in the SARP instrument; and
- b) the size of the SARP memory unit, which limits the volume of processed messages that can be stored.

In the SARP channel, a beacon message arriving at the satellite 406 MHz receiver is assigned in real-time to a specific processing unit of the SARP instrument (see Figure C.2). This SARP Data Recovery Unit (DRU) remains occupied for a given processing time. As 406 MHz beacon message arrival times at the satellite receiver are random within a repetition period (i.e. the beacon transmission times are not synchronised), some bursts may be lost if all DRUs are busy, even when these bursts do not interfere in the frequency domain. Therefore, the number of available DRUs in the SARP instrument directly impacts on the SARP capacity and the probability of successful access to a DRU is a significant parameter that is analysed further in section C.3.

All future SARP instruments in the Cospas-Sarsat LEOSAR system will have 3 on board DRUs, allowing for simultaneous processing of 3 beacon bursts.

Figure C.2: SARP Block Diagram



406 MHz beacon messages could also be lost after on board processing if the processed data in the satellite memory unit is replaced by newer information before its successful retransmission to a LEOLUT. This is dependent upon the number and availability of LEOLUTs in the system, the size of the SARP memory unit and the rate of arrival of new information. On the basis of the current characteristics of the SARP instrument and memory unit, and the number of LEOLUTs in the System, it is assumed that no data is lost before its transmission to a LEOLUT (there are no “blind” orbits, i.e., a LEOSAR satellite will always come into view of at least one LEOLUT during a single orbit). Therefore, the satellite memory is not the critical criteria that determines the system capacity.

In the SARR channel, similar limitations due to the LEOLUT ground processing could also exist. However, it is assumed that the LEOLUT ground processing can be adapted as necessary to meet the required traffic. Therefore, the LEOSAR capacity analysis does not take into

account specific SARR limitations, but is based on the SARP limitation to 3 Data Recovery Units.

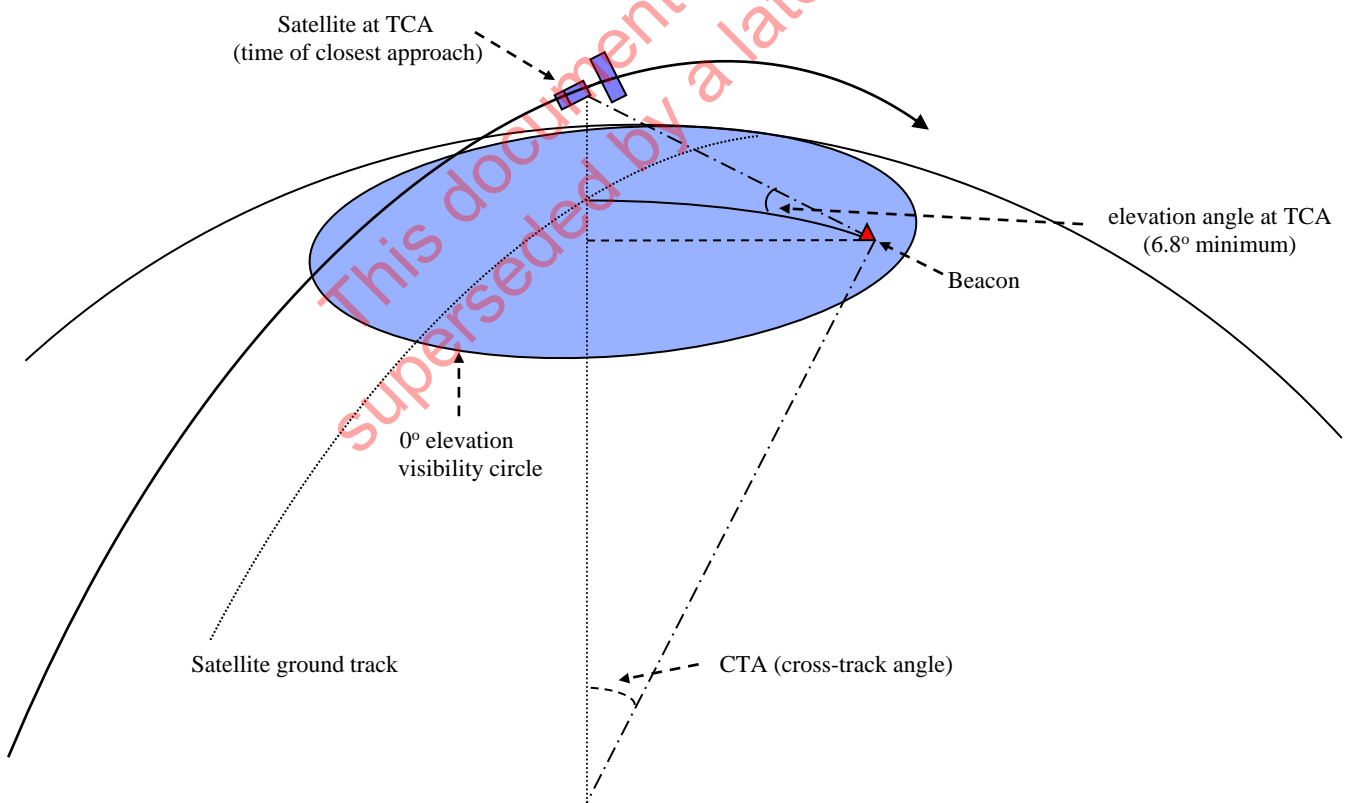
C.2.4 LEOSAR Satellites Visibility Area and Duration of Satellite Passes

406 MHz beacon messages can be detected only when a LEOSAR satellite comes into visibility of the transmitting beacon. The LEOSAR satellite visibility area to be considered in the capacity analysis depends on several parameters, including:

- the altitude of the satellite (for Sarsat satellites at an altitude of about 870 km, the visibility area to 0° elevation is limited to a circle of about 3,000 km radius); and
- the specified minimum beacon to satellite elevation angle (i.e., 5° elevation specified in the document C/S T.001 in respect of beacon antenna diagram);

A beacon remains visible by a satellite for a duration that is a function of the size of the satellite visibility area and the distance from the beacon to the satellite sub-track. This duration is characterised by the Cross-Track Angle, or the maximum beacon-to-satellite elevation angle that is achieved at the time of closest approach (TCA) (see Figure C.3).

Figure C.3: LEOSAR Satellite Visibility Area



Small CTAs correspond to beacons close to the track of the satellite (high maximum elevation angles), which provide long pass durations and the opportunity to receive a large number of bursts from those beacons (up to 15 minutes pass duration and 18 beacon bursts). Large CTAs

correspond to beacons far from the track of the satellite, which provide short duration passes at low elevation angles and fewer bursts received by the satellite.

The requirement for providing a Doppler location, as included in the definition of the LEOSAR capacity, leads to a requirement for a minimum pass duration that allows the reception of a sufficient number of beacon bursts to achieve the required probability of obtaining a good Doppler location. The Cospas-Sarsat document C/S T.002 (Cospas-Sarsat LEOLUT Performance Specification and Design Guidelines) calls for four (4) or more data points that bracket the time of closest approach (TCA) for providing nominal Doppler solutions. For the LEOSAR capacity analysis, we will assume that 4 frequency measurements must be available, and that the minimum duration pass should allow the reception of 5 possible beacon messages with a minimum elevation angle of 5° , which corresponds to passes with an elevation angle at TCA of at least 6.8° . However, the analysis of the probability of collisions in the frequency domain will be made with a 0° elevation angle.

In accordance with a conservative evaluation of the LEOSAR system capacity, the requirement to obtain at least 4 good data points out of 5 possible frequency measurements defines the worst case scenario to be considered in the LEOSAR capacity model. This matter is analysed in more detail in section C.3.

Note: The capacity is defined at 95% probability of good processing. The choice of an elevation angle at TCA of at least 6.8° is conservative, but does not preclude producing Doppler locations when only 3 frequency measurements are available (or 2 complemented by a beacon transmit frequency measurement in the LEO-GEO combined processing technique). However, this capability should not be taken as representing the nominal condition attached to the definition of the LEOSAR system capacity.

This document has been
superseded by a later version

C.3 LEOSAR CAPACITY ANALYSIS

C.3.1 Methodology of LEOSAR Capacity Assessment

C.3.1.1 Probability of Reception of a Single Beacon Message

Firstly, we have to determine the elementary probability for a beacon burst to be correctly received by the satellite SARP instrument. This implies that at least one of the SARP DRUs is free when the beacon burst arrives at the satellite antenna.

Note that if DRUs are free, the collision in time between two arrivals separated by a time $t \leq \tau$, does not directly affect the result of the processing of the messages, provided there is no collision in the frequency domain, i.e. the distance in frequency is greater than the input filter bandwidth “b” (when the distance $|f_1 - f_2|$ is less than, or equal to b, the arriving burst cannot be distinguished from a burst already being processed). Therefore, collisions in the frequency domain and in time will result in both messages being lost. The probability of collisions in the frequency domain and in the time domain need to be assessed prior to addressing the probability of successful recovery of a message in the DRU of the SARP instrument. These probabilities must be determined for N beacons simultaneously active in the satellite visibility area.

Finally, we will assume that a beacon message, if it has access to a free DRU and is not interfered with during its processing time in the DRU, has a probability P_{SP} of being successfully processed by that DRU (i.e. the data in the message are correctly recovered and the Doppler measurement is successful).

We note:

- P_f the probability of burst collisions in the frequency domain when active beacons are uniformly distributed in the satellite visibility area;
- P_U the probability that at least one DRU is free at the time of arrival of the beacon burst;
- P_{NA} the probability that the arriving burst does not collide in time and frequency with other arrivals;
- P_{SP} the probability of successful processing (which may be affected by various factors such as noise, etc.), assuming the arriving burst is assigned to a free DRU and is not interfered with in the frequency domain; and
- P_R the resulting probability of good reception of a beacon burst when N beacons are active in the visibility circle of the LEOSAR satellite, which is a function of the above probabilities.

P_{NA} is a function of P_f and the number of active beacons in the satellite visibility circle.

We will demonstrate in section C.3.2 that P_f varies, depending on the transmitting beacon position in the visibility circle, which is characterised by the Doppler ratio D (the ratio of the actual Doppler shift of a particular transmission to the maximum Doppler shift).

P_U is also a function of the number of active beacons in the visibility circle and of the probability of frequency collision that characterises each of the bursts previously received. However, to compute this probability using the modified Erlang-B model described at Appendix B, we will only consider the minimum value of P_f , which defines the lower limit of P_U .

Note: Although P_U is a function of the probability of frequency collisions, the state of the SARP system at the time “t” of arrival of a new burst is independent of the frequency shift that affects the arriving burst at “t”. The possible collision in time and frequency of the arriving burst with preceding or following bursts received by the SARP is only reflected in the probability P_{NA} (probability of no collisions in frequency during the time interval $[t-\tau, t+\tau]$).

As a consequence, P_R is a function of N and D , and can be expressed as follows:

$$P_R(N,D) = P_U * P_{NA} * P_{SP} \quad \text{C/E.1}$$

The computation of $P_R(N,D)$ will be performed for a single frequency channel and for the multi-channel system, when beacon carrier frequencies are spread over a number of frequency channels, each separated by 3 kHz. This will allow for the computation of a single channel LEOSAR system capacity and a multi-channel LEOSAR system capacity, which are both required for the management of the 406 MHz frequency band.

C.3.1.2 Probability of Successful Doppler Processing

We want to determine the probability of obtaining the Doppler location of a transmitting 406 MHz beacon with an elevation angle at TCA of at least 6.8° (which will be noted P_{DP}), when N beacons are active in the field of view of a LEOSAR satellite. This condition is expressed as the possibility of retrieving at least four (4) bursts out of (M) possible data points.

If each possible point was received with the same probability P_R , the probability of obtaining a Doppler location under the above condition would be the sum of the probabilities of all possible combinations of at least 4 data points out of M possible measurements during the satellite pass (M is a function of the cross-track angle (CTA)), i.e.:

$$P_{DP} = \sum_{i=m}^M C_M^i P_R^i (1 - P_R)^{M-i}; \text{ with } m = 4 \text{ and } M \text{ function of CTA.} \quad \text{C/E.2}$$

However, the computation of P_{DP} must also take into account the fact that P_R is not a fixed value during the satellite pass (see section C.3.2 and Appendix A to Annex C). Therefore, the probability P_{DP} must be computed with the values of P_R obtained for each data point that can be received during a satellite pass with a given cross-track angle (CTA), and a nominal solution (or worst case solution as appropriate) must be selected for the assessment of the LEOSAR capacity. We will demonstrate at Appendix C of Annex C that the worst-case solution corresponds to a cross track angle of 22° ($M = 5$) and use the results of the computation of P_{DP} for that particular case to derive a system capacity figure.

As the selected P_{DP} is a function of the number N of active beacons, the capacity is the value of N when $P_{DP}(N)$ reaches 95%.

C.3.2 Probability of Collision in the Frequency Domain

Two bursts collide in the frequency domain when the distance of their carrier frequency $|f_1 - f_2|$ is smaller than b , the frequency bandwidth of the input filter of the satellite DRUs.

If we assume that the beacon carrier frequencies are uniformly distributed in the available bandwidth B , and noting that b is small compared to B , then (ref TG-1/2000/3/5 and TG-1/2000/4/2):

$$P_f(|f_1 - f_2| < b) = \frac{2b}{B} \quad \text{C/E.3}$$

f_M is defined as the Doppler shift corresponding to $\varphi = 0$ and $\theta = 0$ (see Figures C.4 and C.5), i.e. along the velocity vector of the satellite:

$$f_M = f_B * V_s * \frac{1}{c} = f_B \frac{2\pi(R+h)}{T_s * c} = 10.066 \text{ kHz, with:} \quad \text{C/E.4}$$

f_B beacon carrier frequency = 406.025 MHz;

V_s satellite velocity

c speed of light = 300,000 km/s

R Earth radius = 6,378 km

h altitude of the satellite = 870 km

T_s period of the satellite orbit = 102 minutes

The maximum Doppler shift for a beacon in the satellite visibility area is achieved with the beacon at 0° elevation on the satellite track. This maximum achievable Doppler shift for the channel 406.025 MHz is:

$$f_d^0 = f_M * \cos(\theta_{\min}) = f_M * R / (R+h) = 8.858 \text{ kHz} \quad \text{C/E.5}$$

Therefore, the arriving bursts frequencies are spread over a bandwidth $B = 2 * 8,858 \text{ kHz}$.

Note: Measurements of the beacons' transmit frequency in the 406.025 MHz channel has shown little frequency spreading. Therefore, the spreading of the beacon carrier frequency is not considered further in this analysis (see Annex D on GEOSAR capacity for details on beacon carrier frequency spreading). All beacons in a frequency channel are assumed to transmit at the same frequency.

With an input filter bandwidth $b = 1.2 \text{ kHz}$, and assuming a uniform spreading of the received burst frequencies over the Doppler bandwidth B , the probability of collision P_f would be:

$$p_f \cong \frac{2b}{B} = 0.135 \quad \text{C/E.6}$$

However, the detailed analysis for beacons uniformly distributed in the field of view of the satellite shows that the Doppler spreading is not uniform (see section C.3.2.1 below and Appendix A to Annex C).

Figure C.4: Geometry of the Satellite to Beacon Line of Sight

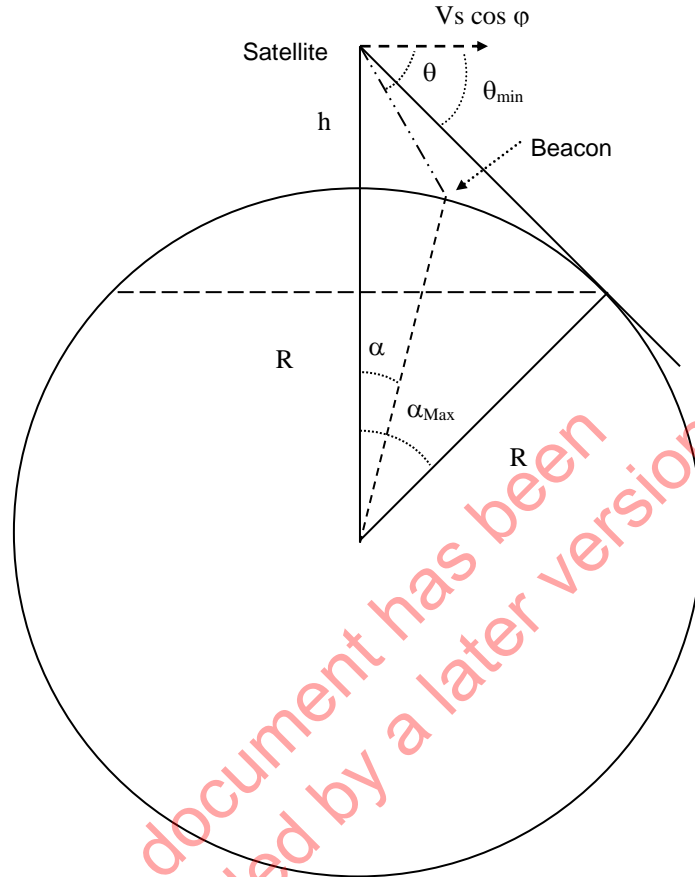
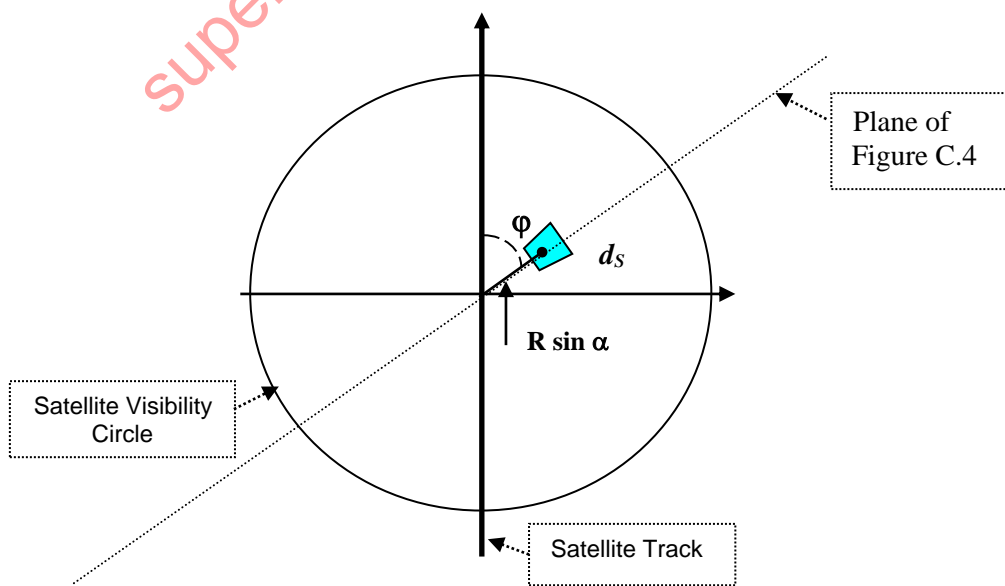


Figure C.5: Geometry of the Satellite Visibility Area



C.3.2.1 Single Channel Frequency Distribution

The frequency shift for a beacon at a position in the visibility circle defined by the angles θ and φ , (see Figures C.4 and C.5) is given by the expression:

$$f_d = f_M * \cos \theta * \cos \varphi \quad \text{C/E.7}$$

where: θ is the look-down angle to the beacon; and

φ is the azimuth of the beacon.

From equation C/E.7 above we can see that the probability of a given beacon burst being interfered with by the bursts of other beacons in the field of view of the satellite depends on the position of that particular beacon in the visibility circle. Therefore, the task is to determine, for the values of the Doppler shift of the bursts received during a particular satellite path (characterised by its CTA), which other beacons would interfere in the frequency domain, and derive a probability of frequency collision for the possible values of the Doppler shift.

The probability of collisions in the frequency domain for a specific Doppler shift f_d is expressed as a function of the Doppler ratio $D = f_d/f_M$, which depends on the position of a transmitting beacon in the satellite visibility circle, and:

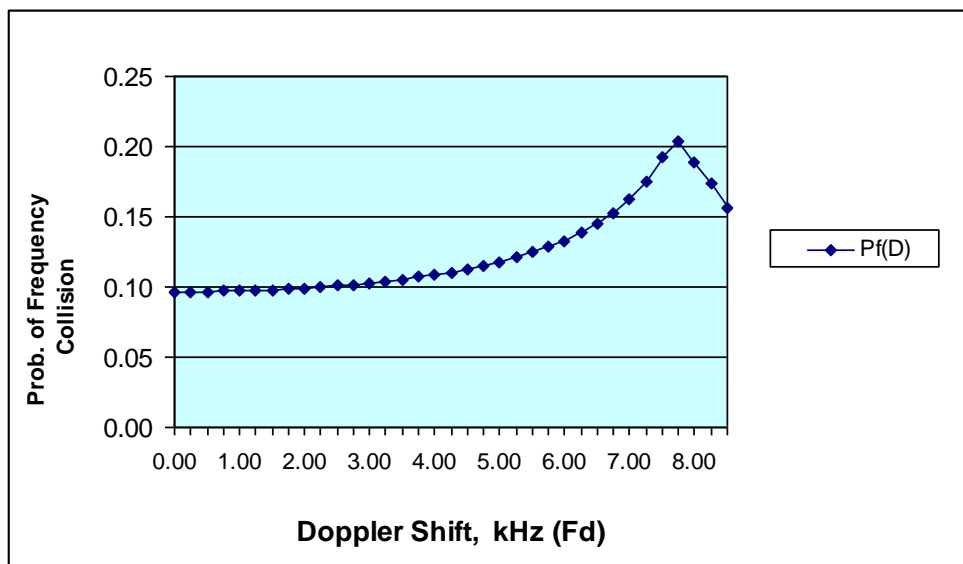
$$P_f(D) = \frac{S_D}{S} \quad \text{C/E.8}$$

where: S is the surface area of the satellite visibility circle; and

S_D is the surface area within the visibility circle where beacon transmissions will collide in frequency with the transmitting beacons that have a Doppler ratio D .

This computation is detailed at Appendix A of Annex C. The results are provided in Table C-A.1 of Appendix A to Annex C and illustrated in Figure C.6. It can be seen from Figure C.6 that the probability of collision in the frequency domain is significantly higher for large Doppler shift values than the probability determined for a uniform distribution in the Doppler bandwidth, and significantly lower for smaller Doppler shift values.

Figure C.6: Probability of Frequency Collision as a Function of the Doppler Shift



C.3.2.2 Multiple Channels Frequency Distribution

The following assumptions are made in respect of the population of active beacons in the visibility circle of the satellite:

- the total number N of active beacons in the visibility circle is uniformly spread amongst k frequency channels, and each channel C_i has the same number of active beacons: $n = N / k$; and
- all beacons in a channel transmit at the same carrier frequency and the carrier frequencies in two adjacent channels are separated by a distance of Δ kHz.

A beacon burst transmitted in channel C_i at a position $B(\alpha, \varphi)$ of the visibility circle is characterised by its Doppler ratio D , and this burst will collide in frequency with the bursts of those beacons in the same channel C_i that are located in the area S_D . We note n_i the number of

beacons in C_i that are located in area S_D . Then, we have: $\frac{n_i}{n} = \frac{S_D}{S} = p_f(D)$

The transmissions of beacon $B(\alpha, \varphi)$ in channel C_i will also collide in frequency with the transmissions of beacons in channel C_{i+1} that are located in the area $S_{D'}$, where:

$$D' = D - (\Delta/f_M) = D - \delta \quad (\text{with } \delta = \Delta / f_M)$$

We have: $\frac{n_{i+1}}{n} = \frac{S_{(D-\delta)}}{S} = p_f(D - \delta)$

Similarly, we find: $\frac{n_{i+j}}{n} = \frac{S_{(D-j\delta)}}{S} = p_f(D - j\delta)$ C/E.9

with the following condition limiting j :

- $S_{(D-j\delta)} \neq 0$ and $n_{i+j} \neq 0$ if $D - j\delta \geq -(D_{\text{Max}} + \varepsilon)$ i.e. Doppler shift $\geq - (8.858 \text{ kHz} + \text{“b”})$, where “b” is the bandwidth of the SARP input filter, and $\varepsilon = b/f_M$ - see Appendix A for the details of these limits, and
- $S_{(D-j\delta)} = 0$ and $n_{i+j} = 0$ if $D - j\delta < -(D_{\text{Max}} + \varepsilon)$ [i.e. $j > (D_{\text{Max}} + \varepsilon + D) / \delta$]

and: $\frac{n_{i-j}}{n} = \frac{S_{(D+j\delta)}}{S} = p_f(D + j\delta)$ C/E.10

with the condition:

- $S_{(D+j\delta)} \neq 0$ and $n_{i-j} \neq 0$ if $D + j\delta \leq D_{\text{Max}} + \varepsilon$
- $S_{(D+j\delta)} = 0$ and $n_{i-j} = 0$ if $D + j\delta > D_{\text{Max}} + \varepsilon$ [i.e. $j > (D_{\text{Max}} + \varepsilon - D) / \delta$],

Therefore, in a system of k channels and with the above conditions on j , the total number of active beacons that collide in frequency with the transmitting beacon $B(\alpha, \varphi)$ in channel C_i is:

$$n(D) = n_i + \sum_{j=1}^{k-i} n_{i+j} + \sum_{j=1}^{i-1} n_{i-j} . \quad \text{C/E.11}$$

The probability of frequency collisions with the transmissions of $B(\alpha, \varphi)$ that operates in channel C_i , is:

$$P_f(D) = \frac{n(D)}{N} = \frac{1}{k} \left[p_f(D) + \sum_{j=1}^{k-i} p_f(D - j\delta) + \sum_{j=1}^{i-1} p_f(D + j\delta) \right] \quad \text{C/E.12}$$

with: $P_f(D-j\delta) \neq 0$ if $j \leq (D_{\text{Max}} + \varepsilon + D) / \delta$,
 $P_f(D-j\delta) = 0$ if $j > (D_{\text{Max}} + \varepsilon + D) / \delta$; and
with: $P_f(D+j\delta) \neq 0$ if $j \leq (D_{\text{Max}} + \varepsilon - D) / \delta$,
 $P_f(D+j\delta) = 0$ if $j > (D_{\text{Max}} + \varepsilon - D) / \delta$;

For the LEOSAR system, with frequency channels separated by $\Delta = 3$ kHz, and with an input filter bandwidth of 1.2 kHz, we have:

$$\delta = \Delta / f_M = 3/10.066 = 0.298$$

$$D_{\text{Max}} = 8.858/10.066 = 0.879$$

$$\varepsilon = b / f_M = 1.2/10.066 = 0.119.$$

The number of channels that can interfere with a burst in channel C_i is:

$$2*(D_{\text{Max}} + \varepsilon) / \delta = 6.$$

The results of the computation of $P_f(D)$ are given in Table C-A.1 of Appendix A and are illustrated in Figure C.7.(a) for the case of five adjacent channels (two above and two below C_i), and in Figure C.7.(b) for the case of ten adjacent channels and twenty channels.

Figure C.7.(a): Probability of Frequency Collisions for Five Adjacent Channels

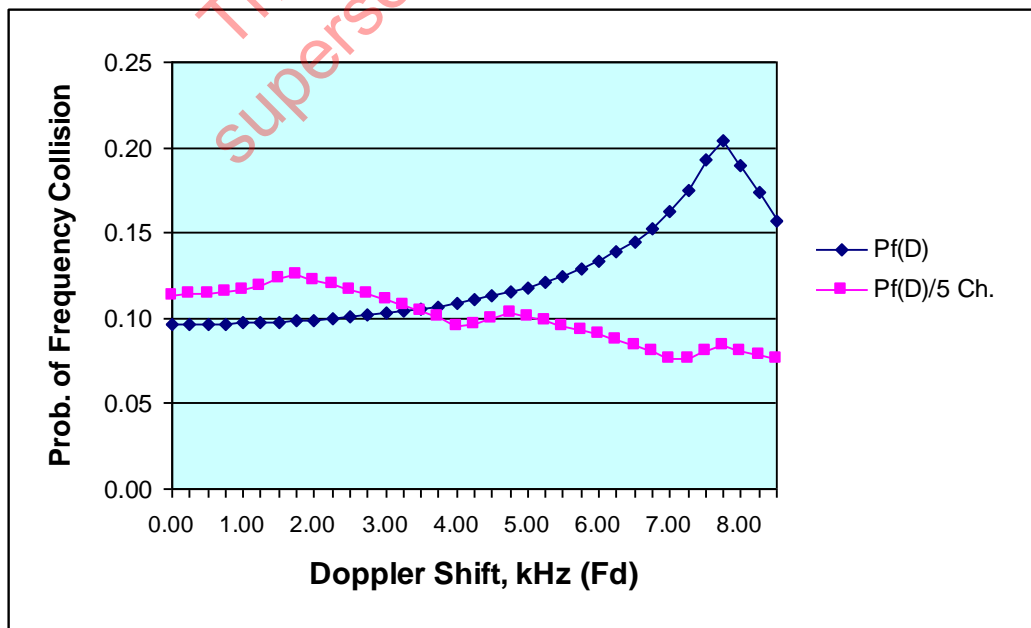
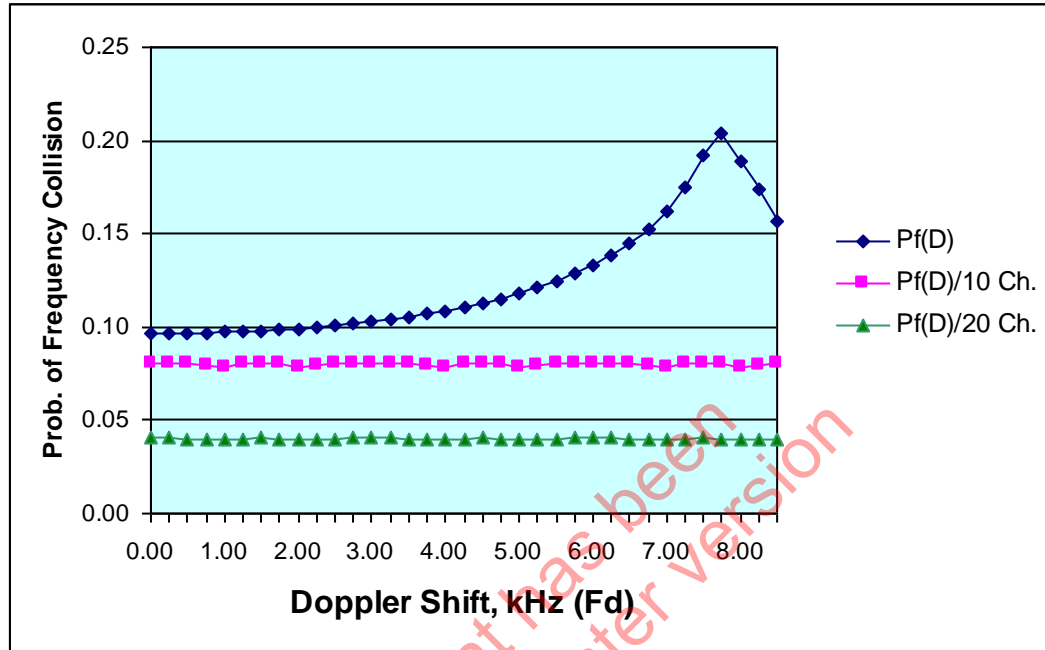


Figure C.7.(b): Probability of Frequency Collisions for Ten and Twenty Adjacent Channels



Note: The above figures C.7.(a) and (b) only present the positive Doppler values of f_d . Negative Doppler values provide a symmetrical graph.

C.3.3 Probability of Beacon Message Access to a Free DRU of the SARP Instrument

P_U is the probability that at least one of the three Data Recovery Units (DRU) of the satellite SARP instrument is free at the time of arrival of the burst, when N beacons are active in the field of view of the satellite (see Figure C.2).

Several assumptions are made for analysing the probability P_U :

- the SARP system includes three Data Recovery Units (DRUs);
- the beacon message arrival times have a Poisson distribution with an arrival rate $\lambda = 1/\gamma$, where γ is the average time interval between arrivals;
- the ‘service’ time (message processing time) of each message is constant, equal to the duration of the beacon message transmission (τ); the service rate is then $\mu = 1/\tau$; and
- messages arriving when all DRUs are occupied are lost, i.e., there are no queues in the system.

For a Poisson distribution, the probability of n arrivals during a time interval t , is given by the expression:

$$P_n(t) = \frac{(\lambda t)^n}{n!} e^{-\lambda t} \quad \text{C/E.13}$$

If (N) is the number of active beacons in the satellite visibility area, τ the duration of a beacon message transmission and T the beacon transmissions’ repetition period, the average density of beacon messages is:

$$\frac{N * \tau}{T} = \frac{\lambda}{\mu}; \text{ and } \lambda = N / T. \quad \text{C/E.14}$$

The various states’ transitions of the SARP system are represented in the diagram of Figure C.8, where $S(i)$ is the state of the system when i servers are occupied.

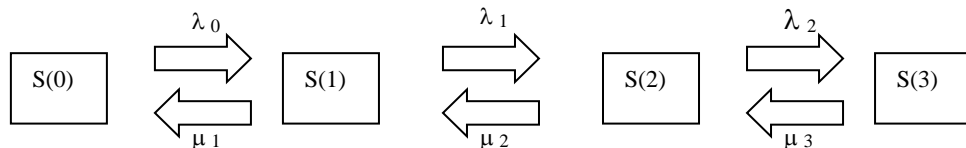


Figure C.8: Diagram of SARP State’s Transitions

The general theory of “birth and death” processes in a system of M servers, illustrated above for three servers only, and the description of the beacon message traffic with the hypothesis of a Poisson distribution of arrivals are detailed in Appendix B of Annex C. The results of this analysis are summarised below.

Under the assumptions made above, the “birth” rate is constant: $\lambda_0 = \lambda_1 = \lambda_2 = \lambda$; and the “death” rate in state $S(i)$ is $i * \mu$, so $\mu_1 = \mu$, $\mu_2 = 2\mu$, $\mu_3 = 3\mu$.

The probability for the SARP system to be in state S(i) is:

$P_i = \frac{\lambda_{i-1}}{\mu_i} P_{i-1}$, and noting that $P_0 = \left[1 + \frac{\lambda}{\mu} + \frac{1}{2!} \left(\frac{\lambda}{\mu} \right)^2 + \frac{1}{3!} \left(\frac{\lambda}{\mu} \right)^3 \right]^{-1}$, the probability of all three

DRUs being occupied is:

$$P_3 = \frac{\left(\frac{\lambda}{\mu} \right)^3 * \frac{1}{3!}}{1 + \frac{\lambda}{\mu} + \frac{1}{2!} \left(\frac{\lambda}{\mu} \right)^2 + \frac{1}{3!} \left(\frac{\lambda}{\mu} \right)^3} \quad \text{C/E.15}$$

The above formula is also known as the Erlang B-formula for a system with 3 service units (i.e., the satellite DRUs) when all ‘blocked’ arrivals are lost (i.e., no queues in the system). However, in the LEOSAR system, the probability P_i of the state S(i) must be modified to account for the fact that no state transition will occur if the arriving burst is not separated in the frequency domain from a burst already under processing. This is achieved by replacing the arrival rate λ with a rate that combines the probability of no collision in frequency: $\lambda_1 = \lambda * (1 - P_f)$. The detail of this calculation is provided at Appendix B of Annex C.

We note $v = \lambda/\mu$, the beacon message traffic expressed in Erlang. Using a modified Erlang-B formula to express the probability of a SARP state P_i , the probability of at least one free DRU in the SARP instrument would be (see Appendix B to Annex C):

$$P_U = \sum_{i=0}^2 P_i = \frac{1 + v + \frac{v^2}{2!} (1 - p_f)}{1 + v + \frac{v^2}{2!} (1 - p_f) + \frac{v^3}{3!} (1 - p_f)(1 - 2p_f)} \quad \text{C/E.16}$$

The above formula assumes the same probability P_f for all messages being processed. To resolve this additional difficulty (each burst under processing actually has a specific probability of collision in the frequency domain, which varies with the position of the beacon in the visibility area), we select the minimum value of P_f (noted $P_f \text{ min}$), which provides the lower limit of P_U (see Appendix B).

P_U depends on $v = \lambda/\mu$, which is a function of N , the number of active beacons in the satellite visibility area. Therefore, $P_U = f(N)$.

C.3.4 Probability P_{NA} of No-Collisions in Time and Frequency

P_{NA} is the probability that the processing of a burst is not affected by another burst at the same frequency, i.e., there are no arrivals of messages at the same frequency during the interval $[t - \tau, t + \tau] = 2\tau$, where τ is the processing time of a single burst and t is the time of arrival of the burst being considered.

Note: P_U , calculated as described in section C.3.3 above, takes into account the probability of collisions in frequency, but only to express the state of the SARP system.

From the assumption that arrivals are distributed according to a Poisson law, we have (C/E.13):

$$P_n(t) = \frac{(\lambda t)^n}{n!} e^{-\lambda t} = \text{probability of } n \text{ arrivals during a time interval 't'}$$

The probability of no-arrivals during the interval $[t - \tau, t + \tau] = 2\tau$ is: $P_0(2\tau) = e^{-2\lambda\tau}$.

This expression must be modified to account for the additional condition: no arrivals at the same frequency (i.e., with a distance of frequencies less than the filter bandwidth of the DRU). Under this additional condition we have to replace λ with $\lambda' = \lambda * P_f$, where P_f is the probability of frequency collision, as detailed in section C.3.2, for the message being processed, which is characterised by a specific Doppler ratio D .

Then:

$$P_{NA} = e^{-2\lambda P_f \tau} \quad \text{C/E.17}$$

The probability P_{NA} is a function of λ and P_f and, therefore, of the number of active beacons (N) and the position in the visibility circle of the beacon $B(\alpha, \varphi)$ being considered, as characterised by its Doppler ratio D .

C.3.5 Probability P_R of Single Beacon Message Reception

We assume that the probability of successful processing when a message has been assigned to a free DRU and is not interfered with during its processing, P_{SP} is 0.99 (ref: TG-1/2000/3/5).

Note: Although a theoretical approach based on the link budget would provide a higher figure for P_{SP} , the figure 0.99, which corresponds to the design specification of the Sarsat SARP, will be retained for the evaluation of the LEOSAR capacity. This also reflects the fact that, in real life, a number of bursts are not received at the nominal power level.

Then, the probability of reception of a single beacon message is: $P_R(N, D) = P_U * P_{NA} * P_{SP}$.

$$P_R(N, D) = 0.99 * e^{-2\lambda P_f \tau} * \frac{1 + v + \frac{v^2}{2!} (1 - P_{f \min})}{1 + v + \frac{v^2}{2!} (1 - P_{f \min}) + \frac{v^3}{3!} (1 - P_{f \min}) (1 - 2P_{f \min})} \quad \text{C/E.18}$$

C.3.6 Probability of Successful Doppler Processing

During a satellite pass, the transmitting beacon will occupy successive positions parallel to the satellite track, at a distance characterised by the cross-track angle (CTA), as illustrated in Figure C.3. The duration of the satellite pass in visibility of the transmitting beacon and, therefore, the number of messages that can be received by the satellite, are a function of the CTA.

We define the probability of successful Doppler processing (P_{DP}) as the probability of receiving at least 4 out of M possible messages. As the probability of reception P_R is specific to each received burst, we cannot apply equation C/E.2 given in section C.3.1.2 and, for $M = 5$, we have the following expression, where P_i is the probability of receiving the burst (i):

$$P_{DP} = P_1 * P_2 * P_3 * P_4 * P_5 + P_1 * P_2 * P_3 * P_4 * (1 - P_5) + P_1 * P_2 * P_3 * (1 - P_4) * P_5 + P_1 * P_2 * (1 - P_3) * P_4 * P_5 \\ + P_1 * (1 - P_2) * P_3 * P_4 * P_5 + (1 - P_1) * P_2 * P_3 * P_4 * P_5; \text{ or:}$$

$$P_{DP} = P_1 * P_2 * P_3 * P_4 * P_5 \left(\frac{1}{P_1} + \frac{1}{P_2} + \frac{1}{P_3} + \frac{1}{P_4} + \frac{1}{P_5} - 4 \right)$$

C/E.19

Similar computations could be performed for $5 < M \leq 18$, but such computations become extremely cumbersome for M greater than 5. Therefore, in Appendix C to Annex C, we will only verify that, for $M > 5$, the probability P_{DP} remains higher than the probability computed for $M = 5$, with a CTA of 22° , and accept the case $M = 5$ as the worst-case situation from which we can derive the system capacity.

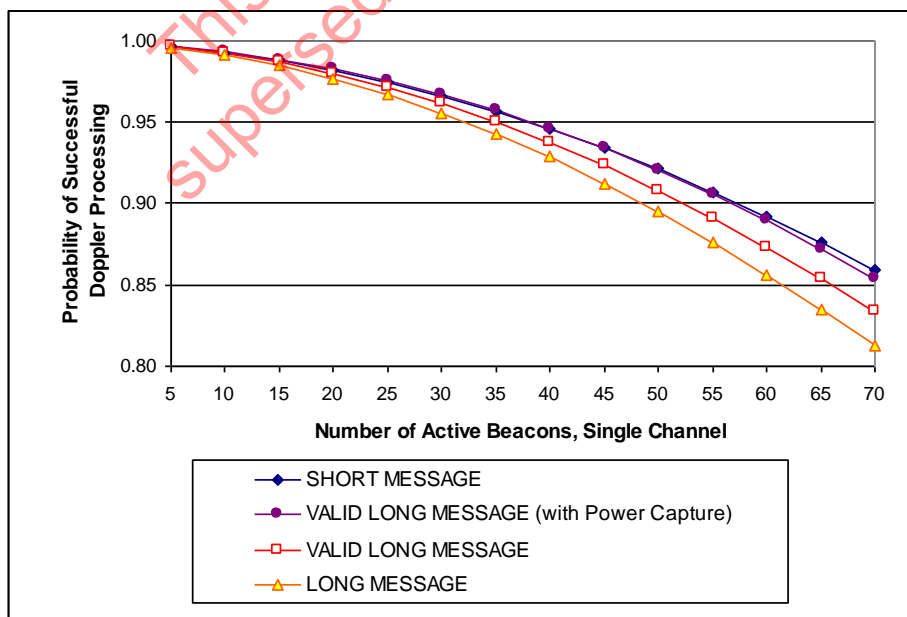
The proposed verification for $M > 5$ is made by applying to all bursts received during the pass the minimum value of P_R (probability of reception of a single message obtained for the maximum of P_i , probability of collision in the frequency domain). With this approximation, equation C/E.2 is applicable.

The detailed computations of the probability of successful Doppler processing for a single frequency channel system and for a multi-channel system are provided in the following sections.

C.3.7 LEOSAR System Capacity

Figure C.9 provides the probability of successful Doppler processing for a CTA of 22° (i.e., $M=5$), as a function of the number N of active beacons in the satellite visibility area, in the case of a single channel, for short beacon messages ($\tau = 0.440s$) and long beacon messages ($\tau = 0.520s$), and also for valid long format messages as discussed below.

Figure C.9: Probability of successful Doppler Processing for CTA = 22° (Elevation angle at TCA = 6.8°), Single Channel Short and Long Beacon Message Formats, and Valid Long Messages



The probability of successful Doppler processing illustrated in Figure C.9 is computed for short and long format messages using the equations C/E.18 and C/E.19 established in sections C.3.5

and C.3.6, and the corresponding values of τ : 0.440 and 0.520 seconds, respectively. However, we have also considered the case of valid long messages, which are used to determine the nominal capacity of a GEOSAR channel (see Annex D “GEOSAR Capacity Model”).

For valid long messages, we assume a population of beacons that all transmit long messages ($\tau = 0.520$ seconds), but we accept that if a collision only affects the second protected field of the message, then the first protected field is successfully retrieved and can be used for the Doppler processing, as the beacon identification is entirely contained in the first protected field (this assumes that the corresponding Doppler frequency measurement is also available). The probability P_U is not modified under this hypothesis, but the probability P_{NA} is now computed with a value $\tau = (0.520+0.425)/2 = 0.473$, considering that no arrivals should occur at the same frequency during the time interval $[t - 0.520, t - 0.425]$ (see the discussion of the recovery of valid long messages in section D.3.2.3 of Annex D).

In addition, on the basis of simulations performed with a Sarsat SARP engineering model, Appendix D to Annex C shows that some form of power capture exists and can be modelled by reducing, in the expression of P_{NA} , the interval during which no collisions should occur to $(0.9*2\tau)$, instead of 2τ .

The resulting probability of successful Doppler processing for valid long messages is reported in Figure C.9 with and without the improvement brought about by the consideration of a possible power capture. It is clear from Figure C.9 that the case “with power capture” cannot be distinguished for the results obtained for short format messages using the unmodified equation C/E.18 of section C.3.5. Therefore, although the following results are provided for short and long format messages using the unmodified equation C/E.18 to avoid an overly conservative approach we will base our final assessment of the LEOSAR capacity on the results obtained for a population of beacons transmitting short format messages.

Figure C.10: Probability of Successful Doppler Processing for CTA = 22° (Elevation angle at TCA = 6.8°), Short Beacon Message Format, with 5, 10 and 20 Frequency Channels

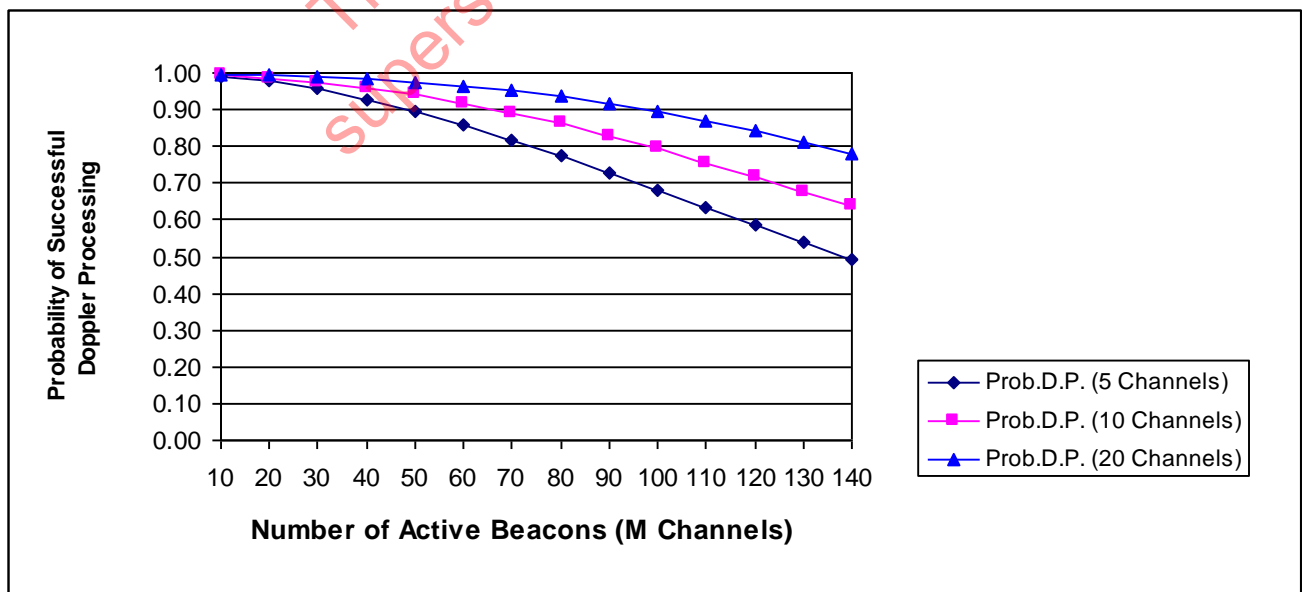


Figure C.10 illustrates the probability of successful Doppler processing computed under the same conditions as above (CTA of 22° (i.e., $M=5$)), for the short message format only, in a

system with 5, 10 and 20 adjacent frequency channels, each channels being assumed to accommodate the same number of beacons.

On the basis of our definition of capacity and the hypotheses made in the preceding analysis, Table C.1 provides the values of the LEOSAR system capacity with a single channel, expressed as the number of active beacons in the satellite visibility area that can be successfully processed with a given probability (assuming all beacons transmit short message formats, or all beacons transmit long message formats), and the corresponding capacity values for a LEOSAR system with 5, 10 or 20 adjacent channels.

Table C.1 shows that a system with 5 adjacent channels would have a lower capacity than a single channel. This result is due to the actual increase of the probability of collisions in the frequency domain for the central channel of the 5-channel system, and particularly when the received frequency of a burst in that channel is not affected by a large Doppler shift (see Figure C.7(a), in particular for Doppler shifts between 0 and 3 kHz). This is specifically the case for the 22⁰ CTA, which is selected as the worst case for the computation of the probability of successful Doppler processing.

With 10 and 20 channels, the total system capacity increases, although not linearly as the DRU limitation affects the probability of reception of individual messages.

These results underline the need to carefully plan the spreading of the beacon carrier frequency on the basis of a decreasing individual channel capacity when additional channels adjacent to existing channels are open for use, or to ensure sufficient frequency separation between existing and new frequency channels so as to ensure that the new channels would not impact on the capacity of the previously opened channels.

Table C.1: Capacity of the LEOSAR System with a Single Frequency Channel, and with “M” Adjacent-Channels

	Number of Active Beacons in Visibility Area			
	Short Message		Long Message	
	$P_{DP} = 0.98$	$P_{DP} = 0.95$	$P_{DP} = 0.98$	$P_{DP} = 0.95$
Single Frequency Channel	21	38	18	32
5 Channels	18	32	15	27
10 Channels	26	45	22	38
20 Channels	45	71	38	60

C.4 CAPACITY OF THE SARP-1 LEOSAR SYSTEM WITH THREE CHANNELS

Three channels have been opened for use with the SARP-1 LEOSAR system, which is limited to the 24 kHz bandwidth of the SARP-1 instrument: 406.022 MHz, 406.025 MHz and 406.028 MHz. All System beacons (orbitography and reference beacons) have been transferred to the first channel: 406.022 MHz. Until the year 2000, all operational beacons have been designed to operate at 406.025 MHz, and this channel will continue to host the vast majority of operational beacons for many years as type approved models will continue to be produced for operation in this channel.

The channel 406.028 MHz has been opened for use since 1 January 2000 and all new beacon models submitted for type approval are required to operate in this channel from 1 January 2002. As long as the population of operational beacons in the channel 406.028 MHz remains small, their impact on the capacity of the 406.025 MHz channel will remain negligible. However, it is essential to assess the longer-term impact of the new channel (406.028 MHz) on the capacity of the 406.025 MHz channel to ensure that capacity requirements are effectively satisfied.

Figure C.11 illustrates the probability of frequency collisions in the channel 406.025 MHz, as a function of the Doppler shift (± 8.8 kHz), when three channels (406.022, 406.025 and 406.028 MHz) are opened for use and each channel is occupied by the same number of beacons.

Although the results illustrated in Figure C.11 assume an equal distribution of beacons in each channel, it can be seen from the resulting curve of probability of frequency collision that this distribution has actually little impact on the curve in the region ± 2.5 kHz, which corresponds to large CTAs of beacons in the 406.025 Channel (e.g., CTA = 22^0 used for the computation of the capacity).

However, Figure C.11 also shows that the probability of frequency collision is higher for beacons in channel 406.028 MHz with large CTAs (corresponding in Figure C.11 to Doppler shifts between 0.5 and 5.5 kHz). Noting also that beacons in channel 406.022 MHz will have a major impact on the probability of frequency collision for beacon transmissions in channel 406.028 MHz, there is no benefits in terms of capacity to opening 406.022 MHz for use by distress beacons. Furthermore, in line with the approach taken to assess the capacity of the LEOSAR system, we must base our assessment of the capacity of the three channel system on the probability of obtaining a Doppler location for beacons in the channel 406.028 MHz (worst case from the point of view of frequency collisions with CTA = 22^0).

The three-channel system capacity is provided in Table C.2 for the probabilities of successful Doppler processing 95% and 98%, and for the short and long message formats. The corresponding world population of beacons is also provided as illustration. However, the world population figure is dependent on the 406 MHz beacon message traffic model provided at Annex G, which may be amended from time to time.

Figure C.11: Probability of Frequency Collision in Channel 406.025 MHz (3-Channel System)

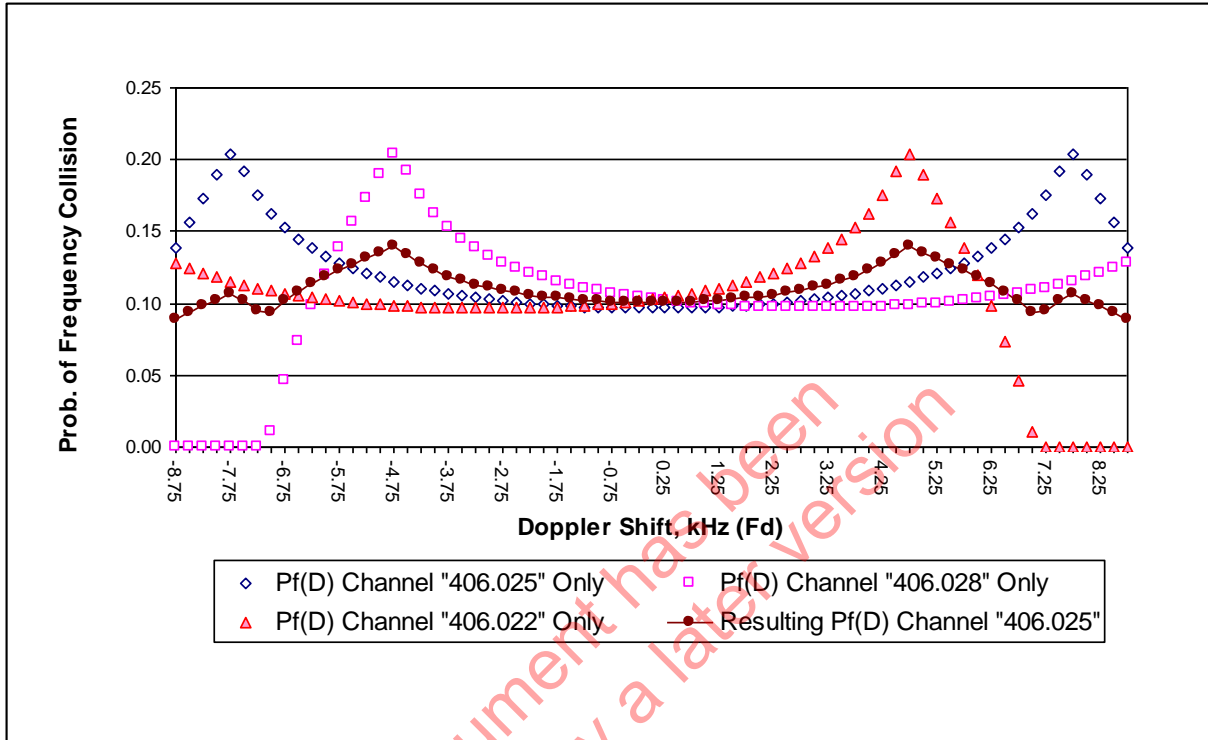


Table C.2: Capacity of the SARP-1 LEOSAR System with Three Channels (Probability of successful Doppler processing computed at edge of coverage assuming a uniform distribution of beacons among 3 channels)

		Short Message		Long Message	
		$P_{DP} = 0.98$	$P_{DP} = 0.95$	$P_{DP} = 0.98$	$P_{DP} = 0.95$
Single Channel (406.025 MHz)	Equivalent Number of Active Beacons in Visibility Area	21	38	18	32
	Corresponding World Population of 406 MHz Beacons x 1,000 (Based on 2002 Traffic Model)	734	1,566	587	1,272
Three Channels (406.022 MHz + 406.025 MHz + 406.028 MHz)	Equivalent Number of Active Beacons in Visibility Area	18	33	16	28
	Corresponding World Population of 406 MHz Beacons x 1,000 (Based on 2002 Traffic Model)	587	1,321	489	1,077

C.5 CAPACITY OF THE SARP-2 LEOSAR SYSTEM WITH 19 CHANNELS

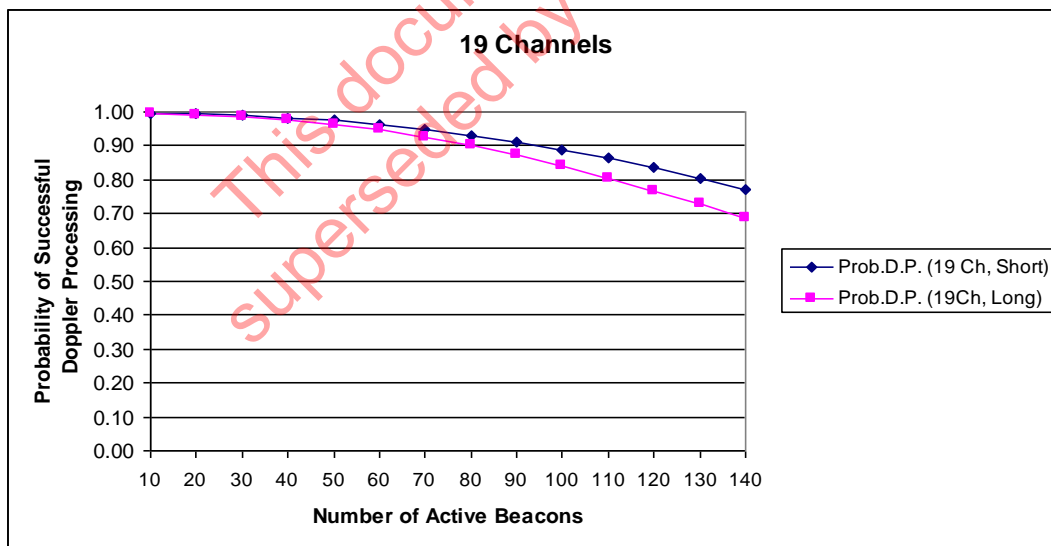
A total of 19 channels with a 3 kHz separation are available for use with the LEOSAR system in the 406.0 – 406.1 MHz frequency band. This takes into account the SARP-2 instrument bandwidth limitations, the maximum Doppler shift that can affect the frequency of the beacon messages received by the satellite, and the possible change of the beacon carrier frequency due to ageing, as specified in the beacon specification, C/S T.001 (see section 5.1 of C/S T.012).

Although, the first channel at 406.022 MHz is currently reserved for the System orbitography and reference beacons, we need to include this channel in the computation of the total capacity as these beacon transmissions can affect other channels through collisions in time and frequency, or by occupying the Data Recovery Units of the SARP instrument. As a consequence, the transmissions of orbitography and reference beacons will need to be accounted for in the model of traffic forecast for the LEOSAR system, which defines the LEOSAR capacity requirements.

Note: The capacity of the channels at the edge of the available frequency band, which have a smaller number of “adjacent” channels that can affect their probability of frequency collision, is slightly higher than the capacity of the “standard” channels in the middle of the frequency band. However, for the purpose of this evaluation, we will assume that all channels are similar.

The results of the computation of the probability of successful Doppler processing for a CTA of 22° , assuming that all channels accommodate the same fraction of the beacon population, are illustrated in Figure C.12 for short and long message formats.

**Figure C.12: Probability of Successful Doppler Processing for CTA = 22°
(Elevation angle at TCA = 6.8°)**



The capacity figures for 19 channels are provided in Table C.3 below, which also shows the corresponding beacon population that can be accommodated world-wide, as provided by the model of 406 MHz beacon message traffic (see Annex G).

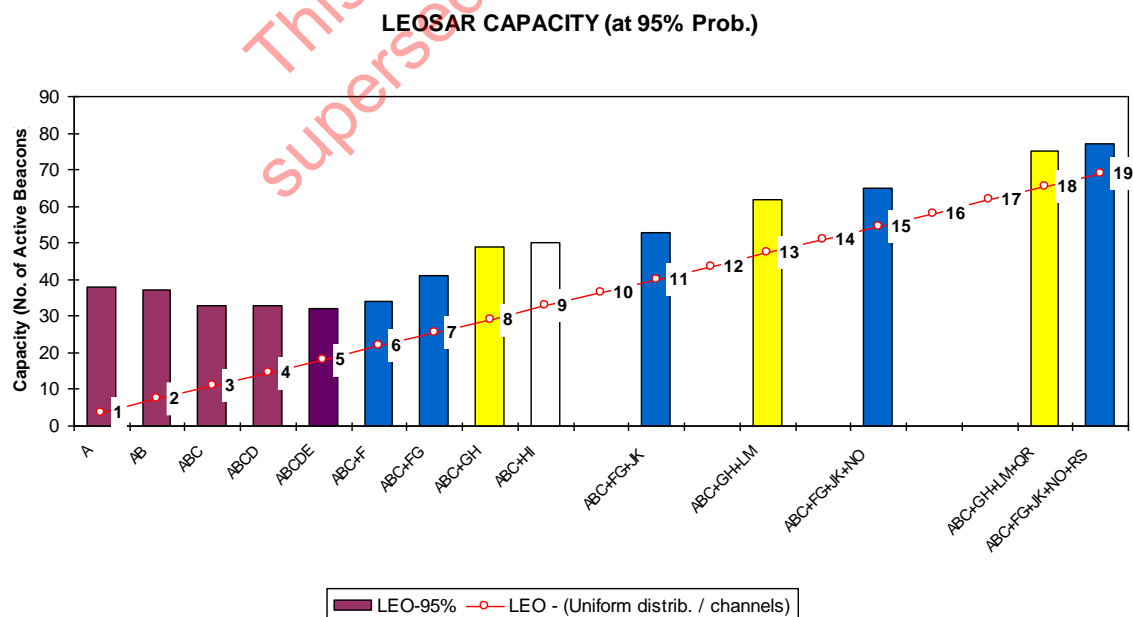
**Table C.3: Capacity of the SARP-2 LEOSAR System with 19 Channels
(Probability of successful Doppler processing computed at edge of coverage
assuming a uniform distribution of beacons among 19 channels)**

	Short Message		Long Message	
	P _{D_P} = 0.98	P _{D_P} = 0.95	P _{D_P} = 0.98	P _{D_P} = 0.95
Equivalent Number of Active Beacons in Visibility Area	43	69	37	58
Corresponding World Population of 406 MHz Beacons x 1,000 (Based on 2002 Traffic Model)	1,811	3,083	1,517	2,545

As shown in section C.4, the capacity of a system of adjacent channels is governed by the probability of collisions in the “worst” channel (i.e., the channel where the probability of collision is highest for small Doppler shifts). As a consequence, three channels have a smaller capacity than one single channel and two adjacent channels have about the same capacity as a single channel.

Table C.4 and Figure C.13 illustrate the LEOSAR capacity for various assignment schemes, assuming 19 possible channels are available, but only some of them are opened for use. The channels are identified with the letters A (i.e., 406.022 MHz) to S (406.76 MHz). The capacity figure for a group is plotted with reference to the highest channel in the group (i.e., ABC+FG+JK is plotted in the K position of the x axis). It is clear that leaving “empty” channels between “opened” channels is a better strategy than opening all available channels without gaps.

Figure C.13: LEOSAR Capacity Under Various Channel Assignment Schemes



The best results for the 19 available channels are achieved with separations of 12 kHz or 9 kHz between channels opened for use. Opening for use pairs of adjacent channels is particularly attractive because of the GEOSAR capacity requirements analysed in Annex D.

The discussion of the optimum assignment strategy is provided at section 4.3 of the document C/S T.012.

Table C.4: LEOSAR Capacity for Various Channel Assignments

Channels	MHz	Channels in Use	LEO Capa
1 - A	406.022	A	38
2 - B	406.025	AB	37
3 - C	406.028	ABC	33
4 - D	406.031	ABCD	33
5 - E	406.034	ABCDE	32
6 - F	406.037	ABC+F	34
7 - G	406.040	ABC+FG	41
8 - H	406.043	ABC+GH	49
9 - I	406.046	ABC+HI	50
10 - J	406.049		
11 - K	406.052	ABC+FG+JK	53
12 - L	406.055		
13 - M	406.058	ABC+GH+LM	62
14 - N	406.061		
15 - O	406.064	ABC+FG+JK+NO	65
16 - P	406.067		
17 - Q	406.070		
18 - R	406.073	ABC+GH+LM+QR	75
19 - S	406.076	ABC+FG+JK+NO+RS	77

This document has been superseded by a later version

APPENDIX A to ANNEX C**COMPUTATION OF THE PROBABILITY OF COLLISION IN FREQUENCY****C-A.1 Curves of Equal Doppler Shift**

The frequency shift for a beacon at a position in the visibility circle defined by the angles θ and φ , is given by the expression (see Figure C.4):

$$f_d = f_M * \cos \theta * \cos \varphi \quad \text{C-A/E.1}$$

where: θ is the look-down angle of the beacon;

φ is the azimuth of the beacon; and

$f_M = 10.066$ kHz (see section 3.2).

A beacon at position B(α, φ) is characterised by a Doppler shift, function of θ and φ , given by the expression C-A/E.1, which can be transformed as follows:

$$\cos \varphi * \cos \theta(\alpha) = D \quad \text{C-A/E.2}$$

where $D = f_d / f_M$, $D_{Max} = 8.858/10.066 = 0.879$, and $D \leq D_{Max}$

C-A/E.2 defines a curve of equal Doppler shift in the visibility area of the satellite. The transmissions of all beacons located on this curve will have the same Doppler ratio D. The function $\theta(\alpha)$ is derived from the consideration of the triangle (satellite, beacon, Earth centre) in Figure C.4, where:

$$\frac{\sin(\pi/2 + \theta - \alpha)}{R + h} = \frac{\sin(\pi/2 - \theta)}{R} = \frac{\cos(\alpha - \theta)}{R + h} = \frac{\cos \theta}{R} \quad \text{C-A/E.3}$$

Therefore:

$$\cos \alpha * \cos \theta + \sin \alpha * \sin \theta = \frac{R + h}{R} \cos \theta = A * \cos \theta; \quad \left(\text{with } A = \frac{R + h}{R}\right)$$

$$\sin \alpha \sqrt{1 - \cos^2 \theta} = \cos \theta * [A - \cos \alpha]$$

$$\sin^2 \alpha * \cos^2 \theta + \cos^2 \theta * [A - \cos \alpha]^2 = \sin^2 \alpha$$

$$\cos^2 \theta = \frac{\sin^2 \alpha}{1 + A^2 - 2A \cos \alpha}$$

$$\cos \theta = \frac{\sin \alpha}{\sqrt{1 + A^2 - 2A \cos \alpha}}$$

$$\theta(\alpha) = \arccos \frac{\sin \alpha}{\sqrt{1 + A^2 - 2A \cos \alpha}} \quad \text{with } A = \frac{R + h}{R} = 1.136 \quad \text{C-A/E.4}$$

From C-A/E.2 we have the equation of the curve that describes all points of the visibility circle with the same Doppler ratio D:

$$\varphi(\alpha) = + \arccos \frac{D}{\cos \theta} = + \arccos \left(\frac{D \sqrt{1 + A^2 - 2 A \cos \alpha}}{\sin \alpha} \right) \quad \text{C-A/E.5}$$

C-A/E.5 is defined within the interval $\alpha \in]0, \alpha_{\text{Max}}]$, with the conditions $\theta \neq \pi/2 \equiv \alpha \neq 0$, as φ can take any value for $\theta = \pi/2$ (i.e., the sub-satellite point). Note that we only have to consider the positive values of $\varphi(\alpha)$ and, because of the symmetry on each side of the satellite track (assuming we do not have to take into account the second order effect of the Earth rotation on the Doppler shift), we will only have to consider $\varphi \in [0, \pi]$.

C-A.2 Probability of Collision in Frequency for a Beacon with a Doppler Ratio D (Single Channel)

The transmissions of the $B(\alpha, \varphi)$ beacon may be interfered with by the transmissions of all beacons that have the same Doppler shift ± 1.2 kHz (1.2 kHz is the frequency bandwidth of the DRUs input filter), i.e. all beacons in positions such as:

$$D - \varepsilon \leq \cos \varphi * \cos \theta(\alpha) \leq D + \varepsilon. \quad \text{C-A/E.6}$$

$$\text{With: } D + \varepsilon = \frac{f_d + 1.2 \text{ kHz}}{f_M} = D + \frac{1.2}{10.066} \cong D + 0.119 \quad (\text{therefore } \varepsilon = 0.119).$$

These interfering beacons belong to an area (S_D) of the visibility circle limited by boundaries defined by the conditions (see Figure C-A.1):

$$\text{curve of equal Doppler } (D + \varepsilon): \cos \varphi * \cos \theta(\alpha) = D + \varepsilon;$$

$$\text{curve of equal Doppler } (D - \varepsilon): \cos \varphi * \cos \theta(\alpha) = D - \varepsilon.$$

$$\varphi \in [0, 2\pi]; \text{ and}$$

$$\theta \in [0_{\text{min}}, +\pi/2] \equiv \alpha \in [0, \alpha_{\text{Max}}];$$

The surface area of S_D can be computed for any value of $D \in [0, D_{\text{Max}}]$ and the ratio S_D/S (where S is the surface area of the visibility circle) is the probability for any other beacon to be located in S_D and to interfere in the frequency domain with transmissions that have a Doppler ratio D (we assume a uniform distribution of the beacons in the satellite visibility area). Therefore, the probability of collision in frequency for a beacon with the Doppler ratio D is:

$$P_f(D) = \frac{S_D}{S} \quad \text{C-A/E.7}$$

An element d_s of the surface of the visibility circle (see Figure C.5) is given by the expression:

$$d_s = (R \sin \alpha * d\varphi) * (R * d\alpha) = R^2 \sin \alpha d\varphi d\alpha \quad \text{C-A/E.8}$$

With $\varphi \in [0, 2\pi]$ and $\alpha \in [0, \alpha_M]$; where α_M is the maximum of α at the edge of the visibility circle, the surface S of the visibility circle is:

$$S = R^2 \int_{\alpha} \int_{\varphi} \sin \alpha \, d\varphi \, d\alpha = 2\pi R^2 (1 - \cos \alpha_M) = 2\pi R^2 (1 - (R/R+h))$$

$$S = 2\pi R^2 \frac{h}{R+h} \quad \text{C-A/E.9}$$

S_D is the surface of the area in the visibility circle where other beacon transmissions will be shifted by a Doppler ratio D' such as $D-\varepsilon \leq D' \leq D+\varepsilon$.

This surface is given by the expression C-A/E.10:

$$S_D = 2 R^2 \int_{\alpha} \int_{\varphi} \sin \alpha \, d\varphi \, d\alpha; \quad \text{C-A/E.10}$$

with: $D_{\min} \leq D - \varepsilon \leq \cos \varphi * \cos \theta(\alpha) \leq D + \varepsilon \leq D_{\max}$
 $D_{\max} = 0.879$ and $D_{\min} = -0.879$
 $\varphi \in [0, +\pi]$
 $\theta \in [\theta_{\min}, +\pi/2] \equiv \alpha \in [0, \alpha_{\max}]$

Note: The above expression uses the symmetry of the beacon-to-satellite path on each side of the satellite track (see Figure C.5).

The limits of the integration domain are:

- the visibility circle (as a consequence of the condition $\theta \geq \theta_{\min} \equiv \alpha \leq \alpha_{\max}$);
- the curve $\varphi(\alpha)$ of equal Doppler shift corresponding to the Doppler ratio $(D + \varepsilon)$, which we will note $\varphi(D + \varepsilon)$; and
- the curve $\varphi(\alpha)$ of equal Doppler shift corresponding to the Doppler ratio $(D - \varepsilon)$, which we will note $\varphi(D - \varepsilon)$.

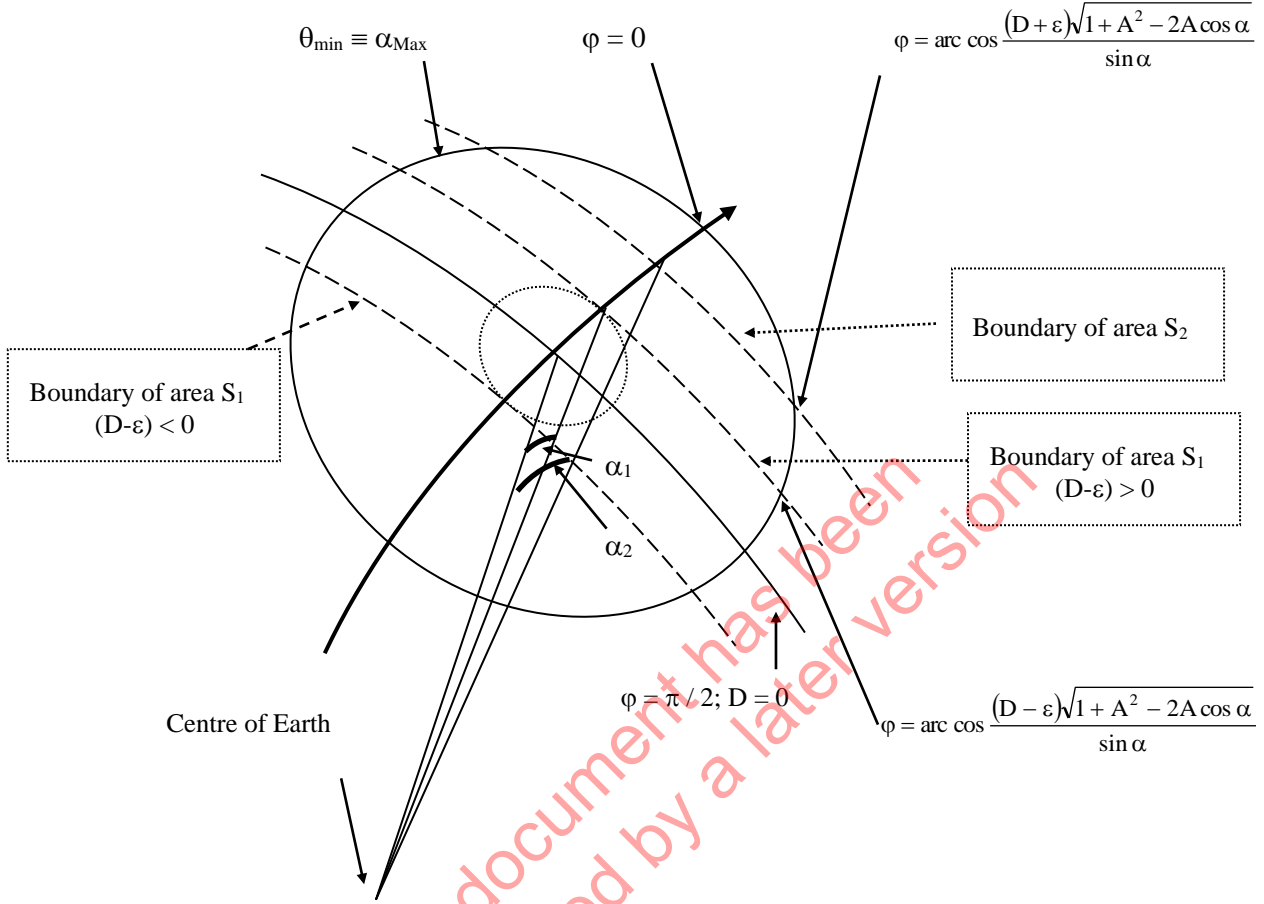
The expressions of $\varphi(D + \varepsilon)$ and $\varphi(D - \varepsilon)$ are derived from C-A/E.5 as follows:

$$\varphi(D + \varepsilon) = \arccos \left(\frac{(D + \varepsilon) \sqrt{1 + A^2 - 2 A \cos \alpha}}{\sin \alpha} \right) \quad \text{C-A/E.11}$$

$$\varphi(D - \varepsilon) = \arccos \left(\frac{(D - \varepsilon) \sqrt{1 + A^2 - 2 A \cos \alpha}}{\sin \alpha} \right) \quad \text{C-A/E.12}$$

The domain of integration of C-A/E.10 is illustrated in Figure C-A.1, which is a representation of the satellite visibility circle.

Figure C-A.1: Integration Domain of C-A/E.10



Note: From Figure C-A.1, we also can see that the case $D < 0$ ($\varphi > \pi/2$) would give an integration domain symmetrical to the domain illustrated in the Figure, and identical results in terms of probability of collision in the frequency domain. Therefore, we can limit the computations to $D \geq 0$.

From Figure C-A.1 above, we see that the expression C-A/E.10 can be further developed as the difference:

$S_D = S_1(D - \epsilon) - S_2(D + \epsilon)$, where:

$S_1(D - \epsilon)$ is the surface area of the visibility circle where all bursts will be received with a Doppler ratio $\geq D - \epsilon$;

$S_2(D + \epsilon)$ is the surface area of the visibility circle where all bursts will be received with a Doppler ratio $\geq D + \epsilon$; and

$$S_D = 2R^2 \underbrace{\int_{\alpha_1}^{\alpha_{Max}} \left[\int_0^{\varphi(D-\epsilon)} d\varphi \right] \sin \alpha \, d\alpha}_{S_1} - 2R^2 \underbrace{\int_{\alpha_2}^{\alpha_{Max}} \left[\int_0^{\varphi(D+\epsilon)} d\varphi \right] \sin \alpha \, d\alpha}_{S_2} \quad \text{C-A/E.13}$$

From the consideration of the triangle (satellite, beacon, earth centre) in Figure C.4 we have:

$\cos(\alpha - \theta) = \frac{R+h}{R} \cos\theta = A \cos\theta$, therefore $(\alpha - \theta) = \pm \arccos(A \cos\theta)$ and, as $(\alpha - \theta) \leq 0$, we have:

$$\alpha = \theta - \arccos(A \cos\theta) \quad \text{C-A/E.14}$$

Considering Figure C-A.1, we find the following relations derived from C-A/E.14, which define the limits α_1 , α_2 and α_{Max} of the integration:

$$\begin{aligned} \varphi = 0 \text{ (or } \pi) \text{ and } \cos\theta = |D-\varepsilon| &\Rightarrow \alpha_1 = \arccos|D-\varepsilon| - \arccos[A|D-\varepsilon|] && \text{C-A/E.15} \\ \varphi = 0 \text{ and } \cos\theta = D+\varepsilon &\Rightarrow \alpha_2 = \arccos(D+\varepsilon) - \arccos[A(D+\varepsilon)], \text{ with } \alpha_2 \leq \alpha_{\text{Max}} && \text{C-A/E.16} \\ \cos\theta_{\text{min}} = R/R+h = 1/A &\Rightarrow \alpha_{\text{Max}} = \arccos(1/A) = \theta_{\text{min}} && \text{C-A/E.17} \end{aligned}$$

The general condition $0 \leq D \leq D_{\text{Max}}$ must be completed with appropriate conditions on $D+\varepsilon$ and $D-\varepsilon$.

C-A.2.1 Modified Expression of S_2 for the Case $D+\varepsilon \geq D_{\text{Max}}$

The condition $D+\varepsilon \leq D_{\text{Max}} = \cos\theta_{\text{min}} = 1/A$ corresponds to the condition $\alpha_2 \leq \alpha_{\text{Max}}$. If $D+\varepsilon \geq D_{\text{Max}}$, then $S_2 = 0$. This can be reflected by introducing a step function such as:

$$\begin{aligned} U(x) &= 0 \text{ when } x < 0, \text{ and} \\ U(x) &= 1 \text{ when } x \geq 0. \end{aligned}$$

The term $D_{\text{Max}} - (D+\varepsilon) = (D_{\text{Max}} - D - \varepsilon)$, can be used as the variable in the step function and the expression of S_2 should be modified as follows:

$$S_2 = 2R^2 * U(D_{\text{Max}} - D - \varepsilon) * \int_{\alpha_2}^{\alpha_{\text{Max}}} \left[\int_0^{\varphi(D+\varepsilon)} d\varphi \right] \sin\alpha \, d\alpha \quad \text{C-A/E.18}$$

C-A.2.2 Modified Expression of S_1 for the Case $D - \varepsilon \leq 0$

The case $0 < D < \varepsilon$ ($D - \varepsilon < 0$) corresponds to the case where $\varphi(D-\varepsilon) > \pi/2$ (i.e., the curve of equal Doppler shift corresponding to the Doppler ratio $(D-\varepsilon)$ is entirely contained in the portion of the visibility circle corresponding to $\pi/2 \leq \varphi \leq \pi$). However, $\cos\theta$ and α_1 always remain positive and this condition is expressed with the absolute value $|D - \varepsilon|$ in the expression of α_1 .

In addition, in that particular case, the expression of S_1 must be modified to account for the fact that S_1 also includes the surface area corresponding to $\alpha \in]0, \alpha_1]$ and $\varphi \in [0, \pi]$. Therefore, S_1 should be written as follows:

$$S_1 = 2 R^2 \int_{\alpha_1}^{\alpha_{\text{Max}}} \left[\int_0^{\varphi(D-\varepsilon)} d\varphi \right] \sin \alpha \, d\alpha + 2 R^2 \int_0^{\alpha_1} \left[\int_0^{\pi} d\varphi \right] \sin \alpha \, d\alpha$$

C-A/E.19

$$S_1 = 2 R^2 \int_{\alpha_1}^{\alpha_{\text{Max}}} \left[\int_0^{\varphi(D-\varepsilon)} d\varphi \right] \sin \alpha \, d\alpha + 2 R^2 * \pi (1 - \cos \alpha_1)$$

As the second part of the above equation for S_1 only appears for $0 < D < \varepsilon$, a general expression is obtained using the step function $U(\varepsilon - D)$, which is equal to 1 for $D \leq \varepsilon$, and equal to 0 for $D > \varepsilon$.

C-A.2.3 General Expression of S_D and $P_f(D)$

With the above modifications, the equation of S_D becomes:

$$S_D = 2 R^2 \left[\begin{array}{l} U(\varepsilon - D) * \pi (1 - \cos \alpha_1) + \int_{\alpha_1}^{\alpha_{\text{Max}}} \left[\int_0^{\varphi(D-\varepsilon)} d\varphi \right] \sin \alpha \, d\alpha \\ - U(D_{\text{Max}} - D - \varepsilon) * \int_{\alpha_2}^{\alpha_{\text{Max}}} \left[\int_0^{\varphi(D+\varepsilon)} d\varphi \right] \sin \alpha \, d\alpha \end{array} \right]$$

C-A/E.20

where: $\alpha_1 = \arccos |D-\varepsilon| - \arccos [A |D-\varepsilon|]$;
 $\alpha_2 = \arccos (D+\varepsilon) - \arccos [A(D+\varepsilon)]$; and
 $\alpha_2 \leq \alpha_{\text{Max}} = \arccos(1/A)$

From C-A/E.7 and C-A/E.9: $P_f(D) = S_D / S = S_D * \frac{R+h}{2\pi R^2 h}$, and after integrating on φ , the general expression of P_f becomes:

$$P_f(D) = \frac{R+h}{\pi h} \left[\begin{array}{l} U(\varepsilon - D) * \pi (1 - \cos \alpha_1) \\ + \int_{\alpha_1}^{\alpha_{\text{Max}}} \left[\arccos \frac{(D-\varepsilon) \sqrt{1+A^2-2A \cos \alpha}}{\sin \alpha} \right] \sin \alpha \, d\alpha \\ - U(D_{\text{Max}} - D - \varepsilon) * \int_{\alpha_2}^{\alpha_{\text{Max}}} \left[\arccos \frac{(D+\varepsilon) \sqrt{1+A^2-2A \cos \alpha}}{\sin \alpha} \right] \sin \alpha \, d\alpha \end{array} \right]$$

C-A/E.21

C-A.3 Probability of Collision in Frequency for a Beacon with a Doppler Ratio D (Multiple Channels)

A beacon burst transmitted in Channel C_i at a position $B(\alpha, \varphi)$ of the visibility circle is characterised by its Doppler ratio D , and this burst (noted $C_i(D)$) will collide in frequency with the bursts of those beacons in the same channel C_i that are located in the area S_D .

In a multi channel system, it will also collide in frequency with the bursts of other channels. If these channels are separated in frequency by Δ kHz, the bursts from beacons in channel C_{i-1} will collide with the burst $C_i(D)$ when they are affected by a Doppler shift such as:

$$D' = D + (\Delta/f_M) \pm \varepsilon = D + \delta \pm \varepsilon; \text{ where } \delta = \Delta/f_M$$

We can compute the surface area of the visibility circle where the above condition on D' is satisfied (i.e., all bursts from beacons in channel C_{i-1} located in this area will collide with $C_i(D)$), in the same way as in section C-A.2 for area S_D , and we will note this surface area $S_{(D+\delta)}$.

From C-A/E.13, 15, 16 and 17 we have:

$$S_{D+\delta} = \underbrace{2R^2 \int_{\alpha_1(D+\delta-\varepsilon)}^{\alpha_{\text{Max}}} \left[\int_0^{\varphi(D+\delta-\varepsilon)} d\varphi \right] \sin \alpha d\alpha}_{S_1} - \underbrace{2R^2 \int_{\alpha_2(D+\delta+\varepsilon)}^{\alpha_{\text{Max}}} \left[\int_0^{\varphi(D+\delta+\varepsilon)} d\varphi \right] \sin \alpha d\alpha}_{S_2} \quad \text{C-A/E.22}$$

This equation provides identical results as for S_D , and the curve representing the evolution of $P_f(D+\delta)$ is similar to the curve $P_f(D)$ shifted by Δ kHz, except for the fact that the translated curve of $P_f(D+\delta)$ is continued for values of $D+\delta$ beyond the D_{Max} limit applied to the computation of $P_f(D)$ in a single channel, as explained below.

In the case of a single channel, we stopped computing S_D when D reached the value D_{Max} , as no bursts could be affected by a Doppler shift greater than $f_D = f_M \cdot \cos \alpha_{\text{Max}}$, α_{Max} being the limit of the visibility circle at 0° elevation. However, to compute $P_f(D+\delta)$ we need to take into account the fact that there are beacons in the visibility circle, transmitting in channel C_{i-1} , that are characterised by the Doppler ratio $D + \delta$, such as:

$$\begin{aligned} D &\leq D_{\text{Max}}, \text{ and} \\ D + \delta - \varepsilon &\leq D_{\text{Max}} \leq D + \delta. \end{aligned}$$

This is illustrated in Figure C-A.2 below, which shows the resulting probability of frequency collisions for beacons bursts in Channel C_i with a Doppler shift f_d , when beacons are transmitting in three channels: C_i , C_{i-1} and C_{i-2} .

The above remark concerning the computation of $P_f(D+\delta)$ for channel C_{i-1} (Channel "B" in Figure C-A.2) is the situation encountered for $f_d = 6.5$ kHz, where:

$$\begin{aligned} f_{d+\Delta} &= 6.5 + 3 = 9.5 \text{ kHz} \geq f_M \cdot \cos \alpha_{\text{Max}} = 8.858 \text{ kHz}; \text{ and} \\ f_{d+\Delta} - b &= 9.5 - 1.2 = 8.3 \text{ kHz} \leq f_M \cdot \cos \alpha_{\text{Max}}. \end{aligned}$$

This corresponds to bursts from beacons in C_{i-1} that are affected by a Doppler shift of at least 8.3 kHz, which can collide with bursts in C_i , affected by a Doppler shift of 6.5 kHz.

The probability of frequency collisions for k adjacent channels is derived from the probability computed in a single channel as described at section C.3.2.2 of Annex C, using equation C/E.12.

$$P_f(D) = \frac{1}{k} \left[p_f(D) + \sum_{j=1}^{k-i} p_f(D-j\delta) + \sum_{j=1}^{i-1} p_f(D+j\delta) \right]$$

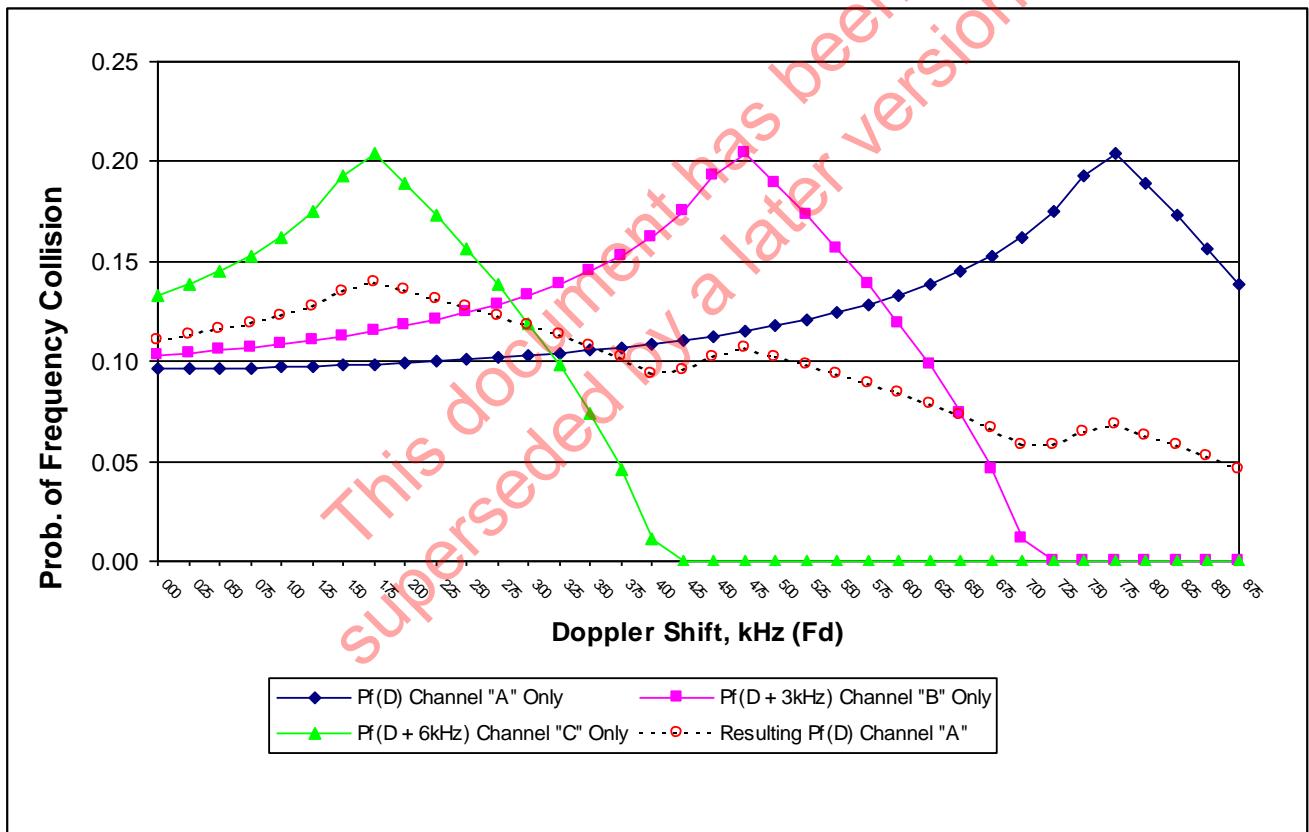
with: $P_f(D-j\delta) \neq 0$ if $j \leq (D_{\text{Max}} + \varepsilon + D) / \delta$,

$P_f(D-j\delta) = 0$ if $j > (D_{\text{Max}} + \varepsilon + D) / \delta$; and

with: $P_f(D+j\delta) \neq 0$ if $j \leq (D_{\text{Max}} + \varepsilon - D) / \delta$,

$P_f(D+j\delta) = 0$ if $j > (D_{\text{Max}} + \varepsilon - D) / \delta$.

Figure C-A.2: Combination of Probabilities of Frequency Collision for Three Adjacent Channels



Although the resulting probability of frequency collisions for beacons in channel C_i (e.g., 406.028 MHz) are on average lower than for a single channel, since beacons are spread over three channels (e.g., 406.022, 406.025 and 406.028 MHz), the probability of frequency collisions for bursts with small values of Doppler shifts (i.e. $f_D \leq 3.5$ kHz) is actually increased in channel C_i (e.g. 406.028 MHz) by comparison with the probability of frequency collisions in a single channel.

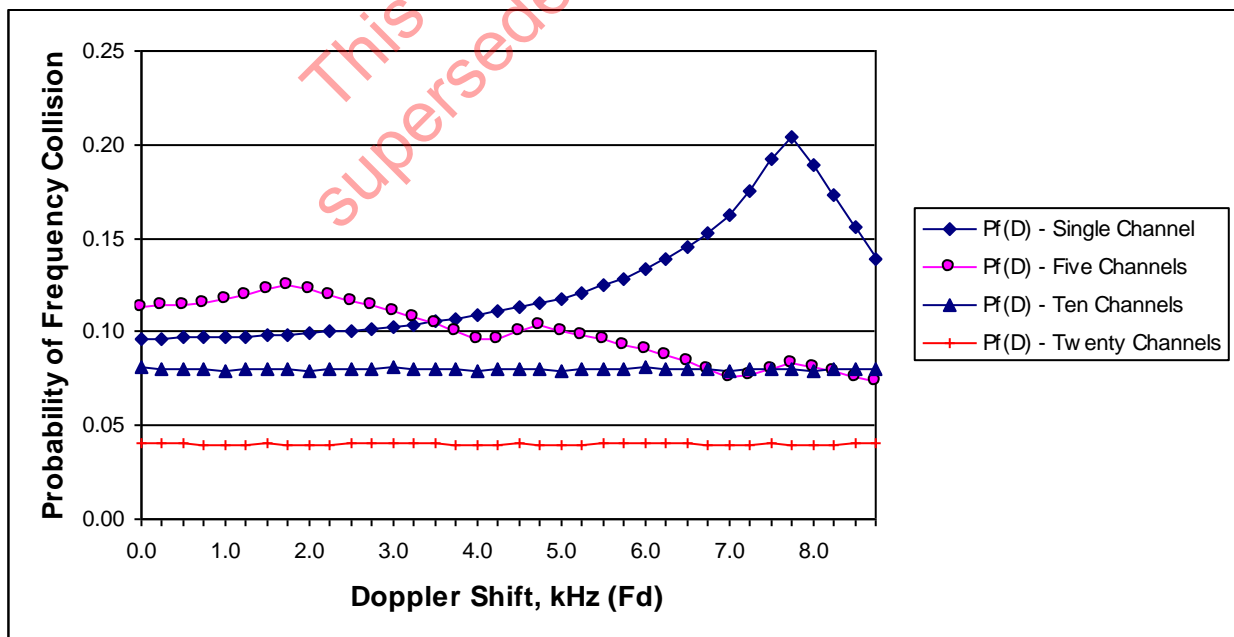
C-A.4 Results of the computation of $P_f(D)$

Table C-A.1 provides the numerical results of the computation of $P_f(D)$ for a single frequency channel, for the central frequency channel of five adjacent channels, ten adjacent channels and twenty adjacent channels. These results are illustrated in Figure C-A.3 below.

Table C-A.1: Probability of Collisions in the Frequency Domain

Fd (kHz)	0.00	0.25	0.50	0.75	1.00	1.25	1.50	1.75	2.00	2.25	2.50	2.75
D = Fd/FM	0.0000	0.0248	0.0497	0.0745	0.0993	0.1242	0.1490	0.1739	0.1987	0.2235	0.2484	0.2732
Pf(D) - Single Channel	0.0966	0.0966	0.0967	0.0969	0.0972	0.0976	0.0980	0.0986	0.0992	0.1000	0.1008	0.1018
Pf(D) - Five Channels	0.1137	0.1139	0.1145	0.1155	0.1171	0.1194	0.1228	0.1253	0.1224	0.1196	0.1168	0.1139
Pf(D) - Ten Channels	0.0807	0.0806	0.0803	0.0797	0.0785	0.0801	0.0807	0.0801	0.0785	0.0797	0.0803	0.0806
Pf(D) - Twenty Channels	0.0403	0.0403	0.0401	0.0399	0.0393	0.0401	0.0403	0.0401	0.0393	0.0399	0.0401	0.0403
Fd (kHz)	3.00	3.25	3.50	3.75	4.00	4.25	4.50	4.75	5.00	5.25	5.50	5.75
D = Fd/FM	0.2980	0.3229	0.3477	0.3725	0.3974	0.4222	0.4470	0.4719	0.4967	0.5216	0.5464	0.5712
Pf(D) - Single Channel	0.1029	0.1041	0.1055	0.1070	0.1087	0.1106	0.1128	0.1152	0.1179	0.1210	0.1245	0.1285
Pf(D) - Five Channels	0.1109	0.1078	0.1044	0.1006	0.0956	0.0963	0.1003	0.1031	0.1007	0.0982	0.0957	0.0931
Pf(D) - Ten Channels	0.0807	0.0806	0.0803	0.0797	0.0785	0.0801	0.0807	0.0801	0.0785	0.0797	0.0803	0.0806
Pf(D) - Twenty Channels	0.0403	0.0403	0.0401	0.0399	0.0393	0.0401	0.0403	0.0401	0.0393	0.0399	0.0401	0.0403
Fd (kHz)	6.00	6.25	6.50	6.75	7.00	7.25	7.50	7.75	8.00	8.25	8.50	8.75
D = Fd/FM	0.5961	0.6209	0.6457	0.6706	0.6954	0.7202	0.7451	0.7699	0.7948	0.8196	0.8444	0.8693
Pf(D) - Single Channel	0.1331	0.1385	0.1449	0.1527	0.1623	0.1748	0.1925	0.2043	0.1892	0.1733	0.1565	0.1385
Pf(D) - Five Channels	0.0903	0.0874	0.0842	0.0806	0.0758	0.0766	0.0807	0.0836	0.0813	0.0789	0.0764	0.0738
Pf(D) - Ten Channels	0.0807	0.0806	0.0803	0.0797	0.0785	0.0801	0.0807	0.0801	0.0785	0.0797	0.0803	0.0806
Pf(D) - Twenty Channels	0.0403	0.0403	0.0401	0.0399	0.0393	0.0401	0.0403	0.0401	0.0393	0.0399	0.0401	0.0403

Figure C-A.3: Probability of Frequency collisions as a Function of the Doppler Shift



APPENDIX B to ANNEX C
ANALYSIS OF A MULTI-SERVER COMMUNICATION SYSTEM
WITH POISSON ARRIVALS

Annex F to the Frequency Management Plan provides a forecast of the 406 MHz beacon population world-wide, and Annex G describes the 406 MHz beacon message traffic model which provides, for a given beacon population, the peak number (N) of active beacons in the visibility circle of a LEOSAR satellite. The system capacity is the value of N that corresponds to a probability of successful Doppler processing of 95%, according to the definition of the capacity given in section 2 of the Frequency Management Plan (C/S T.012).

C-B.1 The Erlang-B Standard Model

The Erlang-B communication system model assumes a limited number of servers and message arrivals that follow a Poisson distribution, i.e., the probability of n arrivals during a time interval t, is given by the expression:

$$P_n(t) = \frac{(\lambda t)^n}{n!} e^{-\lambda t} \quad \text{C-B/E.1}$$

where the average time between arrivals is γ and the arrival rate is $\lambda = 1/\gamma$;

In the LEOSAR system, the ‘service’ time (message processing time) of each message in the system is constant and equal to τ , duration of each message. The service rate is then $\mu = 1/\tau$.

Any message arriving when all DRUs are occupied is lost.

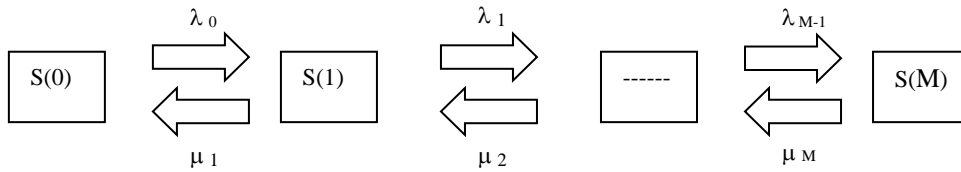
The Erlang-B model assumes that all arrivals are independent occurrences. This is not strictly the case in the LEOSAR message traffic since beacons are transmitting with a fairly stable repetition period. However, the duration of beacon-to-satellite visibility varies as a function of the CTA (Cross Track Angle = distance to the track of the satellite) and, as the satellite visibility area is constantly moving, beacons drop out of visibility while other enter the visibility area. A significant proportion of beacons also start transmitting during a satellite pass. Therefore, there is not a stable number of beacons in the satellite visibility circle, and new beacon arrivals, as well as beacon’s exits of the visibility circle, are clearly independent.

Another aspect of the LEOSAR system random access is that beacon bursts can be destroyed by collisions in time and frequency. This aspect is not reflected in the standard Erlang-B model and we will have to modify the model to account for these occurrences.

Despite the above limitations of the model, we assume that the modified Erlang-B model with a Poisson distribution of arrivals remains valid for the practical case of the LEOSAR system (ref: TG-1/2000/3/5; TG-1/2000/6/7; JC-14/9/7). This assumption has been verified in simulations of traffic loads fed into a test bench of the SARP instrument.

The various state transitions of a system with M servicing units are represented in the diagram of Figure C-B.1, where S(i) is the state of the system when i servers are occupied.

Figure C-B.1: Diagram of System State's Transitions



From the general theory of “birth and death” processes in a system of M servers, as illustrated above, the probability of the state S(i + 1) is

$$p_{i+1} = \frac{\lambda_i}{\mu_{i+1}} p_i \tag{C-B/E.2}$$

Therefore: $p_{i+1} = \frac{\lambda_0 \lambda_1 \dots \lambda_i}{\mu_1 \mu_2 \dots \mu_{i+1}} p_0$, where p_0 is the probability that the system is in state S(0).

As $\sum_{k=0}^M p_k = 1$, then $p_0 = \left(1 + \sum_{k=1}^M \frac{\lambda_0 \lambda_1 \dots \lambda_{k-1}}{\mu_1 \mu_2 \dots \mu_k} \right)^{-1}$, and $p_i = \frac{\lambda_0 \lambda_1 \dots \lambda_{i-1}}{\mu_1 \mu_2 \dots \mu_i} \left(1 + \sum_{k=1}^M \frac{\lambda_0 \lambda_1 \dots \lambda_{k-1}}{\mu_1 \mu_2 \dots \mu_k} \right)^{-1}$.

Under the assumptions made concerning the “birth” rate ($\lambda = \text{constant} = \lambda_0 = \lambda_1 = \dots = \lambda_i \dots$); and the “death” rate in state S(i) (i.e., $\mu_i = i * \mu$, so $\mu_1 = \mu$, $\mu_2 = 2\mu$, $\mu_i = i \mu$), the probability of a state S(i) is:

$$p_i = \frac{\lambda_{i-1}}{\mu_i} p_{i-1} = \frac{\lambda}{i \mu} p_{i-1} = \frac{\lambda^i}{i(i-1)\dots(1)\mu^i} p_0 = \frac{1}{i!} \left(\frac{\lambda}{\mu} \right)^i \left[1 + \frac{\lambda}{\mu} + \dots + \frac{1}{M!} \left(\frac{\lambda}{\mu} \right)^M \right]^{-1}$$

The probability that all (M) servers are occupied is:

$$P_M = \frac{\frac{1}{M!} \left(\frac{\lambda}{\mu} \right)^M}{1 + \frac{\lambda}{\mu} + \frac{1}{2!} \left(\frac{\lambda}{\mu} \right)^2 + \dots + \frac{1}{M!} \left(\frac{\lambda}{\mu} \right)^M}$$

C-B/E.3

The above formula is also known as the Erlang-B formula for a system with M service units when all ‘blocked’ arrivals are lost (i.e., no queues in the system).

In the communications system theory, $v = \lambda / \mu$ is the measure of traffic expressed in Erlang. For convenience, in the analysis of the LEOSAR and GEOSAR system capacity, we chose to express the system capacity as the equivalent number of beacons in the visibility area of the satellite that can be successfully processed with a probability of 95%. Therefore, we will also express the traffic as a number of active beacons in the visibility area of the satellite. This measure of traffic is linked to the Erlang unit as follows (see also section C.3.3 and equation C/E.14).

If (N) is the number of active beacons in the satellite visibility area, τ the duration of a beacon message transmission and T the beacon transmissions’ repetition period, the average density of beacon messages is:

$$\frac{N * \tau}{T} = \frac{\lambda}{\mu}; \text{ and } N = \lambda * T; \mu = 1/\tau. \quad \text{C-B/E.4}$$

C-B.2 Modified Erlang-B Model

In the LEOSAR SARP system, the probability p_i of the state $S(i)$, must be modified to account for the fact that, for a state transition to occur, the arriving beacon burst must be separated in the frequency domain from the bursts occupying the servers. We will assume that the probability of collision in the frequency domain is identical for all received bursts (i.e., $= P_f$) and remains small, and we will derive a modified Erlang-B formula.

Under the above assumption, the arrival rate λ_i is modified to account for the probability of frequency collision between an arriving burst and one of the bursts already under processing by the SARP, and λ_i becomes: $\lambda_0 = \lambda$; $\lambda_1 = \lambda(1 - P_f)$; $\lambda_2 = \lambda(1 - 2 P_f)$; and $\lambda_i = \lambda(1 - i * P_f)$.

We note P_f the probability of collision in the frequency domain, p_i the probability of the state “i”, and we note $\lambda/\mu = v$, then:

$$\begin{aligned} p_1 &= v p_0; \\ p_2 &= \frac{1}{2} v (1 - P_f) p_1; \\ p_3 &= \frac{1}{3} v (1 - 2 P_f) p_2; \text{ and} \end{aligned}$$

$$\text{more generally: } p_i = \frac{v}{i} (1 - (i - 1) P_f) p_i = \frac{v^i}{i!} (1 - (i - 1) P_f) (1 - (i - 2) P_f) \dots (1 - P_f) p_0 \quad \text{C-B/E.5}$$

Assuming a system with M servers, the probability of state $S(0)$, p_0 , should be modified as follows:

$$\begin{aligned} \sum_{k=0}^M p_k = 1 &= p_0 \left[1 + v + \frac{v^2}{2!} (1 - P_f) + \dots + \frac{v^M}{M!} (1 - P_f) (1 - 2 P_f) \dots (1 - (M - 1) P_f) \right] \\ p_0 &= \left[1 + v + \frac{v^2}{2} (1 - P_f) + \dots + \frac{v^M}{M!} (1 - P_f) (1 - 2 P_f) \dots (1 - (M - 1) P_f) \right]^{-1}; \quad \text{C-B/E.6} \end{aligned}$$

and the probability of k servers being busy becomes:

$$p_k = \frac{\frac{v^k}{k!} (1 - P_f) \dots (1 - (k - 1) P_f)}{1 + v + \frac{v^2}{2} (1 - P_f) + \dots + \frac{v^M}{M!} (1 - P_f) (1 - 2 P_f) \dots (1 - (M - 1) P_f)} \quad \text{C-B/E.7}$$

We define p_U as the probability that, in a system of M servers, at least one is free when a beacon burst is received by the satellite. This probability is expressed mathematically as follows:

$$P_U = P[S(0) \cup S(1) \cup S(2) \cup \dots \cup S(M-1)] = p_0 + p_1 + p_2 + \dots + p_{(M-1)}$$

Therefore:

C-B/E.8

$$P_U = \sum_{i=0}^{M-1} P_i = \frac{1 + v + \frac{v^2}{2!}(1 - p_f) + \dots + \frac{v^{M-1}}{(M-1)!}(1 - p_f) \dots (1 - (M-2)p_f)}{1 + v + \frac{v^2}{2!}(1 - p_f) + \dots + \frac{v^M}{M!}(1 - p_f)(1 - 2p_f) \dots (1 - (M-1)p_f)}$$

With $M = 3$ as in the LEOSAR SARP, this expression becomes:

C-B/E.9

$$P_U = \sum_{i=0}^2 P_i = \frac{1 + v + \frac{v^2}{2!}(1 - p_f)}{1 + v + \frac{v^2}{2!}(1 - p_f) + \frac{v^3}{3!}(1 - p_f)(1 - 2p_f)}$$

C-B.3 Application to the LEOSAR SARP

The Erlang-B standard model assumes a stable rate of arrivals (λ). The modified Erlang-B model replaces this stable arrival rate with an arrival rate that depends on the state of the system and the probability of frequency collisions, as arrivals are lost when they occur at the same frequency as that of a message being processed. However, we have shown in section C.3.2 of Annex C and at Appendix A to Annex C that the probability of frequency collision actually depends upon the position of the beacon and the corresponding Doppler ratio D . This means that equation C-B/E.9 is not directly applicable to the SARP system as the value of P_f is not fixed for the various states of the system and depends on the specific messages that are being processed.

However, it should be noted that P_U , the probability of having at least one free DRU when a message arrives, is actually increasing when P_f increases and this result remains true for all values of v (i.e., all values of N , the number of active beacons in the satellite visibility area). Therefore, by choosing the minimum value of P_f we would obtain the lower limit of P_U , which is consistent with a conservative approach to the system capacity.

The function $P_U = f(P_f)$ is illustrated in Figure C-B.2, which shows the evolution of P_U , calculated using C-B/E.9, when P_f increases, for two arbitrary values of N (i.e., $N = 90$ and $N = 180$).

Figure C-B.3 illustrates the evolution of $P_U(N)$ with two values of P_f ($P_{f(\min)} = 0.0966$, and $P_{f(\max)} = 0.2043$).

From Figure C-B.3, it can be seen that the impact of the choice of P_f is minimal for values of $N \leq 40$. Therefore, this aspect of the model will not have a significant impact on evaluation of the capacity of a single frequency channel, as N remains well below 40, but could impact the capacity estimate of a multi-channel system when the number of active beacons (N) in the satellite visibility area is significantly larger.

For the capacity calculation we will retain the minimum value of P_f (i.e., 0.0966 for a single channel, 0.0737 for a system of 5 adjacent channels, 0.0785 for ten channels and 0.0393 for 20 channels).

Figure C-B.2: Evolution of P_U as a Function of P_f

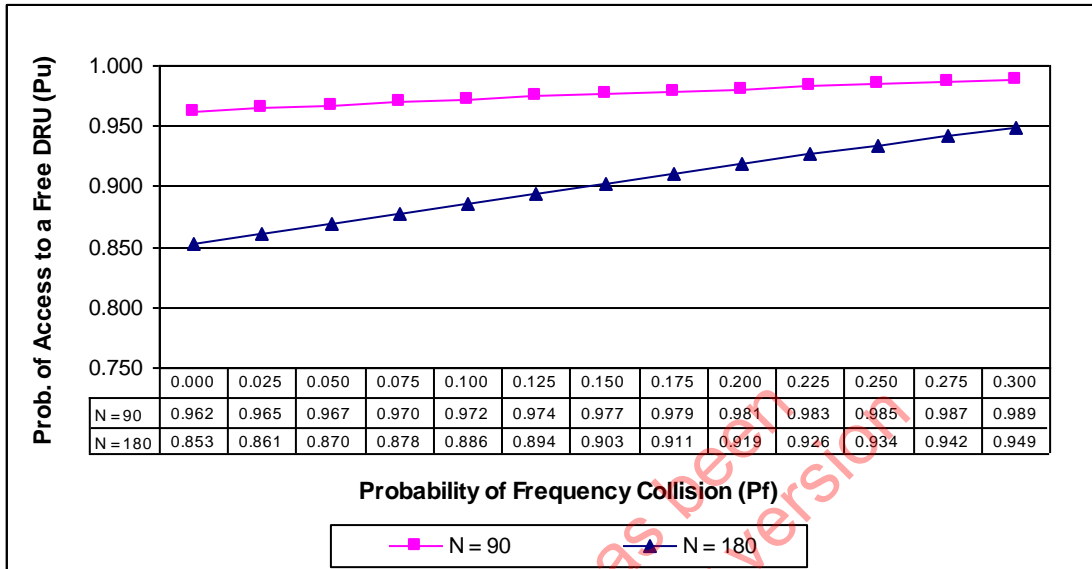
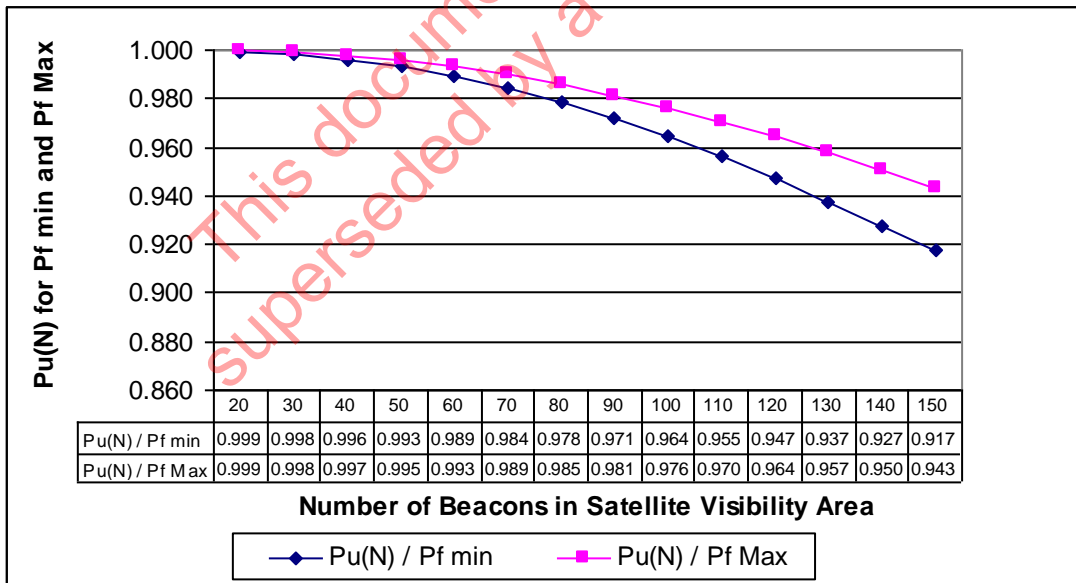


Figure C-B.3: $P_U(N)$ for (a) $P_{f(\min)} = 0.0996$ and (b) $P_{f(\max)} = 0.2043$



APPENDIX C to ANNEX C**PROBABILITY OF SUCCESSFUL DOPPLER PROCESSING
AND LEOSAR SYSTEM CAPACITY**

The definition of the LEOSAR system capacity provided in section 2.1 of the Cospas-Sarsat 406 MHz Frequency Management Plan (C/S T.012) requires achieving a successful Doppler processing (i.e. obtaining a Doppler location using at least four (4) frequency measurements) with a given probability.

The conservative approach adopted for the computation of the LEOSAR capacity requires that the probability of successful Doppler processing should be achieved in a worst case scenario: a satellite pass with a beacon at the edge of the satellite visibility area, which only provides for five (5) possible frequency measurements.

This Appendix summarises the computation of the probability of successful Doppler processing and analyses the evolution of this probability when a greater number of beacon bursts can be received by the satellite. In particular, it shows that the probability of successful Doppler processing improves significantly when the number of bursts that can be received during a satellite pass increases.

As shown in Appendix D, a definition of the capacity based on the average satellite pass duration would considerably increase the capacity figures of the LEOSAR system.

C-C.1 Probability of Successful Doppler Processing

The probability of successful Doppler processing is a function of the probability P_R of good reception of each single beacon burst when N beacons are active in the satellite visibility area.

The probability of reception of each burst is given by the following mathematical expression (equation C/E.18 in section C.3.5), where:

- T is the repetition period of the beacon transmissions and τ is the duration of a beacon burst;
- v is the average density of beacon messages ($N * \tau / T$);
- λ is the rate of beacon message arrivals (N / T);
- P_f is the probability of frequency collision that affects the burst received with a given frequency shift; and
- $P_{f \min}$ is the lower limit of the probability of collision in the frequency domain.

$$P_R = 0.99 * e^{-2\lambda P_f \tau} * \frac{1 + v + \frac{v^2}{2!} (1 - P_{f \min})}{1 + v + \frac{v^2}{2!} (1 - P_{f \min}) + \frac{v^3}{3!} (1 - P_{f \min}) (1 - 2P_{f \min})}$$

Therefore, for a given number “N” of active beacons in the satellite visibility area, the probability P_R varies for each burst received during the satellite pass, depending on the Doppler shift that affects the frequency of the received burst.

C-C.1.1 Computation for a Satellite Pass with a CTA = 22°

The probability of successful Doppler processing is defined as the probability of receiving at least four beacon messages during the satellite pass. For a pass with a CTA of 22°, during which a maximum of five beacon messages can be received, the expression of the probability of successful Doppler processing is given below, with P_i = probability of reception of the burst “i” (equation C/E.19 section C.3.6):

$$P_{DP} = P_1 * P_2 * P_3 * P_4 * P_5 \left(\frac{1}{P_1} + \frac{1}{P_2} + \frac{1}{P_3} + \frac{1}{P_4} + \frac{1}{P_5} - 4 \right)$$

C-C.1.2 Computation for Satellite Passes with CTAs < 22°

Although a similar computation would be possible for all satellite passes, it becomes extremely cumbersome when the number of messages that can be received during a satellite pass (M) increases beyond five. Therefore, a different approach is used.

We select the lowest probability of reception P_R during the pass (which corresponds to the highest probability of frequency collision) and apply it to all bursts that can be received during that pass. This allows the binomial formula (equation C/E.2 copied below) to be used, and provides a low estimate of the probability of successful Doppler processing.

$$P_{DP} = \sum_{i=m}^M C_M^i P_R^i (1 - P_R)^{M-i}; \text{ with } m = 4 \text{ and } M \text{ function of the CTA.}$$

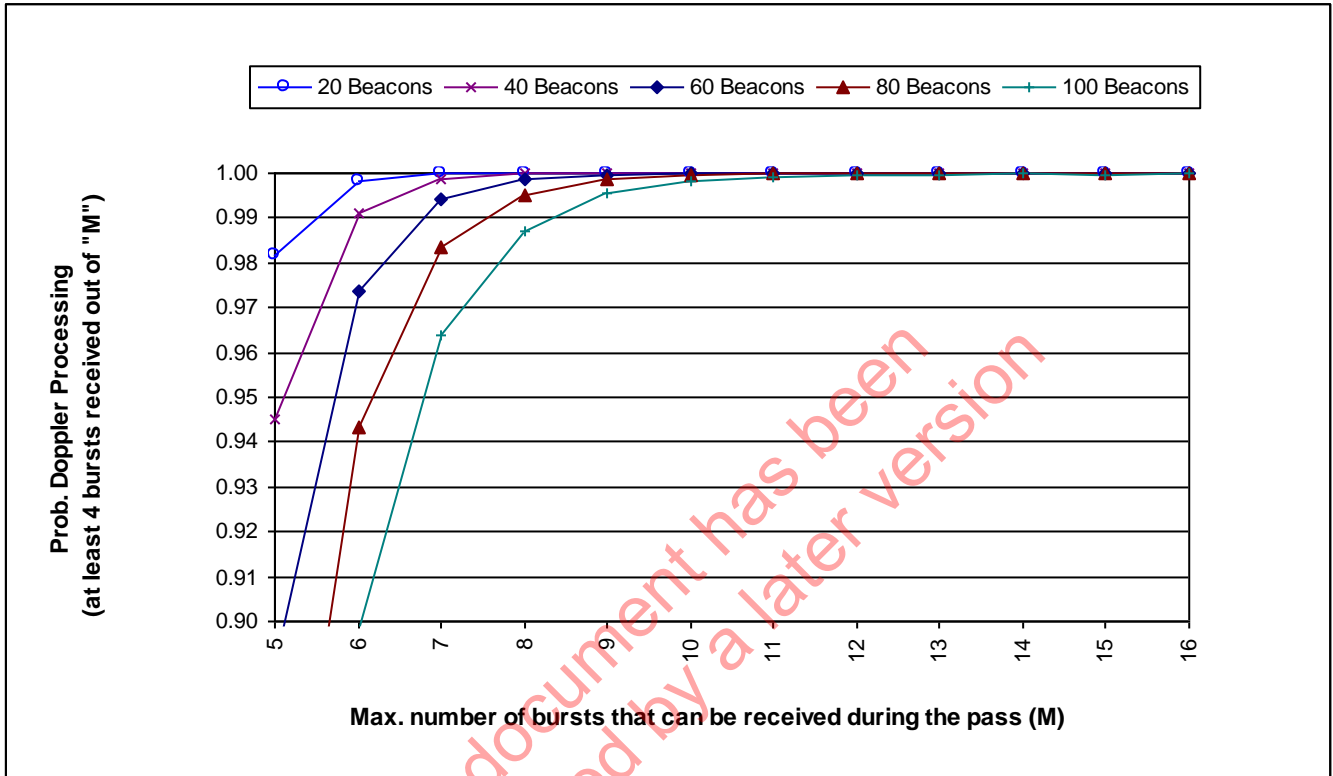
Despite the approximation used for this computation, the results (see Figure C-C.1) clearly show that the CTA of 22° used for the computation of the capacity (i.e. with $M = 5$) is the worst-case scenario.

C-C.2 Comparison of the Probability of Doppler Processing for Various CTAs

Figure C-C.1 provides the results of the computation of the probability of successful Doppler processing as a function of the maximum number of bursts (M) that can be received during a pass, and for various numbers of active beacons in the satellite visibility area (N).

Figure C-C.1 shows that, although the capacity computed in accordance with the hypotheses made in Annex C (CTA = 22°), is only 20 beacons for a single channel with 98% probability, or slightly below 40 beacons with 95% probability, 100 beacons would be processed successfully with a probability over 96% for all passes with a CTA ≤ 20° ($M \geq 7$), or with a probability over 98% for passes with a CTA ≤ 19° ($M \geq 8$).

**Figure C-C.1: Probability of Successful Doppler Processing
Short Messages, Single Channel
Satellite Passes with $CTA \leq 22^\circ$
(Nb of bursts received during pass ≥ 5)**



APPENDIX D to ANNEX C

RESULTS OF A SIMULATION OF THE LEOSAR SARP MULTIPLE ACCESS

C-D.1 Objectives of the Simulation

This appendix summarises the results of simulations of the SARP multiple access capability, performed by CNES using a beacon simulator to feed 406 MHz beacon messages into the engineering model of the SARP-2 instrument. The SARP-2 engineering model contains three data recovering units (DRUs) and is identical to the SARP-2 instruments carried on Sarsat LEOSAR satellites (ref. document JC-16/9/9).

The objectives of the simulations of the Sarsat LEOSAR Search and Rescue Processor (SARP-2) channel were to:

- a) validate the basic hypothesis of the theoretical analysis provided at section C.3 of Annex C;
- b) assess an “average” probability of successful reception of a valid beacon message, independent of the CTA of the beacon; and
- c) assess the number of active beacons in the LEOSAR satellite visibility circle that would achieve a 95% probability of successful Doppler processing if no conditions were imposed on the cross-track angles (CTAs) of the beacons.

C-D.2 Methodology

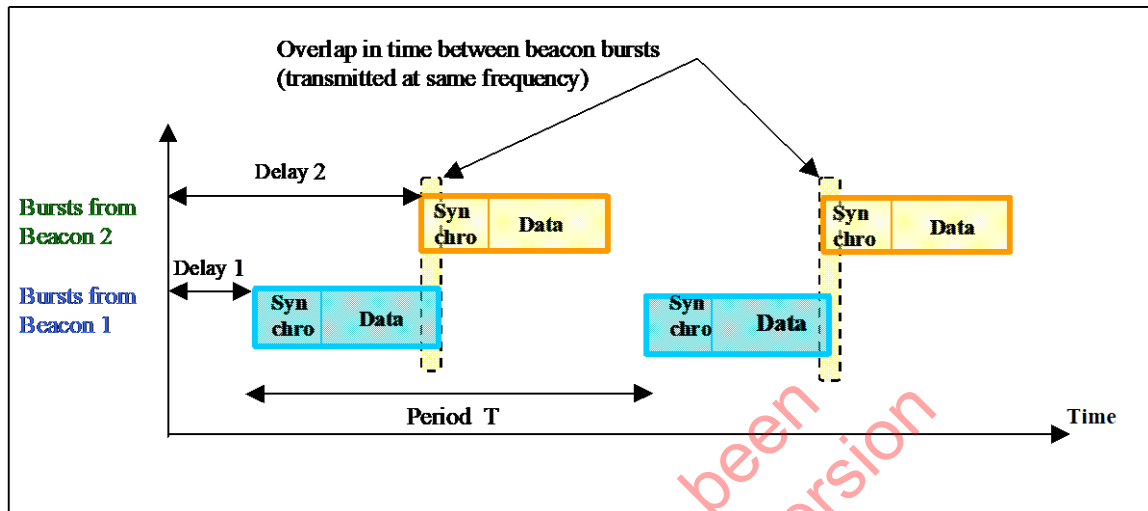
C-D.2.1 Simulation of Collisions in Time and Frequency

The equations provided at Annex C and the computations concerning $P_f(D)$, probability of collision in the frequency domain, have been confirmed using a MATLAB computer simulation for a single channel and three adjacent channels.

The probability P_U of having at least one free Data Recovery Unit (DRU) at the time of arrival of a beacon message at the satellite receive antenna is as given in section C.3.3 of Annex C.

A simulation of random access to the SARP instrument was performed using the CNES beacon simulator and the engineering model of the SARP. The beacon simulator was used to generate messages from two beacons transmitting at the same frequency, but with variable time delays (i.e., a variable overlap in time of two messages at the same frequency), as illustrated in Figure C-D.1.

The simulation results showed that messages could be retrieved even with some overlap in time and frequency, and that the performance of the SARP could be modelled by replacing the time interval of duration 2τ in the expression of the probability of no-arrivals PNA by an interval of duration $2*0.9*\tau$ (see section C.3.4 of Annex C).

Figure C-D.1: Simulation of Collisions in Time and Frequency with Variable Time Overlap

Therefore, the expression of the probability of reception of a single message with N beacons active in the satellite visibility area becomes:

$$P_R(N, D) = 0.99 * e^{-2*0.9*\lambda P_r \tau} * \frac{1 + v + \frac{v^2}{2!} (1 - p_{f \min})}{1 + v + \frac{v^2}{2!} (1 - p_{f \min}) + \frac{v^3}{3!} (1 - p_{f \min}) (1 - 2p_{f \min})} \quad \text{C-D/E.1}$$

The above expression of PR is a function of the number of active beacons (N) and the Doppler ratio (D). The next step is to determine an average probability of reception independent of D, as the simulation cannot provide statistically significant results for specific values of D, particularly those values associated with a CTA of 22°, which have a low occurrence.

C-D.2.2 Multiple Access Simulation – All CTAs (Average) Probability of Reception

As illustrated in Figure C-D.2, the satellite visibility circle is divided in narrow bands, each band being characterised by a typical Doppler ratio value, hence a typical value of the probability of collision in frequency $P_f(D)$ that we will designate $P_f(i)$ for band “i”. These bands are limited by curves of equal Doppler shift, defined by equation C-A/E.5 given at section C-A.1 (Appendix A to Annex C).

The number of active beacons in band “i” is $n(i)$:

$n(i) = N * S(i) / S$ where: N is the total number of active beacons in the satellite visibility area, which are assumed to be uniformly distributed;

S is the surface area of the satellite visibility circle;

S(i) is the surface area of band “i”; and

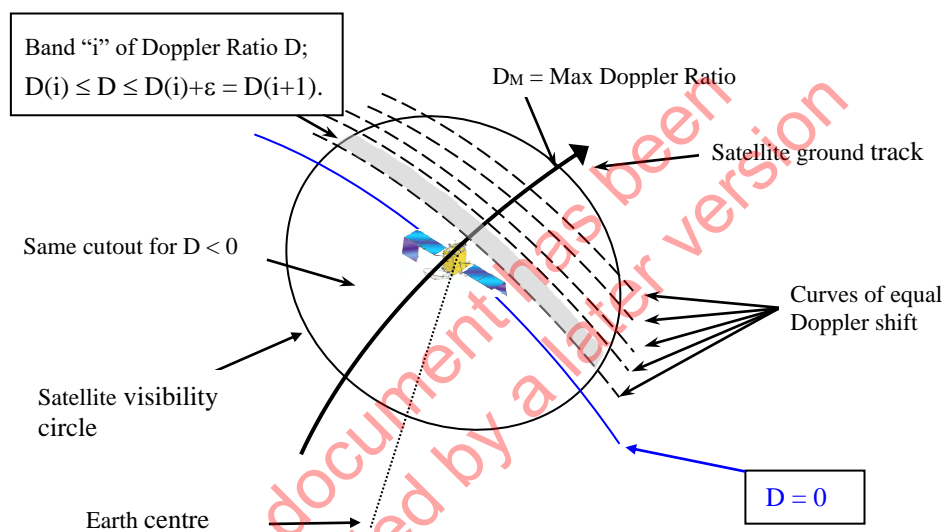
$n(i)$ is the number of active beacons in the band “i”.

The probability of reception for messages from beacons in band “i” is $P_R(i)$, as given by the above equation of $P_R(N,D)$. The average probability of reception of the bursts from the N active beacons in the satellite visibility area will then be given by the expression:

$$P_R(N) = \frac{1}{N} \sum_i n(i) * P_R(i)$$

C-D/E.2

Figure C-D.2: Determination of an “Average” Probability of Reception $P_R(N)$



The “average” probability of successful Doppler processing (designated P_{DS} to differentiate it from the probability P_{DP} defined in the analysis at Annex C as the probability of successful Doppler processing for beacons with a CTA of 22°) is derived from the simulation data, assuming that a minimum of 4 beacon bursts must be correctly received to obtain a Doppler location. It is equal to the ratio of the number of beacons for which at least 4 valid messages have been successfully retrieved, over the total number of beacons in the simulation run.

The simulation consisted of:

- generating a number of scenarios with variable parameters (number of active beacons, number of frequency channels, geographical distribution in the satellite visibility area, repetition periods, etc.); and
- measuring the probability of reception of individual beacon bursts as a function of the number of active beacons in the satellite visibility area.

Due to beacon simulator limitations, a maximum of 10 channels was simulated, with the assumption that the N beacons were evenly distributed amongst the channels. All beacon messages were assumed to be long format messages of duration 0.520 seconds, with a repetition period as specified in document C/S T.001 (i.e., $50 \text{ s} \pm 2.5 \text{ s}$).

C-D.3 Results of the SARP-2 Multiple Access Simulation

The simulation results allow:

- a comparison of the theoretical (as defined above) and measured (from the simulation results) probabilities of reception of individual beacon bursts;
- an assessment of the number of active beacons that would allow a 95% probability of successful Doppler processing “on average” (i.e., with no constraints on the beacon CTAs); and
- the determination of an optimum channel separation, which would maximise the capacity as defined above.

Note, however, that these results are not comparable to the determination of the capacity provided in Annex C, which assumes that the 95% probability of successful Doppler processing must be achieved for beacons with a CTA of 22°.

C-D.3.1 Comparison of Theoretical and Measured Probabilities of Reception

Tables C-D.1 and C-D.2 provide the simulation results for various numbers of active beacons and channel assignments. Each row provides the calculated probability of reception as provided by the equation of section C-D.2 (Theoretical P_R), the measured probability derived from the simulation data (Measured P_R), the ratio of the Theoretical over Measured P_R , and the probability of successful Doppler processing (P_{DS}) derived from simulation data.

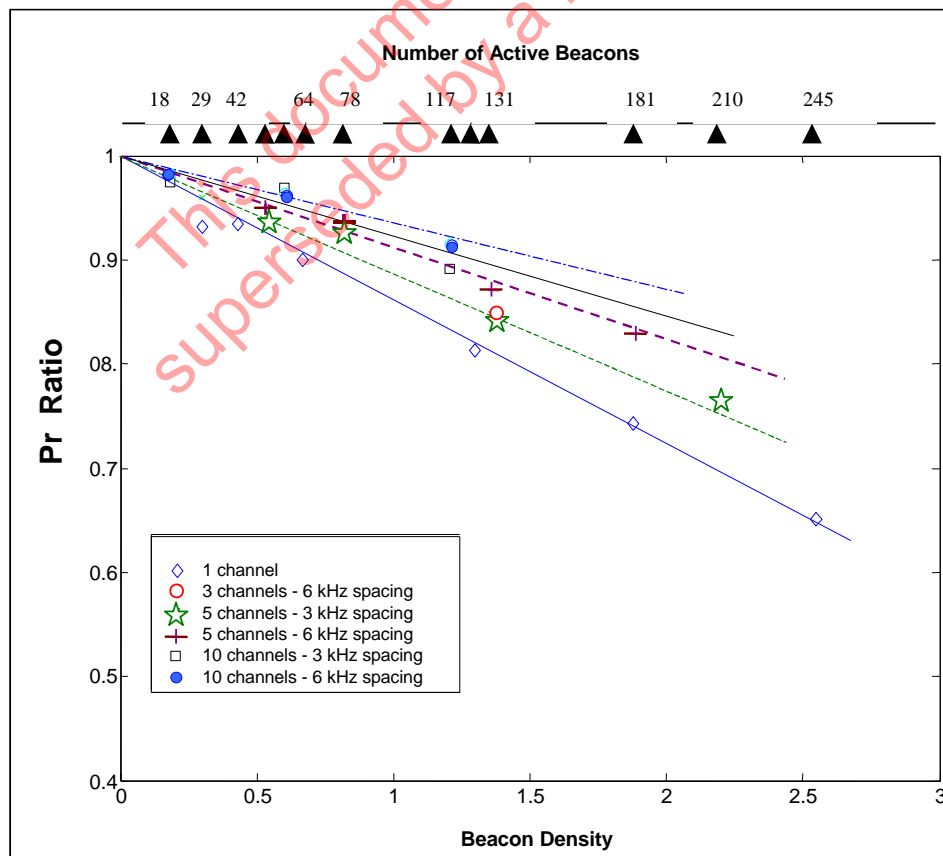
Table C-D.1: Simulation Results for One, Three or Five Channels

Number of Channels	Number of Active Beacons (Density)	Theoretical P_R (%)	Measured P_R (%)	P_R Ratio	Prob. Successful Doppler Processing P_{DS} (%)
1	29 (0.3)	91	98.41	0.93	100.0
5 (3 kHz spacing)	29 (0.3)	94	97.8	0.96	100.0
1	42 (0.43)	89	95.2	0.93	99.7
5 (3 kHz spacing)	52 (0.54)	90	95.62	0.94	99.9
5 (6 kHz spacing)	52 (0.54)	91.8	97.9	0.95	-
1	64 (0.67)	83	92.29	0.91	99.2
5 (3 kHz spacing)	78 (0.81)	84	91.01	0.92	99.5
5 (6 kHz spacing)	78 (0.81)	87.2	93.5	0.93	-
1	125 (1.3)	67	82.4	0.81	96.3
3 (6 kHz spacing)	131 (1.37)	72	84.8	0.85	-
5 (3 kHz spacing)	131 (1.37)	72	86.07	0.84	98.0
5 (6 kHz spacing)	131 (1.37)	76.2	87.7	0.87	-
1	181 (1.87)	54	72.65	0.74	90.0
5 (3 kHz spacing)	210 (2.19)	56	73.3	0.764	-
1	245 (2.55)	42	64.5	0.65	87

Table C-D.2: Simulation Results for Ten Channels

Channel Separation	Number of Active Beacons (Density)		Theoretical P_R (%)	Measured P_R (%)	P_R Ratio	Estimated P_{Ds} (%)
3 kHz spacing	18	(0.19)	96.8	99.54	0.974	100.0
6 kHz spacing	18	(0.19)	97.7	99.54	0.98	100.0
3 kHz spacing	58	(0.61)	91	94	0.968	100.0
6 kHz spacing	58	(0.61)	93.3	97	0.965	-
3 kHz spacing	117	(1.215)	79.8	89.95	0.89	99.0
6 kHz spacing	117	(1.215)	83.8	91.65	0.914	-

Figure C-D.3 illustrates the evolution of the theoretical-to-measured P_R ratio when the beacon density (i.e., the number of active beacons in the satellite visibility circle) increases. In particular, Figure C-D.3 shows that the measured P_R is always higher than the theoretical P_R , and the ratio decreases linearly when the density increases (except for low densities). This observation supports the conclusion that the theoretical values provided by the model are conservative, probably because of a power capture phenomenon that becomes significant when the density of beacons and the probability of collisions increase.

Figure C-D.3: Ratio of Theoretical to Measured P_R as a Function of Beacon Density

The simulation results also indicate that, in a multi-channel system, a 6 kHz separation between channels provides the highest “average” probability of reception.

C-D.3.2 Maximum Number of Active Beacons Providing a 95% Probability of Successful Doppler Processing

Finally, the measured probabilities of successful Doppler processing provided by the simulation are used to derive an estimate of the maximum number of active beacons in various channel assignment scenarios that would allow an average probability of successful Doppler processing of 95% (or 98%). These results are summarised in Table C-D.3 below, and compared with the results of the capacity analysis. Table C-D.3 shows clearly that a definition of the capacity based on an “average” probability of success (with no constraints on the CTA) would provide a much higher number of active beacons in the satellite visibility circle.

As the probability of reception and the probability of successful Doppler processing are computed as an average for all CTAs, the number of active beacons that can be successfully processed with a given probability increases with the number of adjacent channels. This result, which differs from the analysis of the theoretical capacity based on beacons with a CTA of 22°, is nevertheless consistent with the analysis of frequency collisions provided at Annex C, as the probability of frequency collisions does not increase for all CTAs when adjacent channels are in use.

However, as shown in the analysis presented at Annex C, the probability of successful Doppler processing for beacons with higher CTAs (i.e., at the edge of the satellite visibility circle) would be severely impacted if numbers of active beacons significantly greater than the nominal capacity were accepted in the LEOSAR satellite visibility area.

Table C-D.3: Maximum Number of Active Beacons Providing a 95% and 98% Probability of Successful Doppler Processing

	Nominal LEOSAR Capacity (Beacons with 22° CTA)		Max. Number of Active Beacons (All CTAs)	
	P _{DP} = 0.98	P _{DP} = 0.95	P _{DS} = 0.98	P _{DS} = 0.95
Single Frequency Channel	18	32	80	130
5 Channels (3 kHz spacing)	15	27	130	185
10 Channels (3 kHz spacing)	22	38	145	200

ANNEX D

GEOSAR CAPACITY MODEL

D.1 INTRODUCTION

The basic characteristics of the 406 MHz GEOSAR system are presented in section D.2.

The capacity of the Cospas-Sarsat 406 MHz GEOSAR system is defined as follows (see also C/S T.012, section 2):

“The number of 406 MHz distress beacons operating simultaneously in the field of view of a GEOSAR satellite that can be successfully processed by the System to provide beacon message information, under nominal conditions, within 5 minutes of beacon activation 95% of the time.”

However, the capacity could be defined using a different probability of success over a given time, e.g., 98% over 10 minutes. The rationale for using a 95% probability of success within 5 minutes is provided in section D.3. In addition, a number of conditions attached to the “nominal” scenario must be specified before selecting a nominal capacity figure (e.g., length of the beacon message, characteristics of the nominal communication link, etc.). These matters are also addressed in the first stage of the analysis (section D.3), which details the theoretical GEOSAR capacity model.

One of the basic assumptions of the GEOSAR capacity model is that 406 MHz frequency channels separated by 3 kHz are independent (i.e. beacons in adjacent channels do not interfere with each other). This is verified at Appendix A on the basis of frequency data collected from operational 406 MHz beacon transmissions.

The actual determination of the capacity of a GEOSAR channel is presented in section D.4, taking into account the impact of repetitive transmissions analysed in Appendices B and C. Appendix C analyses the distribution of beacon burst transmission times that meet the requirements of the C/S T.001 specification. However, because of the complexity of the analysis, no direct conclusions can be drawn in respect of the nominal GEOSAR capacity. To overcome this difficulty, a “simplified” analytical model is developed at Appendix B.

Finally, Appendix D provides the results of computer simulations that validate the analyses developed at Appendix B and Appendix C, and support the conclusion of the analysis in respect of a nominal GEOSAR channel capacity.

The GEOSAR capacity is determined by two basic aspects of the system.

Beacon transmission times are not synchronised and beacon messages may overlap in time and frequency, which may result in the loss of both messages in the GEOLUT processing. In the first step of the analysis we determine the probability for a beacon message to be received with no collision in time and frequency with another message.

406 MHz beacons transmit either short format or long format messages. The length of the transmitted message (i.e. the duration of the beacon burst) affects the probability of collision in time and, therefore, the system capacity. The analysis addresses the specific issue of retrieving complete long messages, and the associated probability of successful processing, for a population comprised of beacons that only transmit long messages.

In addition, signal processing in the GEOSAR system is characterised by low margins in the link budget, which result from the low power of the beacon signal at the satellite receiver. As a consequence, individual messages may be received with bit-errors and several bursts from the same beacon may need to be integrated before a GEOLUT is able to provide a valid 406 MHz beacon message. This integration process can be implemented in different ways, depending on the specific characteristics of the GEOSAR satellite and the GEOLUT. The second step of the analysis takes into account the need for integrating bursts. A theoretical GEOSAR system capacity is computed as a function of the number of bursts that are required for retrieving a valid beacon message.

The following step of the analysis characterises a nominal GEOLUT performance, by determining the number of bursts required by the integration process to produce a valid message, assuming a beacon signal at low EIRP. The results of the 1997/1998 GEOSAR Demonstration and Evaluation (D&E) are used to define the number of bursts required for the integration process.

The number of bursts selected as representing a nominal GEOLUT performance and the theoretical capacity model are then used to determine the nominal GEOSAR channel capacity.

The nominal GEOSAR channel capacity determined at this stage of the analysis is based on the hypothesis of a uniform distribution of the times of arrival of the beacon bursts at the satellite antenna. Unfortunately, this hypothesis is not consistent with the randomised repetition period of the beacon transmissions, as defined in document C/S T.001. This particular characteristic of the GEOSAR system is addressed in Appendices B, C and D to Annex D, and the nominal GEOSAR capacity is adjusted according to the conclusions derived from the analysis of repetitive transmissions.

Finally, the impact of a low EIRP signal on the time required to recover a valid message and the probability of obtaining a confirmation of a valid or complete beacon message within a given period of time are also assessed.

This document has been
superseded by a later version

D.2 BASIC GEOSAR SYSTEM CHARACTERISTICS

D.2.1 Random Access with Time Diversity

Beacon transmission times are not synchronised, consequently beacon message arrival times at the satellite receiver antenna are random. Therefore, messages (also referred to as beacon bursts in the capacity analysis) from different beacons may overlap in time.

The carrier frequency of a 406 MHz beacon is assigned to particular frequency channels in accordance with the Frequency Management Plan (e.g., 406.025 MHz for the first generation beacons). Within a channel, the beacon carrier frequencies are distributed around the specified centre frequency of the channel, due to variations in oscillator frequencies, aging, temperature, etc. A major difference with the LEOSAR system (see Annex C) is that the frequency of the bursts received by a GEOSAR satellite is not affected by any significant Doppler shift. Therefore, 406 MHz bursts from beacons transmitting in different channels will not collide in the frequency domain, assuming an appropriate frequency separation between channels. However, bursts from beacons in the same frequency channel may overlap both in time and frequency and interfere with each other.

The collision situation could be repeated in successive transmissions as each beacon emits bursts with a repetition period of approximately 50 seconds. The specification for 406 MHz beacons (C/S T.001) requires variations in beacon transmission repetition periods such that “two transmitters should not appear to be synchronised closer than a few seconds over a 5-minute period”. In addition, variations among production units and the diversity of beacon models should ensure a low probability of synchronised emissions repeating the time and frequency collision situation over a large number of successive bursts. However, the matter needs to be investigated further taking into account the actual implementation of the specification by manufacturers (see Appendices B and C to Annex D).

Data bits in the message transmitted by Cospas-Sarsat 406 MHz beacons are directly modulated on the carrier frequency using a narrow band PSK modulation. Any overlay in time and frequency between two beacon messages with an equivalent signal power typically results in the loss of both messages. This is not always the case if the overlapping messages are of distinctly different power, then some form of power capture may come into play and the stronger beacon message might be received correctly, while the weaker message is lost. In particular, this favourable power capture situation is possible with the CW transmission during the first 160 ms of the beacon message. However, the outcome of this situation may vary depending on a number of factors, including the processing capabilities of particular GEOLUTs. Therefore, the analysis addresses the worst-case scenario and assumes that any collision results in the loss of the message, except for the first part of long messages as discussed below.

As depicted in Figure D.1 below, Cospas-Sarsat 406 MHz beacons transmit either a short format or a long format message. Regardless of the message format, each beacon is uniquely identified when the GEOLUT is able to decode the first protected field of the message. This is sufficient to generate a distress alert.

The collision situation can affect the second protected field of a long message format, or the non-protected bits of the short message format, without affecting the first protected field. This situation allows for a correct processing of the alert (i.e., retrieving the correct beacon identification and data encoded in the first protected field), although the additional data encoded

in the second protected field of the long message, or the non-protected bits of the short message, may not be correctly retrieved. The specific case of the second protected field will be further considered below in sections D.2.2 and D.3.3.2, and we will base our assessment of the GEOSAR capacity on the probability of successfully retrieving the first part of the beacon message (i.e., a valid message consisting of the preamble and first protected field, see Figure D.1).

In summary, to remain consistent with the hypotheses made for the evaluation of the LEOSAR system capacity and with a conservative approach to the evaluation of the GEOSAR capacity, we will assume that:

- a) any overlay in time and frequency between beacon messages that affects the first part of a message (preamble, including the CW transmission, and first protected field) results in the loss of that message; and
- b) an active beacon has been successfully processed when a valid beacon message is recovered, as per the definition of valid messages in the GEOLUT specification and design guidelines document (C/S T.009), i.e., the first protected field of the beacon message is recovered with a maximum of two bit errors, which can be reliably corrected using the BCH error correcting code.

Figure D.1: Short and Long Formats of 406 MHz Beacon Messages

Preamble			First Protected Field					Non-Protected Data Field
			First Protected Data Field (PDF-1)				BCH-1	
Unmodulated Carrier	Bit Synchronization Pattern	Frame Synchronization Pattern	Format Flag	Protocol Flag	Country Code	Identification or Identification plus Position Data	21-Bit BCH code	Emergency Code/ National Use or Supplement. Data
Bit No.	1-15	16-24	25	26	27-36	37-85	86-106	107-112
160 ms	←----- 280 ms -----→							

Preamble			First Protected Field					Second Protected Field	
			First Protected Data Field (PDF-1)				BCH-1	Second Protected Data Field (PDF-2)	BCH-2
Unmodulated Carrier	Bit Synchronization Pattern	Frame Synchronization Pattern	Format Flag	Protocol Flag	Country Code	Identification or Identification plus Position Data	21-Bit BCH code	Supplementary and Position or National Use Data	12-Bit BCH code
Bit No.	1-15	16-24	25	26	27-36	37-85	86-106	107-132	133-144
160 ms	←----- 265 ms -----→							←----- 95 ms -----→	

D.2.2 Relationship Between GEOSAR Capacity and 406 MHz Beacon Message Formats

The above assumptions, which characterise the successful processing of a message, would be sufficient for a population consisting of beacons transmitting short format messages, which have only one protected data field. The beacon specification document C/S T.001 also defines long format messages that have a second data field protected by a second BCH error protecting code, as shown in Figure D.1.

In messages from location protocol beacons, the second protected field primarily contains the beacon location data (User Location Protocol), or additional position data that complete the first protected field “coarse” location information to provide a higher resolution of the encoded position (Standard and National Location Protocols).

The probability of collisions is higher in a population that includes beacons transmitting long messages of 520 ms duration, in comparison to the same population comprising only beacons that transmit the short format messages of 440 ms duration. Therefore, a longer time may be needed to obtain the required number of bursts without collisions, which results in a lower system capacity, assuming the same performance requirements (i.e., 95% of valid messages within 5 minutes).

Noting that our assessment of the GEOSAR capacity is based on retrieving valid messages (i.e., the first protected field only), as outlined in section D.2.1 above, we will apply the requirement of a 95% probability of success within 5 minutes under a constraint that assumes a full system load of long messages. However, we will also verify that, under these conditions:

- a) a complete short message, including the non protected field, is retrieved within 5 minutes with a probability greater than 95% when the population includes short messages only; and
- b) a complete long message (i.e., first and second protected fields) is retrieved within 5 minutes with a probability higher than 90% and within 10 minutes with a probability higher than 99%, when the population includes only beacons transmitting long format messages.

D.2.3 Channelisation of the 406.0-406.1 MHz Frequency Band

The probability that a beacon burst may be affected by a collision in time and frequency increases with the number of active beacons in visibility of the satellite. This, in turn, affects the probability of successfully recovering a valid message.

On the basis of the observed dispersion of actual beacon carrier frequencies and the spectrum width of 406 MHz beacon transmissions, Appendix A to Annex D shows that channels with a 3 kHz separation can be considered as independent in the GEOSAR system. Therefore, the obvious solution to increasing the capacity of the GEOSAR system is to spread the beacon population amongst several channels in the 406.0 – 406.1 MHz frequency band, separated by at least 3 kHz.

Frequency channels separated by 3 kHz being independent in the GEOSAR system, the total GEOSAR system capacity will increase linearly with the number of frequency channels opened for use. It is assumed that the load of beacon messages on the satellite transponder does not impact significantly on the system performance. However, channel impairments and interference from other sources may have a severe impact on the ability of the system to successfully process beacon messages, and can significantly decrease its capacity as defined above. The nominal conditions applicable for the definition of the GEOSAR capacity (see Annex B to C/S T.012) assume that there are no significant sources of interference operating in the GEOSAR satellite uplink or downlink bands.

D.2.4 GEOSAR Satellite Characteristics and GEOLUT Processing

The Cospas-Sarsat GEOSAR system uses 406 MHz repeaters installed on-board a variety of geostationary satellites (e.g., the USA Geostationary Operational Environmental Satellites (GOES), satellites in India's INSAT series, the European Meteorological Satellite Organisation (EUMETSAT) Meteosat Second Generation (MSG) series, etc.). These satellites have different 406 MHz transponder implementations, which result in different link budgets.

In addition, although all commissioned GEOLUTs must satisfy minimum performance requirements (see the GEOLUT commissioning standard in document C/S T.010), their characteristics are not identical and both the GEOLUT receiving system and the GEOLUT message processing can introduce performance variations, in particular in respect of the probability of successfully recovering a valid beacon message at a given power threshold. Furthermore, actual environmental conditions may significantly differ amongst various GEOSAR systems, and from the "nominal conditions" applicable to the definition of capacity. It should be noted that the impact of such variations is mitigated by the redundancy built in the GEOSAR ground segment, as several GEOLUTs are tracking each of the GEOSAR satellites and successful processing of the beacon emissions by a single GEOLUT is sufficient to provide an alert message.

From the point of view of the GEOSAR capacity model, these variations can be accounted for in terms of the number of beacon bursts that need to be integrated to recover a valid message. This is directly related to the processing time required for achieving the 95% probability of successful processing.

The evaluation of the capacity of each GEOSAR system should take into account these variations. Nevertheless, a nominal GEOSAR capacity figure has to be selected for the purpose of managing the use of the 406 MHz frequency band. This matter is further addressed in section D.3.4, which analyses the results of the GEOSAR Demonstration and Evaluation (D&E) tests performed in 1997 and 1998 (see the Report of the GEOSAR D&E, C/S R.008).

D.2.5 Repetitive Beacon Burst Collisions in Time and Frequency

Document C/S T.001 (beacon specification) requires the repetition period of the beacon transmissions to be randomised, with a time interval between transmissions of $50 \text{ sec} \pm 5\%$ such that "the repetition period shall not be so stable that any two transmissions appear to be synchronised closer than a few seconds over a 5-minute period". This definition also specifies the intervals between transmissions, which shall vary randomly between 47.5 and 52.5 seconds.

The hypothesis of a uniform distribution of arrival times of beacon bursts at the satellite is valid for analysing the probability of collision that affects the first burst transmitted by a beacon, but the analysis shows that, because of the repetitive nature of beacon transmissions, this hypothesis is not applicable for subsequent bursts. Furthermore, if a collision occurs, subsequent bursts have a higher probability of collision than the statistical average. Consequently, in a worst-case scenario (e.g., first burst collision) a particular beacon could have a much lower probability of successful processing.

Therefore, if the nominal GEOSAR channel capacity is determined on the basis of a non-conditional (or "average") probability of successful processing, (i.e. as opposed to a conditional probability that would assume a first-burst collision), then the analysis must also characterise the system performance in the worst-case scenario, e.g. the time required to achieve successful

processing (including the confirmation process) after a first-burst collision, to verify that acceptable processing times are still achieved.

Beacon bursts experience “on average” the same probability of collision in a uniform distribution of their times of arrival at the satellite antenna and in the distribution that results from the C/S T.001 specification (repetitive transmissions). This is a consequence of the fact that statistically, the average burst density over any 50-second time interval is identical in both distributions. However, computer simulations based on these distributions indicate that the resulting probability of processing success differs between the two distributions. This is verified not only for the conditional probability of success in the worst-case scenario of the C/S T.001 distribution, but also for the non-conditional (average) probability of success under the constraint of repetitive transmissions as defined by the C/S T.001 specification.

Another significant difficulty is that, because the distribution of burst transmission times defined by the C/S T.001 specification does not provide a stable probability of collision for successive bursts, no direct conclusions in respect of the nominal GEOSAR capacity can be drawn from the analysis provided at Appendix C to Annex D for the C/S T.001 distribution.

Therefore, a “simplified” analytical model is developed at Appendix B to Annex D with a different interpretation of the requirement for randomised repetition periods, which allows, by comparison with the results of Appendix C, to draw conclusions on the nominal GEOSAR channel capacity.

The results of the analyses are supported by computer simulation results reported and discussed at Appendix D to Annex D.

This document has been
superseded by a later version

D.3 GEOSAR CAPACITY ANALYSIS

D.3.1 Methodology of GEOSAR Capacity Assessment

D.3.1.1 Probability of No-Collision in Time and Frequency

The first stage of the analysis is to compute the probability of collisions in time and frequency, and to derive a probability of no-collision (P_{NC}). The impact of the length of the beacon message on the probability of collisions is also assessed.

Appendix A to Annex D shows that frequency channels separated by 3 kHz are independent in the context of the GEOSAR system; i.e. bursts from beacons operating in different channels do not collide in the frequency domain with any significant probability. Appendix A also shows that there is little spreading of the beacon carrier frequencies within a given channel, therefore, it can be assumed that bursts from beacons in the same channel always overlap in frequency, i.e., $P_f = 1$. Then, P_{NC} will only depend on the probability of collisions in time for bursts in the same frequency channel.

In the first stages of the analysis presented below in Annex D, the times of arrival of beacon bursts at the satellite antenna are assumed to be random, with a uniform distribution over each period (i.e., the repetition period does not affect the distribution). Appendices B and C address the particular case of repeated collisions in time over successive bursts of the same beacon and analyse the impact of the worst-case scenario (e.g., first-burst collision in Appendix C) on the processing time of a particular beacon.

In Appendix B, we assume a possible specification of the beacon repetition period, whereby the bursts transmission times are randomised around a time defined by a fixed period. Although this interpretation of the repetition period is not in accordance with the specification of document C/S T.001, it is useful for interpreting the following stages of the analysis.

In Appendix C, the repetition period is assumed to be random around the mean value of 50 seconds, as defined in document C/S T.001. The analysis of Appendix C is more complex than that provided in Appendix B, and its results in respect of the probability of frequency collision can only be interpreted by comparison with the results outlined in Appendix B. This matter is further addressed in section D.4, which draws conclusions on the nominal GEOSAR channel capacity. However, for simplicity, the preliminary analysis in section D.3 is performed assuming a uniform distribution of the arrival times, without the added constraint of repetitive transmissions with randomised repetition periods.

D.3.1.2 Theoretical GEOSAR Capacity

Because of the available link budget, and the resulting bit error rates, a single burst processed by the GEOLUT may not produce a valid message, and several successive bursts from the same beacon may need to be integrated. The number of bursts that need to be integrated to produce a valid message characterises the performance of a particular GEOSAR link. Therefore, the second stage is to analyse how the GEOLUT integration process affects the system capacity.

A thorough mathematical analysis of the GEOSAR capacity would require a detailed knowledge of the integration process and of the probability of successfully retrieving a valid message for each number of bursts used in an integration. This information is not available as it depends on a large number of factors, which vary with the specific GEOSAR system under consideration. Therefore, we will analyse the system capacity for various values of “K”, the

number of bursts required for a successful integration, assuming a probability of successful integration equal “1” if the number of bursts received with no collision is equal to or greater than K , and a probability of success equal “0” if the number of bursts is lower than K .

The results of this analysis provide a “theoretical” GEOSAR capacity, as a function of the number of bursts that need to be integrated to achieve successful processing. This is used to derive the “nominal” GEOSAR system capacity in the final stage of the analysis.

D.3.1.3 Nominal GEOSAR System Capacity

Depending on the actual performance of the GEOSAR satellite link and GEOLUT processing, different GEOSAR system implementations may exhibit different capacities. Furthermore, the actual environmental conditions, and particularly the actual beacon EIRP can show great variations depending on the circumstances of the distress event (e.g., beacon position relative to the satellite, floating EPIRB at sea, or ELT from a crashed aircraft on land). However, for the purpose of the management of the 406 MHz frequency band, we must establish a model that provides the “nominal” GEOSAR system capacity.

We analyse the results of tests performed during the GEOSAR D&E phase in 1997 and 1998, and define a nominal scenario characterised by a minimum beacon EIRP (or the corresponding minimum C/No of the input signal at the GEOLUT). This nominal scenario provides the required input for the theoretical capacity model, expressed as a number of bursts required for the successful processing of a beacon signal at the minimum EIRP selected for the nominal scenario.

At this stage, the determined nominal GEOSAR channel capacity must be adjusted to take into account the conclusions of the analysis of repetitive transmissions provided at Appendices B and C, and the computer simulation results provided at Appendix D.

Finally, we compute, for a traffic load at the nominal capacity level, the probabilities for obtaining “confirmed” valid or complete messages, as defined in the GEOLUT specification (i.e., obtaining a second valid or complete alert message identical to the first alert message, within a given time).

D.3.2 Probability of Burst Collisions in the GEOSAR System

If P_c is the probability of collision in time and frequency when 2 beacons are active, the probability of no-collision for the bursts of a specific beacon when N beacons are active is:

$$P_{NC}(N) = (1 - P_c)^{N-1} \quad \text{D/E.1}$$

$P_c = (P_t * P_f)$, where P_t is the probability of collision in time and P_f is the probability of collision in the frequency domain.

The following sections provide the determination of P_f and P_t .

D.3.2.1 Probability of Collision in Frequency (P_f)

This section summarises the analysis of actual beacon frequency spreading provided in Appendix A to Annex D, which shows that channels with a 3 kHz separation are independent, i.e. messages from beacons in different channels do not overlap in frequency, and messages from beacons in the same channel always overlap in frequency.

The specification for Cospas-Sarsat 406 MHz distress beacons (document C/S T.001) requires that, for all beacon models type approved before 1 January 2000, the transmitted frequency be set to 406.025 MHz \pm 2 kHz, and that this carrier frequency not vary more than \pm 5 kHz in 5 years, including the initial offset.

If the beacon carrier frequency had been uniformly distributed in the \pm 2 kHz allowed around 406.025 MHz ($\Delta F = 4$ kHz), then the probability of frequency collision (assuming no additional spreading due to aging, and assuming a GEOLUT receiver filter bandwidth of $\Delta f = 1.5$ kHz) would have been:

$$P_f(|f_1 - f_2| < \Delta f) = P(f \in 2\Delta f) = \frac{2\Delta f}{\Delta F} = \frac{2 * 1.5}{4} = 0.75$$

In such a case, and assuming that ageing would not significantly affect the distribution of carrier frequencies, a separation of at least 4 kHz between frequency channels would be required to achieve a uniform distribution of beacon carrier frequencies throughout the frequency band used by Cospas-Sarsat beacons.

However, available data on actual beacon transmitted frequencies show that 95% of all carrier frequencies are within a 1.5 kHz bandwidth, which is quite far from a uniform distribution in the theoretical 4 kHz bandwidth allowed by the specification.

The actual distribution of beacon carrier frequencies is approximately Gaussian (ref. TG-1/2000/4/2), i.e. the probability density function satisfies the equation:

$$f(x) = \frac{1}{\sigma\sqrt{2\pi}} e^{-\frac{(x-\mu)^2}{2\sigma^2}} \quad \text{D/E.2}$$

where:

- x is the variable representing the frequency (to avoid confusion with the density function f);
- μ is the mean value of the beacons carrier frequency (406.025 MHz); and
- σ is the standard deviation of the distribution (290 Hz on average).

The detailed analysis of actual data provided by the USA Cospas-Sarsat Mission Control Centre (USMCC) is at Appendix A to Annex D. This analysis demonstrates that:

- less than 4.2% of bursts from beacons in the same channel would be separated in frequency by more than 1.5 kHz (filter bandwidth) and, therefore, the probability of collision in frequency P_f is greater than 0.958; and
- a 3 kHz separation between channels ensures that two beacons in adjacent channels will have a probability of collision of about 2% and, therefore, adjacent channels separated by 3 kHz can be considered independent.

For simplicity, we will assume that, in the GEOSAR system, $P_f = 0$ for beacons in different frequency channels, and $P_f = 1$ for beacons in the same frequency channel.

D.3.2.2 Probability of Collision in Time (P_t) for Short or Long Format Messages

Each active beacon in the system transmits a burst of duration τ with a repetition period T . Two bursts collide in time when the distance in time of their arrivals $|t_1 - t_2|$ is less than τ , the duration of one burst.

If we assume that any two beacons are independent and the times of arrival of the bursts at the satellite receiver antenna conform to a uniform distribution over the time period T , then the probability for a message $M(1)$ to overlap in time with another message $M(2)$ is:

$$p_t(|t_1 - t_2| < \tau) = p(t \in 2\tau) = \frac{2\tau}{T} \quad \text{D/E.3}$$

406 MHz beacons transmit either a short format message of 440 ms duration, or a long format message of 520 ms duration, with a repetition period of 50 s. The message structure is illustrated in Figure D.1.

With $T = 50\text{s}$ and $\tau = 0.44\text{s}$ for short format messages, $P_t = 0.0176$.

With $T = 50\text{s}$ and $\tau = 0.52\text{s}$ for long format messages, $P_t = 0.0208$.

Note: In the GEOSAR capacity analysis, we have to consider a large, static visibility area. The random beacon activation times and the random distribution of beacons in the satellite visibility area result in random arrival times at the satellite antenna, which, in the first stages of the analysis, are assumed to conform to a uniform distribution over one beacon repetition period. This hypothesis is not valid when the repetition period of the beacon transmissions is taken into consideration, but it simplifies the preliminary consideration developed in section D.3 (see D.3.2.4). The impact of repetitive transmissions is further considered in section D.4 and at Appendices B and C to Annex D.

D.3.2.3 Probability of Collision in Time for the First Protected Field of Long Format Messages

The above expressions of P_t apply to populations of beacons that are either all transmitting short format messages, or all transmitting long format messages. In this section we will determine the probability that, in a population of beacons that all transmit long format messages, the first part of the message, which contains the preamble and the first protected field (see Figure D.1), is not interfered with by collisions in time and frequency.

If a long format message $M(1)$ arrives at the time “ t_1 ”, it will collide in time with long format messages $M(2)$ that arrive at a time t_2 if:

$$t_2 \geq (t_1 - 0.520 \text{ s}) \text{ and } t_2 \leq (t_1 + 0.520 \text{ s}).$$

However, if the message $M(2)$ arrives at t_2 such as $t_2 > (t_1 + 0.425 \text{ s})$, then, the interfering message $M(2)$ will not affect the first protected field of message $M(1)$. Therefore, the probability of collisions that would affect the first protected field of a long message is:

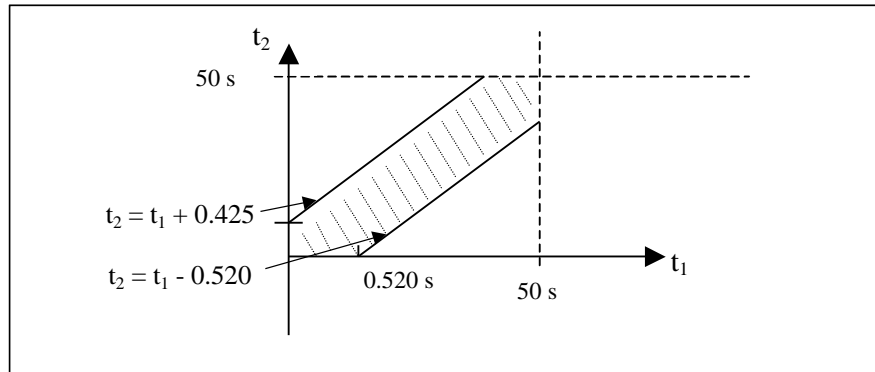
$$P[t_2 \geq (t_1 - 0.520 \text{ s})] \cap P[t_2 < (t_1 + 0.425 \text{ s})]$$

Figure D.2 provides a graphic representation of the probability of collision for the first part of long messages (preamble + first protected field), assuming the message arrival times t are uniformly distributed over the period $T = 50 \text{ s}$.

The mathematical expression of this probability is:

$$P_t = \frac{1}{T^2} \left(T^2 - \frac{1}{2}(T - \tau_1)^2 - \frac{1}{2}(T - \tau_2)^2 \right) \text{ with } \tau_1 = 0.425 \text{ and } \tau_2 = 0.520;$$

$$P_t = \frac{\tau_1 + \tau_2}{T} + \frac{\tau_1^2 + \tau_2^2}{2T^2} \cong \frac{\tau_1 + \tau_2}{T} = 0.0189 \quad \text{D/E.4}$$

Figure D.2: Probability of Collision in Time for the First Part of Long Messages

D.3.2.4 Repetitive Transmissions with Randomised Periods

The implementation of the C/S T.001 specification on the beacon message repetition period could result in two, or more, beacons experiencing repeatedly a probability of burst collisions much higher than the probability computed in the above sections, which assumed a uniform distribution of transmission times over the period T.

The impact of randomised transmission times as specified in document C/S T.001 (406 MHz beacon specification) is analysed in detail in Appendix C to Annex D. Unfortunately, this analysis shows that no direct conclusions can be drawn in terms of a probability of processing success, hence in terms of a nominal GEOSAR capacity. Another possible implementation of randomised transmission times with a 50 s repetition period, which provides for similar probabilities of burst collision, is analysed at Appendix B to Annex D.

This second analysis and the computer simulation results provided at Appendix D to Annex D show that the nominal capacity is reduced from 17 active beacons (as determined below assuming a uniform distribution of beacon bursts) to 14. In the worst-case scenario of Appendix B, the retrieval of valid or complete long messages of a particular beacon, as well as the confirmation process, are delayed by a few minutes when the system experiences a traffic load equal to the nominal capacity. However, under this traffic constraint and in the worst-case scenario, the probability of recovering valid and complete long messages remains greater than 85 % within 5 minutes and greater than 99 % over 10 minutes (see Table D-B.1 with N = 14).

The conclusions of the analysis of randomised repetition periods are further discussed in section D.4, but at this stage of the analysis of the GEOSAR channel capacity we will not address the matter of periodic transmissions, and we will assume that the burst arrival times are uniformly distributed over each period.

D.3.2.5 Probability of No Collision (P_{NC})

From the above analysis, the probability of no-collision for a given burst when N beacons are active in a given channel becomes:

$$P_{NC}(N) = (1 - P_t * P_f)^{N-1} = (1 - P_t)^{N-1} \quad D/E.5$$

The probability of no-collision for beacons in different frequency channels is $P_{NC} = 1$.

As a consequence, the total GEOSAR system capacity will be the sum of the capacities of all frequency channels opened for use. The following stages of the analysis will only consider the capacity of a single frequency channel.

D.3.3 Probability of Successful GEOSAR Processing

Because of the available link budget, the energy of several bursts from the same beacon may need to be integrated to obtain a valid message. The number of bursts to be integrated will depend on a number of factors, including:

- the actual environmental conditions and specific characteristics of the GEOSAR link;
- the actual beacon EIRP; and
- the actual performance of the GEOLUT integration algorithm.

The C/N_0 observed at the GEOLUT receiver depends on the GEOSAR link budget, which is affected by the actual beacon EIRP. From the GEOSAR capacity analysis perspective, the actual performance of the GEOLUT for a given C/N_0 is translated into a number of bursts required to achieve successful processing. In the following sections we will analyse the probability of successful GEOLUT processing as a function of the number of bursts required to obtain a valid message.

Note: All computations in the theoretical analysis provided in this section assume a probability of collisions in time based on the hypothesis of a uniform distribution of the beacon burst arrival times at the satellite antenna.

D.3.3.1 Theoretical Analysis of the GEOSAR Channel Capacity for Short Messages

With a repetition period of beacon bursts of 50 seconds, a maximum of 6 messages are transmitted by the beacon within 5 minutes, and a maximum of 12 messages are transmitted within 10 minutes. Let “ M ” designate the number of bursts transmitted during the time period considered. The probability of receiving “ m ” bursts with no collisions is:

$$P_m = C_M^m P_{NC}^m (1 - P_{NC})^{M-m} \quad \text{D/E.6}$$

where P_{NC} is the probability of receiving a single burst with no collision, as expressed in equation D/E.5.

P_{NC} is a function of N , the number of active beacons in the satellite visibility area, and depends on the probability of collision in time P_t for an individual message (e.g. $P_t = 0.0176$ for beacons transmitting short format messages only).

Figure D.3: Probability of Receiving at least “K” Messages with No Collisions Within 5 Minutes (Short Format Messages)

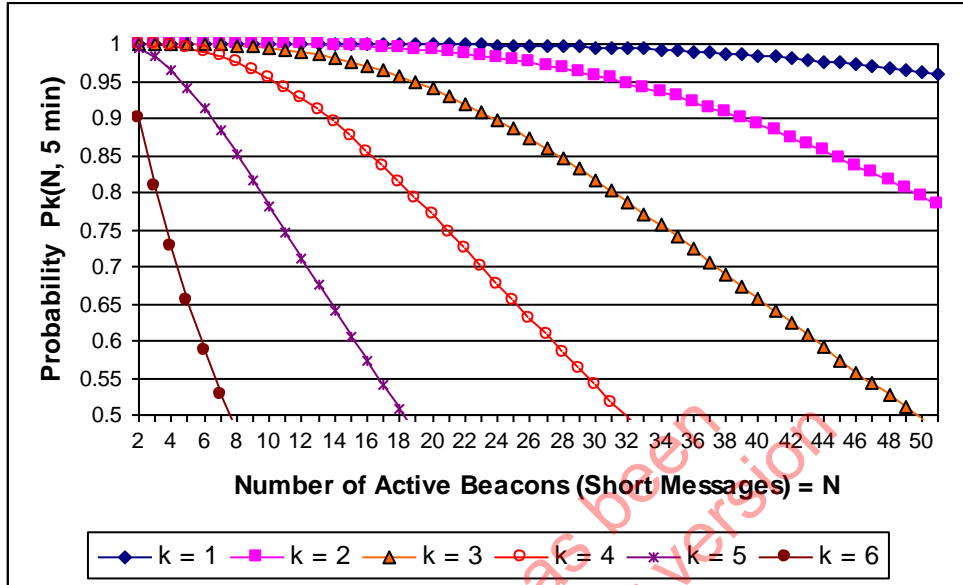
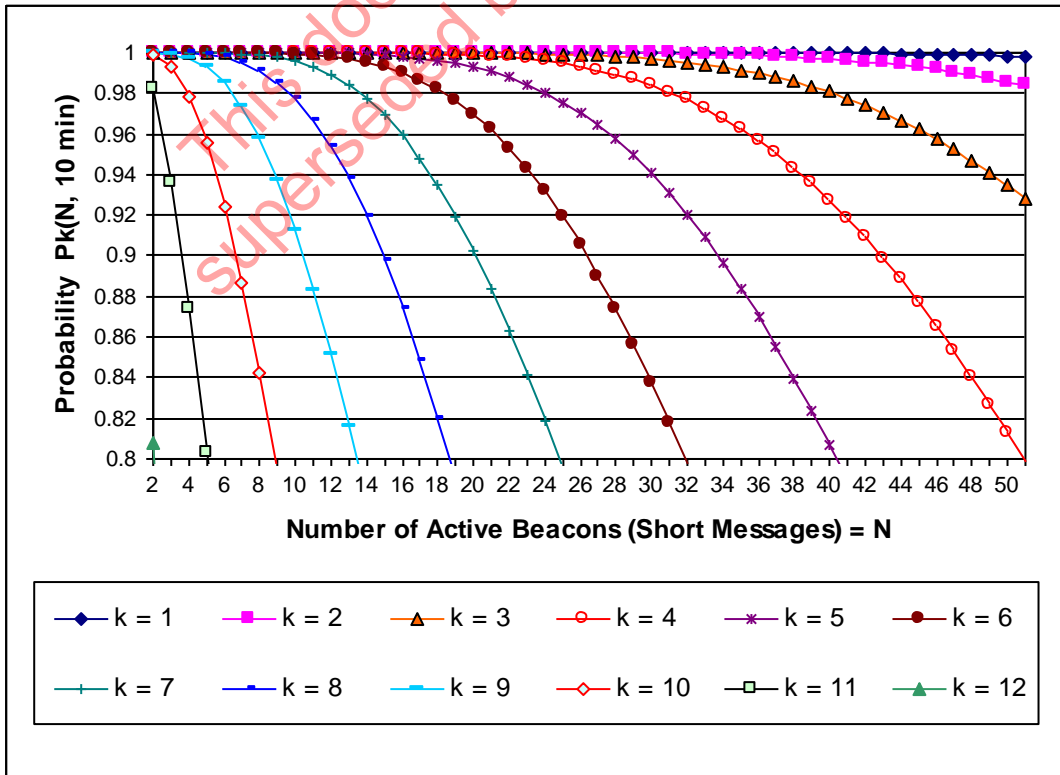


Figure D.4: Probability of Receiving at least “K” Messages with No Collisions Within 10 Minutes (Short Format Messages)



We have assumed that bursts must be received with no collision in time and frequency to be used in the integration process. If the probability of processing success (obtaining a valid message) for “m” non-interfering bursts is P_m , and the probability of receiving m messages with no collisions assuming N beacons are active in the satellite visibility area is P_m , then the probability of successful processing during a time period that allows for the transmission of M beacon messages is:

$$P(N, M) = \sum_{m=1}^M P_m * P_m = \sum_{m=1}^M P_m C_M^m P_{NC}^m (1 - P_{NC})^{M-m} \quad D/E.7$$

However, the probabilities of processing success P_m are not available. Therefore, we will calculate the GEOSAR capacity for possible values of the number of non-interfering bursts “K” required for a successful integration, assuming that $P_m = 0$ if $m < K$, and $P_m = 1$ if $m \geq K$.

The probability $P(N, M)$ is then the probability of receiving at least “K” bursts with no collisions, expressed as follows:

$$P_k(N, M) = \sum_{m=k}^M C_M^m P_{NC}^m (1 - P_{NC})^{M-m} \quad D/E.8$$

Figures D.3 and D.4 show the evolution of $P_k(N, M)$ for $M = 6$ (within 5 minutes) and $M=12$ (within 10 minutes), respectively.

The results of the analysis can be interpreted as follows: if a minimum of K non-interfering bursts are required to obtain a valid message, then the value of N for K at a given probability (e.g. 95%) is the capacity of the system.

Figure D.5 illustrates the evolution of N for various probabilities and values of K, when the capacity is defined for short messages, with processing times of 5 minutes (i.e. 6 bursts maximum), and 10 minutes (i.e. 12 bursts maximum). The calculated GEOSAR capacity figures, as shown in Figure D.5, are reported in Table D.1 below.

Table D.1: GEOSAR Capacity as a Function of the Number of Non-Interfering Bursts Required (Short Format Messages)

K	1	2	3	4	5	6	7	8	9	10	11	12
N(99%, 10')	65	47	35	27	21	16	11	8	5	3	0	0
N(98%, 10')	73	52	40	31	24	18	13	9	6	3	2	0
N(95%, 10')	86	61	47	37	28	22	16	12	8	5	2	0
N(90%, 10')	99	71	54	42	33	26	20	14	10	6	3	0
N(99%, 5')	36	20	11	5	2	0	0	0	0	0	0	0
N(98%, 5')	42	24	14	7	3	0	0	0	0	0	0	0
N(95%, 5')	53	31	18	10	4	0	0	0	0	0	0	0
N(90%, 5')	65	38	23	13	6	0	0	0	0	0	0	0

Figure D.5: Evolution of the Capacity Computed with Various Probabilities for Short Format Messages and for Processing Times = 5 Minutes and 10 Minutes

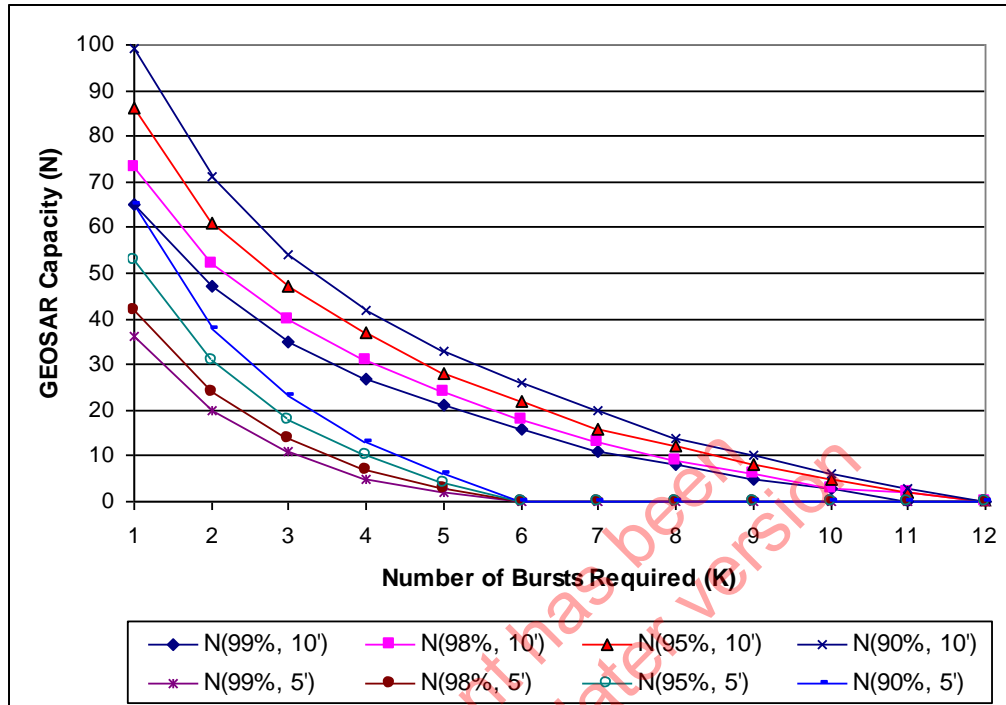


Figure D.5 and Table D.1 clearly show that the condition 95 % probability within 5 minutes is more restrictive, from a capacity viewpoint, than the condition 99 % probability within 10 minutes. This is the result of the time limitation, which directly impacts on the integration process.

Figure D.5 also clearly shows a rapid degradation of the capacity when the minimum number of non-interfering bursts that need to be integrated increases. This illustrates the consequences of low link budget margins on the GEOSAR processing, and the fact that any significant degradation of C/No is likely to impact the probability of quickly recovering valid messages.

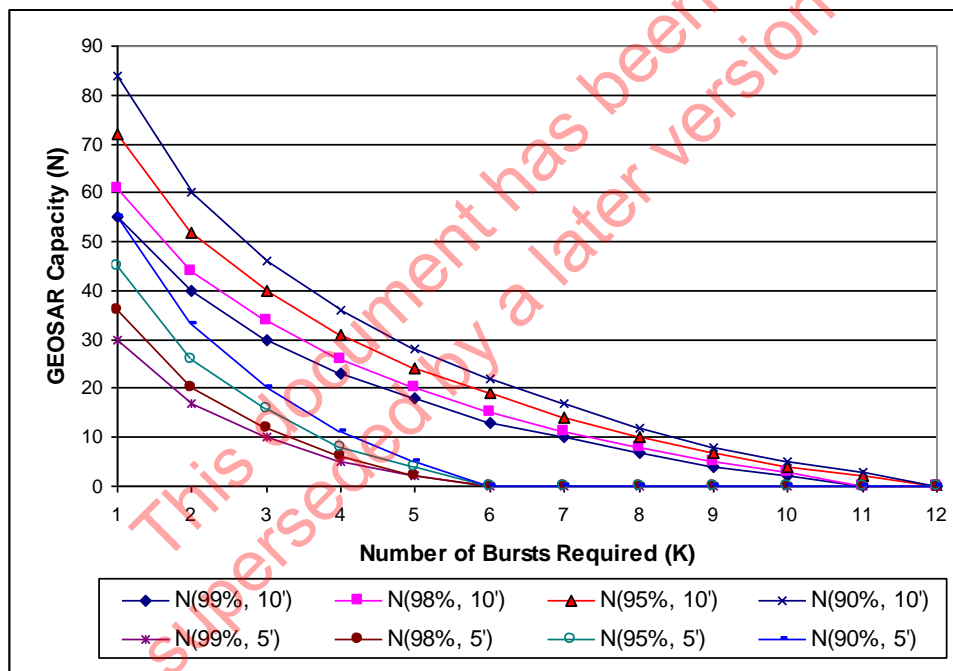
D.3.3.2 Theoretical Analysis of the GEOSAR Channel Capacity for Complete Long Messages

The same analysis as above is performed for a population of beacons that transmit long format messages only, characterised by $P_t = 0.0208$.

The results are illustrated in Figure D.6 and summarised in Table D.2 below. Figure D.6 illustrates the evolution of N for various probabilities of successful processing and values of K, when the capacity requirement is set to obtaining complete long messages within 5 minutes (i.e. 6 bursts maximum), or 10 minutes (i.e. 12 bursts maximum).

Table D.2: GEOSAR Capacity as a Function of the Number of Non-Interfering Bursts Required (Complete Long Format Messages)

K	1	2	3	4	5	6	7	8	9	10	11	12
N(99%, 10')	55	40	30	23	18	13	10	7	4	2	0	0
N(98%, 10')	61	44	34	26	20	15	11	8	5	3	0	0
N(95%, 10')	72	52	40	31	24	19	14	10	7	4	2	0
N(90%, 10')	84	60	46	36	28	22	17	12	8	5	3	0
N(99%, 5')	30	17	10	5	2	0	0	0	0	0	0	0
N(98%, 5')	36	20	12	6	2	0	0	0	0	0	0	0
N(95%, 5')	45	26	16	8	4	0	0	0	0	0	0	0
N(90%, 5')	55	33	20	11	5	0	0	0	0	0	0	0

Figure D.6: Evolution of the Capacity Computed with Various Probabilities for Complete Long Format Messages and for Processing Times = 5 Minutes and 10 Minutes

D.3.3.3 Theoretical GEOSAR Capacity for the First Protected Field of Long Messages

The results of Tables D.1 and D.2 show that, if we assume that the same number of non-interfering bursts are required for retrieving a valid short message or a complete long message, then the capacity figure for long messages at 99% within 10 minutes always exceeds the capacity figure for short messages at 95% within 5 minutes. This means that, if the capacity is selected to allow a short message to be retrieved within 5 minutes with a probability of 95%, then long messages would be retrieved within 10 minutes with a probability higher than 99%.

However, we have determined that the probability of collisions in time is 0.0189 for the first part of long messages (assuming all beacons transmit long messages), instead of 0.0176 for short messages only. Therefore, the condition 95% within 5 minutes might not be satisfied for the retrieval of the first protected field of a long message (a valid long message) when the

traffic corresponds to the maximum load (i.e. at full capacity) and all beacons transmit long format messages.

Table D.3 summarises the results of the computation of the capacity for various probabilities under the conditions:

- $P_t = 0.0176$ (short messages only);
- $P_t = 0.0189$ (first protected field of long messages, i.e. “valid” long messages), and
- $P_t = 0.0208$ (complete long messages only).

Table D.3: Comparison of Capacity for Various Probabilities of Retrieving: Valid Short and Long Messages and Complete Long Messages

Capacity (N) for Short Messages Only (for a given probability of retrieving a valid short message)							
No. of Bursts required: k =		1	2	3	4	5	6
(within 5 minutes)	N(99%, 5')	36	20	11	5	2	0
(within 5 minutes)	N(98%, 5')	42	24	14	7	3	0
(within 5 minutes)	N(95%, 5')	53	31	18	10	4	0
(within 5 minutes)	N(90%, 5')	65	38	23	13	6	0
(within 10 minutes)	N(99%, 10')	65	47	35	27	21	16
Capacity (N) for Long Messages Only (for a given probability of retrieving a valid long message)							
No. of Bursts required: k =		1	2	3	4	5	6
(within 5 minutes)	N(99%, 5')	33	19	10	5	2	0
(within 5 minutes)	N(98%, 5')	39	22	13	7	3	0
(within 5 minutes)	N(95%, 5')	49	29	17	9	4	0
(within 5 minutes)	N(90%, 5')	60	36	22	12	6	0
(within 10 minutes)	N(99%, 10')	60	44	33	25	19	15
Capacity (N) for Long Messages Only (for a given probability of retrieving a complete long message)							
No. of Bursts required: k =		1	2	3	4	5	6
(within 5 minutes)	N(90%, 5')	55	33	20	11	5	0
(within 10 minutes)	N(99%, 10')	55	40	30	23	18	13
(within 10 minutes)	N(98%, 10')	61	44	34	26	20	15
(within 10 minutes)	N(95%, 10')	72	52	40	31	24	19
(within 10 minutes)	N(90%, 10')	84	60	46	36	28	22

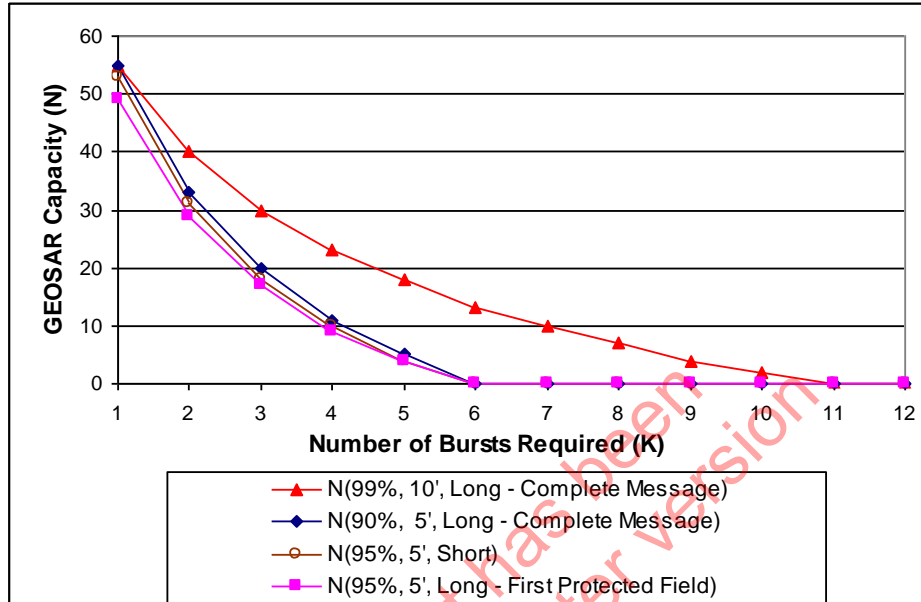
Figure D.7 illustrates the comparison of the capacity figures for short messages (95% within 5 minutes), complete long messages (90% within 5 minutes, and 99% within 10 minutes), and valid long messages, i.e., first protected field only (95% within 5 minutes), as provided in Table D.3.

Assuming we have determined the number of non-interfering bursts required for successful processing, the system capacity can be selected to ensure a probability of 95% of retrieving valid long messages (i.e., the first protected field) within 5 minutes. As this is clearly the more restrictive constraint in terms of capacity, this would ensure that:

- valid short messages are retrieved within 5 minutes with a probability greater than 95%; and
- complete long messages are retrieved within 5 minutes with a probability greater than 90% and within 10 minutes with a probability greater than 99%.

In section D.4 we will use the constraint outlined above (95% valid long format messages must be retrieved within 5 minutes) to determine the nominal GEOSAR channel capacity.

**Figure D.7: Comparison of GEOSAR Capacity as Computed for:
Complete Long Messages (90% within 5 minutes - 99% within 10 minutes)
Short Messages (95% within 5 minutes), and
Valid Long Messages (First Protected Field, 95% within 5 minutes)**



D.3.3.4 Probability of Confirmed Messages at Full System Load

Valid messages are forwarded to a Cospas-Sarsat MCC for distribution to SAR services. However, the GEOLUT specification (C/S T.009) also calls for a confirmation of a valid or complete message with a second independent integration providing an identical valid or complete message. This section considers the probability of obtaining confirmed messages within given time periods, when the system load is at the capacity limit.

The probability $P_k(N, M)$ computed in the previous sections is the probability of obtaining a valid or complete message within a given period of time (M transmitted messages), assuming K non-interfering bursts are required for a successful integration, and N beacons are active in the satellite visibility area. With the assumption made (see D.3.3.1), it is equal to the probability of receiving at least K bursts with no collisions. Therefore, assuming that we have determined the appropriate value of K and the corresponding capacity N that satisfies the requirement to retrieve a valid message within 5 minutes with a probability of 95%, then the probability of obtaining one valid (or complete) message after M beacon emissions is given by equation D/E.8:

$$P_k(N, M) = \sum_{m=k}^M C_M^m p^m (1-p)^{M-m} ; \text{ where } p \text{ is the probability of no-collisions}$$

In accordance with the above logic for retrieving one valid message (or one complete message) during a given period of time, a second valid (or complete) message will be retrieved during a given period of time (after transmission of a given number of bursts “ M ”) if at least $2 \cdot K$ messages can be retrieved without collisions.

Therefore, we will write:

$$P_{\text{confirmed}} = P_{2k}(N, M) = \sum_{m=2k}^M C_M^m p^m (1-p)^{M-m} \quad \text{D/E.9}$$

We will compute $P_{\text{confirmed}}$ in section D.4, after having determined the nominal GEOSAR channel capacity.

D.3.4 Analysis of the GEOSAR D&E Results

The GEOSAR Demonstration and Evaluation (D&E) tests performed in 1997/1998 were designed to characterise the GEOSAR/GEOLUT link performance, and did not specifically address the issue of GEOSAR capacity. Therefore, these results do not directly provide the required input for the capacity model developed above (i.e., the typical number of bursts with no collisions required to achieve a successful processing and retrieve a valid or complete message).

D.3.4.1 Processing Threshold and System Margin (GEOSAR D&E Test T-1)

The processing threshold was defined, for the purpose of the D&E, as the minimum value of the ratio of beacon carrier power to noise density (C/N_0) received at the GEOLUT that resulted in a 99% probability of detection of an error free message (i.e., a valid message) at the GEOLUT. The system margin was defined as the difference between the effective isotropic radiated power (EIRP) of the beacon at the threshold C/N_0 and the EIRP of a nominal beacon, i.e., 37 dBm.

The procedure for test T-1 consisted of transmitting, from a beacon simulator, series of 20 unique beacon messages, each separated in time and frequency to avoid collisions. Each beacon message was transmitted 20 times. The total sequence of beacon messages was repeated for different beacon EIRPs. The recovery of at least one error-free (valid) message during the sequence of 20 bursts transmitted for each beacon message was deemed a processing success. The probability of recovery of an error free message was defined as the ratio of the number of processing successes over the number of 20 burst sequences transmitted. The detailed test procedure and results are provided in the Report of the Demonstration and Evaluation of the 406 MHz GEOSAR System (see also the Summary Report of the D&E, document C/S T.009).

The results of test T-1 showed significant discrepancies amongst the GEOLUTs and the GEOSAR satellites used during the D&E, with variations in the processing threshold (26 to 28 dBHz) and the system margins (12 to 6 dB), which may reflect differences between GEOLUT performance, and also variation of environmental conditions (e.g., interference in the frequency band, distance of the GEOLUT to the satellite, etc.) that affect the link budget. The D&E T-1 test results did confirm the feasibility of a GEOSAR/GEOLUT system, but are not directly relevant to the GEOSAR capacity evaluation.

D.3.4.2 Message Transfer Time (GEOSAR D&E Test T-2)

For the purpose of the D&E, the message transfer time (MTT) was defined as the time between activation of a beacon with an EIRP at the GEOLUT threshold and the time the GEOLUT produced the first error-free message (i.e., valid message). The same test procedure was used as for test T-1. The results were reported for two probabilities: MTT-90% and MTT-50% (i.e., the

time of transfer for 90% and 50%, respectively, of the valid messages recovered at the GEOLUT threshold). The results also showed significant variations from less than one minute to 4 minutes for MTT-50%, and from less than 6 minutes to over 12 minutes for MTT-90%, which were probably a consequence of the experimental nature of the GEOLUTs.

Table D.4 below provides detailed MTT results obtained with GOES 8 and a Canadian GEOLUT during the GEOSAR D&E, for various beacon EIRPs and various MTT probabilities.

Table D.4: Message Transfer Times as a Function of Beacon EIRPs

EIRP (dBm)	MTT/50% (seconds)	MTT/90% (seconds)	MTT/95% (seconds)	MTT/98% (seconds)
37	0	0	0	50
32	0	0	50	50
27	0	100	150	250
26	100	400	500	900
25	150	600	750	900
24	-	-	-	-
22	300	700	800	900
21	350	800	850	900
20	450	850	900	900

Note: An MTT = 0 in Table D.4 means that a valid message was obtained after processing the first burst. All MTTs are multiples of 50 s, the repetition rate of beacon bursts. The MTT results provided for 24 dBm were inconsistent for all MTT probabilities and, therefore, have not been reported. No tests were performed for the other EIRP values not reported in Table D.4.

Although the 406 MHz bursts transmitted by the beacon simulator did not collide in time and frequency, some collisions with actual distress beacon transmissions were possible during the test.

The results of Table D.4 illustrated in Figure D.8 show that the distribution of MTTs is significantly affected by the decrease of the beacon EIRP below a threshold of about 27 dBm (i.e., 10 dB below the nominal 37 dBm EIRP of the beacon), however, the integration process allows for the recovery of valid messages even at low EIRPs, but with increasing transfer times. Note that the shape of the curve obtained for MTT-98% is probably a consequence of the test procedure, which limited the transmissions to 20 bursts for each beacon message (i.e. which would correspond to a MTT of 950 seconds in Table D.4) and the particular processing implemented in this GEOLUT.

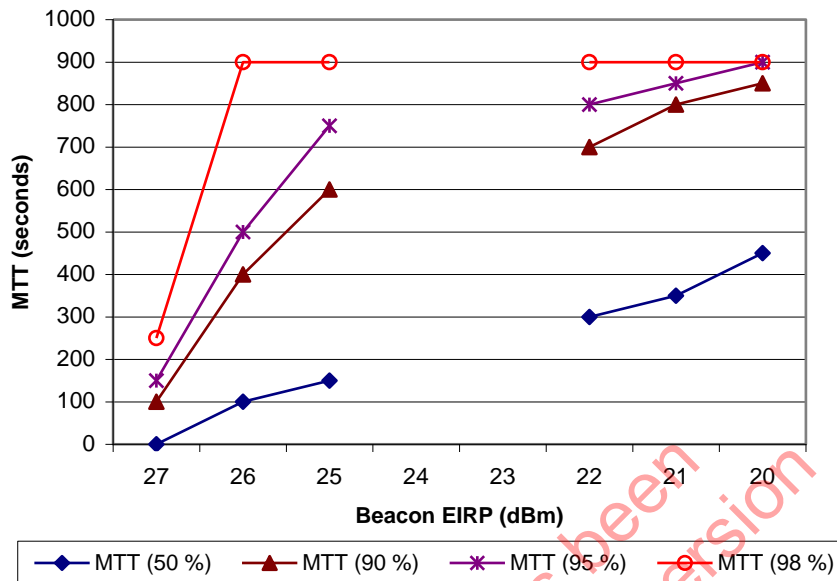
Figure D.8: Message Transfer Times at Various EIRPs

Figure D.8 shows that valid messages were obtained with 95% probability within 300 seconds (5 minutes) if the beacon transmitted with an EIRP of at least 26.5 dBm (10.5 dB below the nominal EIRP of 37 dBm) and with 98% within 600 seconds (10 minutes) at the same EIRP. The test results also clearly indicate shorter MTTs when the beacon transmissions were closer to the nominal EIRP (i.e., see 37 dBm and 32 dBm MTT results in Table D.4, not shown in Figure D.8). However, the actual beacon EIRP in a distress situation, particularly for ELTs after an aircraft incident, may be severely affected by a number of factors (e.g., antenna orientation), which are likely to reduce the available EIRP of the transmission. Therefore the capacity of the GEOSAR system must be assessed assuming a critical beacon with an EIRP lower than the nominal 37 dBm.

It should also be noted from the D&E test data illustrated above, that messages from beacons transmitting with EIRPs well below the threshold were also recovered, although with increasing delays. The major impact of high loads on the GEOSAR system will be to increase the recovery time of weaker messages, or to raise the EIRP threshold at which the requirement to recover 95% of valid messages within 5 minutes will be met.

D.3.4.3 GEOSAR D&E Test T-4 on Beacon Processing Capacity

The USA test results are reported in document JC-16/8/2 (May 2002). The purpose of the test was to assess the capacity of the GEOSAR system, i.e., the system loading, including test beacons and “background” loading of operational beacons active during the test, which resulted in a system performance such that the transmissions of a newly activated test beacon would be successfully processed (production of a valid “Error Free Message”) within five minutes with a probability of 95%.

The background load was generated using the USA Beacon Simulator Signal Generator (BSSG). Real 406 MHz transmissions from operational beacons were also monitored to assess the exact system load. Transmissions from five Field Test Units (FTUs) were used to assess the probability of retrieving valid messages within 5 minutes. The FTUs transmitted short message formats, with an EIRP of 37 dBm.

Data were collected using both GOES-8 and GOES 10 geostationary satellites and the Canadian GEOLUTs at Trenton. The test results indicate that the GOES GEOSAR system has a capacity of 33 active beacons (single channel).

For comparison, Table D.1 indicates that a capacity of 31 beacons transmitting short messages can be achieved for a selected value of $K = 2$ (i.e., 2 transmissions required for retrieving a valid message).

D.3.4.4 Selection of the Value of “K” for the Nominal GEOSAR System Capacity

Although the test data suggest that 2 bursts with a 37dBm EIRP were required on average to achieve a successful processing with the GOES satellites, it would seem prudent for the purpose of the GEOSAR capacity assessment to accept that a minimum of 3 bursts would be required to ensure the recovery of a valid, or complete, message at low EIRP. Therefore, the value $K = 3$ will be used to define the nominal GEOSAR system capacity.

*This document has been
superseded by a later version*

D.4 GEOSAR SYSTEM CAPACITY

On the basis of the GEOSAR capacity analysis provided at section D.3, and for the purpose of managing the use of the 406.0-406.1 MHz frequency band, the nominal GEOSAR channel capacity is defined as the maximum number of active beacons in the GEOSAR satellite visibility area, all transmitting long format messages, that allow for the retrieval of valid messages (first protected field only) with a probability of 95% within 5 minutes.

Under this capacity definition, the analysis shows (see D.3.3.3), for all values of K (the number of bursts received with no collisions that need to be integrated to obtain a valid message), that:

- valid short messages would be retrieved with a probability slightly greater than 95% within 5 minutes; and
- complete long messages would be retrieved within 5 minutes with a probability greater than 90%, and within 10 minutes with a probability greater than 99%.

From the considerations of the GEOSAR D&E test results in section D.3.4, we have selected a value of K equal to 3, that characterises the nominal scenario used to determine the nominal GEOSAR channel capacity. Under this hypothesis, and assuming that the times of arrival of the beacon bursts are always uniformly distributed in the repetition period, the nominal capacity of a single GEOSAR channel would be $N = 17$ (see Table D.3 and Figure D.7).

However, the analysis of repetitive transmissions provided at Appendices B and C to Annex D, and the results of the computer simulations provided at Appendix D to Annex D, show that the hypothesis of a uniform distribution of the bursts arrival times is not consistent with the repetitive nature of the beacon transmissions, and the actual probability of processing success is dependent upon the C/S T.001 specification of randomised repetition periods. The conclusions of the analyses of Appendices B, C and D are addressed in section D.4.1 below. In summary, for beacons designed to the specification of document C/S T.001, the GEOSAR channel capacity is $N = 14$.

The probability of obtaining confirmed valid or complete messages is provided in section D.4.2 for the nominal scenario assuming a message traffic at full system load (i.e., equal to the channel capacity).

Finally, the probabilities of retrieving single or confirmed messages for values of $K > 3$, are provided in section D.4.3 to illustrate non-nominal scenarios where the GEOSAR link is degraded (low C/N_0 , low beacon EIRP below the threshold of the GEOLUT).

D.4.1 Channel Capacity Under the Nominal Scenario ($K = 3$)

For the value $K = 3$, the theoretical GEOSAR capacity model developed in section D.3.3 provides the number of simultaneously active beacons ($N = 17$) that can be processed within 5 minutes with a 95% probability of retrieving a valid message, assuming all transmitted bursts are long format messages and the distribution of burst arrival times is uniform over the period "T" (see Table D.3).

However, the analysis of Appendix C shows that, if the repetition period as specified in C/S T.001 is taken into consideration, the probability of collision is increased after a burst collision in time and frequency (see Figure D-C.5 in Appendix C). This is confirmed by the results of computer simulations reported at Appendix D.

Furthermore, although the analysis of Appendix C shows that, on average, the probability of burst collisions is the same as in the hypothesis of a uniform distribution, the simulation results of Appendix D clearly indicate that the probability of success, under the Appendix C distribution of burst transmission times, is lower than in the case of a uniform distribution. Similar results are obtained with the distribution of burst transmission times of Appendix B, confirming that equation D/E.8, which provides adequate results for a uniform distribution (as confirmed by the computer simulations), cannot be used to compute the non-conditional probability of successful processing in the cases of Appendix B and Appendix C distributions. Instead, a “weighted average” is defined in Appendix B to Annex D and compared to the simulation results of Appendix D to Annex D (see sections D-B.4/D-B.5 and D-D.3.2/D-D.4.2).

D.4.1.1 Nominal GEOSAR Channel Capacity for C/S T.001 Burst Distribution

The analysis at Appendix C does not allow a direct conclusion in respect of the probability of successful processing. However, a comparison with the results of the analysis in Appendix B, as shown in Figure D-C.6, indicates that similar performance is obtained in respect of the probability of burst collisions “on average” (non-conditional probabilities) with the distribution of burst arrival times of Appendix B. This similarity is confirmed by the simulation results of Appendix D to Annex D.

In addition, Appendix D simulation results (Figure D-D.6 and Table D-D.1) show that:

- the non-conditional probability of processing success is identical for the distributions of Appendix B (i.e., “fixed periods” with randomised transmission times) and Appendix C (i.e. the C/S T.001 specification for the randomised repetition period), therefore, the analytical model of Appendix B should provide a good estimate of the GEOSAR capacity; and
- the computer simulation results for the C/S T.001 specification (i.e., Appendix C distribution) provide a reasonable match with the results of the analysis provided at section D-B.4 of Appendix B, using equation D-B/E.30 that provides the non-conditional probability of success for the burst distribution of Appendix B (referred to as the “weighted average”).

Note: The simulation results for the distribution of Appendix C (i.e., the C/S T.001 specification) actually indicate slightly lower probabilities of processing success than the analytical results (for numbers of active beacons between 10 and 20 - see Figure D-B.8), using the “weighted average” (equation D-B/E.30) of the Appendix B probability of success. However, the burst collision criteria used for the simulation are very stringent (no overlap allowed, even for the CW portion of the burst). Similarly, the condition $K = 3$ (3 bursts received with no collision) is probably conservative. Therefore, we will base our assessment of the GEOSAR channel capacity on the results of the analysis to avoid an overly conservative approach.

On the basis of the above considerations, we will use the results obtained at Appendix B, i.e., the non-conditional probability of processing success as determined by the “weighted average” defined by equation D-B/E.30, to assess the nominal GEOSAR channel capacity. As shown in Table D-D.1 and Figures D-D.6 / D-B.8, the 95% probability of processing success within 5 minutes is achieved with 14 beacons simultaneously active in a GEOSAR channel.

Therefore, we will select $N = 14$ as the nominal channel capacity of the GEOSAR system.

The GEOSAR system performance under this traffic load is summarised in Table D.5 below.

**Table D.5: Summary of GEOSAR Performance with 14 Active Beacons (K = 3)
Probability of Successful Processing of Single Valid or Complete Long Messages**

14 Active Beacons All Long Format Messages	Non-Conditional Probability *		“Worst-Case” Probability (Conditional, First Burst Collision)*	
	5 minutes (6 bursts)	10 minutes (12 bursts)	6 minutes (7 bursts)	11 minutes (13 bursts)
Single Valid Message (First Protected Field)	95 %	99.9 %	89 %	> 99 %
Single Complete Message (First and Second Protected Field)	94 %	99.9 %	>85 %	> 99 %

Note (*): The results provided in Table D.5 for the non-conditional probability of the C/S T.001 specification, analysed in Appendices C and D are copied from Table D-B.2

The results provided for the “worst-case” scenario, which consists of a first-burst collision followed by 6 additional bursts (a total of 7 bursts or about 6-minute emission), or a first-burst collision followed by 12 additional bursts (a total of 13 bursts or about 11-minute emission) are copied from Table D-B.1 in Appendix B (14 active beacons, valid long and complete long messages over 5 and 10 minutes). Table D-B.1 provides the results of the analysis of Appendix B worst-case scenario, which are shown to match the simulation results of the C/S T.001 worst-case distribution (see section D.4.1.2 below).

D.4.1.2 System Performance for the “Worst-Case” Scenario (First-Burst Collision)

Figures D-D.6, D-D.7 and Table D-D.1 also show that:

- the conditional (worst-case) probability of success is lower in the worst-case scenario of Appendix C (6 bursts transmitted within 5 minutes, with a first-burst collision) than in the worst-case scenario of Appendix B ($|\Delta| \leq \tau$), which does not impose a first-burst collision;
- however, the analysis of the Appendix B distribution (worst-case over 5 minutes) provides a slightly conservative but reasonable match with the simulation results of the Appendix C worst-case scenario, if one additional burst is allowed (7 bursts transmitted instead of 6, with a first-burst collision).

We deduce from the above remarks that, for the worst-case scenario, the probability of success computed for the Appendix B distribution using equation D-B/E.8 provides an acceptable analytical model of the worst-case scenario performance under the C/S T.001 specification (Appendix C), assuming a first-burst collision followed by 6 additional bursts over a total duration of approximately 6 minutes (or assuming a first-burst collision followed by 12 additional bursts over a total duration of about 11 minutes).

Considering the probabilities of successful processing provided in Table D-B.1 of Appendix B for the worst-case scenario ($|\Delta| \leq \tau$), we can conclude that, under the traffic load determined above ($N = 14$), and assuming the above Appendix C scenarios (first burst collision followed by 6 or 12 bursts), a valid long message would be retrieved within 6 minutes with a probability of approximately 89%, or within 11 minutes with a probability greater than 99%.

Similarly, Table D-B.1 indicates that, in the worst-case scenario of Appendix C (first-burst collision), single complete long messages would be retrieved within 6 minutes with a probability greater than 85 % and within 11 minutes with a probability greater than 99 %.

These results confirm that, even in the worst-case scenario of a first burst collision, the performance of the system remains acceptable with a traffic load at the proposed capacity limit of a channel.

Table D.5 summarises the performance of the GEOSAR system at full channel load, in the nominal scenario ($K = 3$), on average (i.e., non-conditional probabilities), and in the worst-case situation that follows a first-burst collision (conditional probabilities corresponding to the situation $\Delta \leq \tau$ analysed at Appendix B). The detailed results of the computations are provided in Tables D-B.1 of Appendix B to Annex D, and Tables D-D.1 of Appendix D to Annex D.

Table D.5 also confirms that the condition “95 % within 5 minutes” selected for the definition of the GEOSAR channel capacity, is a rather severe constraint, as a non-conditional (average) probability of success of 99.9 % is achieved within 10 minutes, and a conditional (worst-case) probability greater than 99 % is achieved within 11 minutes after a first-burst collision.

D.4.2 Probability of Obtaining Confirmed Messages (Nominal Scenario: $K = 3$)

In comparing the computer simulation results (Figure D-D.7 and Table D-D.2) with the results of the theoretical analysis of Appendix B we have noted that the analysis of the worst-case scenario of the Appendix B distribution (i.e. $\Delta \leq \tau$), using equation D/E.9 to define the probability of success, provided an acceptable analytical model of the GEOSAR system performance in respect of the probability of obtaining confirmed complete messages over 10 minutes (12 transmitted bursts) under the constraints of repetitive transmissions.

In Appendix B and Appendix D to Annex D we have also noted that the “weighted average” of the probability of success for the Appendix B distribution, defined by equation D-B/E.30, provided an acceptable analytical model of the GEOSAR performance in respect of the non-conditional probability of success. Therefore, for the assessment of non-conditional probability of obtaining confirmed messages, we will use this weighted average, computed for $K' = 2K$ as in equation D/E.9.

Figure D.9 provides a comparison of the computer simulation results for the Appendix C distribution with the results of the Appendix B analysis, for confirmed complete long messages, in respect of the non-conditional and the conditional probabilities of success in both distributions, when the number of transmitted bursts increases from 10 to 18 (i.e., up to 15 minute beacon transmissions).

Although the analytical results provided for the Appendix B distribution are slightly higher than the computer simulation results based on the Appendix C distribution, these results are close enough to justify the use of the Appendix B analysis to characterise the GEOSAR system performance in respect of the probability of obtaining confirmed messages over 10 or 15 minutes, assuming a nominal scenario ($K = 3$). This is further developed in Figure D.10, which provides the results of the analysis for confirmed valid, and confirmed complete, long messages.

Under message traffic conditions corresponding to the selected nominal capacity ($N=14$), the probability of obtaining confirmation of a valid message within 10 minutes is 97.7 % and the probability of obtaining confirmation of a complete long message within 10 minutes is 96.6 %. These probabilities of confirmed messages are degraded in the worst-case situation that follows a first-burst collision (92 % and 88 %, respectively, within 10 minutes), but remain above 99 % within 15 minutes. The computation results in respect of confirmed messages in the worst-case scenario are provided in Table D-D.2 of Appendix D.

These results are summarised in Table D.6 for 10 and 15 minute transmissions (12 and 18 transmitted bursts).

**Figure D.9: Comparison of Analysis and Simulation Results
Probability of Confirmed Complete Long Messages
For Non-Conditional and “Worst-Case” Scenarios**

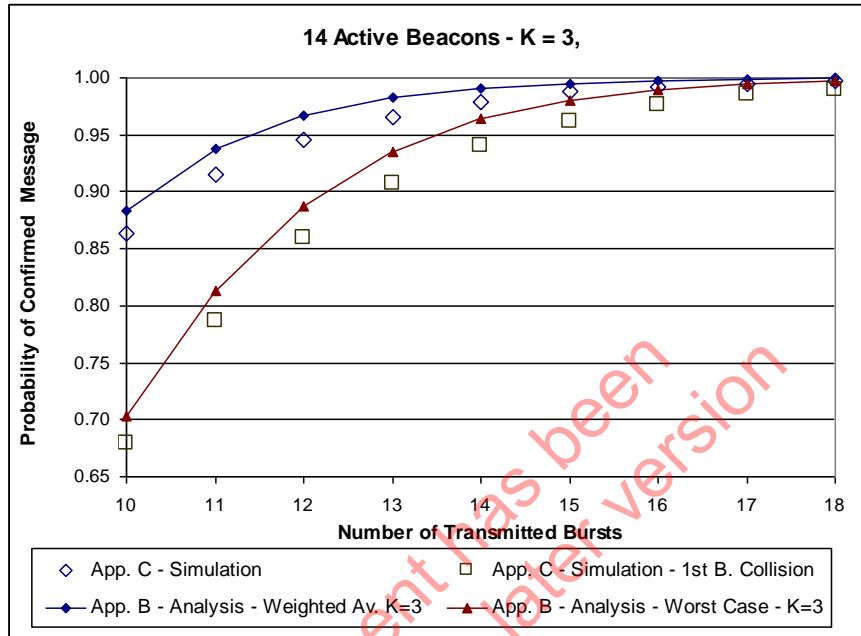


**Figure D.10: Evolution in Time of the Non-Conditional and Conditional
Probability of Confirmed Valid / Complete Long Messages
With K = 3 and 14 Active Beacons
(Appendix B Weighted Average and Worst-Case Scenario)**

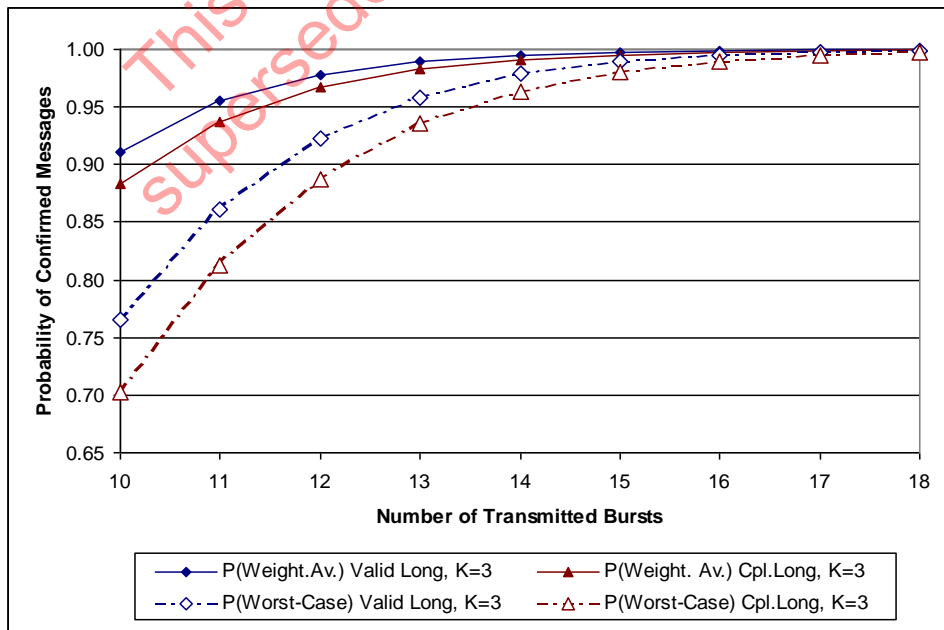


Table D.6: Summary of GEOSAR Performance with a Traffic Load Equal to the Channel Capacity (14 Active Beacons, K = 3) Probability of Confirmed Valid or Complete Long Messages

14 Active Beacons All Long Format Messages	"Average" Probability (non-conditional)		"Worst-Case" Probability (conditional, first-burst coll.)	
	10 minutes (12 bursts)	15 minutes (18 bursts)	10 minutes (12 bursts)	15 minutes (18 bursts)
Analysis of Confirmed Valid Messages (First Protected Field)	97.7 %	99.9 %	92.2 %	99.8 %
Analysis of Confirmed Complete Messages (First and Second Protected Field)	96.6 %	99.9 %	88.7 %	99.7 %
Simulation of Confirmed Complete Messages (First and Second Protected Field)	94.5 %	99.7 %	85.5 %	99.1 %

D.4.3 GEOSAR Performance Under Non-Nominal Scenarios (K > 3)

Figure D.11 compares computer simulation and analytical results for K = 4 and K = 5, which characterise degraded GEOSAR links. It is worth noting that for K = 5, the analysis provides a more conservative evaluation of the performance than the computer simulations. This is also observed for K = 4, but to a lesser degree.

Figure D.11: Comparison of Analysis and Simulation Results Probability of Confirmed Complete Long Messages for K = 4 and K = 5

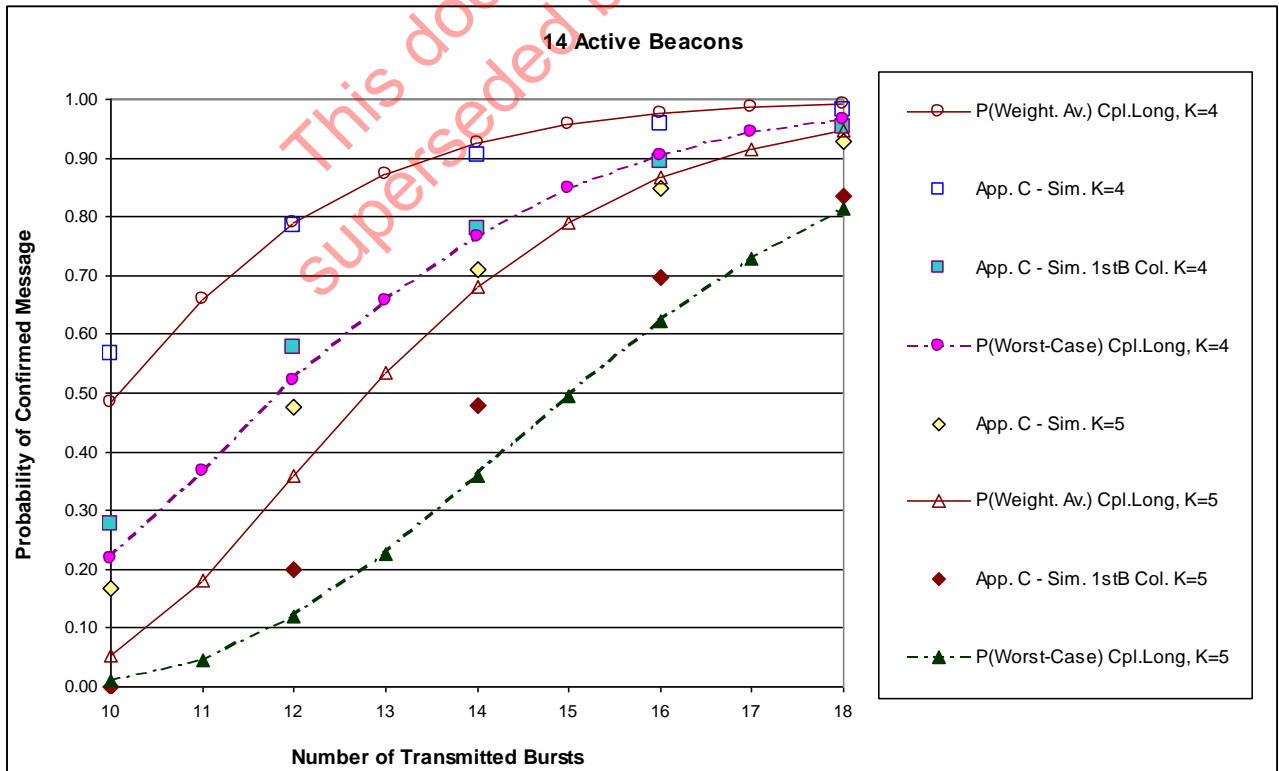
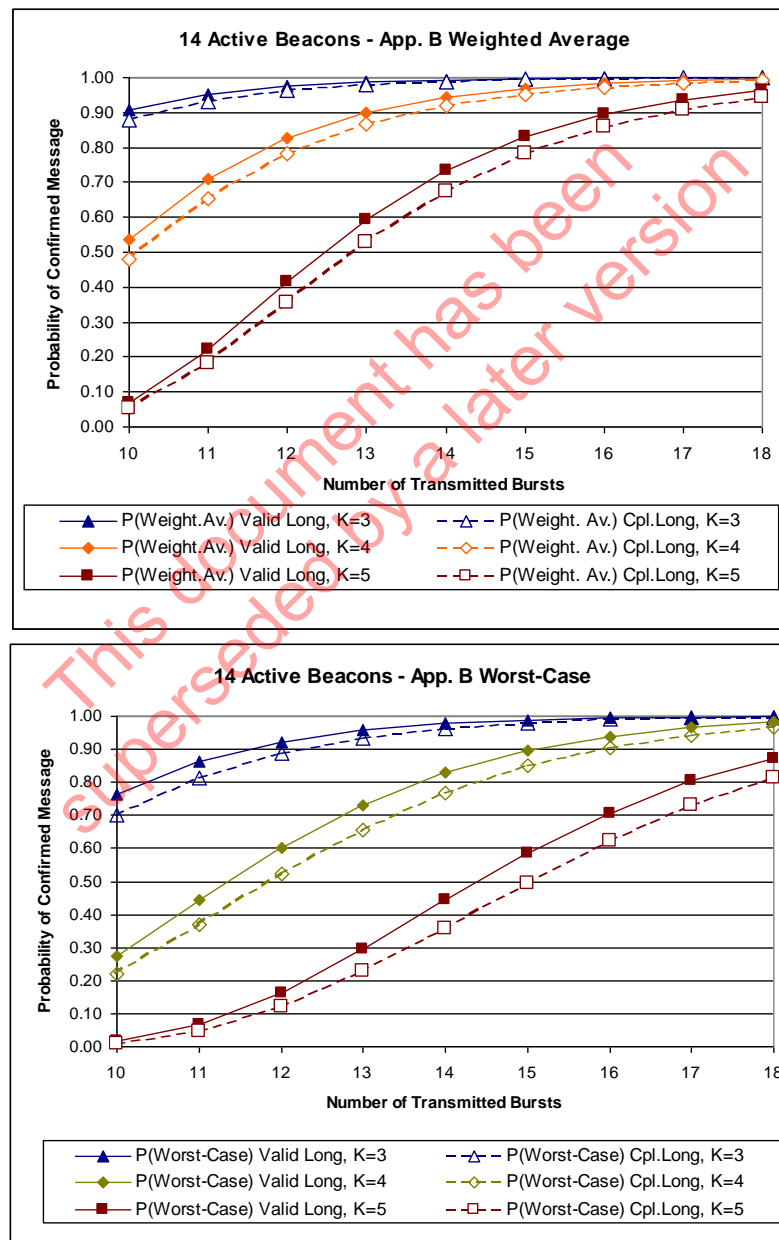


Figure D.12 illustrates the impact of beacon EIRPs below the GEOLUT threshold, or degraded links with low C/No (i.e., $K > 3$) on the probability of recovering confirmed valid or complete long messages. The results illustrated in Figure D.12 are provided by the analysis of the Appendix B distribution for the non-conditional probability of success (weighted average defined by equation D-B/E.30) and conditional probability (worst-case computed as per D/E.9).

**Figure D.12: GEOSAR Channel Performance for $K \geq 3$
 Evolution of the Probability of Confirmed Messages
 with Time for Nominal ($K = 3$) and Degraded Links ($K = 4, 5$)
 Non-Conditional and Conditional (Worst-Case) Probabilities**



From the analysis and the computer simulation results, it is possible to draw several conclusions in respect of the GEOSAR capacity when the quality of the communication link is degraded.

With a degraded link, the system capability of providing a confirmation within 10 minutes (12 transmitted bursts) for complete long messages, decreases from approximately 96 % ($K = 3$) to about 79 % if $K = 4$, and less than 50 % if $K = 5$. In the worst-case scenario of a first-burst collision, these probabilities decrease from 88 % ($K = 3$) to about 50 % ($K = 4$) and 20 % ($K = 5$).

However, over 15 minutes (18 transmitted bursts), these probabilities increase significantly to over 95 % ($K = 4$) or 80 % in the worst-case ($K = 5$).

Therefore, although degraded links will significantly impact on the performance of the GEOSAR system at maximum load, particularly its capability to produce confirmation messages within 10 minutes, the above results show that beacons will still be successfully processed by the GEOLUT to provide single and confirmed messages, but with increasing processing times.

This document has been
superseded by a later version

APPENDIX A to ANNEX D**ANALYSIS OF FREQUENCY CHANNEL SEPARATION****D-A.1 Scope and Objectives**

This appendix summarises the analysis of the distribution of operational beacon frequencies, as reported in document TG-1/2000/4/2. The data used in this analysis, i.e., measured beacon carrier frequencies provided by the USMCC (USA Cospas-Sarsat Mission Control Centre), was collected from operational 406 MHz beacons observed during the time period June 1993 – March 1994. Figure D-A.1 illustrates the distribution of frequency data provided by the French Mission Control Centre (FMCC) for the year 1999.

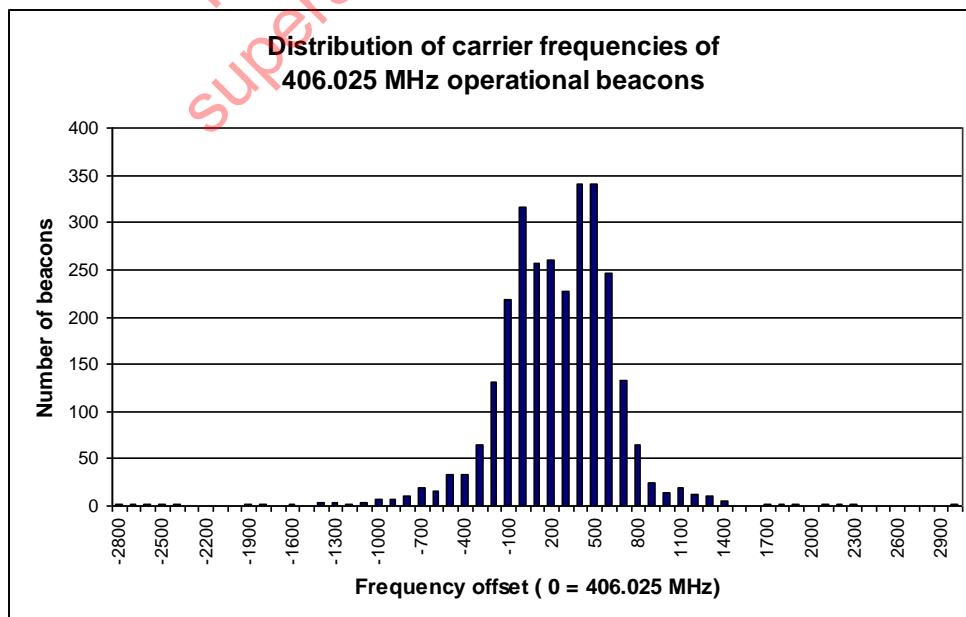
The objectives of the following sections are to:

- characterise the actual distribution of beacon carrier frequencies in the channel 406.025 MHz used by all operational beacons in the time period;
- assess a probability of collision in the frequency domain for beacons in the same channel; and
- verify that channels separated by 3 kHz are independent for the purpose of computing the nominal GEOSAR channel capacity.

D-A.2 Methodology

The beacon carrier frequencies collected from operational beacon transmissions are not distributed uniformly in a frequency channel, 95% are within a 1.5 kHz bandwidth from the nominal carrier frequency 406.025 MHz (USMCC data).

Figure D-A.1: FMCC Statistics on Operational Beacon Carrier Frequencies (1999)



The frequency data from actual beacon transmissions processed by the USMCC between June 1993 and March 1994 are analysed to determine their offset from the reference 406.025 MHz, and the parameters of the distribution are assessed, assuming that the actual distribution is approximately Gaussian.

The probability of collisions in frequency for two beacons in the same channel is assessed on the basis of the estimated carrier frequency distribution. Finally, the probability of frequency collisions between transmissions from beacons in two adjacent channels is also estimated.

D-A.3 Operational Beacons' Frequency Distribution

If we assume that the distribution is Gaussian $G(\mu, \sigma^2)$ around the value 406.025 MHz, we can write the density function of the carrier frequencies (x) as follows:

$$f(x) = \frac{1}{\sigma\sqrt{2\pi}} * e^{-\frac{(x-\mu)^2}{2\sigma^2}} \quad \text{D-A/E.1}$$

where μ is the mean value of the carrier frequency (i.e. 406.025 MHz), and σ^2 is the variance.

To determine the parameters of the Gaussian distribution $G(\mu, \sigma^2)$, we will use the tabulated function $G(0,1)$ of the variable $Z = (X-\mu) / \sigma$.

Table D-A.1 summarises the distribution of frequency offsets from 406.025 MHz, as obtained from USA data (406 MHz Beacon Carrier Frequencies USMCC Composite Sites; June 1993 – March 1994).

Table D-A.1: Analysis of Beacon Carrier Frequency Distribution

	Frequency Offset: $ \Delta f $ (Hz)	Number of observations $f < 406.025$ MHz	Number of observations $f > 406.025$ MHz	Average number of observations	Number of observations relative to total (718)	$(f-\mu)/\sigma$	σ
	(1)	(2)	(3)	(4)	(5)	(6)	(7)
1.	> 1500	3	0	1.5	0.0021	2.88	520
2.	> 1000	9	0	4.5	0.0063	2.5	400
3.	> 750	23	13	18	0.0251	1.96	380
4.	> 500	50	39	44.5	0.0620	1.53	330
5.	> 250	114	98	106	0.1476	1.04	240
6.	> 150	181	165	173	0.2409	0.7	210
7.	> 100	220	204	212	0.2953	0.53	190
8.	> 50	279	261	270	0.3760	0.32	160
9.	> 25	327	310	318.5	0.4436	0.14	180
10.	>0	366	352	359	0.5		

Column 1 provides the classes of the analysis: $|\Delta f|$. Columns 2 and 3 provide the number of observations greater than the offset $|\Delta f|$, above or below the expected mean value of the frequency: 406.025 MHz. Column 4 provides an average number of observations, assuming the distribution should actually be symmetrical around $\Delta f = 0$. Finally, column 5 provides the ratio: “(number of observations with an offset greater than Δf) / (total number of observations)”. This relative number of observations can be used as an entry in the tabulated function $G(0,1)$, which provides the value of $Z = (f-\mu)/\sigma$.

The estimated value of σ is derived from the corresponding value of the offset: $\sigma = (f-\mu) / Z$.

A strictly Gaussian distribution would give a stable estimate for σ . This is obviously not the case in the data set provided. However, we can still consider that the Gaussian approximation remains valid, at least up to an offset of 250 Hz.

D-A.4 Probability of Frequency Collisions Within a Channel

The transmissions from two beacons may collide in frequency if they are separated by less than 1.5 kHz, i.e., the GEOSAR demodulator filter bandwidth. If “Y” designates the frequency separation, the condition of no-collision is:

$$|Y| = |(f_1 - f_2)| \geq 1,500 \text{ Hz}$$

The probability of no-collision is:

D-A/E.2

$$P(|Y| \geq 1,500) = P((x_1 - x_2) \geq 1,500) + P((x_1 - x_2) \leq -1,500) = 2 * F(1,500)$$

where $F(1,500)$ is the value of the distribution function $F(Y)$ for $Y = 1,500$ Hz.

The random variable Y is a linear function of the random variables x_1 and x_2 that are supposed to follow the same Gaussian distributions $G(\mu, \sigma)$. Then, the distribution of Y is also Gaussian, with the parameters:

$$\mu' = \mu_1 - \mu_2 = 0; \text{ and}$$

$$(\sigma')^2 = (\sigma_1)^2 + (\sigma_2)^2 = 2\sigma^2.$$

Proceeding as in D-A.3, we can use the tabulated normal distribution $G(0,1)$ to determine the probability of $|Y| \geq 1,500$ Hz. Noting that the value of σ determined in section D-A.3 varies from 160 to 520, we would have:

$$160 \leq \sigma \leq 520$$

$$226 \leq \sigma' = \sqrt{2} * \sigma \leq 735$$

We find: - for $\sigma' = 226$;

$$P(|Y| \geq 1,500) = 2 * F(1,500) \cong 0; \text{ and}$$

D-A/E.3

- for $\sigma' = 735$;

$$P(|Y| \geq 1,500) = 2 * F(1,500) = 0.0412.$$

Note: A similar analysis performed on FMCC data illustrated at Figure C-A.1, gave σ values between 400 and 550.

For the largest σ , which corresponds to the lowest probability of collision within a channel, only 4.2% of all transmissions from beacons in the same channel would not collide in the frequency domain.

Therefore, the probability of beacon bursts collision in frequency for beacons in the same channel is:

$$P_f \geq 0.958$$

D-A/E.4

D-A.5 Probability of Frequency Collisions for Beacons in Adjacent Channels

We assume two frequency channels are separated by ΔFc kHz. Our objective is to determine the probability of frequency collisions between bursts from two beacons, when one is in channel (1), e.g. 406.025 MHz, and the other is in channel (2) e.g. 406.028 MHz.

We proceed as above, but with $\mu_1 = 0$, $\mu_2 = \Delta Fc$ (Hz), and assuming σ is the same in both channels.

We designate f_1 the frequency of the beacon in channel (1): $f_1 = \mu_1 + \delta f_1$

We designate f_2 the frequency of the beacon in channel (2): $f_2 = \mu_2 + \delta f_2 = \mu_1 + \Delta Fc + \delta f_2$

Therefore: $\Delta f = f_2 - f_1 = \Delta Fc + (\delta f_2 - \delta f_1)$.

If the required distance in frequency to avoid a collision is 1,500 Hz, we have, assuming $\Delta Fc \geq 0$ and $f_2 \geq f_1$:

$$\begin{aligned} P(|\Delta f| > 1,500) &= P(\Delta Fc + (\delta f_2 - \delta f_1) > 1,500) + P(\Delta Fc + (\delta f_2 - \delta f_1) < -1,500) \\ &= P((\delta f_2 - \delta f_1) > 1,500 - \Delta Fc) + P((\delta f_2 - \delta f_1) < -1,500 - \Delta Fc) \end{aligned}$$

$$P(|\Delta f| > 1,500) = P((\delta f_2 - \delta f_1) > 1,500 - \Delta Fc) + P((\delta f_2 - \delta f_1) < -(1,500 + \Delta Fc))$$

D-A/E.5

The new variable $Y = (\delta f_2 - \delta f_1)$, follows the normal distribution $G(\mu', \sigma')$ with $\mu' = \Delta Fc$ and $\sigma' = \sqrt{2} * \sigma$ and we can determine the probability $P[|Y/\sigma'| \geq (1,500 - \mu')/\sigma']$ from the tabulated normal distribution $G(0,1)$.

Table D-A.2 summarises the results (i.e., probability of frequency collisions) for various channel separations, assuming beacons in each channel have the distribution described in section D-A.3 (i.e. we will use the values $\sigma' = \sqrt{2} * 520 = 735$ and $\sigma' = \sqrt{2} * 160 = 226$).

On the basis of these results, the probability of frequency collision between beacons in two adjacent channels separated by 3 kHz would be 2% with the worst σ for the distribution ($\sigma = 520$), and negligible for $\sigma = 160$. Therefore, we will consider that channels are independent in respect of frequency collisions in the GEOSAR system.

Table D-A.2: Probability of Frequency Collision as a Function of the Channel Separation

Channel Separation ΔF_c (Hz)	$(\delta f_2 - \delta f_1) > \theta$ $(\delta f_2 - \delta f_1) < \theta'$	$\lambda = (\pm 1,500 - \mu')/\sigma'$ ($\sigma' = 735$)	$F(\lambda)$	P. Coll. ($\sigma = 520$)	$\lambda = (\pm 1,500 - \mu')/\sigma'$ ($\sigma' = 226$)	$F(\lambda)$	P. Coll. ($\sigma = 160$)
3,000	$> -1,500$	-2.041	0.9794	0.0206	-6.637	1	0
	$< -4,500$	-	0				
2,500	$> -1,000$	-1.360	0.9131	0.0869	-4.425	1	0
	$< -4,000$	-	0				
2,000	> -500	-0.680	0.7517	0.2483	-2.212	0.9865	0.0135
	$< -3,500$	-	0				
1,500	> 0	0	0.5000	0.5000	0	0.5000	0.5000
	$< -3,000$	4.082	0				
1,000	> 500	0.680	0.2483	0.7517	2.212	0.0135	0.9865
	$< -2,500$	3.401	0				
500	$> 1,000$	1.360	0.0869	0.9098	4.425	0	1
	$< -2,000$	2.721	0.0033				
0	$> 1,500$	2.041	0.0206	0.9588	6.637	0	1
	$< -1,500$	2.041	0.0206				

Note: The probability of collision is: $P. Coll. = 1 - \sum F(\lambda)$, with $\lambda = (\pm 1,500 - \mu')/\sigma'$

D-A.6 Probability of Frequency Collisions for the GEOSAR Channel Capacity Model

For the purpose of the GEOSAR capacity model, on the basis of the above results and for simplicity, we will accept, that:

- channels separated by 3 kHz are considered independent in respect of frequency collisions; and
- beacons in the same frequency channel always collide in the frequency domain (i.e., $P_f = 1$).

APPENDIX B to ANNEX D**ANALYSIS OF COLLISIONS IN TIME OVER "M" SUCCESSIVE BURSTS
WITH FIXED PERIOD AND RANDOMISED TRANSMISSION TIMES****D-B.1 Synchronised Transmissions with Random Spreading**

The Cospas-Sarsat System document C/S T.001 “Specification for Cospas-Sarsat 406 MHz Distress Beacons” specifies as follows the repetition period of successive beacon transmissions (section 2.2.1 of C/S T.001):

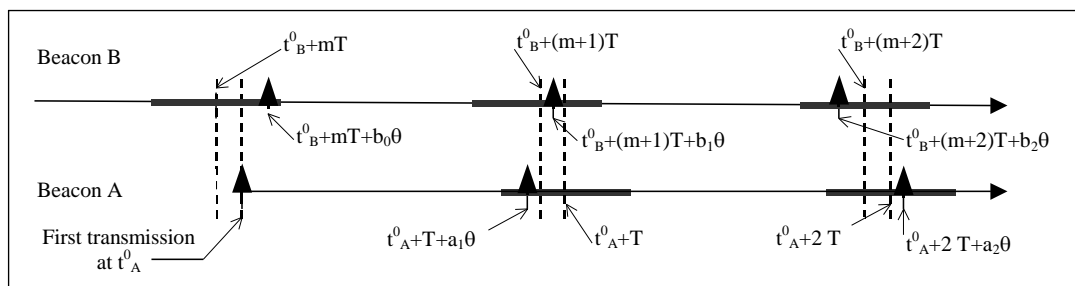
“The repetition period shall not be so stable that any two transmitters appear to be synchronised closer than a few seconds over a 5-minute period. The intent is that no two beacons will have all their bursts coincident. The period shall be randomised around a mean value of 50 seconds, so that time intervals between transmissions are randomly distributed on the interval 47.5 to 52.5 seconds.”

The analysis of the probability of collision for successive transmissions of the same beacon, with a repetition period randomised as specified above is provided at Appendix C to Annex D. However, because of its complexity, the analysis of Appendix C does not provide direct conclusions in respect of the probability of successful processing. Therefore, to obtain an acceptable analytical model of the GEOSAR capacity, a different implementation of randomised repetition periods is analysed in this Appendix. Although the random spreading analysed below is not in accordance with the specification, it provides similar results when compared to the analysis of Appendix C, in respect of the probability of burst collision, and the computer simulation results reported at Appendix D to Annex D confirm that the probability of processing success for the Appendix B distribution should be identical to the probability of processing success achieved with the C/S T.001 specification. Therefore, the analysis of the distribution of repetitive beacon burst transmission times provided in this appendix is an acceptable analytical model of the GEOSAR capacity.

We will assume that all beacons have a “fixed” 50 second period. However, we will also assume that the actual burst transmission time is randomised in a time interval of ± 2.5 seconds around the 50 sec period time. This implementation of a randomised transmission time would allow time intervals between transmissions to vary from 45 to 55 seconds (which is not consistent with the specification).

In accordance with the proposed scenario, all active beacons are actually synchronised with a fixed “period separation”, and transmission times are randomly distributed in the interval ± 2.5 seconds, as illustrated in Figure D-B.1 below.

Figure D-B.1: Fixed Repetition Period with Randomised Transmission Times



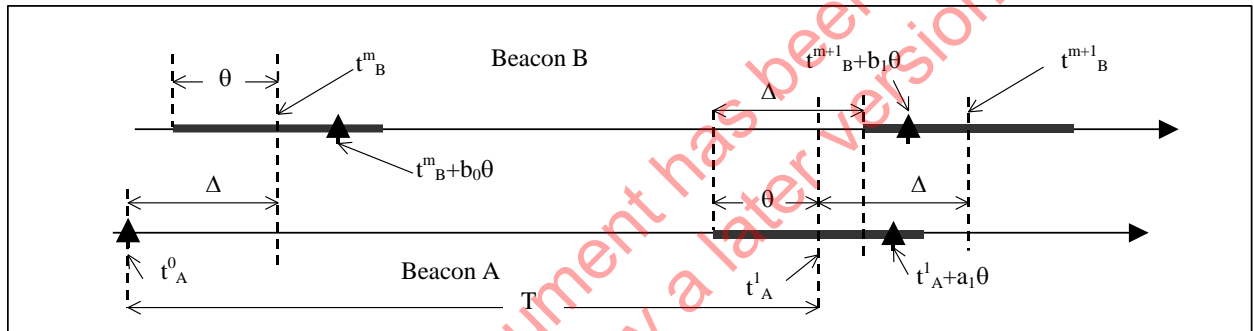
In the above figure, $\theta = 2.5$ sec, and $(x*\theta)$ is the random value (x times 2.5 seconds) added to the fixed period T , with “ x ” a random number uniformly distributed in the interval $[-1, +1]$.

Assuming a population of active beacons in the visibility area of the satellite with the above repetition period characteristic, we need to analyse the probability of repeated collisions, and determine their impact on the probability of processing success.

D-B.2 Probability of Collisions as a Function of the Period Separation (Δ) of Synchronised Beacon Transmissions

We designate t_A^0 and t_B^0 the times of the first transmissions of beacons A and B, which set the origin of the time counters for A and B. B has already transmitted $m-1$ bursts when A is transmitting its first burst (see Figure D-B.2).

Figure D-B.2: Spreading of Second Bursts of A and B after One Period T



B started transmitting at t_B^0 and the following bursts were transmitted at times: $t_B^0 + T + x_1*\theta$, $t_B^0 + 2T + x_2*\theta$, ..., $t_B^0 + mT + x_m*\theta$, etc. with x_1, x_2, \dots, x_m random numbers in the interval $[-1, +1]$. We designate t_B^1, t_B^2, t_B^m the times defined by the fixed repetition period T , such as $t_B^1 = t_B^0 + T$, $t_B^2 = t_B^0 + 2T$, ..., $t_B^m = t_B^0 + mT$. Note that these times are NOT the transmission times, but the centres of the intervals upon which the transmission time is randomly spread. Figure D-B.2 illustrates the situation for the first and second bursts of A (t_A^0 and $t_A^1 + a_1\theta$), for simplicity of notation we designate $a_1\theta$ the random variation of the period of A when the second burst is transmitted, and $b_1\theta$ the random variation of the period of B when the $m+1$ burst is transmitted.

The distance in time between the first burst of A (t_A^0) and the m^{th} burst of B is designated $\Delta = t_A^0 - t_B^m$. The value m is selected such that $|\Delta| \leq T/2$. Note that, in accordance with our hypothesis, we will have: $t_A^1 - t_B^{m+1} = \Delta$, $t_A^2 - t_B^{m+2} = \Delta$, ..., $t_A^n - t_B^{m+n} = \Delta$, etc. Δ is referred to as the fixed "period separation".

D-B.2.1 Probability of First Burst Collision: $P_1(\Delta)$

The first burst of A and the m^{th} burst of B are transmitted at the times:

- t_A^0 , and
- $t_B^0 + mT + b_0\theta = t_B^m + b_0\theta$; with b_0 a random number $\in [-1, +1]$.

They are separated by: $t_A^0 - (t_B^m + b_0\theta) = \Delta - b_0\theta$, and will collide if $|\Delta - b_0\theta| < \tau$, where τ is the duration of one burst.

As a consequence of the above condition, a collision is possible only if $|\Delta| \leq \theta + \tau$.

We designate:

- the probability that the first burst of A collides with the m^{th} burst of B when the period separation is Δ as $P_1(\Delta)$; and
- the density of probability of beacon B transmission times as $f_B(x)$ with the conditions:

$$f_B(x) = 1/2\theta \text{ if } x \in [t_B^m - \theta, t_B^m + \theta], \text{ and } f_B(x) = 0 \text{ if } x \notin [t_B^m - \theta, t_B^m + \theta].$$

$$\text{The probability of collision is expressed as follows: } P_1(\Delta) = \int_{t_A^0 - \tau}^{t_A^0 + \tau} f_B(x) * dx \quad \text{D-B/E.1}$$

However, the integration limits depend on the following conditions:

$$t_A^0 - \tau = t_B^m + \Delta - \tau \geq t_B^m - \theta \text{ for } \Delta < 0, \text{ and } t_A^0 + \tau = t_B^m + \Delta + \tau \leq t_B^m + \theta \text{ for } \Delta > 0, \\ \text{which both translate into the condition } |\Delta| \leq \theta - \tau.$$

Under the above condition $f_B(x) = 1/2\theta$ over the interval $[t_A^0 - \tau, t_A^0 + \tau]$ and

$$P_1(\Delta) = \int_{t_A^0 - \tau}^{t_A^0 + \tau} \left(\frac{1}{2\theta} \right) * dx = \frac{\tau}{\theta} \quad \text{D-B/E.2}$$

If $\theta - \tau \leq |\Delta| \leq \theta + \tau$, then we shall have, assuming $\Delta \geq 0$, $t_A^0 + \tau = t_B^m + \Delta + \tau \geq t_B^m + \theta$. Therefore, $P_1(\Delta)$ must be written as follows:

$$P_1(\Delta) = \int_{t_A^0 - \tau}^{t_A^0 + \tau} f_B(x) * dx = \int_{t_A^0 - \tau}^{t_B^m + \theta} \left(\frac{1}{2\theta} \right) * dx = \frac{1}{2\theta} (\theta - \Delta + \tau) = \frac{\tau}{\theta} \left(1 - \frac{\Delta - \theta + \tau}{2\tau} \right) \quad \text{D-}$$

In summary, noting the symmetry around $\Delta = 0$, we have:

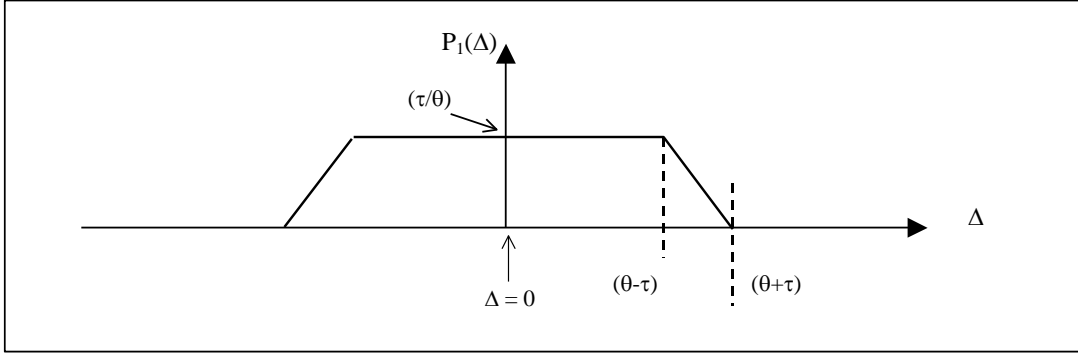
$P_1(\Delta) = \frac{\tau}{\theta} \quad \text{if } \Delta \leq \theta - \tau$	D-B/E.4
$P_1(\Delta) = \frac{\tau}{\theta} \left(1 - \frac{ \Delta - \theta + \tau}{2\tau} \right) \quad \text{if } \theta - \tau \leq \Delta \leq \theta + \tau$	
$P_1(\Delta) = 0 \quad \text{if } \Delta \geq \theta + \tau$	

The probability $P_1(\Delta)$ is graphically illustrated at Figure D-B.3.

We can compute the average value of $P_1(\Delta)$ as follows, assuming a uniform distribution of the Δ values:

$$P_1 = \frac{2}{T} \int_0^{T/2} P_1(\Delta) * d\Delta = \frac{2}{T} \left[\int_0^{\theta - \tau} \frac{\tau}{\theta} d\Delta + \int_{\theta - \tau}^{\theta + \tau} \frac{\tau}{\theta} \left(1 - \frac{\Delta - \theta + \tau}{2\tau} \right) d\Delta \right] = \frac{2\tau}{T} \quad \text{D-B/E.5}$$

Therefore, the average value of $P_1(\Delta)$ is identical to the probability of collision for a uniform distribution of beacon transmission times.

Figure D-B.3: Probability of First Burst Collision $P_1(\Delta)$ **D-B.2.2 Probability of Second Burst Collision: $P_2(\Delta)$**

The following bursts are transmitted at the times:

- $t_{A+T}^0 + a_1\theta = t_{A+T}^1 + a_1\theta$; $t_{A+2T}^0 + a_2\theta = t_{A+2T}^2 + a_2\theta$; etc.; and similarly
- $t_{B+(m+1)T}^0 + b_1\theta = t_{B+(m+1)T}^{m+1} + b_1\theta$; $t_{B+(m+2)T}^0 + b_2\theta = t_{B+(m+2)T}^{m+2} + b_2\theta$; etc.

with $a_1, a_2, b_1, b_2 \in [-1, +1]$.

They are separated by: $(t_{A+T}^0 + a_1\theta) - (t_{B+(m+1)T}^0 + b_1\theta) = \Delta + (a_1 - b_1)\theta$; and

$$(t_{A+2T}^0 + a_2\theta) - (t_{B+(m+2)T}^0 + b_2\theta) = \Delta + (a_2 - b_2)\theta; \text{ etc.}$$

These bursts will collide if $|\Delta + (a_x - b_x)\theta| < \tau$.

As a consequence of the above condition, a collision is possible only if $|\Delta| \leq 2\theta + \tau$.

To simplify the notation, we will also replace the expressions $t_A^1 + a_1\theta$ by $t_A + a\theta$ and $t_B^m + b_1\theta$ by $t_B + b\theta$, with the understanding that t_A is associated with the second burst of A and t_B corresponds to the $(m+1)$ burst of B.

We designate as $P_2(\Delta)$ the probability of a collision between the A and B bursts after one period T, when the periods are synchronised with a separation of Δ seconds. Because of the obvious symmetry around $\Delta = 0$, we will only consider $\Delta \geq 0$ in the following discussion.

We then designate $f_B(x)$ the density of probability of the transmission times of B and $f_A(y)$ the probability of collisions with the second burst of A for $t_A + a\theta = t_A + y$.

$$P(t_B + b\theta = x) = f_B(x) = 1 / 2\theta \text{ if } x \in [t_B - \theta, t_B + \theta] \text{ and } f_B(x) = 0 \text{ outside this interval.}$$

With $y = a\theta$

$$f_A(y) = P(t_B + b\theta \in [t_A + y - \tau, t_A + y + \tau])$$

$$f_A(y) = \int_{t_A + y - \tau}^{t_A + y + \tau} f_B(x) dx$$

D-B/E.6

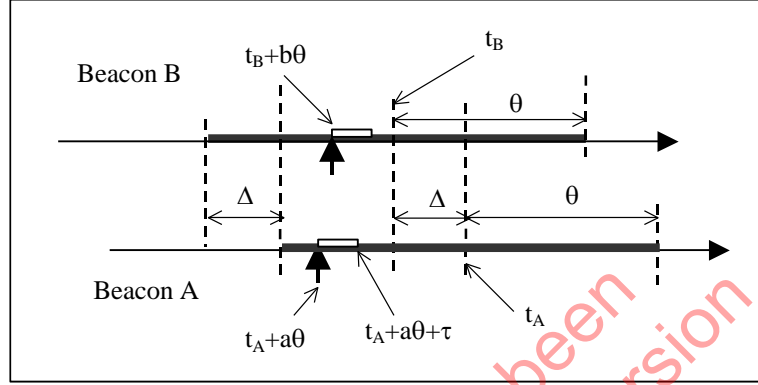
The probability of collision between the second burst of A and the $(m+1)$ burst of B will then be:

$$P_2(\Delta) = \frac{1}{2\theta} \int_{-\theta}^{+\theta} f_A(y) * dy$$

D-B/E.7

However, we have a number of conditions that affect the integration limits of $f_A(y)$.

Figure D-B.4: Second and Subsequent Bursts Collisions



D-B.2.2.1 $0 \leq \Delta \leq \tau$

Noting that, by definition, $t_A - t_B = \Delta$ and $t_A + y = t_A + a\theta \in [t_A - \theta, t_A + \theta]$, under the above conditions we have: $t_B - \theta = t_A - \Delta - \theta \leq t_A - \theta$, and $t_A - \theta - \tau \leq t_A - \theta - \Delta = t_B - \theta$.

Therefore, $\exists y, y \in [-\theta, +\theta]$, such as : $t_A - \theta - \tau \leq t_A + y - \tau \leq t_B - \theta$.

a) From the above condition: $t_A + y - \tau \leq t_B - \theta = t_A - \Delta - \theta$ and $y \leq \tau - \Delta - \theta$.

In addition, if we assume that $\tau < \theta$:

$$t_A + y + \tau \leq t_A + \tau - \theta - \Delta + \tau \leq t_A - \Delta + \theta = t_B + \theta$$

Then
$$f_A(y) = \int_{t_A + y - \tau}^{t_A + y + \tau} f_B(x) * dx = \int_{t_B - \theta}^{t_A + y + \tau} \frac{1}{2\theta} * dx = \frac{y + \tau + \theta + \Delta}{2\theta}$$
 D-B/E.8

with the associated conditions: $-\theta \leq y \leq \tau - \Delta - \theta$

b) If $\tau - \Delta - \theta \leq y$ $t_B - \theta = t_A - \Delta - \theta \leq t_A + y - \tau$

Assuming as above that $\tau < \theta$:

$$t_A + \theta + \tau \geq t_A + y + \tau \geq t_A + \tau + \tau - \theta - \Delta \geq t_A - \Delta + \theta$$

Then $t_A + \theta + \tau \geq t_B + \theta$

Therefore, $\exists y, y \in [-\theta, +\theta]$, such that: $t_A + y + \tau \geq t_B + \theta$, and we will have to address separately this particular situation.

We now consider the case where:

$$t_A + y + \tau \leq t_B + \theta = t_A - \Delta + \theta \quad \text{and} \quad y \leq \theta - \Delta - \tau$$

$$\text{Then} \quad f_A(y) = \int_{t_A+y-\tau}^{t_A+y+\tau} f_B(x) * dx = \int_{t_A+y-\tau}^{t_A+y+\tau} \frac{1}{2\theta} * dx = \frac{\tau}{\theta} \quad \text{D-B/E.9}$$

with the associated conditions: $\tau - \Delta - \theta \leq y \leq \theta - \Delta - \tau$

$$\text{c) If } \theta - \Delta - \tau \leq y \leq \theta \quad t_A + y + \tau \geq t_B + \theta$$

$$\text{Then} \quad f_A(y) = \int_{t_A+y-\tau}^{t_A+y+\tau} f_B(x) * dx = \int_{t_A+y-\tau}^{t_B+\theta} \frac{1}{2\theta} * dx = \frac{\theta - \Delta + \tau - y}{2\theta} \quad \text{D-B/E.10}$$

Finally, we can compute $P_2(\Delta)$ for the conditions $0 \leq \Delta \leq \tau$, using equations D-B/E.8, D-B/E.9, and D-B/E.10:

$$P_2(\Delta) = \frac{1}{2\theta} \int_{-\theta}^{+\theta} f_A(y) * dy = \frac{1}{2\theta} \left[\int_{-\theta}^{\tau-\Delta-\theta} \frac{y + \theta + \tau + \Delta}{2\theta} * dy + \int_{\tau-\Delta-\theta}^{\theta-\Delta-\tau} \frac{\tau}{\theta} * dy + \int_{\theta-\Delta-\tau}^{+\theta} \frac{\theta - \Delta + \tau - y}{2\theta} * dy \right]$$

$$P_2(\Delta) = \frac{\tau}{\theta} - \frac{\tau^2 + \Delta^2}{4\theta^2} \quad \text{D-B/E.11}$$

D-B.2.2.2 $\tau \leq \Delta \leq 2\theta - \tau$

From the above conditions on Δ , we have: $\tau - \Delta \leq 0$ and $\tau - \Delta - \theta \leq a\theta$, $\forall a\theta \in [-\theta, +\theta]$.
Therefore :

$$t_A + \tau - \Delta - \theta - \tau \leq t_A + a\theta - \tau$$

$$t_B - \theta \leq t_A + a\theta - \tau = t_A + y - \tau, \quad \forall y \in [-\theta, +\theta]$$

a) The condition $t_A + a\theta + \tau \leq t_B + \theta = t_A - \Delta + \theta$, is equivalent to $a\theta \leq \theta - \Delta - \tau$. Therefore, we have:

$$f_A(y) = \int_{t_A+y-\tau}^{t_A+y+\tau} f_B(x) * dx = \int_{t_A+y-\tau}^{t_A+y+\tau} \frac{1}{2\theta} * dx = \frac{\tau}{\theta} \quad \text{D-B/E.12}$$

with the conditions $-\theta \leq y \leq \theta - \Delta - \tau$

b) If $y \geq \theta - \Delta - \tau$, the condition $t_A + a\theta - \tau \leq t_B + \theta = t_A - \Delta + \theta$, is equivalent to:

$$a\theta \leq \theta - \Delta + \tau.$$

$$\text{Then} \quad f_A(y) = \int_{t_A+y-\tau}^{t_A+y+\tau} f_B(x) * dx = \int_{t_A+y-\tau}^{t_B+\theta} \frac{1}{2\theta} * dx = \frac{\theta - \Delta + \tau - y}{2\theta} \quad \text{D-B/E.13}$$

with the conditions $\theta - \Delta - \tau \leq y \leq \theta - \Delta + \tau$

For the conditions $\tau \leq \Delta \leq 2\theta - \tau$, $P_2(\Delta)$ is expressed as follows, using D-B/E.12 and D-B/E.13:

$$P_2(\Delta) = \frac{1}{2\theta} \int_{-\theta}^{+\theta} f_A(y) * dy = \frac{1}{2\theta} \left[\int_{-\theta}^{\theta-\Delta-\tau} \frac{\tau}{\theta} * dy + \int_{\theta-\Delta-\tau}^{+\theta} \frac{\theta-\Delta+\tau-y}{2\theta} * dy \right] = \frac{\tau}{\theta} - \frac{\tau\Delta}{2\theta^2}$$

$$P_2(\Delta) = \frac{\tau}{\theta} \left(1 - \frac{\Delta}{2\theta} \right)$$

D-B/E.14

D-B.2.2.3 $2\theta - \tau \leq \Delta \leq 2\theta + \tau$

From the above conditions, we have $t_B + \theta = t_A - \Delta + \theta \leq t_A - 2\theta + \tau + \theta = t_A - \theta + \tau$

As $t_A - \theta + \tau \leq t_A + a\theta + \tau$ we have, $\forall y \in [-\theta, +\theta]$, $t_B + \theta \leq t_A + y + \tau$

A collision is possible only if $t_A + y - \tau \leq t_B + \theta$, which imposes the following condition on y :

$$y \leq \theta - \Delta + \tau$$

Therefore,

$$f_A(y) = \int_{t_A+y-\tau}^{t_A+y+\tau} f_B(x) * dx = \int_{t_A+y-\tau}^{t_B+\theta} \frac{1}{2\theta} * dx = \frac{\theta - \Delta + \tau - y}{2\theta} \text{ and}$$

D-B/E.15

$$P_2(\Delta) = \frac{1}{2\theta} \int_{-\theta}^{+\theta} f_A(y) * dy = \frac{1}{2\theta} \left[\int_{-\theta}^{\theta-\Delta+\tau} \frac{\theta - \Delta + \tau - y}{2\theta} * dy \right] = \frac{\Delta^2 - 2\Delta(2\theta + \tau) + (2\theta + \tau)^2}{8\theta^2}$$

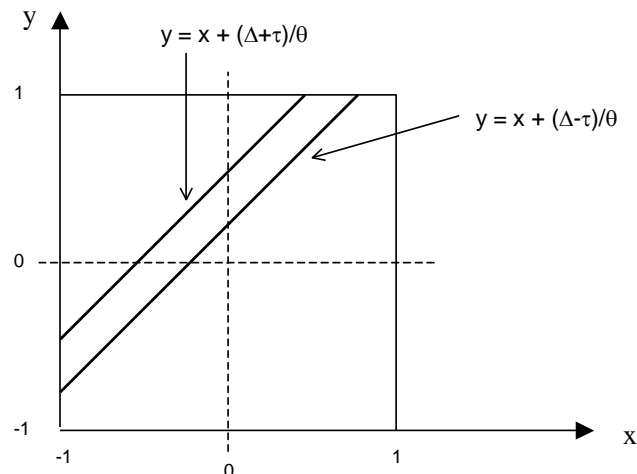
Note: The equations of $P_2(\Delta)$ and the corresponding definition intervals given above (D-B/E.11, D-B/E.14, D-B/E.15) can also be obtained using a graphical representation of the basic conditions for a collision between "A" and "B" bursts:

$$t_B + b\theta \in [t_A + a\theta - \tau, t_A + a\theta + \tau]$$

$$t_B + b\theta = t_A - \Delta + b\theta \geq t_A + a\theta - \tau \Rightarrow b - a \geq (\Delta - \tau)/\theta$$

$$t_B + b\theta = t_A - \Delta + b\theta \leq t_A + a\theta + \tau \Rightarrow b - a \leq (\Delta + \tau)/\theta$$

The above conditions can also be written: $a + (\Delta - \tau)/\theta \leq b \leq a + (\Delta + \tau)/\theta$, which is represented in the figure below by the area above the straight line $\{y = (\Delta - \tau)/\theta + x\}$ and below the straight line $\{y = (\Delta + \tau)/\theta + x\}$. The mathematical expression of the area ($x \ 1/4^{\text{th}}$) is identical to the equations of $P_2(\Delta)$ summarised below.



Equations D-B/E.16 summarise the mathematical expression of the probability of collision between the second burst of A and another beacon burst, as a function of the period separation Δ (see D-B/E.11, D-B/E.14, and D-B/E.15):

D-B/E.16

$$P_2(\Delta) = \frac{\tau}{\theta} - \frac{\tau^2 + \Delta^2}{4\theta^2} \quad \text{if } 0 \leq \Delta \leq \tau$$

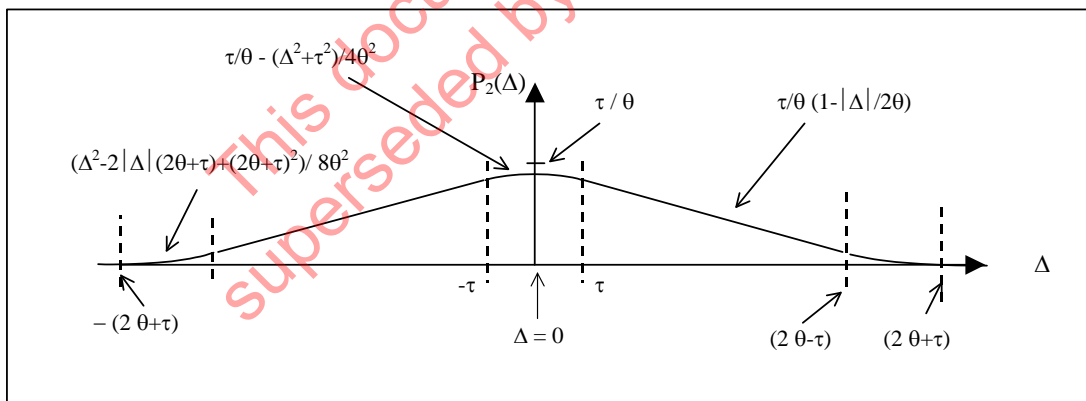
$$P_2(\Delta) = \frac{\tau}{\theta} \left(1 - \frac{\Delta}{2\theta}\right) \quad \text{if } \tau \leq \Delta \leq 2\theta - \tau$$

$$P_2(\Delta) = \frac{(\Delta - (2\theta + \tau))^2}{8\theta^2} \quad \text{if } 2\theta - \tau \leq \Delta \leq 2\theta + \tau$$

$$P_2(\Delta) = 0 \quad \text{if } 2\theta + \tau \leq \Delta$$

As the periods are synchronised with a fixed period separation Δ , the probability of collision for subsequent bursts of A will remain equal to $P_2(\Delta)$. The function $P_2(\Delta)$ is illustrated graphically at Figure D-B.5 below.

Figure D-B.5: Probability of Second and Subsequent Bursts Collisions $P_2(\Delta)$



The average value of $P_2(\Delta)$, assuming a uniform distribution of Δ over the interval $[-T/2, +T/2]$ can be computed as follows:

$$P_2 = \frac{2}{T} \int_0^{T/2} P_2(\Delta) * d\Delta$$

D-B/E.17

$$P_2 = \frac{2}{T} \left[\int_0^{\tau} \left(\frac{\tau}{\theta} - \frac{\Delta^2 + \tau^2}{4\theta^2} \right) * d\Delta + \int_{\tau}^{2\theta - \tau} \left(\frac{\tau}{\theta} - \frac{\Delta\tau}{2\theta^2} \right) * d\Delta + \int_{2\theta - \tau}^{2\theta + \tau} \frac{(\Delta - (2\theta + \tau))^2}{8\theta^2} * d\Delta \right]$$

$$P_2 = \frac{2\tau}{T}$$

The result of the computation of D-B/E.17, i.e., $P_2 = 2\tau/T$, confirms that “on average” P_2 remains equal to the probability of collision computed at Annex D for a uniform distribution of the beacon bursts’ times of arrival.

D-B.2.3 Probability of Collision for Beacon A Bursts, Assuming At Least One Other Beacon With a Period Separation $|\Delta| < \tau$

The average value of $P_2(\Delta)$ is equal to the probability of collisions computed for a uniform distribution (i.e., $2\tau/T$, see above). However, we need to address the “worst-case” scenario whereby at least one beacon has a period separation with beacon “A” less than τ ($|\Delta| \leq \tau$). To that effect we have to compute the average probability of collision between two bursts when $|\Delta| \leq \tau$, as well as the average probability of collision for the other beacons characterised by a period separation from “A” greater than τ ($|\Delta| \geq \tau$).

For the first burst, using the distribution of $P_1(\Delta)$ computed in D-B.2.1 (see D-B/E.4), the statistical average of the probability of collision for $|\Delta| \leq \tau$, and for $|\Delta| \geq \tau$, will be:

$$P_1(|\Delta| \leq \tau) = \frac{1}{\tau} \int_0^{\tau} \frac{\tau}{\theta} * d\Delta = \frac{\tau}{\theta} \quad \text{D-B/E.18}$$

$$P_1(\tau \leq |\Delta| \leq T/2) = \frac{1}{\left(\frac{T}{2} - \tau\right)} \left[\int_{\tau}^{\theta - \tau} \frac{\tau}{\theta} * d\Delta + \int_{\theta - \tau}^{\theta + \tau} \frac{\tau}{2\theta} \left(1 + \frac{\theta - \Delta}{\tau}\right) * d\Delta \right] = \frac{2\tau}{T - 2\tau} \left(1 - \frac{\tau}{\theta}\right) \quad \text{D-B/E.19}$$

From the distribution of $P_2(\Delta)$, provided as D-B/E.16, we find the following average probabilities, as a function of Δ , which characterise all bursts except the first:

$$P_2(|\Delta| \leq \tau) = \frac{1}{\tau} \int_0^{\tau} \left(\frac{\tau}{\theta} - \frac{\Delta^2 + \tau^2}{4\theta^2} \right) * d\Delta = \frac{\tau}{\theta} \left(1 - \frac{\tau}{3\theta}\right) \quad \text{D-B/E.20}$$

$$P_2\left(\tau \leq |\Delta| \leq \frac{T}{2}\right) = \frac{1}{\left(\frac{T}{2} - \tau\right)} \left[\int_{\tau}^{2\theta - \tau} \left(\frac{\tau}{\theta} - \frac{\Delta\tau}{2\theta^2} \right) * d\Delta + \int_{2\theta - \tau}^{2\theta + \tau} \frac{\Delta^2 - 2\Delta(2\theta + \tau) + (2\theta + \tau)^2}{8\theta^2} * d\Delta \right]$$

$$P_2\left(\tau \leq |\Delta| \leq \frac{T}{2}\right) = \frac{2\tau}{T - 2\tau} \left(1 - \frac{\tau}{\theta} + \frac{\tau^2}{3\theta^2}\right) \quad \text{D-B/E.21}$$

Therefore, if we accept to disregard the second order τ/θ terms in the expressions of $P_2(\Delta \leq \tau)$ and $P_2(\Delta \geq \tau)$, we have the same results for $P_1(\Delta \leq \tau)$ and $P_1(\Delta \geq \tau)$ and for all subsequent bursts. While $P_{Av}(\Delta \leq \tau)$ is higher than the mean $2\tau/T$ which characterises the uniform distribution, the probability $P_{Av}(\Delta \geq \tau)$ is lower than $2\tau/T$.

In future computations we will use the expressions D-B/E.20 and D-B/E.21 provided above for the second and subsequent bursts, to express the probabilities of collision $P_{Av}(\Delta \leq \tau)$ and $P_{Av}(\Delta \geq \tau)$.

Note: The probability of occurrence of the worst-case scenario ($|\Delta| \leq \tau$) with two active beacons is: $2\tau/T$. With N active beacons, the probability of having the situation $|\Delta| < \tau$ is $1-(1-2\tau/T)^{N-1}$, i.e. = 0.147 for N=10 (10 active beacons transmitting short messages) and 0.247 if 17 beacons are active.

The next step is to compute the probability of collision for beacon A bursts when a total of N beacons are active (i.e. "A" plus N-1 other beacons).

We assume that, statistically, the values of Δ are uniformly distributed on the time interval $[-T/2, T/2]$. Therefore, with p_{Δ} designating the probability of $|\Delta| \leq \tau$ for two beacons A and B:

$$P(|\Delta| \leq \tau) = p_{\Delta} = 2\tau/T \tag{D-B/E.22}$$

We designate $P_{\Delta(i/N)}$ the probability of "i" beacons with the situation $|\Delta| \leq \tau$ with respect to beacon A, assuming N beacons are active. These probabilities are:

$$\begin{aligned}
 p_{\Delta(0/N)} &= 1-(1-p_{\Delta})^{N-1} \cong 1- p_{\Delta(1/N)} - p_{\Delta(2/N)} - p_{\Delta(3/N)} && \text{D-B/E.23} \\
 p_{\Delta(1/N)} &= (N-1) p_{\Delta} (1-p_{\Delta})^{N-2} && [p_{\Delta(1/17)}= 0.2428 \text{ for 17 active beacons/long msgs}] \\
 p_{\Delta(2/N)} &= [(N-1)(N-2)/ !2] p_{\Delta}^2 (1-p_{\Delta})^{N-3} && [p_{\Delta(2/17)}= 0.0387, \text{ same conditions as above}] \\
 &\dots\dots\dots \\
 p_{\Delta(i/N)} &= [(N-1)(N-2)..(N-i)/ !i] p_{\Delta}^i (1-p_{\Delta})^{N-i-1}
 \end{aligned}$$

As $p_{\Delta(3/17)}= 0.0038$ for long messages and 17 active beacons (which corresponds to the capacity computed for a uniform distribution), we will only consider these probabilities $p_{\Delta(i/N)}$ when $i \leq 3$.

If P_A designates the probability of bursts from A to collide with bursts from B assuming $|\Delta| \leq \tau$, as determined above (i.e. $P_A = P_{A\Delta}(|\Delta| \leq \tau) = \tau/\theta(1-\tau/3\theta)$, see D-B/E.20), the non-conditional (average) probability for a burst from A to experience at least one collision can be expressed as follows:

$$\begin{aligned}
 P_C(A) &= P_{C(N)}*[1 - p_{\Delta(1/N)} - p_{\Delta(2/N)} - p_{\Delta(3/N)}] && \text{D-B/E.24} \\
 &+ p_{\Delta(1/N)}*[P_A + P_{C(N-1)}*(1-P_A)] \\
 &+ p_{\Delta(2/N)}*[2P_A - P_A^2 + P_{C(N-2)}*(1 - 2P_A + P_A^2)] \\
 &+ p_{\Delta(3/N)}*[3P_A - 3P_A^2 + P_A^3 + P_{C(N-3)}*(1 - 3P_A + 3P_A^2 - P_A^3)]
 \end{aligned}$$

Note: The above expression is obtained by considering successively the cases where:

- no beacons have their "period separation" $|\Delta|$ smaller than τ ;
- only one beacon "B" has a period separation such that $|\Delta| \leq \tau$;
- two beacons "B" and "C" have a period separation such that $|\Delta| \leq \tau$; and
- three beacons "B", "C" and "D" have a period separation from "A" such that $|\Delta| \leq \tau$.

The bursts from any beacon in the situation $|\Delta| \leq \tau$ have the same probability P_A to collide with the bursts from "A". If two beacons are in this situation (with the probability $p_{\Delta(2/N)}$) then the probability of one of their bursts colliding with an "A" burst is: $2P_A - P_A^2$ and we must also take into account the probability of collisions from the N-3 other beacons with "A", i.e., $P_{C(N-2)}$. The same reasoning is applied to the case where three beacons are in the situation $|\Delta| \leq \tau$.

In the above expression D-B/E.24, $P_{C(N-i)}$ designates the probability of a collision between A bursts and one or more bursts from the N-i-1 beacons that are characterised by a period separation from "A" greater than τ ($|\Delta| \geq \tau$). This probability is given by the usual expressions:

$$P_{NC(N-i)} = (1-P_C)^{N-i-1} \text{ and } P_{C(N-i)} = 1 - P_{NC(N-i)} \quad \text{D-B/E.25}$$

where P_C is the probability of collision between a burst from A and a burst from one of these N-i-1 beacons. P_C is the probability $P_{Av}(|\Delta| \geq \tau)$ calculated above (D-B/E.21), i.e.:

$$P_C = P_{Av}(\Delta \geq \tau) = \frac{2\tau}{T - 2\tau} \left(1 - \frac{\tau}{\theta} + \frac{\tau^2}{3\theta^2} \right) \quad \text{D-B/E.26}$$

The expression of $P_C(A)$ given as D-B/E.24 provides an "average" probability of collision for the bursts from A, and the computation confirms that it is identical to the probability of collision obtained with a uniform distribution of the times of arrival (see Figure D-B.6). However, we wish to analyse the particular case where beacons A and B are in the situation $|\Delta| \leq \tau$, i.e., at least one beacon has a period separation $|\Delta|$ less than τ from beacon A. This "worst-case" scenario is also illustrated at Figure D-B.6. The expression D-B/E.24 for $P_C(A)$ can be rewritten, noting that $p_{\Delta(i/N)}$ expressed in D-B/E.23 must be recomputed for (N-1) beacons instead of N.

Then, we have:

$$\begin{aligned} P_{C}^*(A) = & [P_A + P_{C(N-1)}*(1-P_A)]*[1 - p_{\Delta(1/N-1)} - p_{\Delta(2/N-1)}] \\ & + p_{\Delta(1/N-1)}*[2P_A - P_A^2 + P_{C(N-2)}*(1 - 2P_A + P_A^2)] \\ & + p_{\Delta(2/N-1)}*[3P_A - 3P_A^2 + P_A^3 + P_{C(N-3)}*(1 - 3P_A + 3P_A^2 - P_A^3)] \end{aligned} \quad \text{D-B/E.27}$$

In the above expression, the probability of a second beacon such that $|\Delta| \leq \tau$ is computed as follows: $p_{\Delta(1/N-1)} = (N-2) p_{\Delta} (1-p_{\Delta})^{N-3}$. D-B/E.28

The probability of a third beacon in the same situation is:

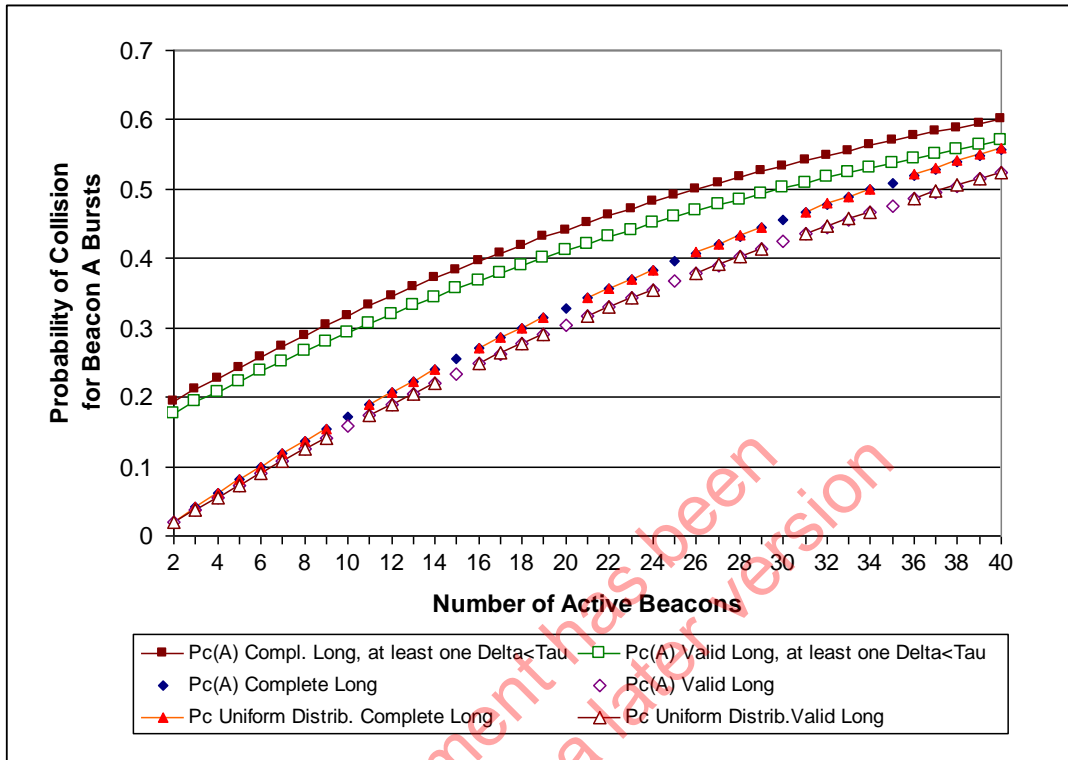
$$p_{\Delta(2/N-1)} = (N-2)(N-3)/!2] p_{\Delta}^2 (1-p_{\Delta})^{N-4}. \quad \text{D-B/E.29}$$

D-B.2.4: Comparison of the Probabilities of Collision $P_C(A)$, $P_{C}^*(A)$ and the Probability of Collision Assuming a Uniform Distribution

Figure D-B.6 below illustrates the results of the computation of the probability of collision for valid long messages and complete long messages, under three hypotheses:

- a uniform distribution of the times of arrival of the bursts for all repetition periods (see Annex D);
- when the fixed repetition period with randomised spreading of the bursts' transmission time is implemented as described in this appendix (D-B/E.24); and
- as per (b) above, but with the added constraint that the "period separation" $|\Delta|$ between a particular beacon "A" and at least one other beacon is smaller than or equal to τ ($|\Delta| \leq \tau$) as in D-B/E.27.

Figure D-B.6: Comparison of the Probability of Collisions Under the Hypothesis of Uniform Distribution and for Fixed Periods with Randomised Transmission Times, - Conditional ($\Delta \leq \tau$) and Non-Conditional Probabilities -



As expected, the probability of collision computed "on average" when all beacons in the population are transmitting in accordance with the hypothesis of "fixed periods and randomised transmission times" (D-B/E.24), is equal to the probability of collision computed with the assumption of a uniform distribution of the bursts' times of arrival. Data points have been removed on the curves obtained for a uniform distribution to show the perfect overlap with the curves obtained for the "average" probabilities of collision, both for complete long messages and for valid long messages.

It is clear from the above Figure D-B.6 that when two beacons have a period separation Δ equal or less than τ , the probability of collision is significantly increased. This is particularly significant for small numbers of active beacons.

From the above results, we might conclude that the required probability of success under the hypothesis of Appendix B (fixed repetition periods and randomised transmission times) will be achieved, on average, with the same number of active beacons as was determined at Annex D under the hypothesis of a uniform distribution, despite the fact that the messages from some beacons may be severely impacted by repetitive collisions, since the "average" probability of collision remains the same. However, this conclusion is NOT supported by the computer simulations reported and discussed at Appendix D to Annex D. This is due to the fact that the binomial formula used to compute the probability of success (see D/E.8) is not applicable when some beacons experience higher probabilities of collision (non-homogeneous population).

The "average" probability of processing success is further analysed in section D-B.4. In sections D-B.3 below, we analyse in more detail the worst-case scenario, particularly in respect

of the time required for obtaining valid or complete long messages, and confirmed valid or complete long messages.

D-B.3 Probability of Successful GEOSAR Processing for Beacon "A" Messages with a Period Separation $|\Delta| < \tau$

The computations detailed in section D.3 of Annex D (equation D/E.8) are repeated with the probability of collision $P_c^*(A)$ computed with the equation D-B/E.27 provided in section D-B.2.3 above, instead of the probability of collision P_i that characterised the uniform distribution over the period T of the times of arrival of the beacon bursts.

Note: The binomial formula remains applicable in this "worst-case" scenario, as shown at Appendix D to Annex D, because it characterises a specific situation with a stable probability of collision. All bursts from all beacons "A" ($\Delta \leq \tau$) have the probability of collision $P_c^*(A)$.

The results assuming $K = 3$ (i.e. three non-interfering messages are required to obtain a valid or complete message) are provided at Table D-B.1 and illustrated in Figure D-B.7 below, which shows the probability $P(A)$ of successfully processing a message from beacon "A" with a period separation $|\Delta| < \tau$ from at least one other beacon, for short messages, valid long messages or complete long messages, and for various processing times (5 or 10 minutes), as a function of the number of active beacons.

Figure D-B.7: Evolution of the Probability of Successful Processing (Assuming $K = 3$) Under the Condition $|\Delta| < \tau$, for 5 and 10 Minute Processing Time

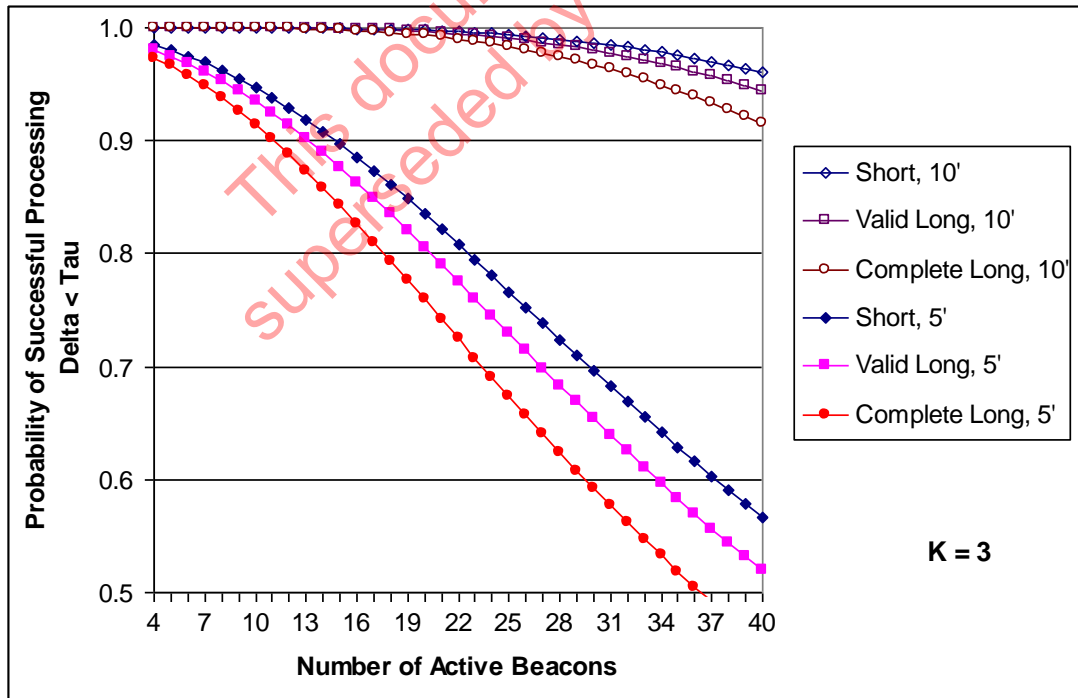


Table D-B.1: Conditional Probability of Successful Processing for N Active Beacons, Assuming K = 3 and At Least One Period Separation $|\Delta| < \tau$

N	5	6	7	8	9	10	11	12	13	14
P(A) Short, 5'	0.9801	0.9750	0.9691	0.9625	0.9552	0.9471	0.9384	0.9291	0.9191	0.9085
P(A) Valid Long, 5'	0.9750	0.9686	0.9614	0.9534	0.9445	0.9349	0.9245	0.9134	0.9016	0.8892
P(A) Complete Long, 5'	0.9660	0.9577	0.9483	0.9380	0.9267	0.9145	0.9015	0.8877	0.8732	0.8581
P(A) Short, 10'	1.0000	1.0000	1.0000	1.0000	0.9999	0.9999	0.9999	0.9998	0.9997	0.9996
P(A) Valid Long, 10'	1.0000	1.0000	1.0000	0.9999	0.9999	0.9998	0.9998	0.9996	0.9995	0.9993
P(A) Complete Long, 10'	1.0000	0.9999	0.9999	0.9999	0.9998	0.9996	0.9995	0.9993	0.9989	0.9986
N	15	16	17	18	19	20	21	22	23	24
P(A) Short, 5'	0.8974	0.8858	0.8737	0.8612	0.8484	0.8353	0.8219	0.8082	0.7944	0.7805
P(A) Valid Long, 5'	0.8763	0.8628	0.8489	0.8347	0.8201	0.8053	0.7903	0.7751	0.7598	0.7445
P(A) Complete Long, 5'	0.8424	0.8264	0.8099	0.7932	0.7762	0.7591	0.7419	0.7247	0.7075	0.6904
P(A) Short, 10'	0.9994	0.9992	0.9990	0.9986	0.9983	0.9978	0.9972	0.9966	0.9958	0.9949
P(A) Valid Long, 10'	0.9990	0.9987	0.9983	0.9978	0.9972	0.9964	0.9956	0.9946	0.9934	0.9921
P(A) Complete Long, 10'	0.9981	0.9974	0.9967	0.9957	0.9946	0.9934	0.9919	0.9901	0.9882	0.9860

Under the worst case scenario of beacon "A" with at least one period separation $|\Delta| < \tau$, the capacity requirement (95% of valid long messages retrieved within 5 minutes) would be achieved with a maximum of 8 active beacons. With 13 active beacons, valid long messages from beacon "A" would be retrieved within 5 minutes with a 90% probability, and with 17 active beacons (i.e., the GEOSAR channel capacity under the hypothesis of uniform distribution of the bursts' arrival times) the messages from "A" would be retrieved with a probability of approximately 84.9% within 5 minutes. However, within 10 minutes, the probability 99% is achieved with 24 active beacons transmitting long messages (probability of recovering a valid message only). Complete long messages would be retrieved with the probability 99% within 10 minutes, with up to 22 active beacons.

The computer simulations described at Appendix D provide results that are consistent with the above analysis. Although the performance requirement is not achieved for beacon "A" if 17 beacons are active (capacity computed for a uniform distribution of the burst arrival times), the performance remains acceptable as the probability of success is well above 99% over 10 minutes. The analysis for confirmed messages presented in section D.4 of Annex D also supports this conclusion.

However, we have yet to determine the population N for which the probability of success "on average" will be 95%.

D-B.4 Non-Conditional (Average) Probability of Successful GEOSAR Processing with Fixed Periods and Randomised Transmission Times

Appendix D to Annex D shows that, in the context of repetitive transmissions, the probability of success computed on the basis of an "average" probability of collision (D-B/E.24) using the binomial formula (equation D/E.8) is not consistent with statistics derived from computer simulations. However, Appendix D to Annex D also shows that the results of the computer simulations for the worst-case scenario of Appendix C (i.e., the C/S T.001 specification) match the probability of success determined by the analysis provided in sections D-B.3 above. Therefore, we will make the assumption that:

- if a beacon "A" is in the situation where at least one other beacon is synchronised with a period separation $\Delta \leq \tau$, it has a probability of success $P_K(1)$ as determined in section D-B.3, using the binomial formula (D/E.8) and the probability of collision $P^*_c(A)$ provided by D-B/E.27;
- if a beacon "A" is in the situation where all other beacons have a period separation with "A" such that $\Delta \geq \tau$, then it has a probability of success $P_K(2)$ as determined in section D.3.3 using

the binomial formula (D/E.8) and the non-conditional probability of burst collision $P_C(A)$ determined by D-B/E.24, which is also the probability of collision for a uniform distribution;

- c) the probability of experiencing the first situation is $p_{\Delta}(1) = 1 - p_{\Delta}(0/N) = p_{\Delta}(1/N) + p_{\Delta}(2/N) + p_{\Delta}(3/N)$ as defined in (D-B/E.23);
- d) the probability of experiencing the second situation is:
 $p_{\Delta}(2) = p_{\Delta}(0/N) = 1 - (1 - p_{\Delta})^{N-1} \cong 1 - p_{\Delta}(1/N) - p_{\Delta}(2/N) - p_{\Delta}(3/N)$ as defined in (D-B/E.23); and
- e) the “average” probability of success for beacon “A” is computed as the weighted average of the probabilities of success in each situation:

$$P^*_K(N,M) = P_K(1) * p_{\Delta}(1) + P_K(2) * p_{\Delta}(2) \qquad \text{D-B/E.30}$$

Table D-B.2: Non-Conditional Probability of Successful Processing for N Active Beacons - Weighted Average for Valid and Complete Long Messages, Assuming K = 3

	N	5	6	7	8	9	10	11	12	13	14
P(A) Valid Long, 5'		0.9978	0.9963	0.9943	0.9916	0.9881	0.9837	0.9785	0.9723	0.9652	0.9571
P(A) Complete Long, 5'		0.9968	0.9946	0.9917	0.9879	0.9831	0.9771	0.9700	0.9617	0.9523	0.9416
P(A) Valid Long, 10'		1.0000	1.0000	1.0000	1.0000	1.0000	1.0000	1.0000	0.9999	0.9999	0.9998
P(A) Complete Long, 10'		1.0000	1.0000	1.0000	1.0000	1.0000	0.9999	0.9999	0.9998	0.9998	0.9996
	N	15	16	17	18	19	20	21	22	23	24
P(A) Valid Long, 5'		0.9481	0.9381	0.9272	0.9154	0.9028	0.8895	0.8755	0.8608	0.8456	0.8299
P(A) Complete Long, 5'		0.9299	0.9170	0.9032	0.8884	0.8727	0.8563	0.8391	0.8215	0.8033	0.7847
P(A) Valid Long, 10'		0.9997	0.9996	0.9995	0.9993	0.9990	0.9987	0.9983	0.9977	0.9971	0.9964
P(A) Complete Long, 10'		0.9995	0.9992	0.9990	0.9986	0.9981	0.9975	0.9967	0.9958	0.9947	0.9934

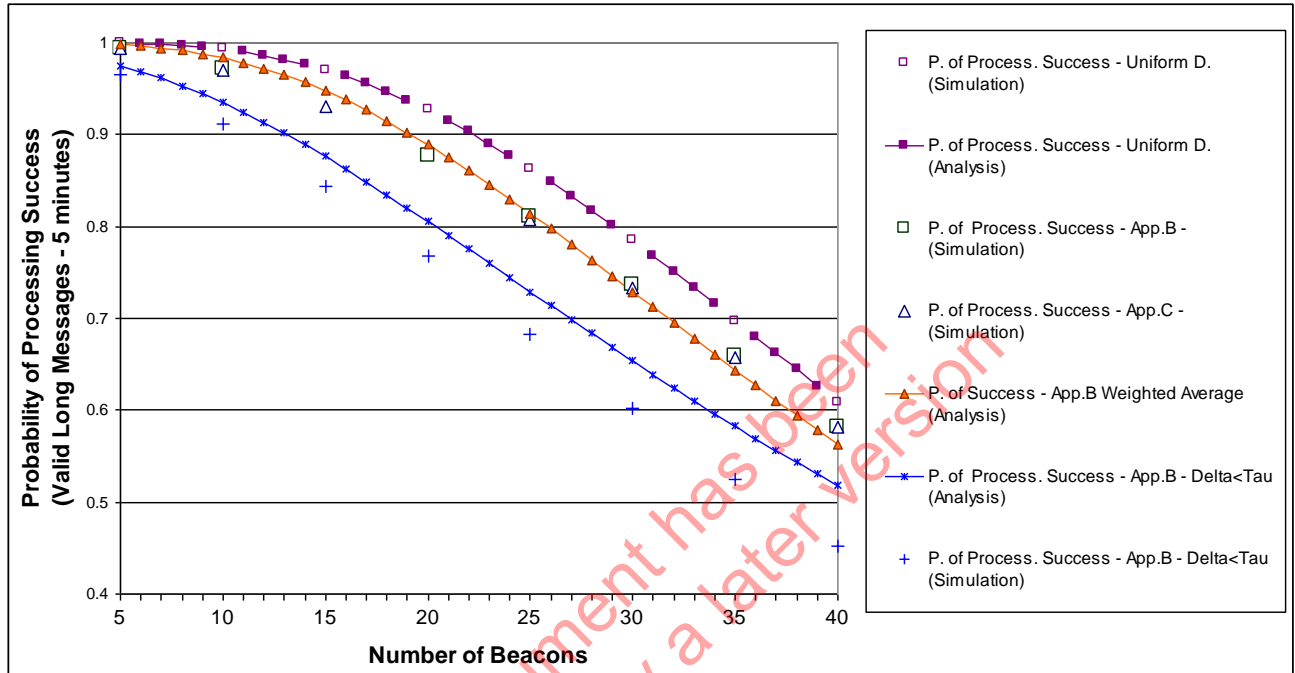
Equation D-B/E.30 provides results that adequately match the computer simulation results provided at Appendix D to Annex D for the transmission time distributions of Appendix B and of Appendix C. Therefore, it provides an acceptable analytical model that can be used to determine the nominal capacity of the GEOSAR system, i.e., the maximum number of active beacons for which the performance criteria of 95% success within 5 minutes is met.

According to the above computation of the “weighted average” for the non-conditional probability of processing success of valid long messages over 5 minutes and assuming a nominal link (K = 3), the 95 % probability would be achieved with a maximum of 14 active beacons. This result is further discussed at section D.4 of Annex D

Figure D-B.8 illustrates the comparison of the probability of successful processing for (a) a uniform distribution of beacon bursts arrival times, (b) the “weighted average” probability computed with the distribution of Appendix B (D-B/E.30), and (c) the conditional ($\Delta \leq \tau$) “worst-case” of the Appendix B distribution as computed in section D-B.3. The results of the corresponding computer simulations are also shown for reference in Figure D-B.8. Although the analytical results for the worst-case of Appendix B seem rather optimistic when compared to the simulation results, the discussion in Appendix D to Annex D show that Appendix B provides a useful model of the performance under the worst-case scenario of the C/S T.001 specification (Appendix C, after 1st burst collision).

**Figure D-B.8: Comparison of Probabilities of Successful Processing
(Valid Long Messages, 5 Minutes)**

- (a) Uniform Distribution of Bursts Arrival Times,
(b) Non-Conditional - App.B Weighted Average, and
(c) Conditional - App.B Worst-Case



D-B.5 Summary of Conclusions of the Analysis of Collisions Over "M" Successive Bursts from Beacons with Fixed Repetition Periods and Randomised Transmission Times

The results of the analysis provided in this appendix clearly show that the hypothesis of uniform distribution of the beacon burst transmission times is not applicable, and the required performance (95 % success over 5 minutes for valid long messages) cannot be achieved with the capacity previously determined (i.e., 17 active beacons). The Appendix B analytical model indicates a maximum GEOSAR channel capacity of 14 active beacons (see Table D-B.2).

The most significant impact of the "worst-case scenario" on the GEOSAR performance is an increased delay for obtaining a valid or a complete long message. However, over 10 minutes, with a maximum load of 14 active beacons, a probability of processing success over 99.9 % would be achieved for single complete long messages.

Although the hypothesis made in respect of the spreading of transmission times is not in accordance with the C/S T.001 requirements, Appendix D to Annex D confirms that:

- the GEOSAR system performance is adequately represented by the mathematical model developed at Appendix B, with a non-conditional probability of success as defined above in section D-B.4 (with equation D-B/E.30 providing the "weighted average" probability of success); and
- the conditional probabilities computed as per the analysis of Appendix B indicate that the system should retain acceptable performance in the worst-case scenario.

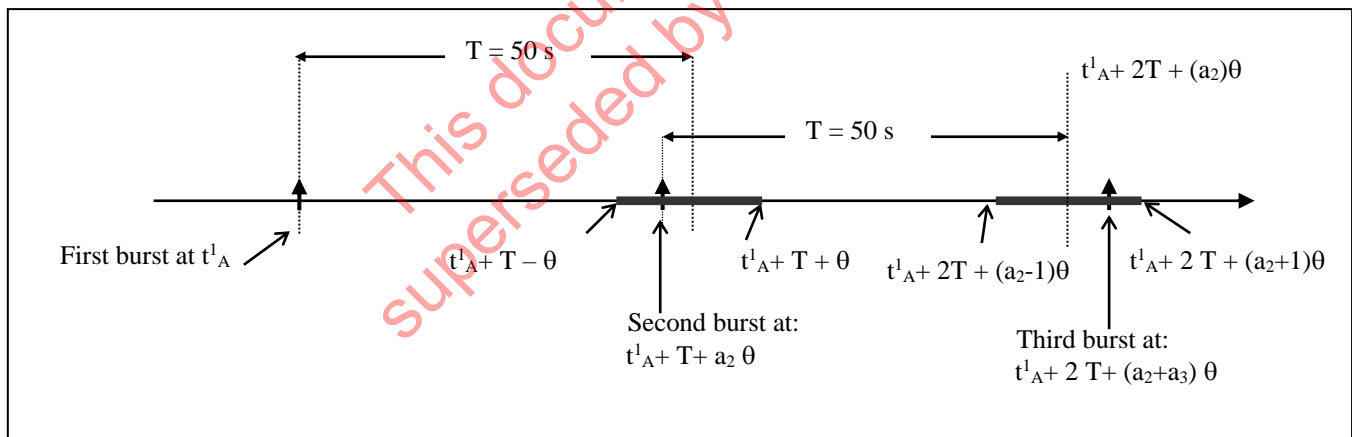
APPENDIX C to ANNEX D**ANALYSIS OF COLLISIONS IN TIME WITH RANDOMISED REPETITION PERIODS****D-C.1 Transmission Times with Random Period Spreading**

The Cospas-Sarsat System document C/S T.001 “Specification for Cospas-Sarsat 406 MHz Distress Beacons” specifies as follows the repetition period of successive beacon transmissions (section 2.2.1 of C/S T.001):

“The repetition period shall not be so stable that any two transmitters appear to be synchronised closer than a few seconds over a 5-minute period. The intent is that no two beacons will have all their bursts coincident. The period shall be randomised around a mean value of 50 seconds, so that time intervals between transmissions are randomly distributed on the interval 47.5 to 52.5 seconds.”

Appendix B to Annex D analyses a possible implementation of fixed repetition periods with random transmission times. This appendix addresses the implementation of “randomised repetition periods” as specified in C/S T.001, where the time intervals between two successive bursts are set randomly between 47.5 seconds and 52.5 seconds, with a uniform distribution of these time intervals centred on 50 seconds, as illustrated in Figure D-C.1 below for a beacon “A”.

Figure D-C.1: Transmission Times with Randomised Repetition Period



The analysis provided in this appendix assesses the impact of the repetition period specification on the probability of repeated collisions for successive bursts from the same beacon, with the objective of verifying whether the hypothesis of a random distribution of arrival times over the period T is still applicable after the bursts from two beacons have collided, and determining the impact of such collisions on the GEOSAR performance.

Unfortunately, the complexity of the analysis will not allow direct conclusions in respect of the probability of successful processing. We will instead verify that, in terms of probability of burst collisions, the distribution of burst transmission times in Appendix C provides results similar to those of Appendix B.

D-C.2 Transmission Times Spreading over "n" Successive Bursts from Beacon "A"

The transmission time of n^{th} burst is noted: $t_A^n = t_A^{n-1} + T + a_n\theta$, where T is the 50 second period, θ is the maximum spreading allowed by the specification (e.g., 2.5 seconds = 5% of T) and a_n is a random number belonging to the interval $[-1, +1]$.

The first burst of beacon A is emitted at the time $T_1 = t_A^1$ ($a_1 = 0$).

The second burst is emitted at the time $t_A^2 = t_A^1 + T + a_2\theta$, which belongs to the time interval $[T_2 - \theta, T_2 + \theta]$ centred on $T_2 = T_1 + T$.

Similarly, we have:

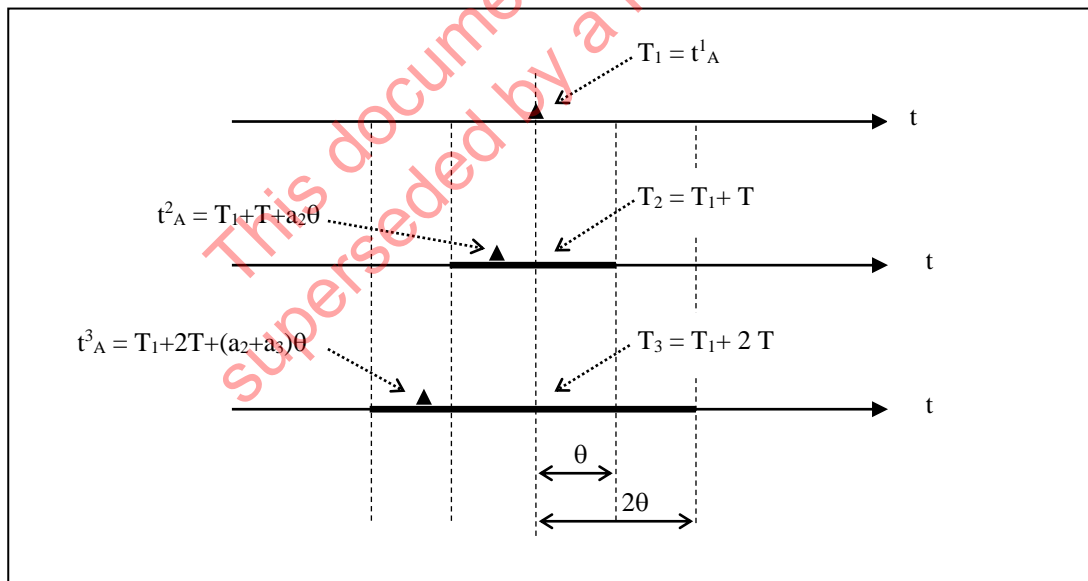
$$t_A^3 = t_A^2 + T + a_3\theta = t_A^1 + 2T + (a_2 + a_3)\theta, \text{ and}$$

$$t_A^n = t_A^1 + (n-1)T + (a_2 + a_3 + \dots + a_n)\theta.$$

The time t_A^3 belongs to the time interval $[T_3 - 2\theta, T_3 + 2\theta]$ centred on $T_3 = T_1 + 2T$.

The time t_A^n belongs to the time interval $[T_n - (n-1)\theta, T_n + (n-1)\theta]$ centred on $T_n = T_1 + (n-1)T$.

Figure D-C.2: Transmission Times Spreading



D-C.2.1 Density of Probability of the Second Burst Transmission Time

The probability density of the second burst transmission time, t_A^2 , illustrated in Figure D-C.3, is:

$$P(t_A^2 = t) = f_2(t) = 0 \quad \forall t \notin [T_2 - \theta, T_2 + \theta], \text{ and}$$

D-C/E.1

$$P(t_A^2 = t) = f_2(t) = 1/2\theta \quad \forall t \in [T_2 - \theta, T_2 + \theta].$$

D-C.2.2 Density of Probability of the Third Burst Transmission Time

Similarly, we have (see Figure D-C.3):

$P(t_A^3 = t) = f_3(t) = 0$ outside the time interval $[T_3-2\theta, T_3+2\theta]$, and

$$P(t_A^3 = t) = f_3(t) = \int_{T_2-\theta}^{T_2+\theta} f_2(x) * f_X(t) dx \quad \text{if "t" is inside the time interval } [T_3-2\theta, T_3+2\theta], \quad \text{D-C/E.2}$$

where $f_X(t)$ is the density function of t_A^3 knowing the transmission time "x" of the second burst.

We have $f_2(x) = 1/2\theta, \forall x \in [T_2-\theta, T_2+\theta]$ centred on the time $T_2 = t_A^1 + T$.

We also have $f_X(t) = 1/2\theta, \forall t \in [x+T-\theta, x+T+\theta]$ and $f_X(t) = 0, \forall t \notin [x+T-\theta, x+T+\theta]$.

However, the above condition on "t" can also be written as follows:

$$x+T-\theta \leq t \leq x+T+\theta; \text{ or}$$

$$t-T-\theta \leq x \leq t-T+\theta$$

The condition $t-T-\theta \leq x \leq t-T+\theta$ must be satisfied to have $f_X(t) \neq 0$ and $f_X(t) = 1/2\theta$, and the condition $T_2-\theta \leq x \leq T_2+\theta$ must be satisfied to have $f_2(x) \neq 0$ and $f_2(x) = 1/2\theta$.

If $T_3 \leq t \leq T_3+2\theta$, then: $T_2-\theta \leq t-T-\theta \leq T_2+\theta \leq t-T+\theta$ (as $T_2-\theta = T_3-T-\theta$ and $T_2+\theta = T_3-T+\theta$).

$$\text{Therefore:} \quad f_3(t) = \frac{1}{4\theta^2} \int_{t-T-\theta}^{T_2+\theta} dx = \frac{1}{4\theta^2} * [T_2 + \theta - t + T + \theta] = \frac{2\theta - (t - T_3)}{4\theta^2} \quad \text{D-C/E.3}$$

If $T_3-2\theta \leq t \leq T_3$, then: $t-T-\theta \leq T_2-\theta \leq t-T+\theta \leq T_2+\theta$.

$$\text{Therefore:} \quad f_3(t) = \frac{1}{4\theta^2} \int_{T_2-\theta}^{t-T+\theta} dx = \frac{1}{4\theta^2} * [t - T + \theta - T_2 + \theta] = \frac{2\theta - (T_3 - t)}{4\theta^2} \quad \text{D-C/E.4}$$

We designate $\delta = t - T_3$. The general form of the equation of the density function of t_A^3 , illustrated graphically in Figure D-C.3, is then:

$$f_3(\delta) = 0, \quad \forall \delta \notin [-2\theta, +2\theta] \quad \text{D-C/E.5}$$

$$f_3(\delta) = \frac{1}{2\theta} - \frac{|\delta|}{4\theta^2}, \quad \forall \delta \in [-2\theta, +2\theta]$$

D-C.2.3 Density of Probability of the Fourth Burst Transmission Time

We can now compute the probability density of the fourth burst, $P(t_A^4 = t) = f_4(t)$, as follows:

$P(t_A^4 = t) = f_4(t) = 0$ outside the time interval $[T_4 - 3\theta, T_4 + 3\theta]$, and

D-C/E.6

$$P(t_A^4 = t) = f_4(t) = \int_{T_3 - 2\theta}^{T_3 + 2\theta} f_3(x) * f_X(t) dx \text{ if "t" is inside the time interval } [T_4 - 3\theta, T_4 + 3\theta],$$

where $f_X(t)$ is the density function of t_A^4 knowing the transmission time "x" of the third burst.

$$\text{We have } f_3(x) = \frac{1}{2\theta} - \frac{|x - T_3|}{4\theta^2}, \quad \forall x \in [T_3 - 2\theta, T_3 + 2\theta] \text{ and } f_3(x) = 0 \quad \forall x \notin [T_3 - 2\theta, T_3 + 2\theta].$$

We also have $f_X(t) = 1/2\theta$, $\forall t \in [x + T - \theta, x + T + \theta]$, and $f_X(t) = 0$, $\forall t \notin [x + T - \theta, x + T + \theta]$. This last condition can be expressed as:

$$x + T - \theta \leq t \leq x + T + \theta, \text{ or} \\ t - T - \theta \leq x \leq t - T + \theta$$

Noting that $T_4 = T_3 + T$, the above conditions lead to the following relations:

a) If $T_4 - 3\theta \leq t \leq T_4 - \theta$, then $t - T - \theta \leq T_3 - 2\theta \leq T_3$, and

$t - T + \theta \leq T_3 \leq T_3 + 2\theta$; therefore:

$$f_4(t) = \int_{T_3 - 2\theta}^{T_3 + 2\theta} f_3(x) * f_X(t) dx = \frac{1}{2\theta} \int_{T_3 - 2\theta}^{t - T + \theta} \left(\frac{1}{2\theta} - \frac{T_3 - x}{4\theta^2} \right) dx$$

$$f_4(t) = \frac{1}{2\theta} \int_{T_4 - T - 2\theta}^{t - T + \theta} \left(\frac{T + 2\theta - T_4}{4\theta^2} - \frac{x}{4\theta^2} \right) dx$$

$$f_4(t) = \frac{9}{16\theta} \left(1 + \frac{t - T_4}{3\theta} \right)^2 \quad \text{D-C/E.7}$$

b) If $T_4 + \theta \leq t \leq T_4 + 3\theta$, then for reason of symetry around T_4 , we will have:

$$f_4(t) = \frac{9}{16\theta} \left(1 - \frac{t - T_4}{3\theta} \right)^2 \quad \text{D-C/E.8}$$

c) If $T_4 - \theta \leq t \leq T_4 + \theta$, then $T_3 - 2\theta \leq t - T - \theta \leq T_3$, and

$T_3 \leq t - T + \theta \leq T_3 + 2\theta$; therefore:

$$f_4(t) = \int_{T_3 - 2\theta}^{T_3 + 2\theta} f_3(x) * f_X(t) dx = \frac{1}{2\theta} \int_{t - T - \theta}^{T_3} \left(\frac{1}{2\theta} - \frac{T_3 - x}{4\theta^2} \right) dx + \frac{1}{2\theta} \int_{T_3}^{t - T + \theta} \left(\frac{1}{2\theta} - \frac{x - T_3}{4\theta^2} \right) dx$$

$$f_4(t) = \frac{1}{2\theta} \int_{t-T-\theta}^{T_4-T} \left(\frac{2\theta - T_4 + T}{4\theta^2} + \frac{x}{4\theta^2} \right) dx + \frac{1}{2\theta} \int_{T_4-T}^{t-T+\theta} \left(\frac{2\theta + T_4 - T}{4\theta^2} - \frac{x}{4\theta^2} \right) dx$$

$$f_4(t) = \frac{3}{8\theta} - \frac{(t-T_4)^2}{8\theta^3}$$

D-C/E.9

With $\delta = t - T_4$, the general expression of $f_4(t)$ given by D-C/E.7, D-C/E.8 and D-C/E.9 is summarised below and illustrated at figure D-C.3.

$\forall \delta \notin [-3\theta, +3\theta]$	$f_4(\delta) = 0$	D-C/E.10
If $-3\theta \leq \delta \leq -\theta$, or $+\theta \leq \delta \leq +3\theta$ then	$f_4(\delta) = \frac{9}{16\theta} \left(1 - \frac{ \delta }{3\theta} \right)^2$	
If $-\theta \leq \delta \leq +\theta$, then	$f_4(t) = \frac{3}{8\theta} - \frac{(\delta)^2}{8\theta^3}$	

D-C.2.4 Density of Probability of the Fifth Burst Transmission Time

The same computation can be repeated for the density of probability of the fifth burst transmission time, as follows:

$$f_5(t) = \int_{T_4-3\theta}^{T_4-\theta} f_4(x) * f_x(t) dx + \int_{T_4-\theta}^{T_4+\theta} f_4(x) * f_x(t) dx + \int_{T_4+\theta}^{T_4+3\theta} f_4(x) * f_x(t) dx$$

D-C/E.11

However, to simplify the computation, we will rewrite the equation using $\delta = T_5 - t$ and $X = x - T_4$.

$$f_5(\delta) = \int_{-3\theta}^{-\theta} f_4(X) * f_X(\delta) dX + \int_{-\theta}^{+\theta} f_4(X) * f_X(\delta) dX + \int_{+\theta}^{+3\theta} f_4(X) * f_X(\delta) dX$$

D-C/E.12

The usual conditions on "t" can be re-written as follows:

- (i) $t \in [T_5 - 4\theta, T_5 + 4\theta] \Rightarrow -4\theta \leq \delta \leq +4\theta$
- (ii) $f_x(t) \neq 0$ only if $t \in [x+T-\theta, x+T+\theta] \equiv x \in [t-T-\theta, t-T+\theta]$, then
 $t - T_5 + T_4 - \theta \leq x \leq t - T_5 + T_4 + \theta$
 $t - T_5 - \theta \leq x - T_4 \leq t - T_5 + \theta \Rightarrow \delta - \theta \leq X \leq \delta + \theta$
 where $x - T_4 = X$.
- (iii) $f_4(x) \neq 0$ only if $x \in [T_4 - 3\theta, T_4 + 3\theta] \Rightarrow -3\theta \leq X \leq +3\theta$

We will use the symmetry of the density function around T_5 to simplify the computation further, i.e. considering only the interval $0 \leq \delta \leq 4\theta$.

The above conditions lead to the following relations:

a) If $0 \leq \delta \leq 2\theta \Rightarrow \delta - \theta \leq \theta \leq \delta + \theta \leq 3\theta$, therefore, $f_5(\delta)$ becomes:

$$f_5(\delta) = \int_{\delta-\theta}^{+\theta} f_4(X) * f_X(\delta) dX + \int_{+\theta}^{\delta+\theta} f_4(X) * f_X(\delta) dX$$

$$f_5(\delta) = \frac{1}{2\theta} \left[\int_{\delta-\theta}^{\theta} \left(\frac{3}{8\theta} - \frac{X^2}{3\theta^3} \right) dX + \frac{9}{16\theta} \int_{\theta}^{\delta+\theta} \left(1 - \frac{2X}{3\theta} + \frac{X^2}{9\theta^2} \right) dX \right] \quad \text{D-C/E.13}$$

$$f_5(\delta) = \frac{1}{3\theta} - \frac{\delta^2}{8\theta^3} + \frac{\delta^3}{32\theta^4}$$

b) If $2\theta \leq \delta \leq 4\theta \Rightarrow \theta \leq \delta - \theta \leq 3\theta \leq \delta + \theta$, therefore, $f_5(\delta)$ becomes:

$$f_5(\delta) = \int_{\delta-\theta}^{+\theta} f_4(X) * f_X(\delta) dX = \frac{1}{2\theta} \int_{\delta-\theta}^{3\theta} \frac{9}{16\theta} \left(1 - \frac{2X}{3\theta} + \frac{X^2}{9\theta^2} \right) dX \quad \text{D-C/E.14}$$

$$f_5(\delta) = \frac{2}{3\theta} - \frac{\delta}{2\theta^2} + \frac{\delta^2}{8\theta^3} - \frac{\delta^3}{96\theta^4}$$

Using the symmetry around T_5 , we find the general expression of $f_5(\delta)$ illustrated in Figure D-C.3:

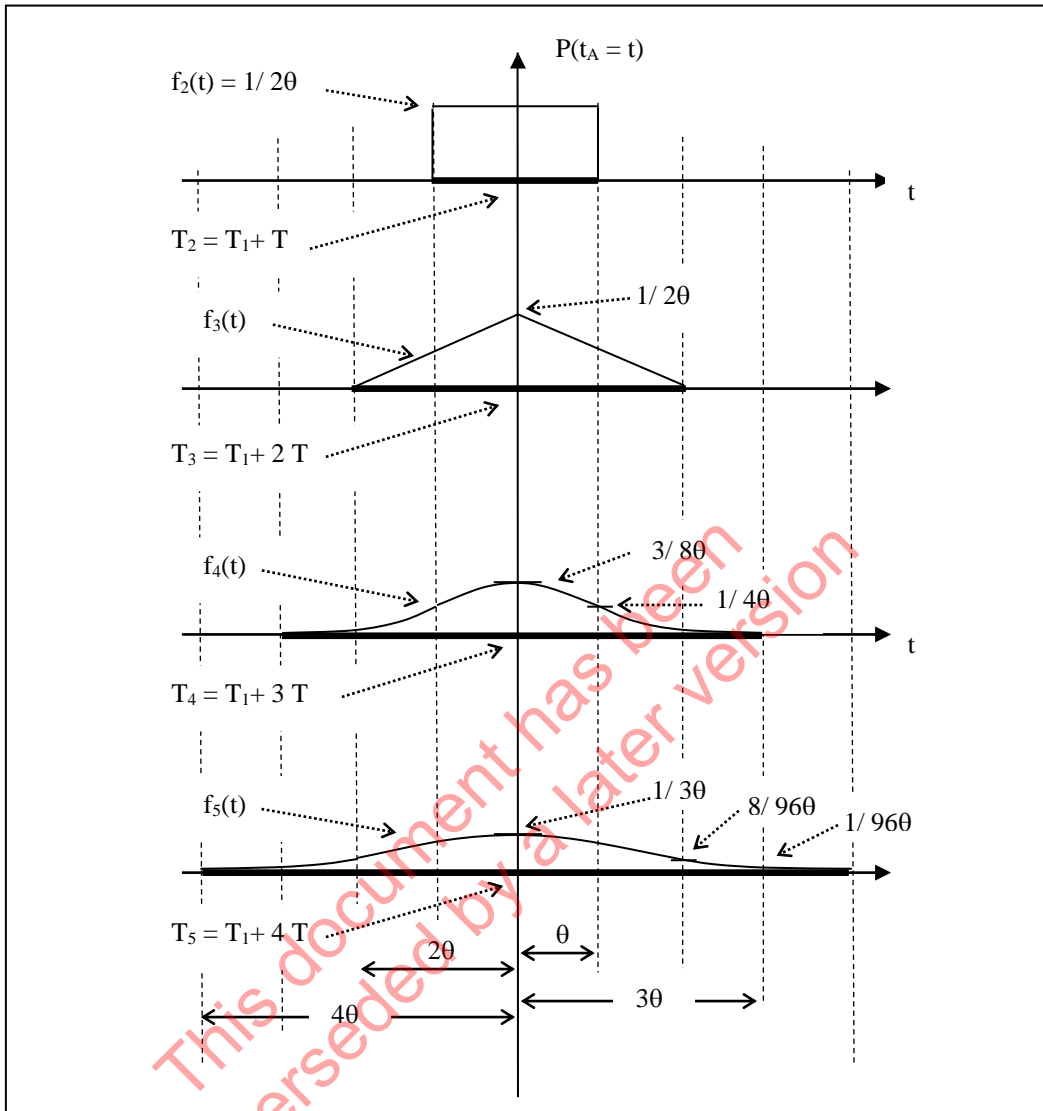
$\forall \delta \notin [-4\theta, +4\theta]$	$f_5(\delta) = 0$	D-C/E.15
If $-4\theta \leq \delta \leq -2\theta$, or $2\theta \leq \delta \leq 4\theta$ then	$f_5(\delta) = \frac{2}{3\theta} - \frac{ \delta }{2\theta^2} + \frac{\delta^2}{8\theta^3} - \frac{ \delta ^3}{96\theta^4}$	
If $-2\theta \leq \delta \leq 2\theta$,	$f_5(\delta) = \frac{1}{3\theta} - \frac{\delta^2}{8\theta^3} + \frac{ \delta ^3}{32\theta^4}$	

D-C.2.5 Density of Probability of the n^{th} Burst Transmission Time

We could proceed as above and continue the computations for subsequent bursts of the beacon "A". The transmissions would continue to spread on a time interval of increasing length, centred on the period ($T_n = T_1 + (n-1)T$), but with decreasing probability densities, particularly for large values of δ .

However, the computations would become extremely cumbersome, particularly when the corresponding equations are used to assess the probability of repeated collision between the bursts from beacon "A" and the bursts of beacon "B" over successive transmissions, as presented in the following section D-C.3. Therefore, we will simply note that, as the probability density decreases, the probability of repeated collisions between "A" and "B" bursts also decreases (see section D-C.3).

Figure D-C.3: Density of Probability of Transmission Times of "A"



D-C.3 Evolution of the Probability of Collision in Time Between Bursts from Beacons "A" and "B", Assuming an Initial Collision or No Collision at T_1

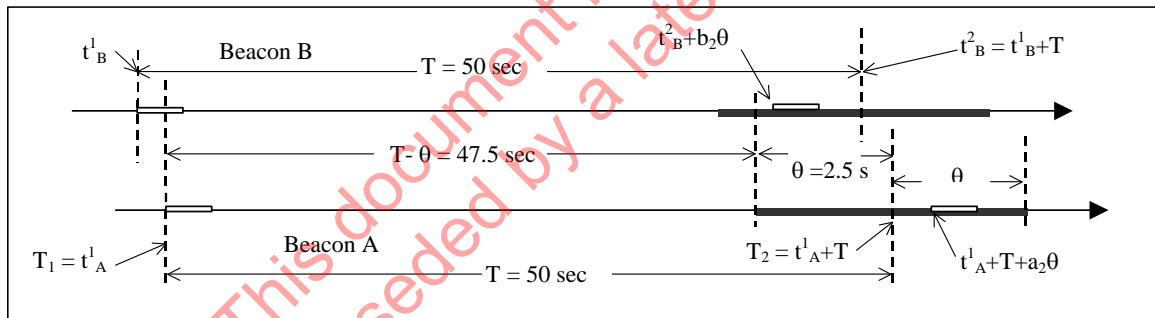
In sections D-C.3.1 to D-C.3.3 we assume that beacons "A" and "B" collide at the time $T_1 = t_A^1$, i.e. $t_B^1 \in [t_A^1 - \tau, t_A^1 + \tau]$, where τ is the burst duration, and we compute the conditional probability of collision for the second, third and fourth bursts. In section D-C.3.4 we consider the case when A and B did not collide at T_1 and analyse the probability of collision of the following burst. These conditional probabilities will be used in section D-C.4 to verify that the "average" probability of collision remains close to the values determined for the uniform distribution of the bursts transmission times, and to compute the probability of collision in the "worst case" scenario of a first burst collision.

D-C.3.1 Second Burst Collision After a Collision at T_1

The following bursts (the second bursts after the initial collision) from A and B will be spread with a uniform distribution on the time interval $[T_2 - \theta, T_2 + \theta]$, with a probability density $1/2\theta$.

Since "A" and "B" messages collided at T_1 , we are, for this second burst, in a configuration illustrated in the figure below, which is identical to the repetitive collisions described at Appendix B under the condition $\Delta \leq \tau$ (see section D-B.2.2 and Figure D-B.4).

Figure D-C.4: Transmission Spreading After First Burst Collision



The probability of collision $P_2(A/B)$ is then as given at Appendix B (equation D-B/E.20):

$$P_2(A/B) = p_c(\Delta \leq \tau) = \frac{\tau}{\theta} * \left(1 - \frac{\tau}{3\theta}\right)$$

D-C/E.16

D-C.3.2 Third Burst Collision Assuming a First Burst Collision

The next bursts (third bursts after the initial collision) from A and B will be spread over the time interval $[T_3 - 2\theta, T_3 + 2\theta]$ with the probability densities $f_3(t)$ calculated above in D-C.2.2. We designate δ the distance between t_A^3 and T_3 , i.e. $t_A^3 = T_3 + \delta$.

For a given value of $\delta \in [0, +2\theta]$, the probability of collision with the third burst from B is:

$$\int_{\delta-\tau}^{\delta+\tau} f_B(x) dx = \int_{\delta-\tau}^{\delta+\tau} \left(\frac{1}{2\theta} - \frac{x}{4\theta^2} \right) dx = \frac{\tau}{\theta} - \frac{\tau\delta}{2\theta^2} = \frac{\tau}{\theta} \left(1 - \frac{\delta}{2\theta}\right)$$

D-C/E.17

The probability of collision for all possible values of $\delta = t_A^2 - T_3$, noting the symmetry around $\delta = 0$, is:

$$P_3(A/B) = 2 \int_0^{2\theta} \frac{\tau}{\theta} \left(1 - \frac{\delta}{2\theta}\right) \left(\frac{2\theta - \delta}{4\theta^2}\right) d\delta$$

$$P_3(A/B) = \frac{2\tau}{3\theta}$$

D-C/E.18

Notes: The above computation is an approximation. The complete analysis, as for the second burst collision described in section D-B.2.2 of Appendix B, should take into account a number of boundary conditions which introduce higher order terms in the above formula. However, for the limited purpose of this analysis, and noting that we will not be able to use this result to compute a probability of processing success, the higher terms can be disregarded.

The probability $P_3(A/B)$ does not depend on whether a collision occurred on the second transmission. Under this analysis, a second burst collision may, or may not, have occurred at T_2 .

The above remarks are also valid for the fourth burst collision analysed below.

D-C.3.3 Fourth Burst Collision Assuming a First Burst Collision

The following bursts (fourth bursts after the initial collision) will be spread over the time interval $[T_4 - 3\theta, T_4 + 3\theta]$ with the probability densities $f_4(t)$ calculated above in D-C.2.3. We accept the same approximation as above for the third burst collision and disregard the boundary conditions at the edge of the transmission time intervals.

As above, we designate δ the distance between t_A^4 and T_4 , i.e. $t_A^4 = T_4 + \delta$.

We have to consider two cases, using the symmetry around T_4 , where:

a) $0 \leq t_A^4 \leq T_4 + \theta$, i.e. $0 \leq \delta \leq \theta$

For a given value of $\delta \in [0, \theta]$, the probability of collision with the fourth burst from B is:

$$\int_{\delta-\tau}^{\delta+\tau} f_B(x) dx = \int_{\delta-\tau}^{\delta+\tau} \left(\frac{3}{8\theta} - \frac{x^2}{8\theta^3} \right) dx = \frac{3\tau}{4\theta} - \frac{\tau(\tau^2 + 3\delta^2)}{12\theta^3} \quad \text{D-C/E.19}$$

The probability of a collision for $\delta \in [-\theta, \theta]$ noting the symmetry around T_4 , is then:

$$P_4^a(A/B) = 2 \int_0^{\theta} \left(\frac{3\tau}{4\theta} - \frac{\tau(\tau^2 + 3\delta^2)}{12\theta^3} \right) \left(\frac{3}{8\theta} - \frac{\delta^2}{8\theta^3} \right) d\delta = \frac{9}{20} \frac{\tau}{\theta} - \frac{8}{144} \frac{\tau^3}{\theta^3} \quad \text{D-C/E.20}$$

b) $T_4 + \theta \leq t_A^4 \leq T_4 + 3\theta$, i.e. $\theta \leq \delta \leq 3\theta$

$$\int_{\delta-\tau}^{\delta+\tau} f_B(x) dx = \int_{\delta-\tau}^{\delta+\tau} \frac{9}{16\theta} \left(1 - \frac{x}{8\theta}\right)^2 dx = \frac{\tau}{8\theta} \left(9 + \frac{\tau^2}{3\theta^2} - \frac{6\delta}{\theta} + \frac{\delta^2}{\theta^2}\right) \quad \text{D-C/E.21}$$

The probability of a collision for $\delta \in [\theta, 3\theta]$ is then:

D-C/E.22

$$P_4^b(A/B) = \frac{\tau}{8\theta} * \frac{9}{16\theta} * \int_{\theta}^{3\theta} \left(9 + \frac{\tau^2}{3\theta^2} - \frac{6\delta}{\theta} + \frac{\delta^2}{\theta^2}\right) \left(1 - \frac{\delta}{3\theta}\right)^2 d\delta = \frac{1}{20} \frac{\tau}{\theta} + \frac{1}{144} \frac{\tau^3}{\theta^3}$$

c) $T_4 - 3\theta \leq t_A^4 \leq T_4 - \theta$, i.e. $-3\theta \leq \delta \leq -\theta$

This situation is symmetrical to (b) above and we will have $P_4^c(A/B) = \frac{1}{20} \frac{\tau}{\theta} + \frac{1}{144} \frac{\tau^3}{\theta^3}$

The probability of collision on the interval $[T_4 - 3\theta, T_4 + 3\theta]$ is then:

$$P_4(A/B) = P_4^a(A/B) + P_4^b(A/B) + P_4^c(A/B) = \frac{9}{20} \frac{\tau}{\theta} - \frac{8}{144} \frac{\tau^3}{\theta^3} + 2 \left(\frac{1}{20} \frac{\tau}{\theta} + \frac{1}{144} \frac{\tau^3}{\theta^3} \right)$$

$$P_4(A/B) = \frac{11}{20} \left(\frac{\tau}{\theta} \right) - \frac{3}{72} \left(\frac{\tau}{\theta} \right)^3 \cong \frac{11}{20} \left(\frac{\tau}{\theta} \right)$$

D-C/E.23

The probability of collision clearly decreases as a result of the spreading of the possible transmission times. Because of the complexity of the calculations (see also sections D-C.4 and D-C.5) we will not attempt to compute the probability of collisions for subsequent bursts.

D-C.3.4 Second Bursts Collision Assuming No-Collision at T_1

If A and B bursts did not collide at T_1 , then their transmission times t_A^1 and t_B^1 were separated by more than τ , i.e., $|t_A^1 - t_B^1| \geq \tau$. This is the situation described at Appendix B under the condition $\Delta \geq \tau$ (see equation D-B/E.21) and the probability of collision, on average, is:

$$P_2^*(A/B) = p_c(\Delta \geq \tau) = \frac{2\tau}{T - 2\tau} * \left(1 - \frac{\tau}{\theta} + \frac{\tau^2}{3\theta^2}\right)$$

D-C/E.24

If N beacons are active and no other beacon transmissions collided with the transmission of A at T_1 , then the probability of a collision between the second burst of A and at least one of the following bursts of the N-1 other beacons is:

$$P_c^*(N) = 1 - (1 - P_2^*)^{N-1}$$

D-C/E.25

where P_2^* as given above (D-C/E.24) replaces the probability of burst collision of the uniform distribution: $p = 2\tau/T$.

D-C.4 Probability of Collision in Time, Assuming N Active Beacons

In D-C.3 we have assessed the probability of collision between bursts from two beacons, "A" and "B", assuming an initial collision at the time T_1 . To compute an "average" probability of collision for the bursts of beacon "A", we must also take into account possible multiple collisions at T_1 , and possible collisions at t^2_A, t^3_A, \dots , between bursts from "A" and from the N-1 other beacons already active in the satellite visibility area, which did not collide at T_1 with the burst from "A".

The results of the computation are summarised in Figure D-C.5 and discussed in section D-C.6.

D-C.4.1 Probability of Collision at T_1 (First Burst)

At time $T_1 = t^1_A$, there is no "history" for the first burst transmitted by "A" and we can only assume a uniform distribution of the times of arrival of the bursts from the N-1 beacons other than A, already active in the satellite visibility area. Because of the uniform distribution hypothesis, the probability of collision between bursts from A and from any other beacon is $p = 2\tau / T$.

We will designate $P^1(0/N)$ the probability of no collisions at T_1 , and similarly $P^1(1/N), P^1(2/N), \dots, P^1(i/N)$ the probabilities of one, two or "i" simultaneous collisions with the burst from A.

$$P^1(0/N) = (1-p)^{N-1} \tag{D-C/E.26}$$

$$P^1(1/N) = (N-1) p (1-p)^{N-2}$$

$$P^1(2/N) = [(N-1)(N-2) / !2] p^2 (1-p)^{N-3}$$

.....

$$P^1(i/N) = [(N-1) \dots (N-i) / !i] p^i (1-p)^{N-i-1}$$

The probabilities $P^1(i/N)$ verify the following relation: $\sum_{i=0}^N P^1(i/N) = 1$, and the probability of at least one collision with the first "A" burst is:

$$P^1_C(N) = \sum_{i=1}^N P^1(i/N) = 1 - P^1(0/N) = 1 - (1-p)^{N-1} \tag{D-C/E.27}$$

The probability of bursts from three beacons A, B and C colliding at T_1 , for N=17 beacons, would be: $P(2/17) = (N-1)(N-2)/2 * (2\tau/T)^2 * (1-2\tau/T)^{N-3} = 0.0387$ in the case of long messages. For A, B, C and D bursts to collide simultaneously, with N = 17 beacons transmitting long messages, we would have the probability $P(3/17) = 0.0038$.

Therefore, in the following computations we will only consider the cases where $i \leq 3$.

$P^1_C(N) = 1 - P^1(0/N) = 1 - (1-p)^{N-1} \cong \sum_{i=1}^3 P^1(i/N)$	D-C/E.28
---	-----------------

D-C.4.2 Probability of Collisions at t_A^2 (Second Burst)

At the time t_A^2 we have to consider several cases, depending on the number of collisions experienced by the first burst from A.

D-C.4.2.1 No Collision at $T_1 = t_A^1$

As there is no "history" of collision at t_A^1 , we must assume that the bursts from the N-1 beacons other than A, already active in the satellite visibility area, satisfied the condition $|t_A^1 - t_B^1| \geq \tau$. The conditional probability of collision for the second burst of A is as described in section D-C.3.4, with equation D-C/E.24:

$$P_2^* = \frac{2\tau}{T - 2\tau} * \left(1 - \frac{\tau}{\theta} + \frac{\tau^2}{3\theta^2} \right)$$

Therefore, with $P_C^2(N,0)$ designating the probability of no collision at T_1 AND at least one collision between the second burst of "A" and bursts from the N-1 other beacons, we have:

$$P_C^2(N,0) = P^1(0/N) [1 - (1 - P_2^*)^{N-1}] \quad \text{D-C/E.29}$$

D-C.4.2.2 One Collision at $T_1 = t_A^1$

The probability of a collision at t_A^2 between the bursts from A and B that already collided at t_A^1 is as determined in section D-C.3.1 with equation D-C/E.16:

$$P_2(A/B) = p_c(\Delta \leq \tau) = \frac{\tau}{\theta} * \left(1 - \frac{\tau}{3\theta} \right).$$

For simplicity, we will abbreviate the designation as P_2 .

In addition, we may have collisions with bursts from the N-2 beacons other than A and B, with the probability: $P_C^*(N-1) = 1 - (1 - P_2^*)^{N-2}$ (see D-C/E.25).

Therefore the probability of at least one collision at t_A^2 assuming one (and only one) collision at t_A^1 is:

$$P_C^2(N,1) = P^1(1/N) * \left[P_2 + (1 - P_2) * \left(1 - (1 - P_2^*)^{N-2} \right) \right] \quad \text{D-C/E.30}$$

D-C.4.2.3 Two Collisions at $T_1 = t_A^1$

The same reasoning as above is applied. However, with two collisions at t_A^1 the probability of at least one collision between the second burst from A and the second bursts from B or C at t_A^2 becomes:

$$P_2(A/B+C) = 2 P_2 - (P_2)^2 \quad \text{D-C/E.31}$$

Therefore, taking into account the N-3 other beacons, the probability of at least one collision at t_A^2 for the second "A" burst, assuming two (and only two) collisions at t_A^1 is:

$$P_C^2(N,2) = P^1(2/N) * \left[2P_2 - P_2^2 + (1 - 2P_2 + P_2^2) \left(1 - (1 - P_2^*)^{N-3} \right) \right] \quad \text{D-C/E.32}$$

D-C.4.2.4 Three Collisions at $T_1 = t^1_A$

With three collisions at t^1_A the probability of at least one collision between the second burst from "A" and the second bursts from beacons B, C or D at t^2_A becomes:

$$P_2(A/B+C+D) = 3 P_2 - 3(P_2)^2 + (P_2)^3 = P_2(3 - 3 P_2 + P_2^2) \quad \text{D-C/E.33}$$

Taking into account the N-4 other beacons, the probability of at least one collision at t^2_A assuming three (and only three) collisions at t^1_A is:

$$P_C^2(N,3) = P^1(3/N) * \left[P_2(3 - 3P_2 + P_2^2) + (1 - P_2(3 - 3P_2 + P_2^2)) \left(1 - (1 - P_2^*)^{N-4} \right) \right] \quad \text{D-C/E.34}$$

D-C.4.2.5 Probability of Collisions for "A" Bursts at t^2_A

We now have to sum up the probabilities determined above, noting that we consider a maximum of three possible simultaneous collisions (see D-C.4.1) and that:

$$P(0/N) + P(1/N) + P(2/N) + P(3/N) < 1.$$

$$\begin{aligned} P_C^2(N) &= P_C^2(N,0) + P_C^2(N,1) + P_C^2(N,2) + P_C^2(N,3) & \text{D-C/E.35} \\ P_C^2(N) &= P^1(0/N) * \left[1 - (1 - P_2^*)^{N-1} \right] \\ &+ P^1(1/N) * \left[P_2 + (1 - P_2) \left(1 - (1 - P_2^*)^{N-2} \right) \right] \\ &+ P^1(2/N) * \left[2P_2 - P_2^2 + (1 - 2P_2 + P_2^2) \left(1 - (1 - P_2^*)^{N-3} \right) \right] \\ &+ P^1(3/N) * \left[P_2(3 - 3P_2 + P_2^2) + (1 - P_2(3 - 3P_2 + P_2^2)) \left(1 - (1 - P_2^*)^{N-4} \right) \right] \end{aligned}$$

D-C.4.3 Probability of Collisions at t^3_A (Third Burst)

The same computations have to be carried out, however, with the added complication of new collisions at t^2_A (i.e., beacons bursts that did not collide with "A" bursts at t^1_A).

We will proceed as in section D-C.4.2, addressing successively the possible occurrences at t^1_A .

D-C.4.3.1 No Collision at $T_1 = t^1_A$

- If no collision occurred at t^1_A AND t^2_A , there is no history of previous collisions and the probability of a collision between the third burst from beacon A and a bursts from any of the N-1 other beacons is as described in section D-C.4.2.1 (equation D-C/E.29), with the probability $[1 - (1 - P_2^*)^{N-1}]$.

Under these conditions, the probability for a burst from "A" to experience a collision at t_A^3 is then:

$$\begin{aligned} P_C^3(N,0,0) &= \text{Prob. no coll. at } t_A^1 * \text{Prob. no coll. at } t_A^2 * \text{Prob. at least one coll. at } t_A^3 \\ &= P^1(0/N) * P^2(0/N) * [1 - (1 - P_2^*)^{N-1}] \end{aligned} \quad \text{D-C/E.36}$$

where: $P^1(0/N)$ is the probability $(1-p)^{N-1}$ used in section D-C.4.2, where "p" is the probability of collision between two bursts (see D-C/E.26).

$P^2(0/N)$ is the also a probability of no collisions, but assuming no collisions occurred at t_A^1 , which imposes that all previous bursts were separated from "A" bursts by a time greater than τ . This probability is $(1-P_2^*)^{N-1}$, where P_2^* is computed as per equation D-C/E.24.

- If no collision occurred at t_A^1 AND one collision occurred at t_A^2 , the probability of a collision with "A" bursts at t_A^3 is:

$$P_C^3(N,0,1) = P^1(0/N) * P^2(1/N) * [P_2 + (1 - P_2)(1 - (1 - P_2^*)^{N-2})] \quad \text{D-C/E.37}$$

where: $P^2(1/N)$ is the probability that one collision (and only one) occurred at t_A^2 , assuming no collision occurred at t_A^1 , which is $(N-1)P_2^*(1-P_2^*)^{N-2}$.

(Note that a collision at t_A^3 that follows a collision at t_A^2 between bursts from the same beacons, has the probability of occurrence P_2)

- If no collision occurred at t_A^1 AND two collisions occurred at t_A^2 , the probability of a collision with "A" bursts at t_A^3 is:

$$P_C^3(N,0,2) = P^1(0/N) * P^2(2/N) * [2P_2 - P_2^2 + (1 - 2P_2 + P_2^2)(1 - (1 - P_2^*)^{N-3})] \quad \text{D-C/E.38}$$

- If no collision occurred at t_A^1 AND three collisions occurred at t_A^2 , the probability of a collision with "A" bursts at t_A^3 is:

$$P_C^3(N,0,3) = P^1(0/N) * P^2(3/N) * [P_2(3 - 3P_2 + P_2^2) + (1 - P_2(3 - 3P_2 + P_2^2))(1 - (1 - P_2^*)^{N-4})] \quad \text{D-C/E.39}$$

As we don't consider the possibility of more than 3 simultaneous collisions at t_A^2 , the probability of collision at t_A^3 , assuming NO collision at t_A^1 is:

$$P_C^3(N,0) = P_C^3(N,0,0) + P_C^3(N,0,1) + P_C^3(N,0,2) + P_C^3(N,0,3) \quad \text{D-C/E.40}$$

Which can be simplified as follows, noting the similarity with the expression of the probability of collisions at t_A^2 (see D-C/E.35):

$$P_C^3(N,0) = P^1(0/N) * \tilde{P}_C^2(N) \quad \text{D-C/E.41}$$

where $P_{\square C^2}$ is formally similar to the expression of the probability P_C^2 (equation D-C/E.35) provided in section D-C.4.2.5. However, it is important to note that $P_{\square C^2}$ is different from the probability P_C^2 , as $P^2(0/N)$, $P^2(1/N)$, $P^2(2/N)$, and $P^2(3/N)$ that appear in the expression of $P_C^3(N,0)$ – see D-C/E.36 to D-C/E.40 – are different from the conditional probabilities $P^1(0/N)$, $P^1(1/N)$, $P^1(2/N)$ and $P^1(3/N)$ in equation D-C/E.35.

D-C.4.3.2 One Collision at $T_1 = t^1_A$

For beacon bursts that collided with "A" bursts at t^1_A , the probability of collision at t^3_A is as computed at section D-C.3.2, i.e., equation D-C/E.18: $P_3(A/B) = 2\tau / 3\theta$. To simplify, we will abbreviate the designation as P_3 . This probability is NOT dependent on possible collisions that may have occurred at t^2_A between the second burst of "A" and the second burst of "B".

Therefore, $P_C^3(N,1)$ will have the form:

$$P_C^3(N,1) = P^1(1/N) * [P_3 + (1-P_3) * [P_C^x(N-1)]] \quad \text{D-C/E.42}$$

where P_C^x designates the probability of collision at t^3_A between the burst from beacon A and bursts from the N-2 beacons other than A and B.

The bursts of the N-2 other beacons did not collide with "A" bursts at t^1_A . However, we now have to consider each possible case of collision with these bursts at t^2_A as this would affect their probability of collision at t^3_A .

- If none of the bursts from the N-2 other beacons collided with the "A" burst at t^2_A , we have:

$$P_C^x(N-1,0) = P^2(0/N-1) * [1 - (1-P_2^*)^{N-2}] \quad \text{D-C/E.43}$$

where $P^2(0/N-1)$ is the probability of no collisions at t^2_A with bursts from N-2 beacons other than A and B, given as: $(1-P_2^*)^{N-2}$.

- If one of the bursts from the N-2 other beacons collided with the "A" burst at t^2_A , we have:

$$P_C^x(N-1,1) = P^2(1/N-1) * [P_2 + (1-P_2) * (1 - (1-P_2^*)^{N-3})] \quad \text{D-C/E.44}$$

where $P^2(1/N-1)$ is: $(N-2)P_2^*(1-P_2^*)^{N-3}$.

- If two of the bursts from the N-2 other beacons collided with the "A" burst at t^2_A , we have:

$$P_C^x(N-1,2) = P^2(2/N-1) * [P_2(2-P_2) + (1-P_2(2-P_2)) * (1 - (1-P_2^*)^{N-4})] \quad \text{D-C/E.45}$$

where $P^2(2/N-1)$ is: $(N-2)(N-3)(1/2)(P_2^*)^2(1-P_2^*)^{N-4}$.

- If three of the bursts from the N-2 other beacons collided with the "A" burst at t^2_A , we have:

$$P_C^x(N-1,3) = P^2(3/N-1) * [P_2(3-3P_2+P_2^2) + (1-P_2(3-3P_2+P_2^2)) * (1 - (1-P_2^*)^{N-5})] \quad \text{D-C/E.46}$$

where $P^2(3/N-1)$ is: $(N-2)(N-3)(N-4)(1/3)(P_2^*)^3(1-P_2^*)^{N-5}$.

As we don't consider the possibility of more than 3 simultaneous collisions at t^2_A , the probability of collision at t^3_A with bursts from the N-2 beacons that did not collide with the "A" burst at t^1_A is:

$$P_C^x(N-1) = P_C^x(N-1,0) + P_C^x(N-1,1) + P_C^x(N-1,2) + P_C^x(N-1,3) \quad \text{D-C/E.47}$$

$$\begin{aligned}
P_C^x(N-1) = & P^2(0/N-1) * \left(1 - (1 - P_2^*)^{N-2}\right) \\
& + P^2(1/N-1) * \left[P_2 + (1 - P_2) \left(1 - (1 - P_2^*)^{N-3}\right)\right] \\
& + P^2(2/N-1) * \left[P_2(2 - P_2) + (1 - P_2(2 - P_2)) \left(1 - (1 - P_2^*)^{N-4}\right)\right] \\
& + P^2(3/N-1) * \left[P_2(3 - 3P_2 + P_2^2) + (1 - P_2(3 - 3P_2 + P_2^2)) \left(1 - (1 - P_2^*)^{N-5}\right)\right]
\end{aligned}
\tag{D-C/E.48}$$

Noting the similarity of form with the expression of $P_C^2(N)$ in D-C/E.35, and with $P_{\square C}^2(N)$ in D-C/E.41 where the symbol \square denotes that the probability $P^2(i/N)$ is different from $P^1(i/N)$, as shown in section D-C.4.3.1, we can write:

$$P_C^x(N-1) = \tilde{P}_C^2(N-1) \tag{D-C/E.49}$$

Therefore, the probability of collision at t_A^3 , assuming ONE collision at t_A^1 is:

$$P_C^3(N,1) = P^1(1/N) * \left[P_3 + (1 - P_3) * \tilde{P}_C^2(N-1)\right] \tag{D-C/E.50}$$

D-C.4.3.3 Two Collisions at $T_1 = t_A^1$

We apply the same reasoning as above in D-C.4.3.2 and we find:

$$P_C^3(N,2) = P^1(2/N) * \left[P_3(2 - P_3) + (1 - P_3(2 - P_3)) * \tilde{P}_C^2(N-2)\right] \tag{D-C/E.51}$$

D-C.4.3.4 Three Collisions at $T_1 = t_A^1$

Similarly we will find:

$$P_C^3(N,3) = P^1(3/N) * \left[P_3(3 - 3P_3 + P_3^2) + (1 - P_3(3 - 3P_3 + P_3^2)) * \tilde{P}_C^2(N-3)\right] \tag{D-C/E.52}$$

D-C.4.3.5 Probability of Collisions for "A" Bursts at t_A^3

We can now sum up the probabilities determined above:

$$\begin{aligned}
P_C^3(N) &= P_C^3(N,0) + P_C^3(N,1) + P_C^3(N,2) + P_C^3(N,3) \\
P_C^3(N) &= P^1(0/N) * \tilde{P}_C^2(N) \\
&+ P^1(1/N) * \left[P_3 + (1 - P_3) * \tilde{P}_C^2(N-1)\right] \\
&+ P^1(2/N) * \left[P_3(2 - P_3) + (1 - P_3(2 - P_3)) * \tilde{P}_C^2(N-2)\right] \\
&+ P^1(3/N) * \left[P_3(3 - 3P_3 + P_3^2) + (1 - P_3(3 - 3P_3 + P_3^2)) * \tilde{P}_C^2(N-3)\right]
\end{aligned}
\tag{D-C/E.53}$$

D-C.5 Probability of Collision Assuming N Active Beacons AND At least One Collision at T_1

In section D-C.4, we have determined the “average” (or non-conditional) probabilities of collision for the bursts from beacon A at the times t_A^1 (first burst), t_A^2 (second burst), and t_A^3 (third burst). The results provided in Figure D-C.5 show that these average probabilities of collision remain equal to the probability of collision for N active beacons computed for a uniform distribution of transmission times.

However, we need to address the “worst-case” scenario of a first burst collision to assess the impact of that condition on the GEOSAR system performance. This will also allow a comparison with the worst-case scenario analysed at Appendix B (i.e., a period separation $|\Delta| \leq \tau$). Therefore, we need to compute the same probabilities as above in section D-C.4, under the additional condition of a collision at time T_1 .

Under this new constraint, the probabilities $P^1(0/N)$, $P^1(1/N)$, $P^1(2/N)$ and $P^1(3/N)$ are replaced by:

D-C/E.54

- $P^\square(0/N) = 0$ (as the collision at t_A^1 between bursts from "A" and "B" is imposed);
- $P^\square(1/N) = P^1(0/N-1)$ (i.e., only one collision = no collision with bursts from N-2 beacons other than "A" and "B");
- $P^\square(2/N) = P^1(1/N-1)$ (i.e., one collision with bursts from N-2 other beacons); and
- $P^\square(3/N) = P^1(2/N-1)$ (i.e., two collisions with bursts from N-2 other beacons).

Replacing $P^1(0/N)$, $P^1(1/N)$, $P^1(2/N)$ and $P^1(3/N)$ with the new probabilities $P^\square(0/N)$, $P^\square(1/N)$, $P^\square(2/N)$, $P^\square(3/N)$ in the expressions of $P_c^1(N)$, $P_c^2(N)$, and $P_c^3(N)$ computed as in section D-C.4, we obtain:

$$P_c^1(N) = 1 - \tilde{P}(0/N) = 1 \quad \text{D-C/E.55}$$

$$\begin{aligned} P_c^2(N) = & P^1(0/N-1) * \left[P_2 + (1-P_2) * (1 - (1-P_2^*)^{N-2}) \right] \\ & + P^1(1/N-1) * \left[P_2(2-P_2) + (1-2P_2+P_2^2) * (1 - (1-P_2^*)^{N-3}) \right] \\ & + P^1(2/N-1) * \left[P_2(3-3P_2+P_2^2) + (1-P_2(3-3P_2+P_2^2)) * (1 - (1-P_2^*)^{N-4}) \right] \end{aligned}$$

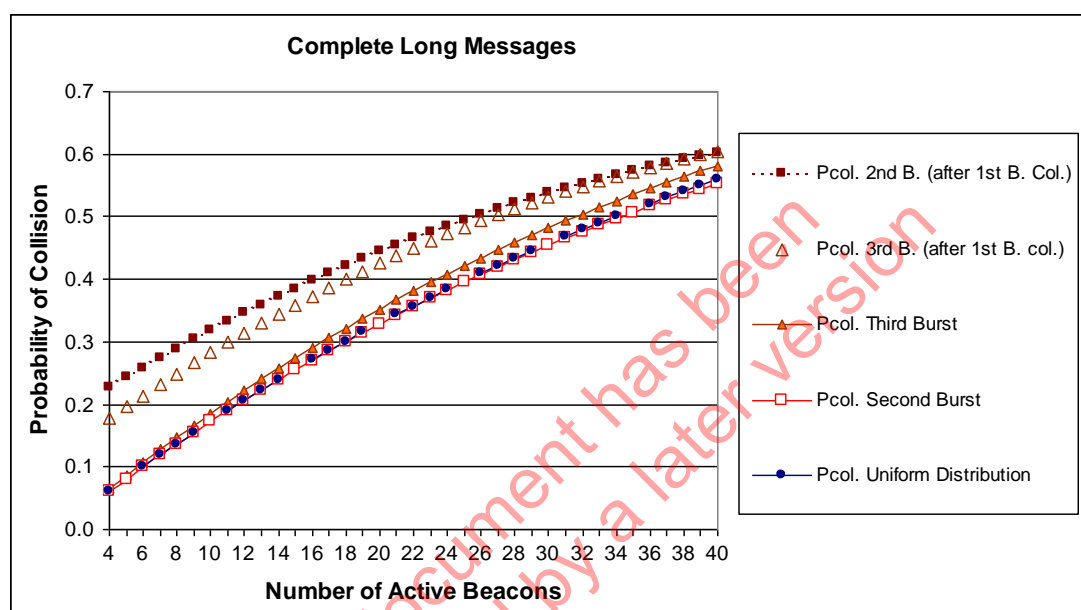
$$\begin{aligned} P_c^3(N) = & P^1(0/N-1) * \left[P_3 + (1-P_3) * \tilde{P}_C^2(N-1) \right] \\ & + P^1(1/N-1) * \left[P_3(2-P_3) + (1-P_3(2-P_3)) * \tilde{P}_C^2(N-2) \right] \\ & + P^1(2/N-1) * \left[P_3(3-3P_3+P_3^2) + (1-P_3(3-3P_3+P_3^2)) * \tilde{P}_C^2(N-3) \right] \end{aligned}$$

The results of this calculation are presented in Figure D-C.5 and discussed in section D-C.6.

D-C.6 Discussion of the Probabilities of Collision Under the Hypothesis of Random Repetition Periods.

The results of the computations described in sections D-C.4 and D-C.5, in the case of complete long messages, are summarised below in Figure D-C.5.

Figure D-C.5: Comparison of Probabilities of Collision for Individual Bursts Assuming A Uniform Distribution (Annex D), or Randomised Periods (Appendix C)



Note: Some data points have been removed to show the exact overlap of the curves for the fourth and the fifth entries of the legend.

Figure D-C.5 highlights two major conclusions. Firstly, the “average” (or non-conditional) probabilities computed as per section D-C.4 for the first (D-C/E.28), the second (D-C/E.35) and the third bursts (D-C/E.53) are identical to the probability of collision obtained with the hypothesis of a uniform distribution of transmission times. This could be expected as it reflects the fact that the randomised period under Appendix C remains on average equal to $T = 50$ seconds. The small variation that we observe for the third burst (Pcol. Third Burst in Figure D-C.5) is only due to the approximation made for the calculation of $P_3(A/B)$, equation D-C/E.18 in section D-C.3.2, which artificially increases the probability of collision.

Secondly, the worst-case (or conditional) probabilities, for the second and third bursts - after first burst collision - are clearly higher than the non-conditional “average” probability, but are decreasing gradually in time towards the average. This is the result of the spreading of the probability densities computed at section D-C.2 and the corresponding decrease of the probability of collision after a collision at T_1 (first burst). Note that the computation slightly overstates the 3rd burst probability of collision for large numbers of active beacons.

Since the non-conditional probability of burst collision is identical to that of the uniform distribution, we might conclude that the randomisation requirement of the specification C/S T.001 analysed in this appendix does not affect the capacity of the system, i.e., the 95% probability of successful processing is met with the same number of active beacons as was computed in the case of a uniform distribution of bursts transmission times. However, this conclusion is NOT supported by the results of the

computer simulation provided at Appendix D, and the matter is further discussed at section D.4 of Annex D and section D-D.4 of Appendix D to Annex D.

In addition, we also have to assess the impact of the worst-case scenario on the probability of success for beacon “A”, and we should now compute the probability of receiving “K” bursts with no-collision over “M” successive transmissions, assuming a first burst collision. Unfortunately, we are faced with the difficulty that the probability of collision changes from burst to burst, and the probability $P_K(N,M)$ cannot be calculated using the binomial formula provided in section D.3.3.1 (equation D/E.8), i.e.:

$$P_k(N, M) = \sum_{m=k}^M C_M^m P_{NC}^m (1 - P_{NC})^{M-m}$$

where P_{NC} designates the probability of no collisions, which also varies from burst to burst.

As we have 20 possible combinations of 3 burst in $M = 6$ possible bursts, or 924 possible combinations of 6 bursts in $M = 12$ possible bursts, it would clearly be impractical to compute the probabilities of successful processing as was done at Annex D and in Appendix B to Annex D, even if we could determine the correct probability of collision for each successive burst up to the 6th or the 12th order. To draw a conclusion from the analysis of randomised repetition periods, we will have to compare the probabilities of collision determined in Appendix C with the probabilities determined in Appendix B.

D-C.7 GEOSAR System Performance Under the Hypothesis of Randomised Repetition Periods

Because of the above considerations, instead of computing the probability $P_K(N,M)$ of successful processing, we will compare the “average” (non-conditional) probability of collision for individual bursts as computed in D-C.4, and the probability assuming an initial collision at T_1 as computed in D-C.5, with the probability of collision obtained in the cases analysed at Appendix B to Annex D (i.e. a fixed repetition period with random transmission times, and the “worst-case” where beacon “A” has a fixed “period separation” Δ from beacon “B” such that $\Delta \leq \tau$). This comparison is illustrated at Figure D-C.6, which provides the same data as in Figure D-C.5, plus:

- the Appendix B probability of collision “on average” (no constraint on the fixed period separation Δ which is assumed to be uniformly distributed); and
- the probability assuming at least one beacon “B” with $|\Delta| \leq \tau$ from beacon “A” (worst-case scenario of Appendix B).

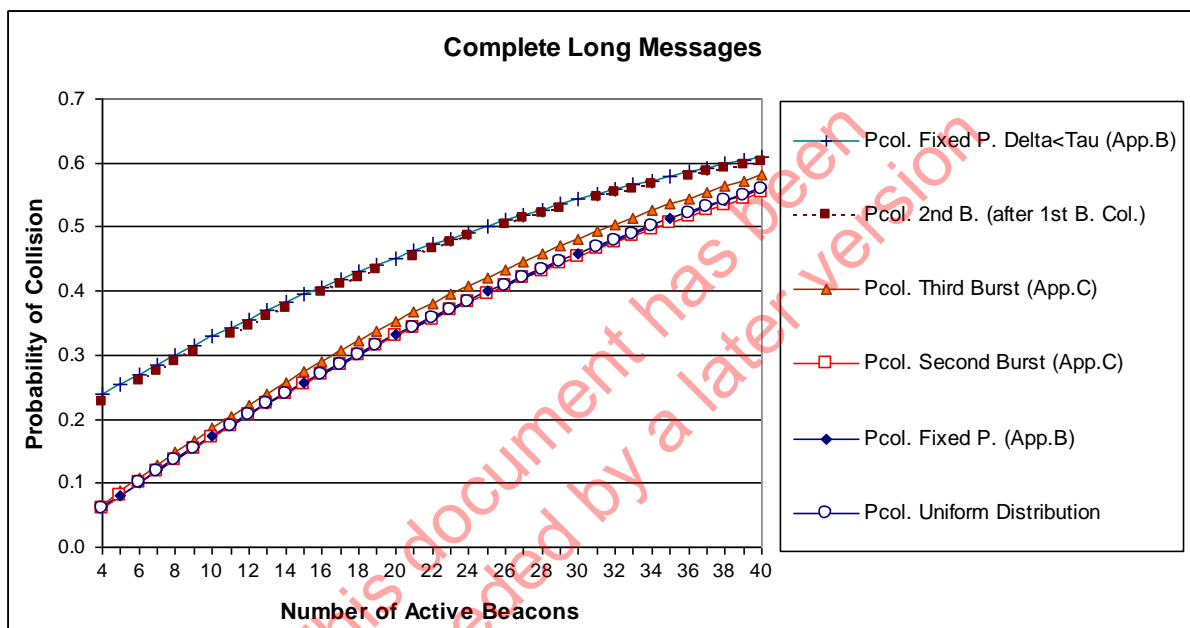
Note: Although the worst-case scenario of Appendix C (first-burst collision) and the worst-case scenario of Appendix B are not identical, since under the condition $\Delta \leq \tau$, there may or may not be a collision for the first burst of beacon “A”, both scenarios have the same probability of occurrence $[1 - (1 - 2\tau/T)^{N-1}]$ when N beacons are active.

Figure D-C.6 shows that the “average” (non-conditional) probability of collision for the second burst as computed under the hypothesis of Appendix C (Pcol. Second Burst (App.C) in Figure D-C.6) and the probability “on average” computed at Appendix B (Pcol. Fixed P. (App.B)) are identical and equal to the probability of collision under a uniform distribution of the beacon bursts. The same remark can be made for the third burst under the distribution of Appendix C (see Pcol. Third Burst (App.C) in Figure D-C.6) although, as noted above in section D-C.6, the approximation of the computation overstates this probability.

Similarly, the probability of collision for the second burst after collision at T_1 (Pcol. 2nd B. (after 1st B. Col.)) is identical to the probability of collision under the worst-case scenario of Appendix B (Pcol. Fixed P. $\Delta < \tau$ (App.B)) i.e., assuming one beacon with $|\Delta| \leq \tau$.

The same match is observed with valid long messages or short messages, which are not reported in this appendix. These results of the mathematical analysis are confirmed by the results of the computer simulation described at Appendix D to Annex D.

Figure D-C.6: Comparison of Probabilities of Collision for Individual Bursts Assuming A Uniform Distribution (Annex D), or Randomised Periods (Appendix C), or Fixed Period and Randomised Transmission Times (Appendix B)



Note: Some data points have been removed to show the exact overlap of the curves for the first and second entries of the legend, and the overlap of the curves for the fifth and sixth entries of the legend.

From this comparison of the probability of collision under the hypotheses analysed in Appendix C and in Appendix B, we can conclude that the performance of the GEOSAR system should be rather similar under both distributions of the bursts transmission times, and that the results obtained at Appendix B in respect of the delay of the confirmation process in the worst-case scenario are also applicable (with minimal adjustment) to the worst case scenario considered under Appendix C.

There are, however, discrepancies between the two distributions, which are highlighted in section D.4 of Annex D, in respect of the worst-case scenario (conditional probabilities of success). In Appendix C we assume a first-burst collision, which has a severe impact on the probability of processing success within 5 minutes, while no such collision is forced under the worst-case scenario of Appendix B (i.e. $\Delta \leq \tau$). Furthermore, the spreading of transmission times observed in Appendix C, lessen the impact of the first-burst collision over time, while no such spreading occurs under the distribution of Appendix B. Over time, the distribution of Appendix C provides better performance than the distribution of Appendix B.

APPENDIX D to ANNEX D

GEOSAR CAPACITY COMPUTER SIMULATION

D-D.1 Scope and Objectives of Computer Simulations

This appendix briefly describes the computer algorithms that were used to validate the mathematical analysis of the GEOSAR capacity model described in Annex D and Appendices B and C of Annex D. The computer model provides the probability of beacon burst collision in time and the probability of successful GEOSAR processing for specific numbers of active beacons by:

- setting the specified number of active beacons and assigning beacon burst transmission times for every burst of every active beacon;
- comparing all the burst transmission times with each other to determine which bursts collided;
- calculating the number of conflicting and non-conflicting bursts for each beacon; and
- identifying those beacons that have a sufficient number of non-conflicting bursts to be “successfully processed” and “confirmed”.

Statistically valid results are obtained by running the simulation a large number of times and averaging the results of the large sample.

The statistical results from the computer model for various numbers of active beacons are then compared to the results of the mathematical model: i.e., the probability of obtaining a valid or complete message by integrating K bursts received without a collision amongst M bursts transmitted during a given period of time (5 or 10 minutes), as determined in section D.3 and in Appendices B and C of Annex D.

D-D.2 Computer Simulation Methodology

D-D.2.1 Computer Assignment of the Beacon Burst Transmission Times

The Computer model initialises the environment by assigning each beacon a random “turn-on” time between 0 and 50 seconds. Thereafter, the burst transmission times are calculated differently for each of the three scenarios (i.e., uniform distribution of transmission times: Annex D; fixed period and randomised transmission times: Appendix B to Annex D; and C/S T.001 specification transmission times: Appendix C to Annex D).

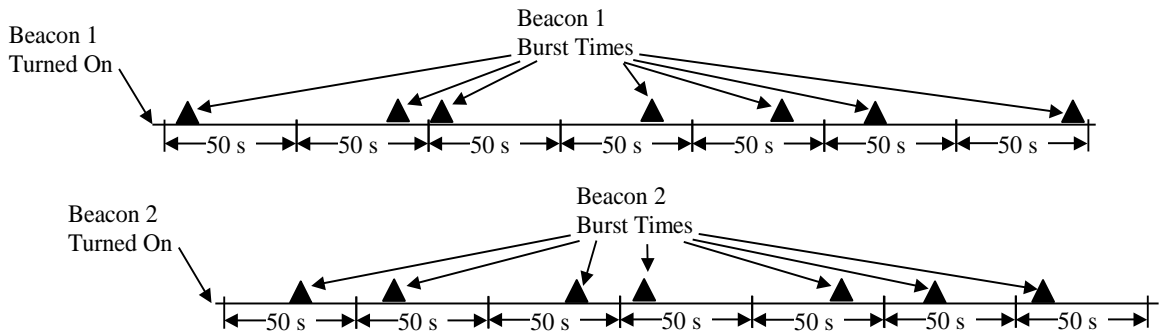
D-D.2.1.1 Uniform Distribution of Burst Transmission Times

As indicated at Figure D-D.1, the computer algorithm creates a series of 50-second time windows for each beacon event, with the first time window starting at the time the beacon was turned on. The transmission times for beacon bursts are assigned randomly such that the beacon transmits one burst in each of its windows.

The distribution of transmission times illustrated at Figure D-D.1 is not representative of the Cospas-Sarsat specification in document C/S T.001, as it allows intervals between transmissions of successive bursts from the same beacon to vary between 0 and 100 seconds, although the average remains at 50 seconds. It is, however, a good illustration of the “uniform

distribution” of transmission times that ignores the characteristic of repetitive transmissions and is used as the basis of the analysis of the theoretical GEOSAR capacity developed at Annex D.

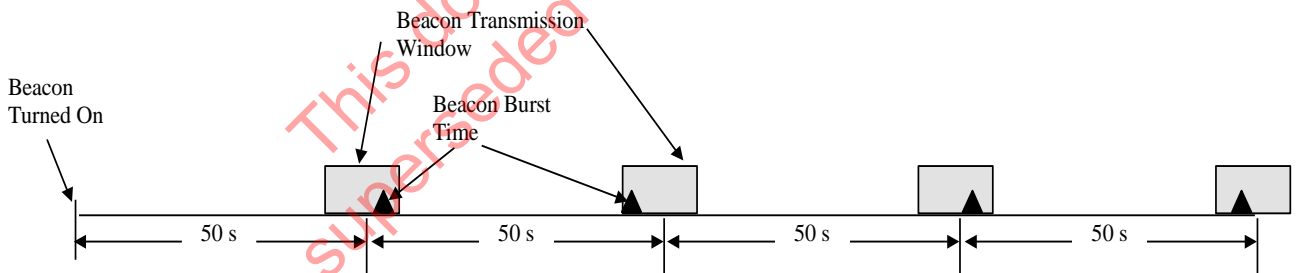
Figure D-D.1: Uniform Distribution of Transmission Times



D-D.2.1.2 Fixed Period and Randomised Transmission Times (Appendix B Distribution)

As indicated at Figure D-D.2, the computer algorithm creates a series of transmission windows for each beacon. The centres of each window are at multiples of 50 seconds after the beacon was turned on; the width of each window is 5 seconds. The transmission times of beacon bursts are assigned randomly such that one burst is transmitted in each window.

Figure D-D.2: Fixed Period and Randomised Transmission Times

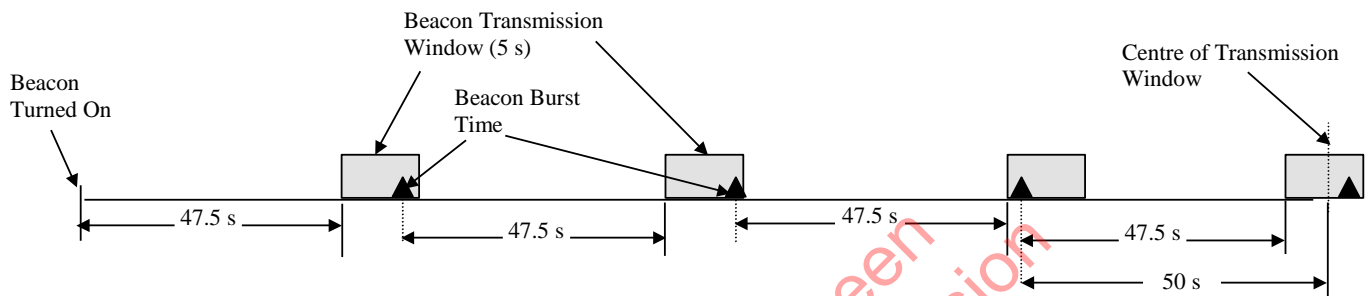


This distribution is not representative of the Cospas-Sarsat C/S T.001 specification as it allows time intervals between transmissions of successive bursts to vary between 45 and 55 seconds, although the average time interval remains 50 seconds. However, this distribution shows interesting characteristics for the mathematical analysis as it exhibits a stable probability of collision for successive bursts, which is a function of the fixed time difference between the centres of the transmission windows of each pair of beacons (also referred to as the “period separation”). The computer simulation shows that the system performance “on average” under Appendix B is equivalent to the system performance under the C/S T.001 specification, and that the system performance in the worst-case scenario defined for both distributions of bursts transmission times remains close.

D-D.2.1.3 C/S T.001 Specification Transmission Times (Appendix C Distribution)

As indicated at Figure D-D.3, the computer creates a series of transmission windows for each beacon. Each window is 5 seconds wide. The first window starts 47.5 seconds after the beacon has been turned on, and subsequent windows start 47.5 seconds after the start of the preceding burst. The transmission times of beacon bursts are assigned randomly such that one burst is transmitted in each window.

Figure D-D.3: C/S T.001 Specification Transmission Times



D-D.2.2 Simulating “Worst-Case” Scenarios

Appendix B also considers the situation where the start time of a beacon’s transmission window coincides with the start time of another beacon’s transmission window, either completely or such that the “window separation” is less than the duration of a beacon burst. This is described at Appendix B as the condition $\Delta \leq \tau$ ($\Delta \leq \tau$). The computer model replicates this situation by forcing the beacon turn on time to be within the burst duration of the turn on time of another beacon. Thereafter, the model gathers performance statistics based only on those two beacons whose turn-on times were forced. Note that forcing the windows to overlap does not force a first-burst collision under the distribution of Appendix B.

Appendix C also considers a worst-case scenario, similar to the case $\Delta \leq \tau$ of Appendix B, whereby the first burst of a particular beacon experiences a collision, which obviously impacts on the probability of collision of follow-on bursts, and on the probability of recovering the beacon message within a given time. The computer model simulates this situation by forcing the first bursts of two beacons to collide. Thereafter, performance statistics are gathered on those two beacons only.

D-D.2.3 Identifying Burst Collisions

The model determines if a burst experienced a fatal collision by comparing its start time with the start time of every other beacon burst. Burst start times that occur within the length of a beacon burst are deemed to have collided. If complete messages were required this type of collision would be considered fatal to all the bursts involved.

The simulation accommodates the specific situation of long valid messages by first identifying which bursts collided, then determining if the collision occurred such that it disrupted a portion of the beacon’s message first protected field or preamble, in which case the collision would be fatal, or if the collision only disrupted the second protected field, in which case the burst could still be processed.

D-D.3 Results of the Computer Simulations for Various Distributions of Transmission Times

The detailed data presented below in section D-D.3 is provided in Table D-D.1

D-D.3.1 Probability of Collision with N active Beacons

Figure D-D.4 shows the probability of collision (first protected field of valid long messages) for specific numbers of active beacons in each of the scenarios:

- Uniform distribution;
- Appendix B (fixed repetition periods and randomised transmission times);
- Appendix C (C/S T.001 specification);
- Appendix B – Worst-Case scenario with $\Delta \leq \tau$; and
- Appendix C – Worst-Case scenario with first-burst collision.

Figure D-D.4: Simulation Results - Probability of Collision for N Active Beacons

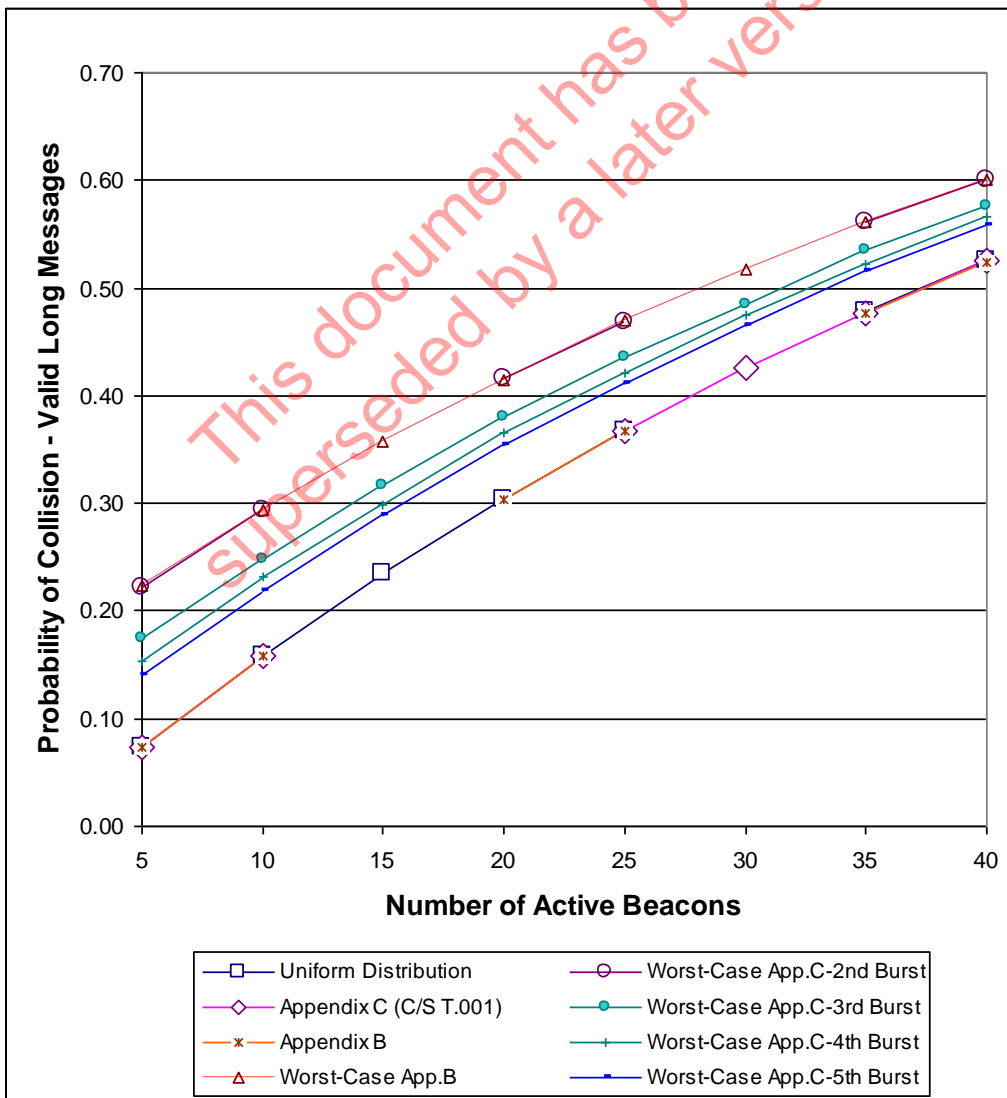


Figure D-D.4 clearly shows that the Uniform distribution, as well as Appendix B and Appendix C distributions, have the same probability of burst collision for N active beacons. The highest probability of burst collision is experienced with the worst-case scenario of Appendix B (at least one couple of beacons such that $\Delta \leq \tau$). With the C/S T.001 specification (Appendix C) distribution of transmission times, the computer results show that, if a collision occurred on the first burst, then the second burst probability of collision is identical to that obtained in the worst-case scenario of Appendix B ($\Delta \leq \tau$). However, the follow-on bursts of that beacon will experience a decreasing probability of collision (see Worst-Case App.C-3rd, 4th and 5th Burst), which in time will converge towards the “average” probability of collision, identical to the probability obtained for a uniform distribution.

These results of the simulation accurately match the results of the analyses of the various distributions presented in Annex D, and at Appendix B and Appendix C of Annex D (see also Figure D-D.5)

D-D.3.2 Probability of Successful Processing with N Active Beacons

The probability of successful processing, defined as obtaining at least 3 messages without collisions affecting the first protected field or the message preamble (i.e., valid long messages) within a given time (5 minutes equivalent to 6 bursts transmitted), is assessed for each of the scenarios described in D-D.3.1 above. The results are illustrated in Figure D-D.6.

In respect of the non-conditional (average) probability of success, Figure D-D.6 shows that:

- the uniform distribution provides the highest probability of success; and
- Appendix B and Appendix C distributions exhibit an identical probability of success, but significantly less than for the Uniform distribution, despite the fact that, on average, they have the same probability of burst collision as the uniform distribution.

The observation noted above reflects the fact that in the presence of repetitive collisions, some beacons experience a much lower probability of success, which is not fully compensated, by the higher probability of success of other beacons. In other words, the best result is obtained when the collisions are evenly spread amongst all beacons.

In respect of the conditional probabilities of success (worst-case scenarios), because the condition of a first burst collision imposed in the worst-case scenario of Appendix C is extremely severe, in particular for a comparison with the worst-case scenario of Appendix B that does not impose a first-burst collision, two results are presented in respect of the C/S T.001 (Appendix C) distribution: i.e. the probability of processing success within 5 minutes, corresponding to the transmission of 6 bursts, and also the probability of success within 6 minutes, which allows for the transmission of 7 bursts. This provides for an assessment of the impact of the first burst collision on the measured performance, and the improvement that is provided after a one-burst delay.

Figure D-D.6 indicates that, on the basis of computer simulation results:

- the worst-case scenario of Appendix C has the lowest probability of success within five minutes, as a result of the imposed condition (first burst collision); and
- however, after the seventh transmission (i.e., within 6 minutes to allow for one additional burst), the performance of the Appendix C distribution (based on C/S T.001 specification) is better than the worst-case scenario of Appendix B ($\Delta \leq \tau$).

**Figure D-D.5: Analysis and Simulation Results
Probability of Collision
for N Active Beacons and Valid Long Messages**

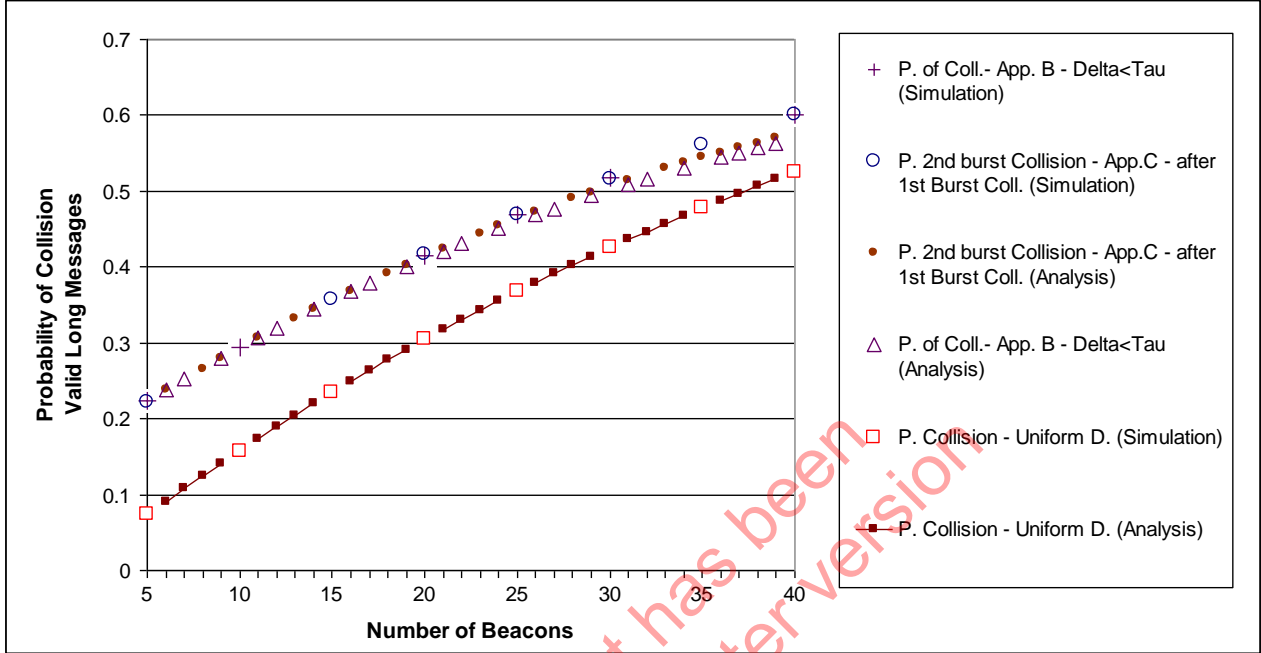
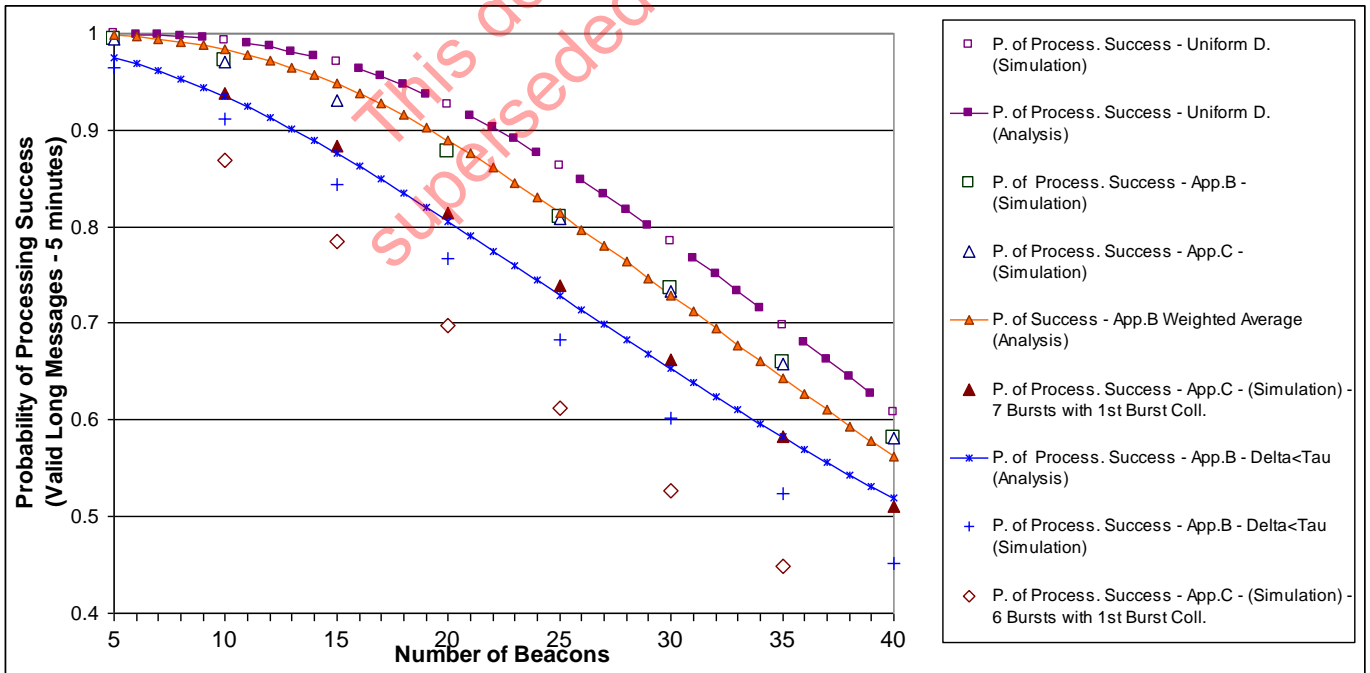


**Figure D-D.6: Analysis and Simulation Results
Probability of Success for N Active Beacons
for Valid Long Messages within 5 Minutes**



Note: In the above figures, data points have been removed where necessary to show the overlap of various curves.

D-D.4 Comparison of Computer Simulations Results with the Results of the Mathematical Analysis

In this section, the results provided by the mathematical analysis and those provided by the computer simulation for the case of valid long messages are compared. The detailed data is provided at Tables D-D.1 and D-D.2.

D-D.4.1 Comparison of Probability of Collision (Valid Long Messages)

Figure D-D.5 highlights the perfect match of the analysis and simulation results for the probability of burst collision assuming a uniform distribution of burst transmission times. Therefore, on the basis of the analysis results reported at Appendix B (section D-B.2.4 and Figure D-B.6) and at Appendix C (section D-C.6 and Figure D-C.5) and the simulation results reported above in section D-D.3.1 and Figure D-D.4, we can conclude that:

- simulation and analysis results in respect of the non-conditional probabilities of burst collision are in good agreement for all three distributions; and
- all three distributions provide, on average, the same probability of collision for a given number “N” of active beacons.

In addition, Figure D-D.5 confirms previous results of the analysis, in particular that the probability of burst collision for the worst-case scenario of Appendix B and for the second burst that follows a first burst collision under the distribution of Appendix C are identical, although the simulation results and the analysis results diverge slightly for large numbers of beacons.

D-D.4.2 Comparison of Probability of Processing Success within 5 Minutes for Valid Long Messages

Figure D-D.6 and Table D-D.1 show that:

- identical simulation results are obtained for the distributions of Appendix B and Appendix C, in respect of the non-conditional probability of processing success, but these results do not match the results obtained for the uniform distribution as noted in section D-D.3.2 above;
- there is a fairly good match between the simulation results and the “weighted average” computed for the distribution of Appendix B as discussed in section D-B.4 of Appendix B; and
- the results of the analysis of the worst-case scenario of Appendix B ($\Delta \leq \tau$) are significantly above the simulation results obtained for the worst-case of the Appendix B distribution, however, the analysis provides a good match with the probability of success under the C/S T.001 (Appendix C) distribution within 6 minutes after first-burst collision (statistic established on 7 transmitted bursts).

The conclusion of this comparison is that the probability of success $P_K(N < M)$ determined in the mathematical analysis on the basis of the binomial formula (Equation D/E.8) using a computed probability of collision, is not consistent with the simulation results in the cases of Appendix B and Appendix C distributions. However, the Appendix B analysis provides a fairly good match with the simulation results:

- when a “weighted average” is used to compute the non-conditional probability of success; and

- when comparing the Appendix B “worst-case” to the Appendix C simulation results, assuming a first-burst collision followed by a 6-burst transmission (i.e., 7 transmitted bursts within about 6 minutes).

In summary, we can conclude that the Appendix B analysis provides an acceptable analytical model of the GEOSAR channel capacity.

Table D-D.1: Comparison of Mathematical Analysis and Computer Simulation Results Obtained for Valid Long Messages with Various Distributions of the Bursts Transmission Times

Number of Active Beacons	10	11	12	13	14	15	16	17	18	19	20
UNIFORM DISTRIBUTION (5-minute transmissions)											
<i>P. Collision - Uniform D. (Simulation)</i>	0.1577					0.2343					0.3040
<i>P. Collision - Uniform D. (Analysis)</i>	0.1578	0.1737	0.1893	0.2046	0.2197	0.2344	0.2489	0.2631	0.2770	0.2907	0.3041
<i>P. of Process. Success - Uniform D. (Simulation)</i>	0.9930					0.9701					0.9266
<i>P. of Process. Success - Uniform D. (Analysis)</i>	0.9929	0.9899	0.9861	0.9816	0.9762	0.9700	0.9630	0.9551	0.9463	0.9367	0.9262
APPENDIX B (5-minute transmissions)											
<i>P. of Coll. - App. B - Delta<Tau (Simulation)</i>	0.2932					0.3575					0.4143
<i>P. of Coll. - App. B - Delta<Tau (Analysis)</i>	0.2931	0.3062	0.3191	0.3316	0.3438	0.3557	0.3674	0.3787	0.3897	0.4005	0.4110
<i>P. of Process. Success - App.B - (Simulation)</i>	0.9721					0.9327					0.8772
<i>P. of Success - App.B Weighted Average (Analysis)</i>	0.9837	0.9785	0.9723	0.9652	0.9571	0.9481	0.9381	0.9272	0.9154	0.9028	0.8895
<i>P. of Process. Success - App.B - Delta<Tau (Simulation)</i>	0.9121					0.8434					0.7676
<i>P. of Process. Success - App.B - Delta<Tau (Analysis)</i>	0.9349	0.9245	0.9134	0.9016	0.8892	0.8763	0.8628	0.8489	0.8347	0.8201	0.8053
APPENDIX C (C/S T.001 Specification)											
<i>P. Coll. 2nd burst - App.C - Worst Case (Simulation)</i>	0.2945					0.3574					0.4160
<i>P. Coll. 2nd burst - App.C - Worst Case (Analysis)</i>	0.2934	0.3066	0.3196	0.3323	0.3447	0.3568	0.3687	0.3803	0.3916	0.4027	0.4134
<i>P. of Process. Success - App.C - 6 bursts - (Simulation)</i>	0.9705		0.9562	0.9479	0.9393	0.9302					0.8743
<i>P. of Process. Success - App.C - 6 Bursts/1st Burst Coll. (Simulation)</i>	0.8694		0.8373	0.8199	0.8039	0.7851					0.6984
<i>P. of Process. Success - App.C - 7 Bursts/1st Burst Coll. (Simulation)</i>	0.9379					0.8831					0.8140
Number of Active Beacons	20	21	22	23	24	25	26	27	28	29	30
UNIFORM DISTRIBUTION (5-minute transmissions)											
<i>P. Collision - Uniform D. (Simulation)</i>	0.3040					0.3677					0.4249
<i>P. Collision - Uniform D. (Analysis)</i>	0.3041	0.3172	0.3301	0.3428	0.3552	0.3674	0.3794	0.3911	0.4026	0.4139	0.4250
<i>P. of Process. Success - Uniform D. (Simulation)</i>	0.9266					0.8625					0.7846
<i>P. of Process. Success - Uniform D. (Analysis)</i>	0.9262	0.9150	0.9030	0.8902	0.8768	0.8627	0.8481	0.8329	0.8172	0.8010	0.7845
APPENDIX B (5-minute transmissions)											
<i>P. of Coll. - App. B - Delta<Tau (Simulation)</i>	0.4143					0.4698					0.5179
<i>P. of Coll. - App. B - Delta<Tau (Analysis)</i>	0.4110	0.4212	0.4311	0.4408	0.4502	0.4593	0.4682	0.4769	0.4853	0.4934	0.5014
<i>P. of Process. Success - App.B - (Simulation)</i>	0.8772					0.8105					0.7363
<i>P. of Success - App.B Weighted Average (Analysis)</i>	0.8895	0.8755	0.8608	0.8456	0.8299	0.8138	0.7973	0.7805	0.7635	0.7464	0.7292
<i>P. of Process. Success - App.B - Delta<Tau (Simulation)</i>	0.7676					0.6828					0.6017
<i>P. of Process. Success - App.B - Delta<Tau (Analysis)</i>	0.8053	0.7903	0.7751	0.7598	0.7445	0.7291	0.7138	0.6986	0.6835	0.6685	0.6537
APPENDIX C (C/S T.001 Specification)											
<i>P. Coll. 2nd burst - App.C - Worst Case (Simulation)</i>	0.4160					0.4691					0.5155
<i>P. Coll. 2nd burst - App.C - Worst Case (Analysis)</i>	0.4134	0.4239	0.4342	0.4442	0.4539	0.4634	0.4726	0.4815	0.4902	0.4986	0.5068
<i>P. of Process. Success - App.C - 6 bursts - (Simulation)</i>	0.8743					0.8077					0.7338
<i>P. of Process. Success - App.C - 6 Bursts/1st Burst Coll. (Simulation)</i>	0.6984					0.6127					0.5274
<i>P. of Process. Success - App.C - 7 Bursts/1st Burst Coll. (Simulation)</i>	0.8140					0.7396					0.6622

D-D.4.3 Probability of Obtaining Confirmed Complete Messages Within 10 Minutes

Figure D-D.7 illustrates the comparison of the mathematical analysis and the computer simulation results in respect of:

- the probability of processing success within 10 minutes (12 messages) for single complete long messages in the worst-case scenario of Appendix B ($\Delta \leq \tau$) and Appendix C (1st burst collision);
- the non-conditional probability of obtaining a confirmed complete long message within 10 minutes; and
- the conditional (worst-case) probability of obtaining a confirmed complete long message within 10 minutes.

The detail of the data is provided at Table D-D.2. Figure D-D.7 shows that the analysis results based on the worst-case scenario of Appendix B are above the simulation results for the same distribution (worst-case scenario of Appendix B). The discrepancy is particularly significant for single complete messages over 10 minutes, when the number of active beacons increases. This highlights the limits of the Appendix B distribution analysis as a model for the GEOSAR capacity.

However, the analysis also provides an acceptable match, slightly above the simulation results, for the worst-case scenario of Appendix C (confirmed messages within 10 minutes / 12 bursts transmitted). In addition, the weighted average of the Appendix B analysis remains close to the simulation results of Appendix C, which confirms the usefulness and the validity of the analysis at Appendix B for confirmed messages over 10 minutes.

**Figure D-D.7: Comparison of Analysis and Simulation Results
 Probability of Processing Success within 10 Minutes for
 Single Complete Long Messages (Worst-Case Scenario) and
 Confirmed Complete Long Messages**

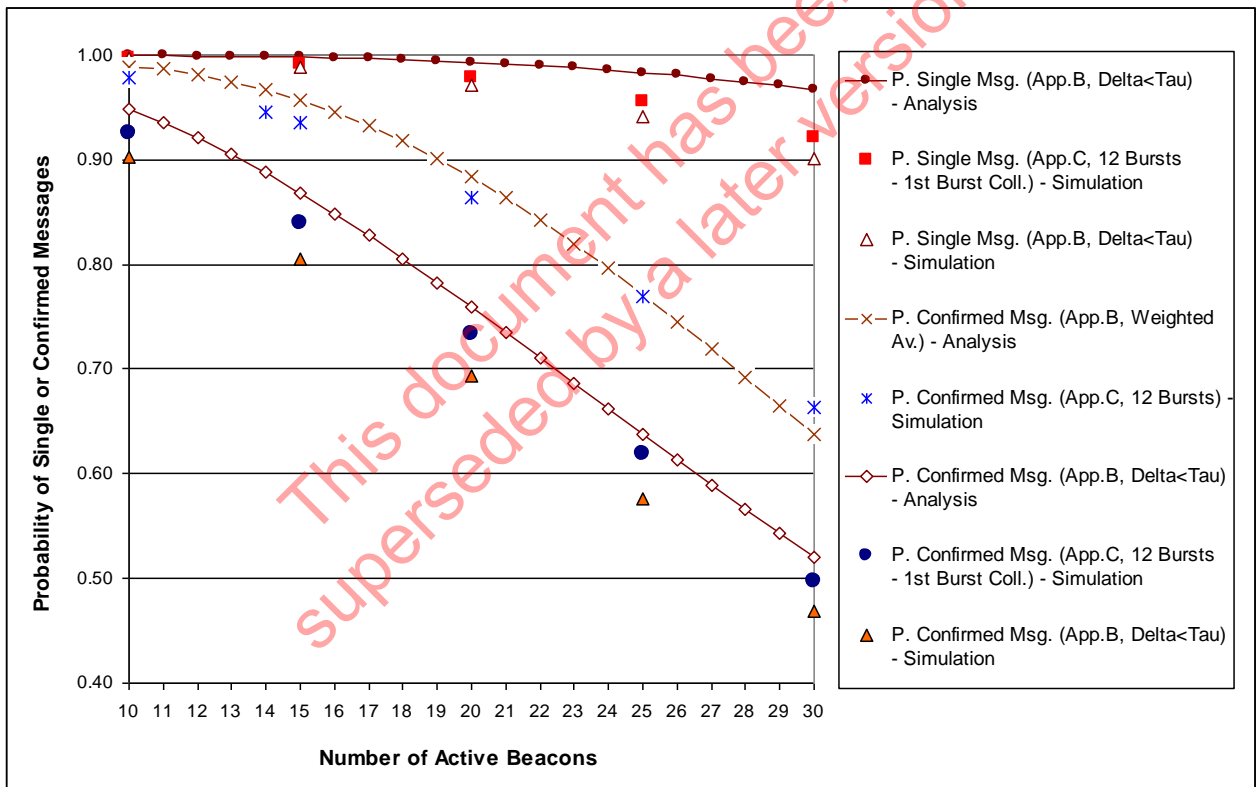


**Table D-D.2: Comparison of Mathematical Analysis and Computer Simulation Results
Obtained for Confirmed Complete Long Messages with Various Distributions
of the Bursts Transmission Times**

Number of Active Beacons	10	11	12	13	14	15	16	17	18	19	20
APPENDIX B - (10 minute transmissions)											
P. Single Msg. (App.B, Delta<Tau) - Simulation	0.9967					0.9880					0.9707
P. Single Msg. (App.B, Delta<Tau) - Analysis	0.9996	0.9995	0.9993	0.9989	0.9986	0.9981	0.9974	0.9967	0.9957	0.9946	0.9934
P. Confirmed - Simulation of App. B					0.9353						
P. Confirmed Msg. - Analysis (Weighted Average)	0.9892	0.9864	0.9812	0.9747	0.9667	0.9571	0.9458	0.9328	0.9181	0.9016	0.8834
P. Confirmed Msg. (App.B, Delta<Tau) - Simulation	0.9024				0.8218	0.8055					0.6933
P. Confirmed Msg. (App.B, Delta<Tau) - Analysis	0.9479	0.9352	0.9208	0.9050	0.8876	0.8689	0.8489	0.8277	0.8057	0.7828	0.7593
APPENDIX C (C/S T.001 Specification)											
P. Single Msg. (App.C, 12 Bursts - 1st Burst Coll.) - Simulation	0.9977					0.9917					0.9778
P. Single Msg. (App.C, 13 Bursts - 1st Burst Coll.) - Simulation	0.9990					0.9954					0.9861
P. Confirmed Msg. (App.C, 12 Bursts) - Simulation	0.9791				0.9461	0.9357					0.8637
P. Confirmed Msg. (App.C, 12 Bursts - 1st Burst Coll.) - Simulation	0.9254				0.8601	0.8391					0.7335
P. Confirmed Msg. (App.C, 13 Bursts - 1st Burst Coll.) - Simulation	0.9569					0.8955					0.8054
Number of Active Beacons	20	21	22	23	24	25	26	27	28	29	30
APPENDIX B - (10 minute transmissions)											
P. Single Msg. (App.B, Delta<Tau) - Simulation	0.9707					0.9413					0.9014
P. Single Msg. (App.B, Delta<Tau) - Analysis	0.9934	0.9919	0.9901	0.9882	0.9860	0.9835	0.9808	0.9778	0.9745	0.9710	0.9672
P. Confirmed Msg. - Analysis (Weighted Average)	0.8834	0.8636	0.8424	0.8198	0.7960	0.7712	0.7455	0.7192	0.6924	0.6653	0.6381
P. Confirmed Msg. (App.B, Delta<Tau) - Simulation	0.6933					0.5763					0.4681
P. Confirmed Msg. (App.B, Delta<Tau) - Analysis	0.7593	0.7353	0.7110	0.6865	0.6620	0.6376	0.6134	0.5895	0.5660	0.5430	0.5205
APPENDIX C (C/S T.001 Specification)											
P. Single Msg. (App.C, 12 Bursts - 1st Burst Coll.) - Simulation	0.9778					0.9550					0.9212
P. Single Msg. (App.C, 13 Bursts - 1st Burst Coll.) - Simulation	0.9861					0.9688					0.9423
P. Confirmed Msg. (App.C, 12 Bursts - 1st Burst Coll.) - Simulation	0.7335					0.6184					0.4976
P. Confirmed Msg. (App.C, 13 Bursts - 1st Burst Coll.) - Simulation	0.8054					0.6985					0.5873

- END OF ANNEX D -

This document has been superseded by a later version

ANNEX E

TEST PROCEDURES FOR VALIDATING THE GEOSAR CAPACITY MODEL

This annex describes the methodology and test procedures to be followed for evaluating the capacity of individual 406 MHz channels in the GEOSAR system.

E.1 BACKGROUND

- The channel capacity in the 406 MHz GEOSAR system is the number of simultaneously active beacons for which the system can provide a valid beacon message within 5 minutes of beacon activation, 95% of the time.

The capacity of a GEOSAR 406 MHz channel is determined by generating traffic loads from known numbers of active beacons in the channel, and evaluating the capability of the GEOSAR system to produce valid 406 MHz alert messages for each beacon in the channel.

The traffic load generated for the test should be comprised of beacon messages which are representative of the nominal conditions as stated at Annex B. Specifically the test transmissions should:

- simulate the performance of operational beacons as specified in Cospas-Sarsat document C/S T.001 (beacon specification);
- be all long format beacon messages, however, a combination of short and long format messages is acceptable provided the precise composition of the population is known;
- transmit at an EIRP of 32 ± 0.5 dBm in the direction of the GEOSAR satellite;
- originate from within the coverage area of the GEOSAR satellite with a beacon to satellite elevation angle not less than 4 degrees, furthermore, there should be no obstructions shielding test source transmitters from the satellite; and
- include an appropriate number of beacons that overlap in time and frequency as required to simulate beacon activations starting randomly in time.

Finally, the ambient conditions during the test should be monitored to ensure that there were no sources of significant interference or real beacons operating in the channel being tested, since these could significantly affect the results.

E.2 TEST PROCEDURE USING A BEACON SIMULATOR

Beacon simulators are capable of transmitting overlapping as well as non-overlapping beacon messages, thus allowing all necessary testing to be performed using only the simulator's transmissions. Two approaches can be used to generate overlapping beacon transmissions that are representative of actual operational beacon transmissions.

- a. All Simulated Signals with C/S T.001 Burst Repetition Interval
Transmission times of all beacons in the simulated population are generated in accordance with the C/S T.001 specification, with pseudo-random start times for the first transmission sequence. The statistical evaluation of the System ability to process successfully beacons within five minutes can be performed using the transmissions of all simulated beacons in the sample population. An example of such a procedure is provided at Appendix A.
- b. Non-overlapping Signals to Generate the Background Load
The simulator is used to generate a background traffic load comprised of simulated beacon signals that do not overlap in time. The simulator is also used to generate "test" signals which can overlap with the background traffic load and each other. The ability of the System to process the "test" signals is evaluated statistically. An example of such a procedure is provided at Appendix B.

This document has been
superseded by a later version

E.3 DATA REDUCTION, ANALYSIS AND RESULTS

The data collected from conducting the test procedures described at either Appendix A or Appendix B is to be recorded at Table E.1. The information listed at Table E.2 should be completed for each simulated traffic load.

Table E.1: Data to be Collected for GEOSAR Capacity Test

Simulated Traffic Load (Number of simultaneously occurring beacon events) _____				
Script Number ____		Date/Time of start of test run 1 _____		
15 Hex ID Tx by Simulator	Time of First Burst in Bcn Event	Time GEOLUT provided First Valid Msg	Time GEOLUT provided first Complete Msg	Time GEOLUT Confirmed Complete Msg

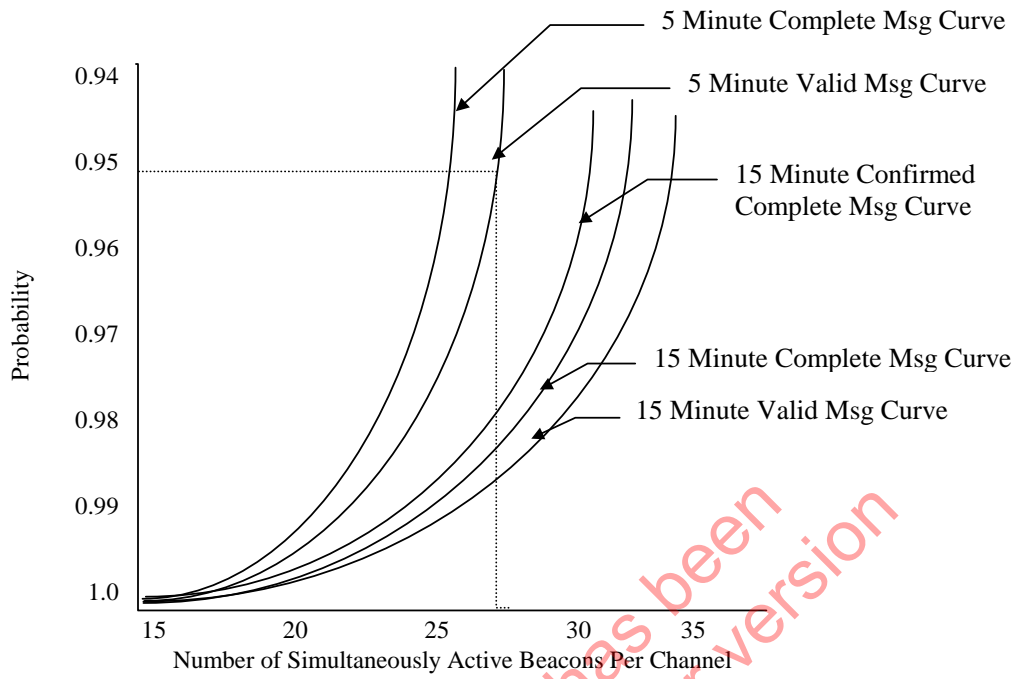
Table E.2: Sample Table for Capacity Statistics

Channel: (Frequency and C/S T.012 Channel Identifier)					
# of Active Bcn Events	% Valid Msg within 5 Min	% Complete Msg within 5 Min	% Valid Msg within 15 Min	% Complete Msg within 15 Min	% Confirmed Complete Msg within 15 Min
15					
20					
25					
30					
35					

The data provided in Table E.2 should be graphed against the respective beacon channel population as indicated at Figure E.1. The capacity of the channel is obtained from the graph as the number of active beacons corresponding to the 95th percentile of the valid message 5-minute curve. Using the fictitious example provided at Figure E.1, the capacity would be 26.5 simultaneously active beacons.

Although the definition of GEOSAR capacity only pertains to the production of valid messages within 5 minutes, the statistics on complete and complete confirmed messages are also calculated as they provide additional information about the performance of the GEOSAR system.

Figure E.1: Graph Depicting Capacity of a 406 MHz Channel in a GEOSAR System



This document has been superseded by a later version

APPENDIX A TO ANNEX E

SAMPLE PROCEDURE FOR GEOSAR CAPACITY TESTING USING TRANSMISSIONS WITH TIME OVERLAPS

The capacity of a 406 MHz channel in a GEOSAR system is determined by generating traffic loads equivalent to known numbers of simultaneously active beacons transmitting long format messages in a Cospas-Sarsat 406 MHz channel. The time required for the GEOLUT to produce a valid beacon message, a complete message and confirm the complete message is recorded for each beacon event. The number of simultaneously occurring beacon events is changed and the time required for the GEOLUT to produce valid, complete and complete confirmed messages is calculated and recorded for the new 406 MHz traffic load.

The test scripts transmitted by the beacon simulator should conform to the nominal conditions detailed in Annex B to C/S T.012. Furthermore, the beacon events transmitted by the simulator should replicate the randomness of the beacon burst repetition period defined in the Cospas-Sarsat 406 MHz beacon specification (C/S T.001). In view of the above, the uplink test signals will include a number of beacon messages that overlap in time and frequency. Nevertheless, due to the randomness of the beacon pulse repetition period, subsequent transmissions of these beacon events might or might not overlap again.

The test should be coordinated to avoid potential interference from non-test sources in both the GEOSAR uplink and downlink channels. Specifically the test scripts should be scheduled to ensure that no signals are uplinked whilst the GEOLUT is in the footprint of a LEOSAR satellite downlink. Furthermore, the 406 MHz channel under test should be free of any signals from operational or test beacons. To minimise the impact on LEOSAR operations, the 406 MHz test channel should be outside the operational processing bandwidth of all LEOSAR SARP instruments.

The test will replicate scenarios of 15, 20, 25, 30 and 35 simultaneously active beacons.

The test should be conducted as follows:

- a. A beacon simulator test script is developed which replicates 15 simultaneously active beacons, with each beacon event having a unique identification (ID). The time of the first burst for each beacon event should be developed using a random process that ensures that the first burst of each beacon is transmitted within 50 seconds of the start of the test. The transmit time for subsequent transmissions for each beacon event shall conform to the repetition period defined in the Cospas-Sarsat beacon specification (C/S T.001). Each beacon event will replicate a beacon being active for a 15 minute period.
- b. After ensuring that the GEOLUT is not in the downlink footprint of a Cospas-Sarsat LEOSAR satellite, the test script is transmitted. The time of the first burst for each beacon event should be recorded in tabular format as provided at Table E.1.

- c. For each beacon event the time when the GEOLUT produces the first valid message, first complete message and first confirmed complete message should be recorded in Table E.1. The time measurements recorded should correspond to the time stamps assigned by the GEOLUT when it produces the respective message, not the time that the message is sent to or received at the MCC.
- d. Repeat the test with different test scripts that also replicate 15 active beacons, until 10 different test scripts have been transmitted.
- e. Compute the probabilities for valid, complete and confirmed complete messages to be recorded in Table E.2.
- f. Repeat the process for scenarios in which the beacon simulator replicates 20, 25, 30, 35 simultaneously active beacons, incrementing the load by 5 beacons until the probabilities recorded in Table E.2 fall below 80%.

*This document has been
superseded by a later version*

APPENDIX B TO ANNEX E**SAMPLE PROCEDURE FOR GEOSAR CAPACITY TESTING USING
NON-INTERFERING BACKGROUND TRANSMISSIONS**

The capacity of the 406 MHz channel is determined by generating traffic loads equivalent to known numbers of active beacons transmitting long format messages in a Cospas-Sarsat 406 MHz channel. The traffic load generated by the beacon simulator is comprised of background signals and test signals. The background signals are transmitted with a constant 50 second burst repetition interval, with start times selected that ensure that the beacon bursts do not collide with each other. The test signals generated by the simulator conform completely to the Cospas-Sarsat beacon specification and, therefore, can collide with each other and with the background signals.

The combination of the background and test signals represent the beacon load on the GEOSAR channel. The time required for the GEOLUT to produce a valid message, a complete message and confirm a complete message is recorded for the test signals (not the background signals). The background traffic load is changed and the process repeated with the new traffic load.

The test should be coordinated to avoid potential interference from non-test sources in both the GEOSAR uplink and downlink channels. Specifically the test scripts should be scheduled to ensure that no signals are uplinked whilst the GEOLUT is in the footprint of a LEOSAR satellite. Furthermore, the 406 MHz channel under test should be free of any signals from operational or test beacons. To minimize the impact on LEOSAR operations, the 406 MHz channel should be outside the operational processing bandwidth of all LEOSAR SARP instruments.

The test will replicate scenarios of 15, 20, 25, 30 and 35 simultaneously active beacons.

The test should be conducted as follows:

- a. A beacon simulator test script is developed which replicates 15 simultaneously active beacons, comprised of 10 background beacons and 5 test beacons. The beacon IDs for the 10 background beacons are provided at Table E-B.1 and are indicated as beacons 1 through 10. The beacon IDs for the test beacons are beacons 60 through 65.

The time of the first burst for each of the test beacon events should be developed using a random process that ensures that the first burst is transmitted within 50 seconds of the start of the test. The transmit time for subsequent test beacon transmissions shall conform to the repetition interval defined in document C/S T.001.

- b. After ensuring that the GEOLUT is not in the downlink footprint of a Cospas-Sarsat LEOSAR satellite, the test script is transmitted. The time of the first burst for each test beacon event should be recorded as per Table E.1.
- c. For each test beacon event the time when the GEOLUT produces the first valid message, first complete message and first confirmed message should be recorded as per

Table E.1. The time measurements recorded should correspond to the time stamps assigned by the GEOLUT when it produces the respective message, not the time that the message is sent to or received at the MCC.

- d. Repeat the test with the same traffic load until a statistically valid amount of data has been recorded.
- e. Compute the probabilities for valid, complete and confirmed complete messages to be recorded in Table E.2.
- f. Repeat steps a) through d) incrementing the background beacon load by 5 beacons, until the probabilities recorded in Table E.2 fall below 80%.

*This document has been
superseded by a later version*

BCN	ID (b26-85)	Bit-Shifted (b25-84)	BCN	ID (b26-85)	Bit-Shifted (b25-84)
1	ADDC078003D0928	56EE03C001E8494	36	ADDC078089549A0	56EE03C044AA4D0
2	ADDC078007A1250	56EE03C003D0928	37	ADDC07808D252C8	56EE03C04692964
3	ADDC07800B71B78	56EE03C005B8DBC	38	ADDC078090F5BF0	56EE03C0487ADF8
4	ADDC07800F424A0	56EE03C007A1250	39	ADDC078094C6518	56EE03C04A6328C
5	ADDC07801312DC8	56EE03C009896E4	40	ADDC07809896E40	56EE03C04C4B720
6	ADDC078016E36F0	56EE03C00B71B78	41	ADDC07809C67768	56EE03C04E33BB4
7	ADDC07801AB4018	56EE03C00D5A00C	42	ADDC0780A038090	56EE03C0501C048
8	ADDC07801E84940	56EE03C00F424A0	43	ADDC0780A4089B8	56EE03C052044DC
9	ADDC07802255268	56EE03C0112A934	44	ADDC0780A7D92E0	56EE03C053EC970
10	ADDC07802625B90	56EE03C01312DC8	45	ADDC0780ABA9C08	56EE03C055D4E04
11	ADDC078029F64B8	56EE03C014FB25C	46	ADDC0780AF7A530	56EE03C057BD298
12	ADDC07802DC6DE0	56EE03C016E36F0	47	ADDC0780B34AE58	56EE03C059A572C
13	ADDC07803197708	56EE03C018CBB84	48	ADDC0780B71B780	56EE03C05B8DBC0
14	ADDC07803568030	56EE03C01AB4018	49	ADDC0780BAEC0A8	56EE03C05D76054
15	ADDC07803938958	56EE03C01C9C4AC	50	ADDC0780BEBEC9D0	56EE03C05F5E4E8
16	ADDC07803D09280	56EE03C01E84940	51	ADDC0780C28D2F8	56EE03C0614697C
17	ADDC078040D9BA8	56EE03C0206CDD4	52	ADDC0780C65DC20	56EE03C0632EE10
18	ADDC078044AA4D0	56EE03C02255268	53	ADDC0780CA2E548	56EE03C065172A4
19	ADDC0780487ADF8	56EE03C0243D6FC	54	ADDC0780CDFEE70	56EE03C066FF738
20	ADDC07804C4B720	56EE03C02625B90	55	ADDC0780D1CF798	56EE03C068E7BCC
21	ADDC0780501C048	56EE03C0280E024	56	ADDC0780D5A00C0	56EE03C06AD0060
22	ADDC078053EC970	56EE03C029F64B8	57	ADDC0780D9709E8	56EE03C06CB84F4
23	ADDC078057BD298	56EE03C02BDE94C	58	ADDC0780DD41310	56EE03C06EA0988
24	ADDC07805B8DBC0	56EE03C02DC6DE0	59	ADDC0780E111C38	56EE03C07088E1C
25	ADDC07805F5E4E8	56EE03C02FAF274	60	ADDC0780E4E2560	56EE03C072712B0
26	ADDC0780632EE10	56EE03C03197708	61	ADDC0780E8B2E88	56EE03C07459744
27	ADDC078066FF738	56EE03C0337FB9C	62	ADDC0780EC837B0	56EE03C07641BD8
28	ADDC07806AD0060	56EE03C03568030	63	ADDC0780F0540D8	56EE03C0782A06C
29	ADDC07806EA0988	56EE03C037504C4	64	ADDC0780F424A00	56EE03C07A12500
30	ADDC078072712B0	56EE03C03938958	65	ADDC0780F7F5328	56EE03C07BFA994
31	ADDC07807641BD8	56EE03C03B20DEC			
32	ADDC07807A12500	56EE03C03D09280			
33	ADDC07807DE2E28	56EE03C03EF1714			
34	ADDC078081B3750	56EE03C040D9BA8			
35	ADDC07808584078	56EE03C042C203C			

Table E-B.1: BSim HEX ID

- END OF ANNEX E -

ANNEX F**FORECAST OF 406 MHz BEACON POPULATION****F.1 POTENTIAL LONG-TERM 406 MHz BEACON POPULATION**

The objective of this exercise is to define realistic lower and upper limits of the potential population of ELTs, EPIRBs and PLBs, for Cospas-Sarsat management planning purposes. However, the world-wide potential 406 MHz beacon population is based on a number of assumptions which are difficult to validate. Therefore, the figures provided in Table F.1 below will be updated as necessary, on the basis of available information.

The actual user base for 406 MHz ELTs, EPIRBs and PLBs is highly dependent on a number of factors which are not under the control of Cospas-Sarsat. These include regulatory decisions by Administrations, the retail cost of beacons, alternative means for providing the distress alerting function, etc. The basic hypotheses used in the following calculations, in particular the world-wide fleet statistics and the percentage of those fleet which may be equipped with 406 MHz beacons, will be reviewed and adjusted from time to time.

No attempt has been made to assess the size of naval and air force fleets world-wide. Even if these figures were known, an educated guess could not be made as to the percentage of these fleets which could be equipped with 406 MHz beacons.

Table F.1: Estimate of Potential 406 MHz Beacon Population

	Estimated size of world-wide fleets	% of craft ¹ with 406 MHz beacons	Numb. per craft	Potential 406 MHz beacon population
Merchant vessels over 100 GT	100,000	100 %	1 at least 2 (20%)	100,000 to 120,000
Fishing vessels over 100 GT	25,000	90 %	1 at least	22,500 to 25,000
Small non-commercial craft	2,000,000 to 2,500,000	30 %	1	600,000 to 750,000
Commercial Aircraft	20,000	80 %	2	32,000
General Aviation Aircraft	400,000 to 500,000	50%	1	200,000 to 250,000
PLB and military	-	-		500,000 to 1,000,000
TOTAL (world-wide)	-	-		1,454,500 to 2,177,000

Note 1: These percentages correspond to the estimated maximum fraction of the total fleet which may be equipped with 406 MHz beacons

The figures provided in Table F.1 show that the larger numbers correspond to potential markets for which little or no statistical data is available (small non-commercial craft and PLBs). As a consequence, the actual beacon populations could be vastly different from the above assessment. For planning purposes, it would be prudent to consider a potential 406 MHz beacon population of at least 1,500,000, with a possible maximum of 2,500,000.

F.2 BEACON POPULATION FORECAST

The forecast for the period 2015-2025 assumes that the population will continue to grow in all segments, but at a decreasing rate after the initial build-up of production. The model is based on estimated growth rates of the annual production for each segment of the population (i.e., EPIRBs, ELTs and PLBs). The annual production covers both the replacement market, based on a beacon life time of about 10 years, and the actual growth of the population.

The model is reviewed annually and updated on the basis of the results of the annual survey of beacon production.

Figure F.1: Forecast of Beacon Population
 (June 2023 Forecast)

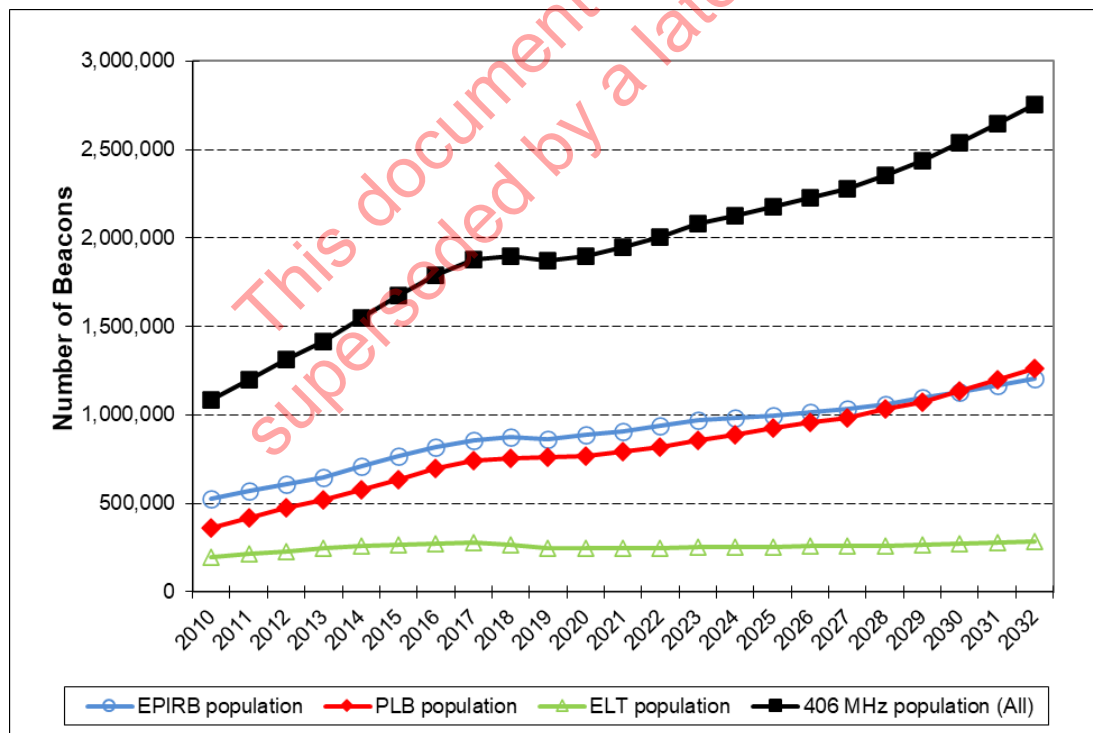


Table F.2: 406 MHz Beacon Population Model
(June 2023 forecast / 2022 manufacturers' production survey)

Year	2016	2017	2018	2019	2020	2021	2022	2023	2024	2025	2026	2027	2028	2029	2030	2031	2032
EPIRB production increase	-1.9%	2.8%	-3.2%	-9.1%	12.4%	-2.6%	5.7%	2%	2%	5%	2%	5%	2%	5%	2%	5%	2%
EPIRB production	95,845	98,552	95,434	86,750	97,472	94,959	100,380	102,388	104,435	109,657	111,850	117,443	119,792	125,781	128,297	134,712	137,406
EPIRB replacement	48,885	58,967	77,733	96,372	76,986	71,838	69,344	68,931	91,374	97,741	95,845	98,552	95,434	86,750	97,472	94,959	100,380
EPIRB population	817,424	857,009	874,710	865,088	885,574	908,695	939,731	973,188	986,249	998,165	1,014,170	1,033,061	1,057,419	1,096,450	1,127,275	1,167,027	1,204,053
PLB production increase	11.4%	10.7%	-14.3%	17.4%	-16.1%	13.4%	3.0%	10%	5%	5%	5%	5%	5%	5%	5%	5%	5%
PLB production	83,608	92,554	79,354	93,186	78,155	88,609	91,254	100,379	105,398	110,668	116,202	122,012	128,112	134,518	141,244	148,306	155,721
PLB replacement	21,533	48,529	66,825	88,860	69,132	60,569	68,862	64,065	72,143	75,076	83,608	92,554	79,354	93,186	78,155	88,609	91,254
PLB population	697,668	741,693	754,222	758,548	767,571	795,611	818,003	854,317	887,573	923,165	955,759	985,217	1,033,975	1,075,307	1,138,396	1,198,093	1,262,560
ELT production increase	-8.8%	21.8%	10.2%	-22.0%	12.9%	-5.3%	-3.0%	5%	2%	5%	2%	2%	5%	2%	2%	5%	2%
ELT production	22,026	26,817	29,554	23,055	26,039	24,656	23,904	25,099	25,601	26,881	27,419	27,967	29,366	29,953	30,552	32,080	32,721
ELT replacement	14,903	20,879	42,089	43,377	26,792	24,318	21,968	23,168	24,982	24,151	22,026	26,817	29,554	23,055	26,039	24,656	23,904
ELT population	274,246	280,184	267,649	247,327	246,574	246,912	248,848	250,779	251,398	254,129	259,521	260,672	260,483	267,381	271,894	279,318	288,135
406 MHz population (All)	1,789,338	1,878,886	1,896,581	1,870,963	1,899,719	1,951,218	2,006,582	2,078,284	2,125,220	2,175,459	2,229,451	2,278,949	2,351,877	2,439,138	2,537,565	2,644,438	2,754,749

This document has been superseded by a later version

The above model estimates appropriate growth rates of beacon production based on an annual survey of manufacturers' forecast and takes into account the regulatory environment. For example, the ICAO decision to mandate 406 MHz ELTs on all aircraft under the ICAO Convention jurisdiction and the phase-out of 121.5 MHz satellite alerting services on 1 February 2009 had a significant impact on the production of ELTs prior to that date. Expected changes to National regulations in respect of PLBs are also factored in the estimated growth rates of PLB production. The production growth model assumes a continuing decrease of beacon retail costs, at least for the next few years.

However, the model does not take into account possible policy decisions by some States which could result in a significant surge of the population over a few years, e.g., mandating the carriage of 406 MHz ELTs on general aviation aircraft in the USA and/or Canada.

- END OF ANNEX F -

*This document has been
superseded by a later version*

ANNEX G

COSPAS-SARSAT 406 MHz MESSAGE TRAFFIC MODEL

G.1. SOURCES OF 406 MHz TRAFFIC

G.1.1 Operational 406 MHz Beacons

There is a direct correlation between the total 406 MHz beacon population and the average number of beacons activated in a given period of time. This relationship is expressed as the ratio of the total number of beacon activations observed during one year over the corresponding beacon population (i.e., the annual activation ratio given as a percentage of the total beacon population). For a given beacon population the average number of active beacons at any point in time will also depend on the average length of time that a distress beacon remains active. It should be noted that annual activation rates and average duration of beacon transmissions can be different for each segment of the beacon population. The actual activation rate and average transmission duration are monitored by Cospas-Sarsat on an annual basis.

An analysis of operational alerts has also shown that alerts are not evenly distributed over the surface of the Earth, rather, there are regions of higher concentrations that must be accounted for in the model. Similarly, the number of active beacons fluctuates as a function of time. The detailed procedures used by Cospas-Sarsat for evaluating the fluctuation of the traffic load caused by the geographic distribution of the beacon population, and for the time fluctuations are detailed in section G.4. These peak-time and density factors are assessed on an annual basis. Because of the large difference in size between the instantaneous coverage area of LEOSAR satellites and the GEOSAR satellite coverage, the peak-time and density factors are specific to each system and are evaluated separately for each system.

G.1.2 Self-Test Mode Transmissions

A review of data collected over an extended period of time has shown that there is a direct correlation between the traffic load resulting from self-test mode transmissions and the beacon population. Furthermore, the factors that influence the peak traffic load as a result of geographic region and time are also applicable to self-test mode transmissions.

G.1.3 System Beacons

The term System beacons is used to describe those 406 MHz beacons active on a permanent or semi-permanent basis which are required for the successful operation of the System.

System beacons provide:

- a. calibrated signals that are used by LUTs to calculate updated satellite orbit vectors;

- b. a method for calculating and distributing time calibration data required for LUTs to use the data from Sarsat SARP instruments; and
- c. a reliable and standardised test source which can be used for evaluating the performance of the System.

Since all System beacons operate in a dedicated frequency channel at 406.022 MHz, for GEOSAR load calculations, they do not contribute to the traffic in the other 406 MHz channels.

With respect to the LEOSAR system, the Doppler shift causes System beacon transmissions to be received at frequencies as high as 406.032 MHz. This is accounted for in the LEOSAR capacity model, which provides a capacity figure that includes the System beacons in channel 406.022 MHz. Therefore, the traffic from System beacons must also be accounted for in the LEOSAR traffic model.

G.1.4 Test Beacons

Test beacons are identical to operational beacons, except that they are coded with a test protocol. They are typically used by national Administrations, beacon manufacturers or LUT operators for conducting tests to evaluate the performance of Cospas-Sarsat equipment. It has been demonstrated that the number of test beacons active at any time is not related to the beacon population, but rather to the amount of testing in the System. Additionally, since the activation of test coded beacons should be co-ordinated with national Administrations it is possible to co-ordinate their use, and, therefore, control their impact on the traffic load.

For the purposes of forecasting the impact of test coded beacons on the beacon message traffic load, the number of active test coded beacons has been tracked over several years, and values for LEOSAR and GEOSAR beacon message traffic models have been determined as shown in section G.5 of Annex G.

G.2. BEACON POPULATION AND 406 MHz MESSAGE TRAFFIC**G.2.1 Evaluation of Peak Traffic as a Function of the Total Beacon Population**

To effectively manage the use of the 406 MHz band, the traffic load for both GEOSAR and LEOSAR systems must be assessed. The following steps are necessary to establish a forecast of the peak volume of 406 MHz beacon message traffic for a given beacon population. The detailed calculation methods and data collection procedures are provided in sections G.3 and G.4, respectively.

G.2.1.1 Methodology for Evaluating the Peak Traffic from Distress Beaconsa. Assess the annual rate of 406 MHz beacon activations (Ra).

The annual rate of 406 MHz beacon activations can be evaluated by Cospas-Sarsat Participants by collecting the following data on an annual basis:

- the number of registered beacons in their database (NRB); and
- the annual number of activations, world-wide, of registered beacons with their country code (NARB).

The rate of activation is the ratio of the number of activations over the number of beacons in the population:

$$Ra = NARB / NRB$$

The product of the total population by the annual rate of beacon activation provides the average number of beacons activated during the year, or a 24-hour period when divided by 365.

b. Assess the Estimated Total Population (ETP)

The ratio of registered beacons (RtR) is the ratio of the number of active beacons for one or several country code(s) that were actually registered (NARB) over the total number of active beacons with the same country code(s) observed during the year (TNAB):

$$RtR = NARB / TNAB$$

The estimated total population for a given country code is the number of registered beacon divided by the ratio of registered beacons:

$$ETP = NRB / RtR$$

Note that the estimated population can be established for each frequency channel if specific NRB, NARB and RtR values are available for each channel. This can then be used to assess the existing traffic in specific channels.

- c. Assess the mean duration of 406 MHz transmissions (D) and the average number of active beacons (NAB)

The beacon transmission duration is the difference in minutes between the last time a beacon was observed in the Cospas-Sarsat System and the first time the same beacon was observed.

The statistical evaluation of the average duration of 406 MHz beacon transmissions can be provided by MCCs for alerts located in their service area, and by nodal MCCs on a global basis.

This average duration, expressed as a fraction of the day, multiplied by the average number of active beacons during 24 hours, provides the average number of active beacons at any time (NAB).

- d. Assess the average number of beacons active in the instantaneous coverage area of a LEOSAR or a GEOSAR satellite.

The average number of active beacons (ANAB) in the coverage area of a satellite is the product of the average number of active beacons, world-wide, as determined in step (c) above, by the fraction of the Earth surface covered by the satellite.

$$\text{ANAB(Leo)} = \text{NAB} * \text{Rleo}, \text{ with } \text{Rleo} = 0.07$$

$$\text{ANAB(Geo)} = \text{NAB} * \text{Rgeo}, \text{ with } \text{Rgeo} = 0.42$$

- e. Assess the geographical distribution of beacon activations to compute a geographic density factor (Df).

The geographical distribution of the located alerts is used to compute:

- the maximum to average ratio of the number of active beacons in the instantaneous coverage area of a LEOSAR satellite (LEO density factor = $Df(\text{leo})$) which is applied to the average number of active beacons in the coverage area of a LEOSAR satellite; and
- the maximum to average ratio of the number of active beacons in the instantaneous coverage area of a GEOSAR satellite (GEO density factor = $Df(\text{geo})$) which is applied to the average number of active beacons in the GEOSAR coverage area.

- f. Assess, over a given period of time, the peak-to-average ratio of beacon messages (Rt):

- in the instantaneous coverage area of a LEOSAR satellite: $Rt(\text{leo})$; and
- in the coverage area of a GEOSAR satellite $Rt(\text{geo})$.

These LEOSAR and GEOSAR peak-to-average ratios (peak-time factors) characterise the uneven distribution in time of 406 MHz beacon transmissions and are applied to the numbers of active beacons determined at step (e) above to obtain a peak number of active beacons in the coverage area of the satellite considered (i.e., LEO or GEO). The determination is made separately for the LEO and the GEO systems (see section G.4).

For consistency with the LEO and GEO capacity determination, which assume a probability of processing success of 95% for the peak traffic, the selected peak-time factor corresponds to the ratio of the number of active beacons that is not exceeded more than 2% of the time over the average number of active beacons, both figures being measured in the highest density region. The detailed computation of the LEO and GEO peak-time ratios is described at section G.4.

G.2.1.2 Other Sources of Traffic

The result of the above computation is an assessment of the peak 406 MHz message traffic from operational beacons as a function of the total beacon population, expressed as a number of active beacons.

Similar computations must be made for the other sources of 406 MHz signals identified in section G.1 above: i.e. self-test mode transmissions and test beacons.

Self-test mode transmissions are proportional to the operational beacon population and must be taken into account accordingly. Their contribution to the total traffic is estimated as a fraction of the operational beacon traffic previously computed (see section G.3).

Test beacon transmissions can be controlled by MCCs and their impact limited as necessary. Their contribution to the total traffic has been evaluated in the worst case as a fixed number of active beacons in the coverage area of the satellite (see section G.3).

System beacons also contribute to the total traffic in the LEOSAR and GEOSAR systems. However, they are all operating at 406.022 MHz and do not affect the traffic in adjacent channels in the GEOSAR system. Therefore, this traffic can be ignored in the GEOSAR traffic model, as long as the 406.022 MHz channel is not expected to accommodate distress beacons.

In the LEOSAR system, System beacon transmissions can interfere in time and frequency with operational beacon transmissions in other channels. As the message traffic from System beacons remains well within the estimated capacity of the 406.022 MHz channel, they have only a limited impact on the capacity requirements of adjacent channels. Nevertheless, this traffic must be evaluated as part of the peak LEOSAR message traffic.

G.2.1.3 Capacity Requirements

The peak of the total 406 MHz traffic demand represents the capacity requirement for the system considered. It is the sum of the contributions of all sources of traffic in the channels open for use by distress beacons, as described above. Faulty beacon transmissions and interference may affect the load of a channel but are not accounted for in the traffic forecast (i.e., the capacity requirement resulting from legitimate transmissions). Their impact is accounted for, where necessary, as a reduction of the channel capacity.

G.2.2 Peak Message Traffic in 3 kHz Channels

The 406 MHz beacon message traffic model is used to determine the beacon population which corresponds to the saturation threshold of the LEOSAR or the GEOSAR systems (i.e. the system capacity expressed as the maximum numbers of typical 406 MHz beacons

transmitting in the LEOSAR satellite coverage area at any point in time, or transmitting in the GEOSAR coverage area, which can be successfully processed with a given probability).

However, a traffic forecast must also be provided for each channel used by Cospas-Sarsat to ensure that the individual capacity of each channel is not exceeded.

G.2.2.1 Actual Population and Traffic in Channel

Several methods can be considered to assess the actual population in the channel under consideration.

The first option is to assess the actual beacon population in the channel by multiplying the total 406 MHz beacon population by the 406 MHz beacon population channel ratio (Cr), which represents the fraction of the actual total traffic resulting from sources operating in the channel under consideration.

The value of Cr is provided by monitoring received alerts and performing the following calculation:

$$Cr = \frac{\text{Number of alerts from beacons in the channel}}{\text{Total number of alerts received}}$$

The second option is to determine the population in each channel using the methodology applied for the forecast of the total population, i.e., determining the population operating in a specific channel on the basis of the history of beacon production at each frequency.

Experience shows that the second method produces estimates that anticipate by one or two years the channel population determined according to the first method, using a channel traffic ratio based on the actual channel traffic. When possible (when actual production data is available for each frequency channel) the second method should be used for estimating the current population in each channel and producing a population forecast for each channel.

G.2.2.2 Forecast Population and Traffic in Channel

On the basis of the assessment of the actual beacon population in a channel, as described above, a forecast of the population in the channel can be developed.

The channel traffic forecast is derived from the population forecast in the channel by following the steps of the computation described in section G.2.1.1 above. Adjustments to the various factors used in the computation may be required to take into account the specific characteristics of the population in a particular channel, e.g., specific activation rates, average beacon transmission duration, etc. (see section G.3.4)

However, it should be noted that the forecast evolution of the beacon population in specific channels can be unreliable as it requires a number of hypotheses concerning the commercialisation of a small number of beacon models. Therefore, adequate margins should be included when comparing the channel traffic demand and the channel capacity.

G.3 MODEL OF 406 MHz BEACON MESSAGE TRAFFIC

The following sections provide the mathematical expression of the computation described in section G.2. The message traffic, expressed as an equivalent number of active beacons, is a function of the beacon population (P). The model described below is applied to the total beacon

population to derive a peak traffic in the entire system. It can also be applied to the actual population of beacons in a particular channel ($P_{\text{channel}} = P \times Cr$, see G.2.2.1), or to the forecast of the beacon population in the channel, subject to appropriate adjustments of the various factors, to compute a peak traffic (actual or forecast) in the channel.

G.3.1 Average Number of Active Beacons World-wide

The number of active distress beacons (NAB) at any time over the surface of the Earth is:

$$NAB = P * Ra/365 * D/(24*60)$$

Where:

- P is the 406 MHz beacon population considered (i.e. total or in a channel, actual or forecast).
- Ra is the annual activation rate (may be global or specific to each channel),
- D is the average duration of 406 MHz beacon transmissions (in minutes),

G.3.2 Equivalent Number of Active Beacons in the LEOSAR System

The peak number of active distress beacons in the LEOSAR coverage area, taking into account the uneven geographical distribution of beacons and the uneven distribution of activations in time, is:

$$PNAB(\text{leo}) = NAB * R_{\text{leo}} * D_{\text{f}}(\text{leo}) * R_{\text{t}}$$

where:

- R_{leo} is the ratio LEOSAR coverage area / Earth surface (R_{leo} = 0.07);
- D_f(leo) is the density factor reflecting the maximum to average ratio of the beacon population in the instantaneous coverage area of a LEOSAR satellite, which depends on the geographical distribution of the 406 MHz beacons;
- R_t is the peak-time factor which corresponds to the ratio of peak (98% probability) over average traffic in the highest density region.

The number of operational beacons activated in self-test mode in the instantaneous coverage area of the satellite (single burst with inverted frame synchronisation received but not processed by the system) can be expressed as a ratio of the beacon population (STR), which may include a specific peak-time factor.

The equivalent traffic from self-test mode transmissions in the coverage area of a LEOSAR satellite is then expressed as:

$$\text{Self-Test Traffic}(\text{leo}) = P * STR * R_{\text{leo}} * D_{\text{f}}(\text{leo})$$

- Where: P is the beacon population considered;
- R_{leo} and D_f(leo) have the same definition as above; and
- STR is a “Self Test Ratio” to be measured for a given population.

The traffic from test coded beacons which is not dependent on the actual beacon population, is expressed as an equivalent number of active beacons in the instantaneous coverage area of the satellite:

$$TB(leo)$$

The traffic from System beacons (orbitography, time reference) expressed as a fixed equivalent number of active beacons in the satellite visibility area.

$$SB(leo)$$

The total traffic to be considered in the coverage area of a LEOSAR satellite (the LEOSAR capacity requirement) is the sum of the traffics calculated above as equivalent numbers of active 406 MHz beacons:

$$\text{LEO Traffic (P)} = \text{PNAB (Leo)} + \text{Self-Test Traffic (leo)} + \text{TB(leo)} + \text{SB(leo)}$$

This expression can be developed as the following mathematical function of the beacon population:

$$\text{LEO Traffic (P)} = \text{TB(leo)} + \text{SB(leo)} + \text{P} * [[(\text{Ra}/365 * \text{D}/24 * \text{Rt}) + \text{STR}] * \text{Rleo} * \text{Df(leo)}]$$

G.3.3 Equivalent Number of Active Beacons in the GEOSAR System

The peak number of active distress beacons in the GEOSAR coverage area, taking into account the uneven geographical distribution of beacons and the uneven distribution of activations in time, is:

$$\text{PNAB (geo)} = \text{NAB} * \text{Rgeo} * \text{Df(geo)} * \text{Rt}$$

where:

R_{geo} is the ratio GEOSAR coverage area / Earth surface ($R_{geo} = 0.42$);

$Df(geo)$ is the density factor reflecting the maximum to average ratio of the beacon population in the coverage area of a GEOSAR satellite, which depends on the geographical distribution of the 406 MHz beacons;

R_t is the peak-time factor which corresponds to the ratio of peak (98% probability) over average traffic in the highest density region.

The number of operational beacons activated in self-test mode in the coverage area of the satellite (single burst with inverted frame synchronisation received but not processed by the system) can be expressed as a ratio of the beacon population (STR), which may include a specific peak-time factor.

The equivalent traffic form self-test mode transmissions in the coverage area of a GEOSAR satellite is then expressed as:

$$\text{Self-Test Traffic (geo)} = P * \text{STR} * R_{\text{geo}} * D_{\text{f}}(\text{geo})$$

where: P is the beacon population considered;
R_{geo} and D_f(geo) have the same definition as above; and
STR is a “Self Test Ratio” to be measured for a given population.

The traffic from test coded beacons which is not dependent on the actual beacon population, is expressed as an equivalent number of active beacons in the instantaneous coverage area of the satellite:

$$\text{TB}(\text{geo})$$

The total traffic to be considered in the coverage area of a GEOSAR satellite (the GEOSAR capacity requirement) is the sum of the traffics calculated above as equivalent numbers of active 406 MHz beacons:

$$\text{GEO Traffic (P)} = \text{PNAB (geo)} + \text{Self-Test Traffic (geo)} + \text{TB}(\text{geo})$$

This expression can be developed as the following mathematical function of the beacon population:

$$\text{GEO Traffic (P)} = \text{TB}(\text{geo}) + P * [[(\text{Ra}/365 * \text{D}/24 * \text{Rt}) + \text{STR}] * R_{\text{geo}} * D_{\text{f}}(\text{geo})]$$

Note: System beacons are not included in this traffic as their transmissions at 406.022 MHz do not impact on the capacity of the distress beacon channels, as computed in accordance with the model of Annex D.

G.3.4 LEOSAR and GEOSAR Traffic Per Channel

The above calculations of the traffic as a function of the total population can also be followed to assess the actual or forecast traffic per channel, using the actual or forecast figure of the population in a given frequency channel.

G.3.4.1 Estimate and Forecast of the Channel Population

The actual figure of the population in a particular channel can be estimated by applying the channel ratio (Cr = fraction of the total traffic load generated from beacons transmitting in that channel) to the total beacon population:

$$Cr = \frac{\text{Number of alerts from beacons in the channel}}{\text{Total number of alerts received}}$$

The actual channel population is then: $P_{\text{Channel}} = P \times Cr$, where P is the total beacon population.

The channel population can also be estimated using manufacturers' production figures for each frequency channel as described in section G.2.2.1.

The forecast beacon population per channel cannot be assessed with a forecast value of the channel traffic ratio, Cr , which would be unreliable. Instead, a specific forecast of the channel population must be established, using information on the beacon models type approved to operate in the channel and manufacturers' forecast of production.

G.3.4.2 Application of the Traffic Model to the Channel Population

The following parameters that are population dependent, may need to be reassessed on a channel basis to account for non-homogenous samples of the beacon population in particular channels.

- a. Annual activation ratio: Cospas-Sarsat has observed that beacons with automatic activation mechanism (g-switch in ELTs or automatic release of EPIRBs) generate a higher number of false alerts than beacons with manual activation only. This results in a higher activation rate for automatically activated beacons. If a channel has a large proportion of manually activated beacons, the annual activation ratio could be significantly lower than for the total population, or other channels with a higher percentage of automatically activated beacons.
- b. Mean duration of 406 MHz transmissions: For the same reason as above, different categories of beacons could have a different average duration of transmissions. This matter may need to be monitored in future.

The other parameters of the model described in section G.2.1 (items d. to f.) seem to be less dependent of the segments of the beacon population and should remain identical in all channels.

G.4 ESTIMATION OF THE MESSAGE TRAFFIC MODEL PARAMETERS

Figure G.1 summarises the global traffic data that are to be collected by France and the USA for the determination of the Rate of Activation (Ra), the Estimated Total Population (ETP) and the Average Transmission Duration (D). The data collection procedures for these parameters plus the Density Factors (Df) and Peak-Time Factors (Rt) are provided in the following sections.

G.4.1 406 MHz Beacon Activation Rate (Ra)

To allow for a possible merging of the data collected, France and the USA should provide:

- the numbers of registered beacons (NRB) for each beacon type (ELT, EPIRB, PLB) as at the middle of the year, including, where appropriate, special beacon programmes; and
- the number of active registered beacon (NARB) from all available sources (LEOLUTs, GEOLUTs or other MCCs), observed during one year, for each beacon type, including single burst activations (SBAs).

For the computation of the rate of activation (Ra), France should consider the French registered beacon population and count only the number of worldwide activations of French registered beacons. The USA should use the USA registered beacon population, including special program beacons as appropriate, and count the number of worldwide activations of USA registered beacons.

The rate of activation is the ratio of the number of activations over the number of beacons in the population:

$$Ra = NARB / NRB$$

The activation rate should be computed for each type of beacon ELT, EPIRB and PLB, and for each population (France or USA). The average activation rate to be used in the beacon message traffic model is obtained after adding the French and US beacon population and beacon activation figures.

G.4.2 Estimated Total Population (ETP)

The ratio of registered beacons (RtR) is the ratio of the number of active beacons for one or several country code(s) that were actually registered (NARB) over the total number of active beacons with the same country code(s) observed during the year (TNAB)

France and the USA should provide the number of observed active beacons in their respective reference populations that were actually registered (NARB) for each beacon type. The estimated total population is derived from the count of registered beacons (NRB) and the observed ratio of active beacons that are actually registered (RtR), as follows:

$$RtR = NARB / TNAB$$

$$ETP = NRB / RtR$$

Figure G.1: Global Traffic Data to Be Collected by France and the USA for the Determination of the Rate of Activation (Ra), the Estimated Total Population (ETP) and the Average Transmission Duration (D)

		ELT	EPIRB	PLB	Other	ALL	Comments
Number of Registered Beacons	NRB						US registered or French registered, Mid-Year (average) population
Number of Active Registered Beacons	NARB						Include all single point alerts (SPA), all data sources (LEO & GEO)
Activation Rate for Registered Beacons	$RaR = NARB/NRB$						Ra, the rate of activation of the model is assumed to be equal to RaR
Total Number of Active Beacons	TNAB						Include registered and non-registered beacons (French or US)
Ratio of Total Active that are Registered	$RtR = NARB/TNAB$						For French or US beacons
Estimated Total Population	$ETP = NRB/RtR$						French or US beacons
US Beacons Activation Duration	$\sum (LTO - FTO) / N$ (US coded beacons)						(Last time observed) minus (First time observed) SPA duration = 60 seconds
French Beacons Activation Duration	$\sum (LTO - FTO) / N$ (French coded beacons)						(Id)

G.4.3 Mean Duration of 406 MHz Transmissions (D)

The beacon transmission duration is the difference in minutes between the last time a beacon was observed in the Cospas-Sarsat System and the first time the same beacon was observed.

Alert data from all available sources (LEOLUTs, GEOLUTs or other MCCs) shall be used to determine the beginning and end of transmission of a beacon, i.e., the first and last detection times. If the first detection is a LEO Doppler solution, the beginning of transmission time is taken as the TCA of the Doppler solution. If the last detection is a LEO Doppler solution, the end of transmission time is taken as the TCA of the Doppler solution. Single burst activations should be included in the statistics with an associated duration of 60 seconds (one minute). In the case of single LEOSAR Doppler solutions for which only a TCA is available, a transmission duration of 8 minutes should be assumed (from TCA - 4 to TCA + 4).

All transmission duration data should be provided separately for each type of beacon (i.e., ELT, EPIRB, PLB, other) and for their combined total. The average transmission duration should be computed separately for French coded beacons and USA coded beacons.

A consolidated average transmission duration will be determined by averaging the durations (France, USA) weighted by the respective estimated populations.

G.4.4 Geographical Distribution Factors (Df (leo) and Df (geo))

France and the USA should annually provide the geographical distribution of all located alerts observed worldwide, using a grid of 15° in latitude per 15° in longitude, for all types of beacons, except orbitography, test or reference beacons. The data should be provided in tabular form (Excel spreadsheet) as well as graphically. All resolved positions or the “A” solution of unresolved Doppler locations should be included.

The LEO density factor is approximated by adding the number of located beacons (N_{leo}) within the area composed of 5 times 4 basic 15° “squares” at mid-latitude, or 4 times 4 at the Equator, and dividing by the average number of locations that should be observed in the same area, assuming a uniform worldwide distribution; i.e. the total number of locations (N_{tot}) multiplied by the ratio of coverage for a LEO satellite ($R_{leo} = 0.07$).

The highest value of the ratio $N_{leo} / (N_{tot} \times R_{leo})$ for various LEO coverage areas is the LEO density factor: Df (leo).

The GEO density factor is obtained by adding the number of located beacons (N_{geo}) within all basic 15° “squares” comprised between the longitudes Long. - 60° to Long. + 60°, and dividing by the average of number of locations that should be observed in the same area assuming a uniform worldwide distribution; i.e. the total number of locations (N_{tot}) multiplied by the ratio of coverage for a GEO satellite ($R_{geo} = 0.42$).

The highest value of the ratio $N_{geo} / (N_{tot} \times R_{geo})$ obtained for the longitudes of existing GEO satellites is the GEO density factor: Df (geo).

G.4.5 406 MHz Beacon Peak-Time Traffic Ratio (Rt)

G.4.5.1 GEO Peak-Time Factor

France and the USA collect all activations that have at least one GEO data point (i.e., GOES-East detections for the USA and MSG detections for France), including single point activations. The corresponding regions (GOES-East coverage area and MSG coverage area) are expected to be regions of high traffic densities.

The beginning of beacon transmission time and end of beacon transmission time are determined for each activation, per the procedure described in section G.4.3 for the assessment of the duration of transmission. For single point activation a duration of sixty seconds is assumed and for single Doppler locations either the number of point times fifty seconds is used or an average 8 minutes pass duration (TCA – 4 to TCA + 4).

For each successive five-minute time slot within the observation period (e.g., May to August), a beacon is considered active during the whole duration of the time slot (i.e., 5 minutes) if the beginning of transmission (BoT) and end of transmission (EoT) span the middle of the time slot.

The cumulative number of slots during which the number of active beacons (NAB) was greater than X is computed to derive the distribution of traffic illustrated at Figure 2.

The GEO peak-time factor (Rt) is the ratio of the number of active beacons in a time slot (NAB) that is exceeded 2 % of the time and the average number of active beacons (ANAB) observed in the GEO area during the year.

The highest Rt as determined for the GOES-East and MSG satellite coverage should be used as GEO peak-time factor for the beacon message traffic model (Rt (geo)).

Alternatively, the highest product Rt*Df for each satellite (GOES-East and MSG) can be considered for use in the traffic model.

G.4.5.2 LEO Peak-Time Factor

France and the USA collect alert data from LEO satellite passes in visibility of the Toulouse LEOLUT or the Maryland LEOLUT, respectively.

The LUT acquisition of signal (LUT AOS) and loss of signal (LUT LOS) are determined for each observed pass to determine the duration of observation. Only real-time alert data are selected, including single points or unlocated alerts acquired in real-time.

The number of active beacons (NAB) observed during each LEO satellite pass is normalised to the duration of the satellite pass as follows:

$$\text{NNAB} = \text{NAB} \times \text{Average D pass} / \text{D pass}$$

with D pass = (LUT LOS – LUT AOS)

The cumulative number of satellite passes with more than X normalised active beacons is computed to derive the distribution of traffic illustrated at Figure G.3.

The LEO peak-time factor (R_t) is the ratio of:

- the normalised number of active beacons that is exceeded during 2% of the passes; and
- the average normalised number of active beacons per pass for the complete data sample.

Alternatively, the number of active beacons (NAB) observed in real-time, is computed for each five-minute slot when a satellite is in visibility of the LEOLUT. The cumulative distribution of five-minute slots during which NAB is greater than X is established and the computation of R_t is performed as described at Figure G.2 for the GEO traffic.

The highest R_t as determined for the Maryland and Toulouse LUTs should be used as LEO peak-time factor for the beacon message traffic model ($R_t(\text{leo})$).

Note: Calculations of R_t for the LEO and GEO traffic models do not have to be performed annually. The need for re-evaluation of the peak-time factors and for separate values for $R_t(\text{leo})$ and $R_t(\text{geo})$ will be reconsidered periodically.

G.4.6 Channel Ratios (Cr)

France and the USA should annually provide the distribution of alerts (absolute numbers of activations and ratios over the total number of alerts) in each channel used by operational beacons, except 406.022 MHz. The distribution should be provided separately for each type of beacon and for the total population.

All beacon transmissions of less than 10 minutes duration should be removed from the sample to eliminate unstable transmission frequencies.

Note that the channel ratio cannot be used to forecast the channel traffic, as it is not fixed in time and the future evolution of a measured ratio is not easily predictable. The main purpose of the measured channel ratio is to provide a means to verify the validity of channel population estimates developed on the basis of manufacturers' production data and the population forecast model.

G.4.7 Self-Test Traffic Ratio (STR)

The beacon self-test traffic should be measured from time to time as follows:

- the total number of points (self-test bursts) is assessed during a certain time period of observation, in a GEOLUT or a LEOLUT coverage area and each point is assumed to have a 50 seconds duration to derive the total duration of self-test transmissions;
- the self-test transmission duration is divided by the duration of the observation period (the total duration of observed satellite passes for a LEOLUT) to obtain the observed self-test traffic (OSTT).

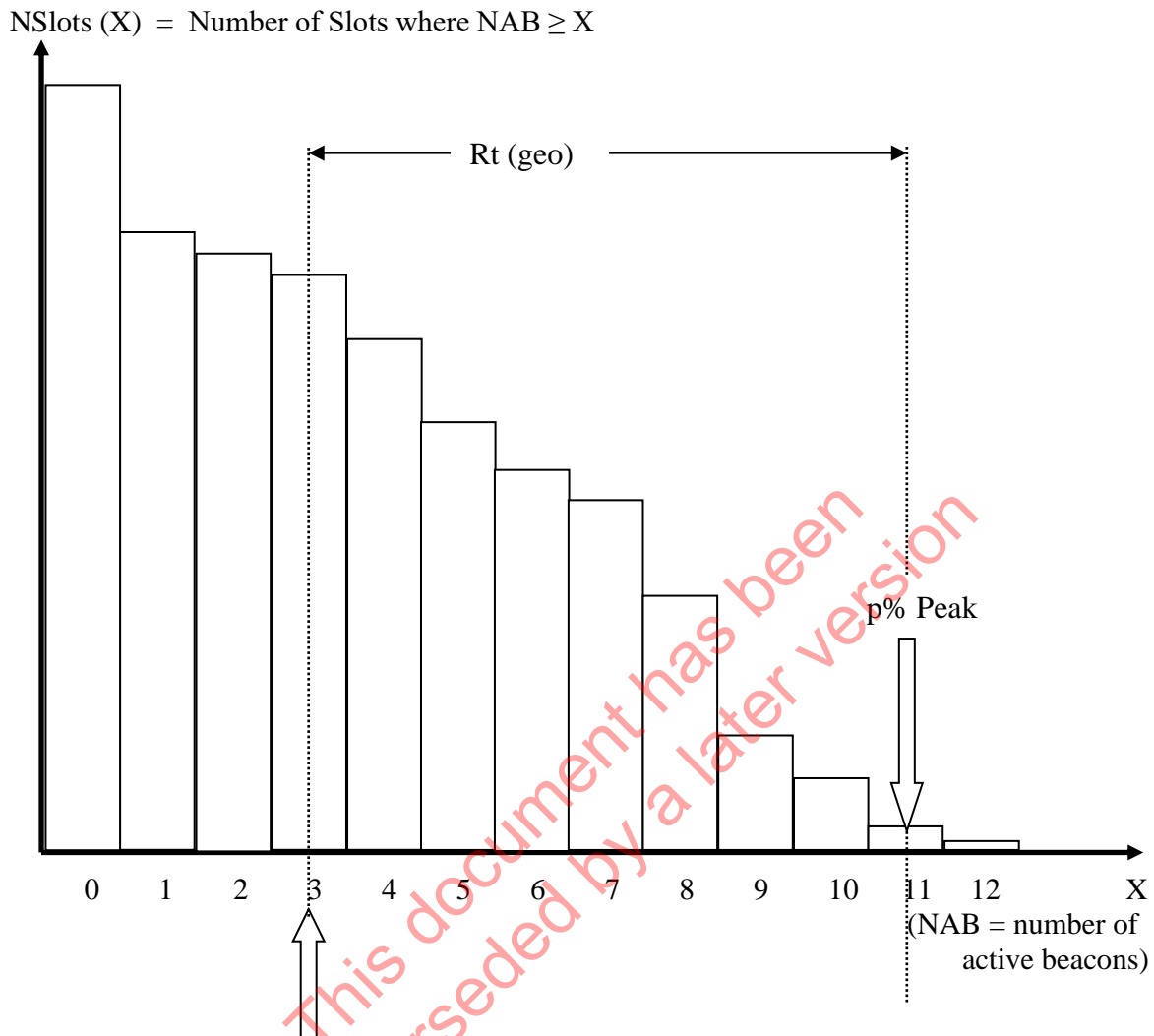
For the computation of the self-test ratio (STR), a peak-time ratio (STR_t) may be introduced. The self-test ratio is:

$$STR = [OSTT \times STR_t] / [R(\text{geo}) \times Df(\text{geo}) \times P]$$

or, as appropriate,

$$STR = [OSTT \times STR_t] / [R(\text{leo}) \times Df(\text{leo}) \times P]$$

where "P" is the worldwide beacon population at the time of the observation.

Figure G.2: Distribution of GEO Traffic in Time

Average NAB over the observation period (ANAB)

$$ANAB = \left[\sum \text{Beacon activation durations} \right] / \text{Duration of observation period}$$

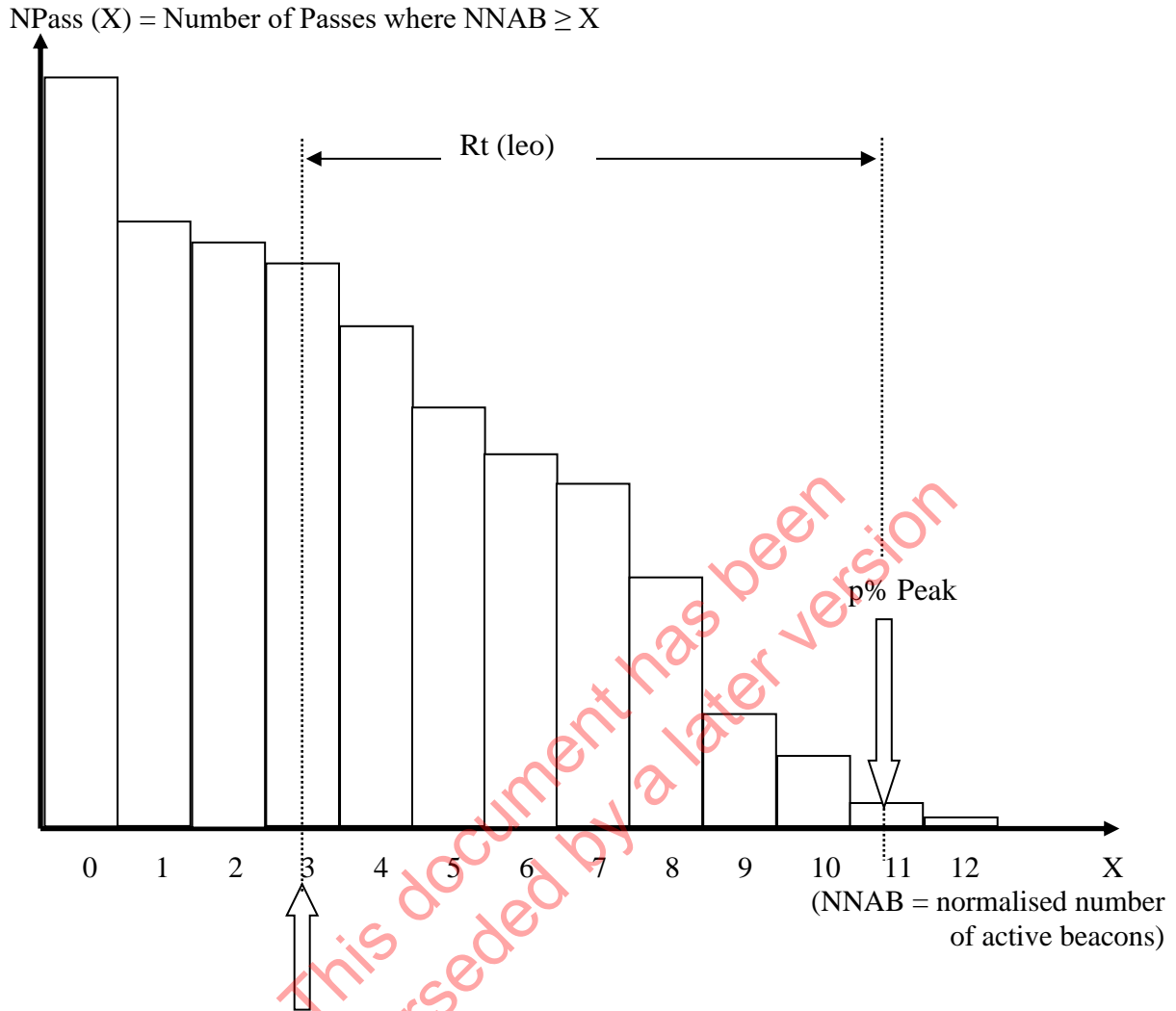
$$= \left[\sum_X (\text{NSlots}(X) - \text{NSlots}(X+1)) * X * 5 \right] / \text{Duration of observation period (in minutes)}$$

Assuming the accepted probability of observing a traffic higher than the selected peak value is p%, then:

$$p\% \text{ Peak} = X, \text{ such that } [\text{NSlots}(X) / \text{NSlots}(0) = p\%]$$

and

$$\mathbf{Rt (geo) = p\% \text{ Peak} / ANAB}$$

Figure G.3: Distribution of LEO Traffic in Time

$$\text{Average per Pass: } APP = \frac{\sum_x [(N_{\text{Pass}}(X) - N_{\text{Pass}}(X+1)) * X]}{N_{\text{Pass}}(0)}$$

Assuming the accepted probability of observing a traffic higher than the selected peak value is p%, then:

$$p\% \text{ Peak} = X \text{ such that } [N_{\text{Pass}}(X) / N_{\text{Pass}}(0) = p\%]$$

and

$$\mathbf{Rt (leo) = p\% \text{ Peak} / APP}$$

G.5 APPLICATION OF THE BEACON MESSAGE TRAFFIC MODEL TO THE LEOSAR AND GEOSAR SYSTEMS

Table G.1 illustrates the computation of the beacon message traffic for the LEOSAR and GEOSAR systems to year 2026, using model parameters updated in 2023 (2022 data).

As activation rates and duration of transmission vary according to the category of beacon (ELT, PLB and EPIRB), the traffic is computed for each category and then summed-up with other traffic sources (self-test, System beacons) to provide a total peak traffic, which represents the capacity requirement for the LEO or the GEO system.

Figure G.4 illustrates the LEOSAR and GEOSAR curves of traffic in time, function of the beacon population forecast provided at Annex F to C/S T.012.

Figure G.4: LEOSAR and GEOSAR Beacon Message Traffic Forecast
 (Peak Traffic – 2023 model parameters/2022 population and traffic data)

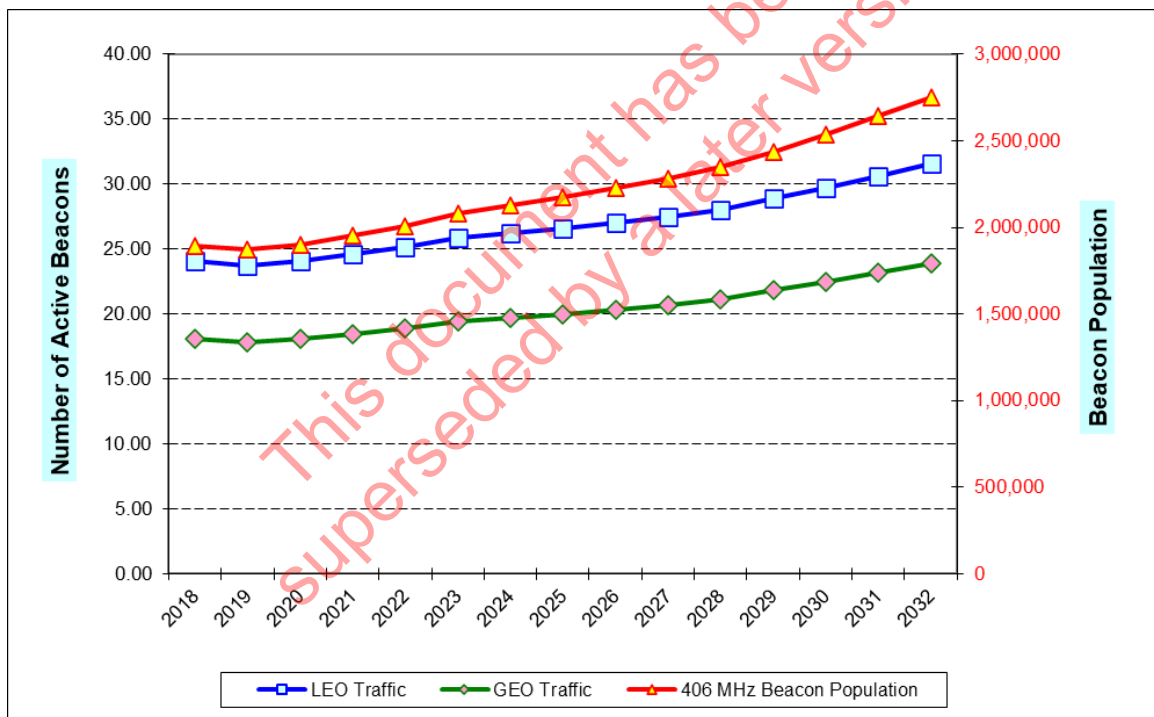


Table G.1: Ten-Year Forecast of Beacon Message Traffic
(2023 Model Parameters based on 2022 population and traffic data)

2022 DATA		ELT	EPIRB	PLB	ALL	ELT	EPIRB	PLB	ALL	ELT	EPIRB	PLB	ALL
		2022	2022	2022	2022	2027	2027	2027	2027	2032	2032	2032	2032
Beacon Population (end of year)	P	248,848	939,731	818,003	2,006,582	260,672	1,033,061	985,217	2,278,949	288,135	1,204,053	1,262,560	2,754,749
Annual Rate of Activation	Ra	4.33%	1.47%	0.49%		4.33%	1.47%	0.49%		4.33%	1.47%	0.49%	
Average Duration of Transmissions	D	55	276	119		55	276	119		55	276	119	
		4.48456E-06	7.71027E-06	1.10671E-06		4.49684E-06	7.73139E-06	1.10974E-06		4.49684E-06	7.73139E-06	1.10974E-06	
Number of Active Beacons	NAB = P x (Ra/365) x (D/1440)	1.12	7.27	0.91	9.29	1.17	7.99	1.09	10.25	1.30	9.31	1.40	12.01
LEOSAR System													
Ratio of coverage	R _{leo}	0.07	0.07	0.07	0.07	0.07	0.07	0.07	0.07	0.07	0.07	0.07	0.07
Density Factor	Df (leo)	5.2	5.2	5.2	5.2	5.2	5.2	5.2	5.2	5.2	5.2	5.2	5.2
Peak-Time Factor	Rt	4	4	4	4	4	4	4	4	4	4	4	4
Peak Number of Active Beacons in LEO Visibility Area	PNAB = P x (Ra/365) x (D/1440) x R_{leo} x Df(l_{leo})	6.52952E-06	1.12261E-05	1.61136E-06	13.53	6.54741E-06	1.12569E-05	1.61578E-06	14.93	6.54741E-06	1.12569E-05	1.61578E-06	17.48
Population for Self-Test Tr. Observed (2017)		1,878,886											
Observed Self-Test Traffic (2016/ LEO / USA) = OSTT		1.5600											
Average Self Test Traffic	ASTT = OSTT / R _{leo} / Df(l _{leo})	4.3											
Self-Test Peak-Time Factor	STPT	4.0											
Self Test Ratio	STR = ASTT x STPT / P	9.124E-06											
Self-Test Peak Traffic (leo)	STT = P x STR x R_{leo} x Df(l_{leo})				6.66				7.57				9.15
Test Beacons	TB (leo)				2				2				2
System Beacons	SB (leo)				3				3				3
TOTAL LEOSAR TRAFFIC	LEO Traffic = TB (leo) + SB (leo) + STT + PNAB				25.19				27.50				31.63
GEOSAR System													
Ratio of coverage	R _{geo}	0.42	0.42	0.42	0.42	0.42	0.42	0.42	0.42	0.42	0.42	0.42	0.42
Density Factor	Df _{geo}	1.2	1.2	1.2	1.2	1.2	1.2	1.2	1.2	1.2	1.2	1.2	1.2
Peak-Time Factor	Rt	2.5	2.5	2.5	2.5	2.5	2.5	2.5	2.5	2.5	2.5	2.5	2.5
Peak Number of Active Beacons in GEO Visibility Area	PNAB = P x (Ra/365) x (D/1440) x R_{geo} x Df(g_{geo})	5.65054E-06	9.71494E-06	1.39445E-06	11.71	5.66602E-06	9.74155E-06	1.39827E-06	12.92	5.66602E-06	9.74155E-06	1.39827E-06	15.13
Population for Self-Test Tr. Observed (2008)		745,451											
Observed Self-Test Traffic (2008 / GEO / France) = OSTT		0.629											
Average Self Test Traffic	ASTT = OSTT / R _{geo} / Df(g _{geo})	1.2											
Self-Test Peak-Time Factor	STPT	2.5											
Self Test Ratio	STR = ASTT x STPT / P	4.185E-06											
Self-Test Peak Traffic (geo)	STT = P x STR x R_{geo} x Df(g_{geo})				4.23				4.81				5.81
Test Beacons	TB (geo)				3				3				3
System Beacons	SB (geo)				0				0				0
TOTAL GEOSAR TRAFFIC	GEO Traffic = TB (geo) + SB (geo) + STT + PNAB				18.94				20.73				23.94

- END OF ANNEX G -

ANNEX H

COSPAS-SARSAT 406 MHz CHANNEL ASSIGNMENT PLAN

The 406 MHz Channel Assignment Plan summarised in Table H.2 is based on the following:

- a. LEOSAR and GEOSAR systems capacities as described at Annexes C and D of the document C/S T.012 “Cospas-Sarsat 406 MHz Frequency Management Plan”;
- b. a 25% capacity margin is applied to the capacity of channels to provide for the continued production of type approved beacons;
- c. a forecast 406 MHz beacon population as presented at Annex F to document C/S T.012; and
- d. a 406 MHz message traffic forecast as presented at Annex G to document C/S T.012 and summarised in Table H.1 below, which shows the LEOSAR and GEOSAR capacity requirements (provided as an equivalent number of 406 MHz beacons in the field of view of a LEOSAR or a GEOSAR satellite) and the corresponding channel requirements.

Table H.1: Summary of 406 MHz Beacon Population Forecast, Capacity Requirements and Channel Requirements (2023 Model Parameters / 2022 Population and Traffic Data)

	2016	2017	2018	2019	2020	2021	2022	2023	2024	2025	2026	2027	2028	2029	2030	2031	2032
Population Forecast (x 1,000)	1,789.3	1,878.9	1,896.6	1,871.0	1,899.7	1,951.2	2,006.6	2,078.3	2,125.2	2,175.5	2,229.5	2,278.9	2,351.9	2,439.1	2,537.6	2,644.4	2,754.7
LEO capacity requirements *	23.0	23.9	24.1	23.8	24.1	24.6	25.2	25.8	26.2	26.6	27.0	27.5	28.0	28.9	29.7	30.6	31.6
LEO Capacity - channels ABC	33	33	33	33	33	33	33	33	33	33	33	33	33	33	33	34	35
LEO Capacity - channels ABC-25%	24.75	24.75	24.75	24.75	24.75	24.75	24.75	24.75	24.75	24.75	24.75	24.75	24.75	24.75	24.75	25.5	26.25
LEO Capacity - channels ABC-F	34	34	34	34	34	34	34	34	34	34	34	34	34	34	34	34	34
LEO Capacity - channels ABC-F -25%	25.5	25.5	25.5	25.5	25.5	25.5	25.5	25.5	25.5	25.5	25.5	25.5	25.5	25.5	25.5	25.5	25.5
LEO Capacity - channels ABC-FG	34	41	41	41	41	41	41	41	41	41	41	41	41	41	41	41	41
LEO Capacity - channels ABC-FG -25%	25.5	30.75	30.75	30.75	30.75	30.75	30.75	30.75	30.75	30.75	30.75	30.75	30.75	30.75	30.75	30.75	30.75
No. of Channels required for LEO	1	1	1	1	1	1	3	3	3	3	3	3	3	3	3	3	4
GEO capacity requirements *	17.2	17.9	18.1	17.8	18.1	18.4	18.9	19.4	19.7	20.0	20.4	20.7	21.1	21.8	22.4	23.2	23.9
GEO Capacity - channels AB																	
GEO Capacity - channels ABC																	
GEO Capacity - (BC-25%)**																	
GEO Capacity - channels ABC+F	42	42	42	42	42	42	42	42	42	42	42	42	42	42	42	42	42
GEO Capacity - (BCF-25%)**	31.5	31.5	31.5	31.5	31.5	31.5	31.5	31.5	31.5	31.5	31.5	31.5	31.5	31.5	31.5	31.5	31.5
No. of GEO channels required ***	2	2	2	2	2	2	2	2	2	2	2	2	2	2	2	2	2
Channels in use for operational beacons' operation	BC+FG	BC+FG	BC+FG	BC+FG	BC+FG	BC+FG	BC+FG	BC+FG	BC+FG	BC+FG	BC+FG	BC+FG	BC+FG	BC+FG	BC+FG	BC+FG	BC+FG
Notes:	Peak number of active beacons in field of view of satellite, based on Annex G traffic model, as updated in March 2023.																
*	25% margin required for continued production of type approved beacon models																
**	Assuming a single GEOSAR channel capacity of 14 active beacons.																
***	Based on the assignment strategy described in CIS T.012, section 4																
****	Channel A = 406.022 MHz (reserved for system beacons), Channel F = 406.037 MHz (closed for new type approval since 2012)																
	Channel B = 406.025 MHz (closed for new type approval since 2002) Channel G = 406.040 MHz (closed for new type approval since 2017)																
	Channel C = 406.028 MHz (closed for new type approval since 2007) Channel J = 406.049 MHz (not open)																

Table H.2: Cospas-Sarsat 406 MHz Channel Assignment Table

Chan. #	Centre Freq. (MHz)	Status for Type Approval of New Beacon Models		Comments Table approved by the Cospas-Sarsat Council at the CSC-43 Session – October 2009 (see Note 1)
		Date open	Date closed	
	406.007	Not available		SARP-2 limitation
	406.010	Not available		Doppler shift limitation
	-----	-----		-----
	406.019	Not available		Doppler shift limitation
A	406.022	C/S orbitography / reference		Reserved for System beacons
B	406.025	1982	1 Jan 2002	Open for beacon models submitted for TA before 01/01/02
C	406.028	1 Jan 2000	1 Jan 2007	Open for beacon models submitted for TA before 01/01/07
D	406.031	1 Jan 2016	1 Jul 2025	Open for beacon models submitted for TA before 01/07/25
E	406.034			Reserved, not to be assigned
F	406.037	1 Jan 2004	1 Jan 2012	Open for beacon models submitted for TA before 01/01/12
G	406.040	1 Jan 2010	1 Jan 2017	Open for beacon models submitted for TA before 01/01/17
H	406.043			Reserved, not to be assigned
I	406.046			Reserved, not to be assigned
J	406.049	TBD	TBD	Available for future assignments / New developments
K	406.052	TBD	TBD	Available for future assignments / New developments
L	406.055			Reserved, not to be assigned
M	406.058			Reserved, not to be assigned
N	406.061	TBD	TBD	Available for future assignments / New developments
O	406.064	TBD	TBD	Available for future assignments / New developments
P	406.067			Reserved, not to be assigned
Q	406.070			Reserved, not to be assigned
R	406.073	TBD	TBD	Available for future assignments / New developments
S	406.076	1 Jan 2025	TBD	Open for beacon models submitted for TA after 01/01/25
	406.079	Not available		Doppler shift limitation
	-----	-----		-----
	406.088	Not available		Doppler shift limitation
	406.091	Not available		SARP-2 limitation

Notes:

- (1) Planned assignments may change if the Cospas-Sarsat Council determines that the beacon population in an active channel differs from the projected population.

TA Type approval

TBD To be determined

- END OF ANNEX H –

- END OF DOCUMENT –

*This document has been
superseded by a later version*

Cospas-Sarsat Secretariat
1250 Boul. René-Lévesque West, Suite 4215, Montreal (Quebec) H3B 4W8 Canada
Telephone: +1 514 500 7999 / Fax: +1 514 500 7996
Email: mail@cospas-sarsat.int
Website: www.cospas-sarsat.int
